Conjugated Polymers with BN Units in the Main Chain

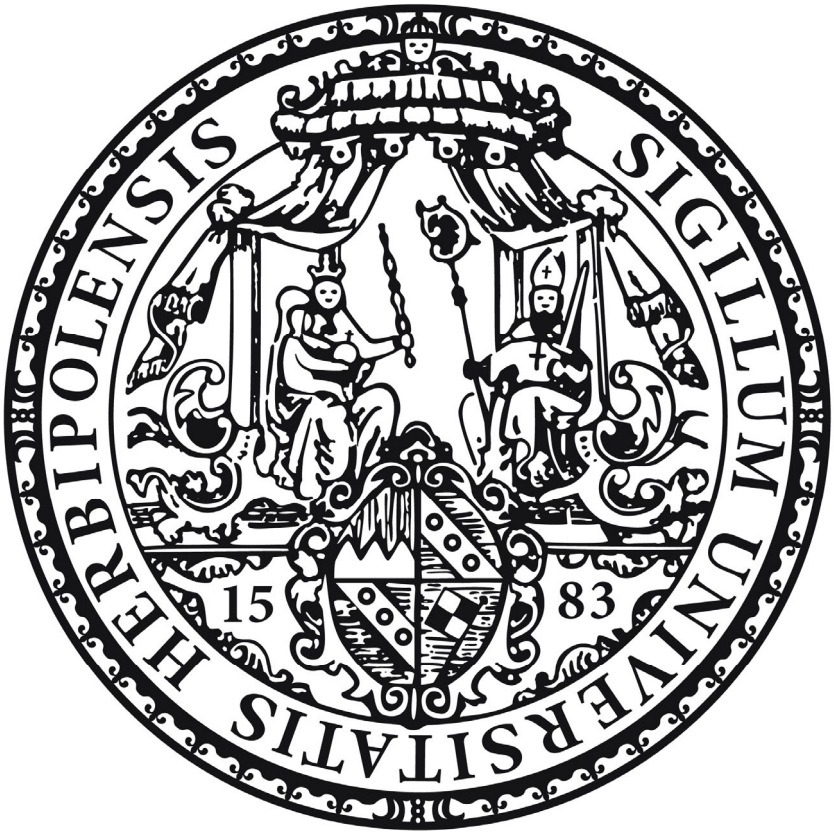

Dissertation zur Erlangung des naturwissenschaftlichen Doktorgrades der Julius-Maximilians-Universität Würzburg

vorgelegt von

Dipl.-Chem.
Thomas Lorenz
aus Bedburg

Würzburg 2020

Eingereicht bei der Fakultät für Chemie und Pharmazie am

_____

Gutachter der schriftlichen Arbeit

1. Gutachter: Prof. Dr. Holger Helten
2. Gutachter: Prof. Dr. Dr. h. c. Todd B. Marder

Prüfer des öffentlichen Promotionskolloquiums

1. Prüfer: Prof. Dr. Holger Helten
2. Prüfer: Prof. Dr. Dr. h. c. Todd B. Marder
3. Prüfer: _____

Datum des öffentlichen Promotionskolloquiums

_____

Doktorurkunde ausgehändigt am

_____

List of Publications

The publications listed below are partly reproduced in this dissertation with permission from Wiley-VCH. The table itemizes at which position in this work the paper has been reproduced.

Publication	**Position**
T. Lorenz, A. Lik, F. A. Plamper, H. Helten, *Angew. Chem. Int. Ed.* **2016**, *55*, 7236-7241; *Angew. Chem.* **2016**, *128*, 7352-7357.	Chapter 4.1
T. Lorenz, M. Crumbach, T. Eckert, A. Lik, H. Helten, *Angew. Chem. Int. Ed.* **2017**, *56*, 2780-2784; *Angew. Chem.* **2017**, *129*, 2824-2828.	Chapter 4.2
F. Brosge, T. Lorenz, H. Helten, C. Bolm, *Chem. Eur. J.*, **2019**, *25*, 12708-12711.	Chapter 4.3

Table of contents

1 Acknowledgements

At first, I would like to thank Prof. Dr. Helten for giving me the opportunity to do my PhD in his group and for working on such an interesting research topic. I am thankful for his continuous support, great advice and inspiring discussions and for providing a kind and productive working atmosphere.

I also would like to thank Prof. Dr. Dr. h. c. Todd B. Marder for taking over the second report on my thesis.

Furthermore, I want to thank the whole Helten group for the enjoyable atmosphere. Thanks to my co-workers Ozan Ayhan, Artur Lik, Merian Crumbach, Lars Fritze, Nicolas Riensch, Abhishek Koner, Matthias Maier, Andreas Helbig and Maximilian Fest for being the great guys they are and for the pleasant atmosphere inside and outside of the laboratory.

I would like to thank Lars Müller, Fabian Thomas, Sebastian Wollnitz and Niklas Möller for their supporting work during their internships and bachelor theses.

A lot of this work would not have been possible without many different analytical measurements, so I want to thank Dr. Klaus Beckerle and Nicolas Riensch for GPC measurements, Toni Gossen, Rachida Bohmarat and Dr. Gerhard Fink for NMR measurements, Brigitte Pütz for MS measurements, Irmgard Kalf for IR measurements, Claudia Schleep for the elemental analysis, Qianqian Guo for collection of X-ray diffraction data and Dr. Thomas Eckert and Dr. Felix Plamper for DLS and SAXS measurements.

I would also like to thank Felix Brosge and Prof. Carsten Bolm from the Institute of Organic Chemistry, RWTH Aachen for the productive cooperation and pleasant discussions.

Finally, I am extremely grateful for my closest family and friends, who have always supported me during my studies.

2 List of Abbrevations

Å	Angström
Ar	aryl
abs	absorbance
anal.	analysis
b.p.	boiling point
BBr_2	dibromoboryl
BBr_3	tribromoborane
BCl_2	dichloroboryl
BCl_3	trichloroborane
$BF_3•OEt_2$	trifluoroborane etherate
BH_3	borane
BPA	boron-doped polyacetylene
BN-PPV	poly(*p*-phenylene iminoborane)
br	broad
Bu	Butyl
cat.	catalyst
cm	centimeter
cod	1,5-cyclooctadiene
d	doublet
DCB	dichlorobenzene
DFB	difluorobenzene
dba	dibenzylideneacetonato
DFT	density functional theory
DLS	dynamic light scattering
DP_n	number average degree of polymerization
dppf	1,1'-bis(diphenylphosphino)ferrocene
dtbpy	4,4'-di-*tert*-butyl-2,2'-bipyridine
EI	electron ionization
elem.	elemental
equiv.	equivalents
Et_2O	diethyl ether
eV	electron volt

g	gram
GPC	gel permeation chromatography
HOMO	highest occupied molecular orbital
HRMS	high-resolution mass spectrometry
Hz	Hertz
ICT	intramolecular charge transfer
i-Pr	*iso*-propyl
J	coupling constant
LED	light-emitting diode
LUMO	lowest unoccupied molecular orbital
m	multiplet
M	molar, mol per liter
max	maximum
Mes	mesityl, 2,4,6-trimethylphenyl
Mes*	supermesityl, 2,4,6-tri-*tert*-butylphenyl
MHz	megahertz
m.p.	melting point
m/z	mass per charge
mbar	millibar
M_n	number average molar mass
M_w	mass average molar mass
NBN unit	diaminoborane unit
nm	nanometer
NMR	nuclear magnetic resonance
Oct	octyl, *n*-C_8H_{17}
OFET	organic field-effect transistor
OLED	organic light-emitting diode
OPV	organic photovoltaic cell
o	ortho
p	para
PA	polyacetylene
PAH	polycyclic aromatic hydrocarbon
Ph	phenyl
PIB	poly(iminoborane)
pin	pinacolato

PLED	polymer light emitting diode
ppm	parts per million
PPP-DIB	poly[*N*-(*p*-phenylene)diimidoborane(3)]
PPV	poly(*p*-phenylen-vinylen)
R	organic substituent
R_h	hydrodynamic radius
r.t.	room temperature
s	singulet
SAXS	small-angle X-ray scattering
sept	septet
SIMS	secondary ion mass spectrometry
t	time
t	tertiary
T	temperature
TADF	thermally activated delayed fluorescence
THF	tetrahydrofuran
Tip	tripyl, 2,4,6-triisopropylphenyl
tol	tolyl
TPA	two-photon absorption
TPEF	two-photon excited fluorescence
UV-vis	ultraviolet-visible
δ	chemical shift
ε	extinction coefficient
Φ_F	quantum yield
λ	wavelength

3 Introduction

In the last decades, the area of research in (semi)conducting π-conjugated organic materials has attracted tremendous attention,[1] due to the applicability of these materials in electronic and optoelectronic devices such as organic light-emitting diodes (OLEDs/PLEDs),[2] organic field-effect transistors (OFETs),[3] and organic photovoltaic cells (OPV).[4,3b] Therein the replacement of established inorganic solids with organic compounds has been of great interest because of the facile processability of these compounds which leads to significantly reduced production costs. Another advantage lies in the possibility of obtaining light-weight materials which can be used in flexible optoelectronic devices,[1-4] for bioimaging, drug delivery,[5] chemical sensing[6] and as electrodes in plastic batteries.[7]

3.1 Conjugated Organoborane Polymers

Through the incorporation of inorganic elements into conjugated polymers various novel hybrid macromolecules with intriguing properties and functions became accessible which cannot be achieved with purely organic compounds.[8] Therein, recent research of conjugated polymers incorporating group 13 elements increased as a result of the inherent electron-deficiency of this group, although the same electron-deficiency makes the preparation of such materials particularly challenging. Nonetheless the interest in organoboron-based conjugated materials owing to their use in organic electronics and optoelectronics and also for bioimaging and sensory applications is tremendously growing.[8,9,10] Due to their vacant p orbital the trivalent boron centers can participate in π-conjugated systems, thereby adding an empty orbital to the π system, which often yields in electron-deficient and potentially n-type semiconducting materials. In OLED devices boron-based chromophores have been incorporated as emitters and electron transporting materials. Due to strong two-photon absorption (TPA) and two-photon excited fluorescence (TPEF) behavior, a lot of organo-borane compounds can be used for biomedical imaging. Other boron compounds show efficient thermally activated delayed fluorescence (TADF).[9q] Some organoboranes, in which a conjugated organoborane is sufficiently Lewis acidic, the ability to bind Lewis bases make such materials applicable as chemosensors, for example, for the detection of certain anions or amines by an optical or electric response.[9] Recent research in graphenes and nanographenes and the chemistry of borophenes lead to growing interest in the incorporation of boron into polycyclic aromatic hydrocarbons (PAHs) and extended 2D structures.[12] Therein air and moisture sensitivity of many organoboron compounds presents itself as problem, which can be overcome by attaching a bulky aryl substituent to the boron center. Various researchers, for example, Wagner and co-workers[13a] used

this concept, by incorporating a mesityl (2,4,6-trimethylphenyl, Mes) group at the boron center for steric protection. Another effective strategy was shown by Yamaguchi and co-workers, who placed boron atoms into internal positions of a fused polycyclic system,[14c] which also led to achieve air- and moisture-stable organoborane compounds.[14-17]

3.1.1 Conjugated Organoborane Polymers with B–Vinyl Linkages

For the synthesis of organoboron polymers different pathways are possible depending on the kind of linkages the polymer chain should contain. Siebert, Corriu, Douglas, and co-workers[18] investigated the hydroboration reaction as a method to prepare poly(vinylene borane)s and, independently, Chujo and co-workers did so as well.[19] Chujo succeeded in the syntheses of well-defined poly(vinylene borane)s **1a,b** by hydroboration polymerization between aromatic or heteroaromatic diynes and the dihydroboranes $MesBH_2$ (Mes = mesityl, 2,4,6-triimethylphenyl) or $TipBH_2$ (Tip = tripyl, 2,4,6-triisopropylphenyl) at ambient temperature (Scheme 3.1.1).[19] This polyaddition reaction follows a step-growth mechanism. The obtained polymers incorporate bulky aryl groups on the boron centers which provide stability against air and moisture and solubility in common organic solvents.[19c] The photophysical characteristics of these macromolecules confirm highly effective π-conjugation along the backbone across the boron centers, e.g. polymer **1a** shows strong blue emission ($\lambda_{max,em}$ = 437 nm) and quantum yields about 0.4–0.5. These properties make these species especially interesting for applications in OLED devices.[19d] By incorporating electron-donating substituents at the phenylene unit, bathochromic shifts of the absorption and emission spectra can be observed. This is characteristic of efficient charge transfer to the boron center. Other related polymers with heteroaromatic units as building blocks showed unusually large Stokes shifts.[19b]

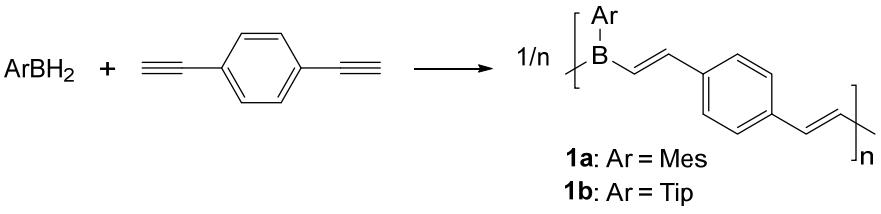

Scheme 3.1.1. Synthesis of polymers **1a,b**.[19]

Chujo and co-workers also demonstrated another pathway for the synthesis of related organoborane polymers using the haloboration–phenylboration polymerization approach, wherein elevated temperatures (~100 °C) are required to obtain *B*–phenyl-substituted products.[20]

Recently, Qin and co-workers used the hydroboration polymerization approach for the synthesis of boron-doped polyacetylenes (BPAs) **2a-c** (Scheme 3.1.2).[21a] These species can be described as poly-acetylenes (PAs) in which every fourth double bond is replaced with a boron atom. Such polymers showed molecular weights of M_n = 5.7 kDa (**2a**), 12.2 kDa (**2b**), and 11.6 kDa (**2c**), respectively. The UV-vis absorption characteristics of **2a-c** in THF indicate a bathochromic shift with increasing length of the cross-conjugated side-chain. Comparing these transitions to those of the related phenyl-enevinylene-bridged polymers such as **1b** (Scheme 3.1.1; $\lambda_{max} \approx 400$ nm), it becomes clear that the former are more red-shifted compared to the latter. This indicates an enhanced main-chain electronic delocalization in **2a-c**. These polymers were also fluorescent, though only **2a** showed a considerable quantum yield (Φ_F = 24.6 %). Another absorption and emission characteristic of **2a-c** is that they showed positive solvatochromic effects. Hereby a bathochromic shifts occurs with increasing solvent polarity. This indicates that in more polar solvents the charge transfer excited states are better stabilized.[21a]

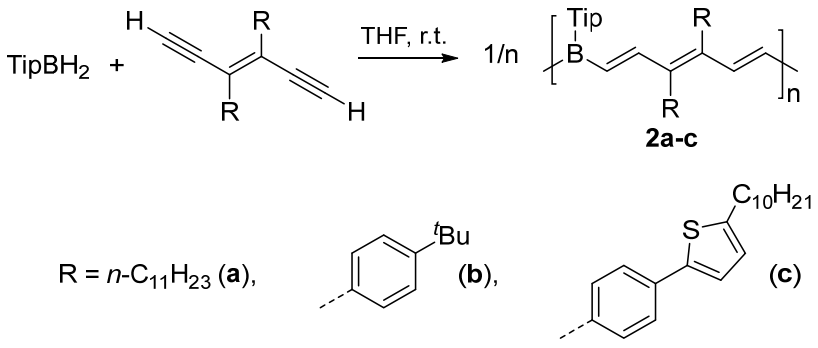

Scheme 3.1.2. Synthesis of boron-doped polyacetylenes **2a-c** by hydroboration polymerization.

The hydroboration polymerization between the ditopic dihydroborane **3** and aromatic dialkynes, which gave 9,10-diboraanthracene-containing polymers **4a,b** was reported by Wagner, Jäkle, Holthausen, and co-workers. These polymers were predominantly *E*-configured (Scheme 3.1.3).[21] The polymeric structure in the solid state of precursor **3**, as shown via single-crystal X-ray diffractometry, results from two-electron-three-center (2e3c) B–H–B bridges. By incorporation of alkoxy-substituents (**4b**) a good solubility in organic solvents can be achieved. During the same time Jia and co-workers published a related study.[22]

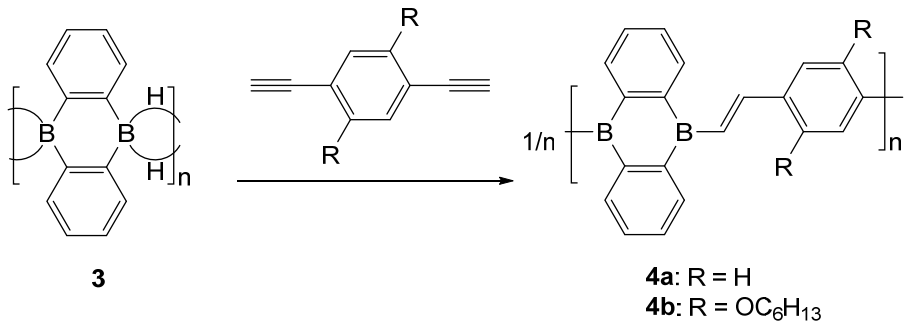

Scheme 3.1.3. Synthesis of polymers **4a,b**.[21]

3.1.2 Conjugated Organoborane Polymers with B–Aryl and B–Alkynyl Linkages

Conjugated organoborane polymers with B–aryl and B–alkynyl linkages cannot be obtained by the above-mentioned hydroboration polymerization. Therefore, polycondensation reactions either via C–C coupling or via B–C coupling were explored. For the C–C coupling reactions preformed organoborane (co)monomers are used and for the B–C coupling organodimetallic reagents and boranes with suitable leaving groups are necessary. Chujo and co-workers successfully prepared poly(*p*-phenylene borane)s[23] and poly(ethynylene *p*-phenylene ethynylene borane)s[24] from reactions of aryldimethoxyboranes with difunctional Grignard reagents or dilithio diacetylides. Jäkle and co-workers applied a milder approach for the synthesis of such polymers by using tin/boron exchange polycondensation. Copolymerization of a bis-stannyl compound either with a dihaloborane (Scheme 3.1.4)[25a,26] or with a bis-haloboryl species (Scheme 3.1.5)[22,25b,c] can be performed in noncoordinating solvents and usually under very mild reaction conditions.

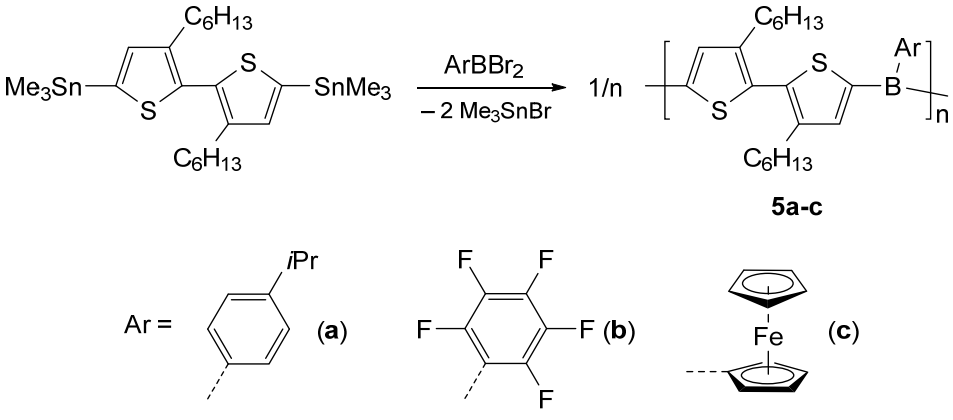

Scheme 3.1.4. Synthesis of polymers **5a-c**.[25a]

The polymers **5a,b** with boron embedded in a polythiophene backbone[9p] show strongly fluorescence emission, which can be modulated by varying the aryl group on the boron center.[25a] The high Lewis acidity of polymers **5a-c**, due to the absence of steric demanding substituents at the boron centers,

though makes them sensitive towards air and moisture, but also makes them interesting for sensory materials by (reversible) binding of pyridine derivatives and in doing so decreasing the absorption and quenching the emission. Jäkle and co-workers were also able to prepare different polymers from common precursor **6** by introducing different boron substituents in a postmodification reaction (Scheme 3.1.5).[25b] These polymers display a strong emission and an optical response to fluoride and cyanide anions. A big disadvantage of these kind of Sn/B exchange reactions is the high toxicity of the used organotin compounds.

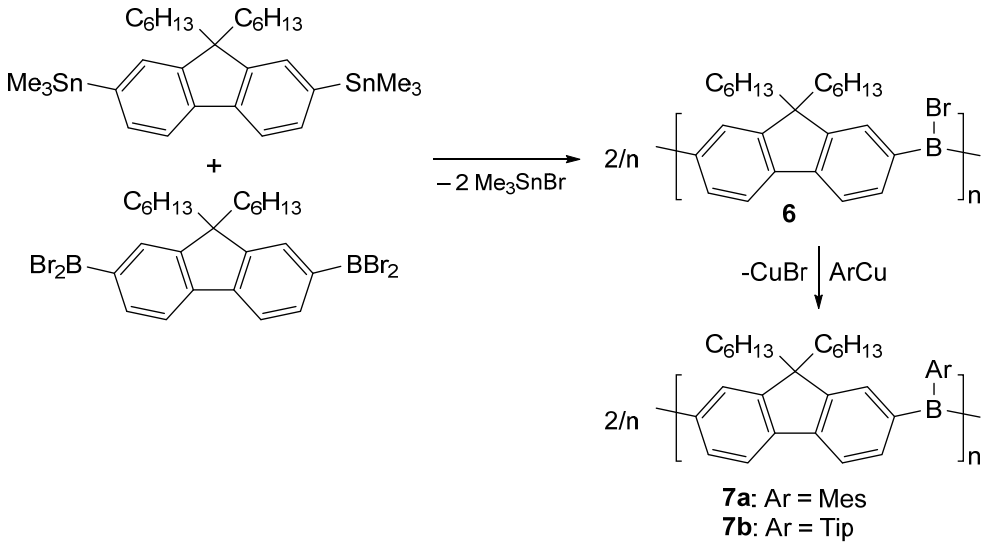

Scheme 3.1.5. Synthesis of polymers **7a,b**.[25b]

Helten and co-workers recently applied another approach by using the less toxic organosilicon compounds to circumvent this issue.[27] Here the drawback initially was that silicon/boron exchange reactions were significantly slower than analogous Sn/B exchange processes. In further studies they showed that it was possible to effectively catalyze the Si/B exchange at ambient temperature with electrophilic silyl compounds like Me_3SiNTf_2 (Tf = SO_2CF_3) (Scheme 3.1.6).[27] Additionally they were able to postmodify the obtained polymers with bulky substituents using TipLi or Mes*Li (Mes* = 2,4,6-tri-*tert*-butylphenyl, supermesityl), respectively, in order to access thienyl- and furylborane oligomers **8a,b** and polymers **8a,b′**.[27] This polycondensation of AB type monomers **7a,b**, comprising of complementary functional groups required for condensation, $SiMe_3$ and BBr_2, in a single molecule are extremely desirable reactions because of their independence of the exact stoichiometry of two monomers.The furylborane compounds show exceptionally intense blue luminescence, with quantum yields of up to Φ_F = 71 %. Incorporating thiophene moieties in furan species Helten et al. demonstrated that the photophysical properties can be effectively modulated by varying the ratio of furan to thiophene rings.[27b]

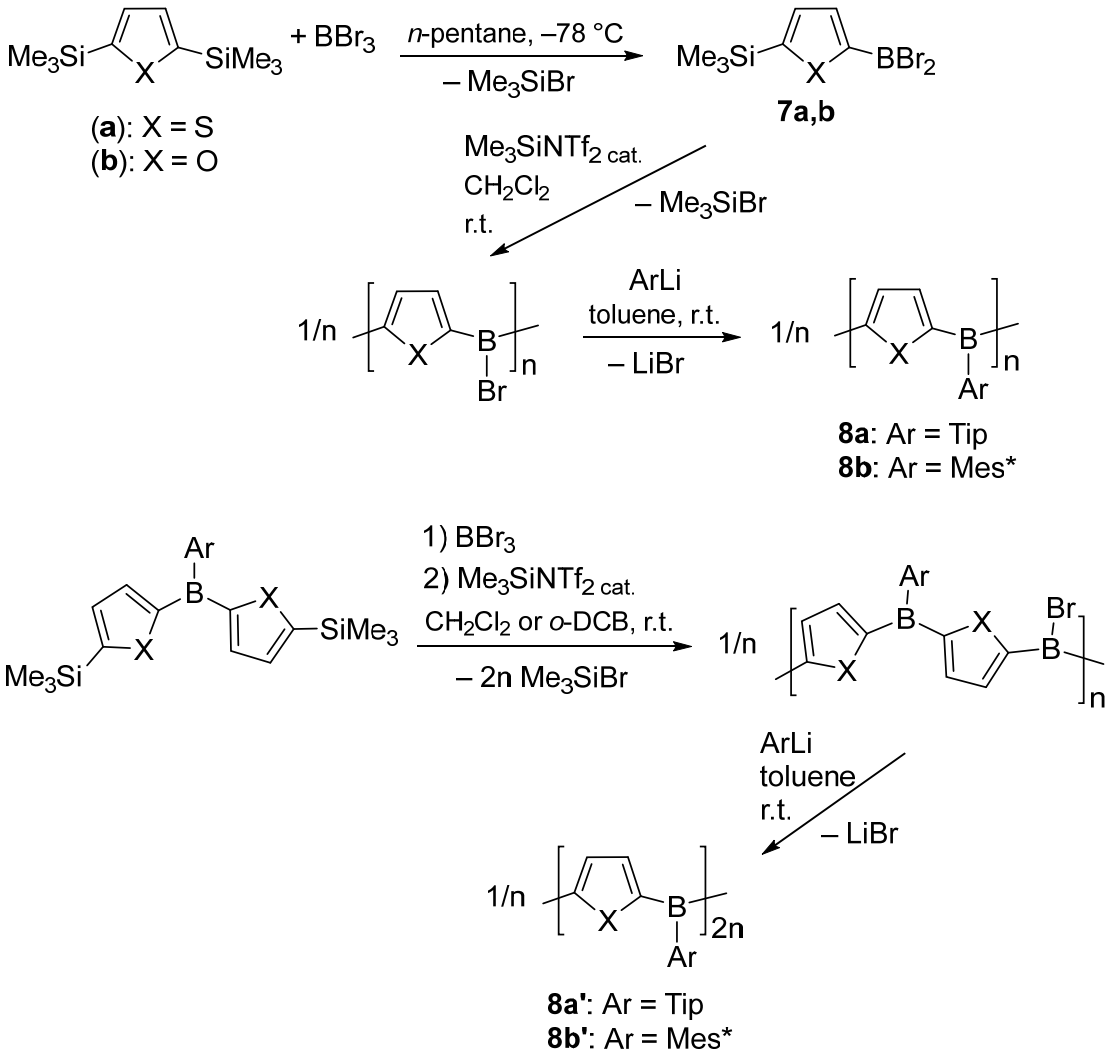

Scheme 3.1.6. Synthesis of oligomers **7a,b** and polymers **8a,b′** by catalytic Si/B exchange polycondensation.[27]

For the synthesis of conjugated organoborane polymers using C–C cross-coupling reactions different type of approaches have been established.[26,28-32] One example is the Stille-type cross-coupling. Wagner and Jäkle were able to incorporate the 9,10-diboraanthracene building block into polymer **9** (Scheme 3.1.7) using this protocol.[29] The resulting polymer **9**, which features mesityl as bulky substituent at the boron center, is air- and moisture-stable.

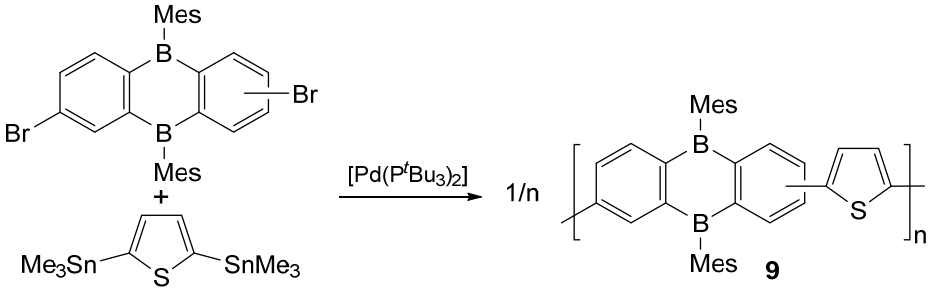

Scheme 3.1.7. Synthesis of polymer **9**.[29]

At about the same time the working groups of Bonifácio et al. and by Rupar et al. developed C−C coupling strategies to incorporate 9-borafluorene (dibenzoborole) units into conjugated polymers (Scheme 3.1.8).[30,31] Upon treating polymer films of **12** with NH_3 vapor, they display a reversible, simultaneous "turn-off/turn-on" fluorescence response.

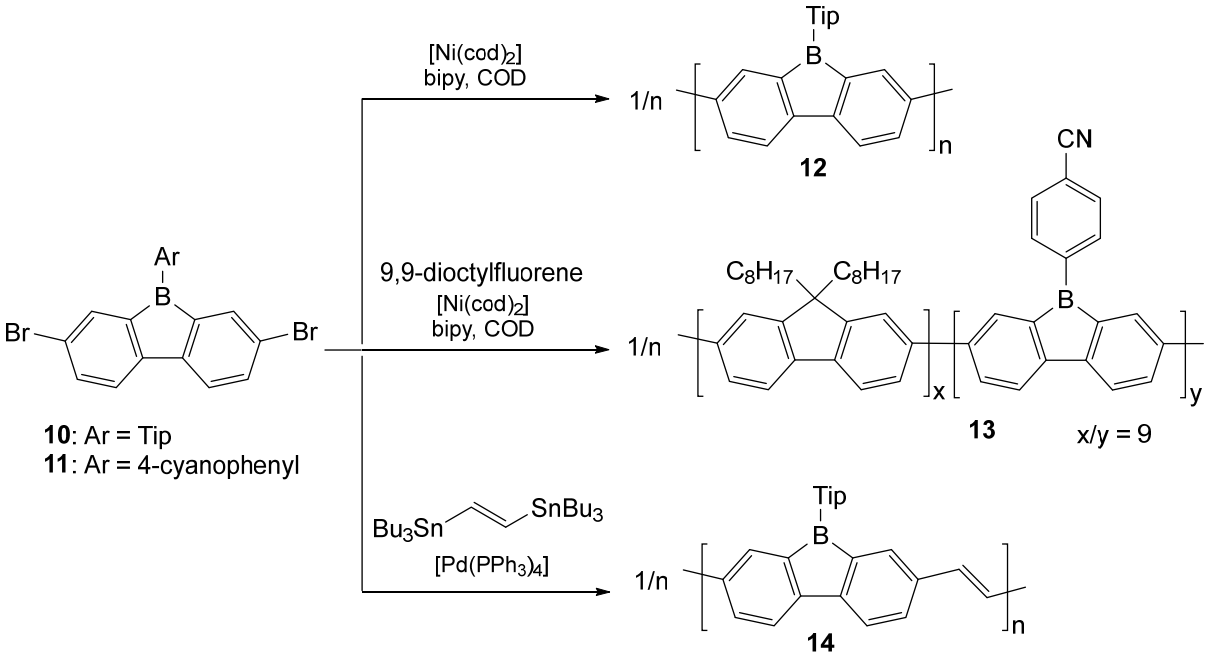

Scheme 3.1.8. Synthesis of borafluorene-containing polymers **12**,[31] **13**,[30] and **14**.[31]

3.1.3 Conjugated Organoborane Polymers with B–N Linkages

The replacement of selected CC fragments in organic compounds by BN units is known as “BN/CC isosterism”. This has been successfully applied in many cases to mono- and polycyclic aromatic hydrocarbons as a concept to produce novel compounds with structural similarities to their all-carbon analogues but fundamentally altered electronic properties.[8, 9a, 9i-r, 33] The application of this concept to polymer chemistry, however, is still in its infancy.

The first examples of π-conjugated polymers that feature B=N units in their main chain were presented by Mulvaney et al. already in 1962.[34] These polymers featured 1,3,2-benzodiazaboroline system as a building blocks and were prepared by polycondensation of diboronic esters with 3,3’-diaminobenzidine. Yamaguchi et al. recently used a Stille-type polycondensation as a novel route to related 1,3,2-benzodiazaboroline-containing polymers.[35] The incorporation of 1,3,2-benzodiazaboroline units into a polymer chain via the 4,7-positions of the benzo core was first explored by Yamamoto and co-workers via Suzuki–Miyaura cross-coupling and subsequent polymer modification.[36] Furthermore, Hayashi et al. prepared a related polymer by electrochemical oxidative polymerization.[37]

By alkoxyboration polymerization of diisocyanates with dimethyl boronates or trialkyl borates, Chujo and co-workers prepared poly(boronic carbamate)s such as **15a,b** which have linear diaminoborane (NBN) units in their main chain (Scheme 3.1.9a).[38] Potentially, the poly(boronic carbamate)s **15a** and **15b**, which have aromatic groups in the main chain, could exhibit extended π-conjugation across the NBN units. However, this aspect was not addressed by the authors for these types of polymers.

Polymers with aminoborane-B=N units in the backbone were prepared by Chujo and co-workers using addition boration polymerization methods as well.[39] Initial attempts employing diynes, diisocyanates, and $PhBCl_2$ in a one-pot reaction gave random copolymers such as **16a** via haloboration and phenylboration reactions (Scheme 3.1.9b). However, the content of the unit originating from the diyne monomer was much lower in the products than expected from the feed ratio. This was attributed to the relatively low reactivity of the diyne monomers towards haloboration. Moreover, the derivative **16b**, having a backbone composed of π systems with no aliphatic interruption, did not form under these conditions.

With a view to increase the content of the alkenylborane unit, a stepwise procedure was developed (Scheme 3.1.9c).[39] In the first step, selective twofold bromoboration of the diyne monomer was achieved under mild conditions. Various aromatic diynes as well as 1,2-diethynyl-1,1,2,2-tetramethyldisilane were employed to give compounds **17a-e** as intermediates. Competing phenylboration of the diynes was not oberserved, as this should require more forcing conditions (~70 °C). On the other hand, phenylboration of isocyanates proceeds smoothly at room temperature. Therefore, the subsequent reaction of **17a-e** with tolylene-2,4-diisocyanate afforded the alternating copolymers **18a-e** at ambient temperature. The polymers **18a-d** are exclusively comprised of π systems along the main chain. However, for **18a**, poorly extended conjugation was deduced from its UV–vis absorption spectrum. This was attributed to effectively interrupted conjugation at the cross-links. Polymer **18d** showed a relatively bathochromic shifted absorption edge. Upon UV irradiation of a dilute $CHCl_3$ solution of **18d**, visible green light emission was observed. It was supposed that this effect might not originate from extended conjugation, but from the dialkenylborane structural defects in the polymer chains. The polymer **18e**, bearing disilanylene units, showed an intense visible violet emission when irradiated in solution with UV light. This was tentatively attributed to the local σ–π-conjugated unit, possibly including a B=N bond.[39b]

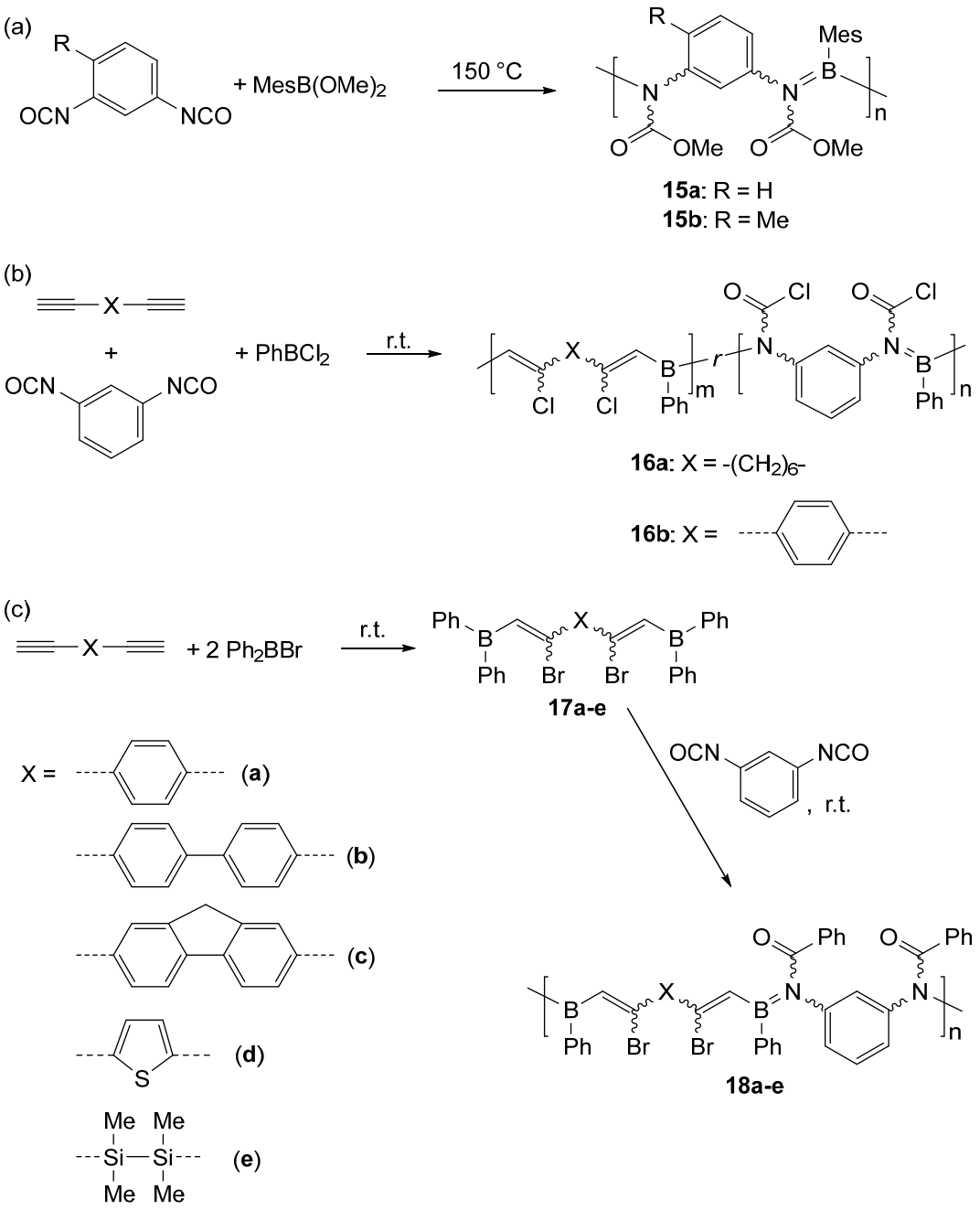

Scheme 3.1.9. Synthesis of polymers **15a,b**,[38] **16a,b** (*r* denotes random copolymers),[39] and **18a-e**.[39]

Recently, Liu, Jäkle, and co-workers presented the first conjugated 1,2-azaborinine polymer, **21**, and related oligomers, **19** and **20**, as molecular model systems for **21** (Scheme 3.1.10).[40] The synthesis was achieved using Suzuki–Miyaura cross-coupling methods. The polymer was formed in strictly regioregular fashion, and the heterocycles adopt an almost perfectly coplanar *syn* arrangement. This was deduced from a single-crystal X-ray study of the dimer, **20**, which also suggested that N–H···π(Mes) interactions play an important role. It should be mentioned that mesityl groups attached to boron are often sufficiently bulky to effectively shield the boron center and prevent hydrolysis or the attack of small nucleophiles in general.

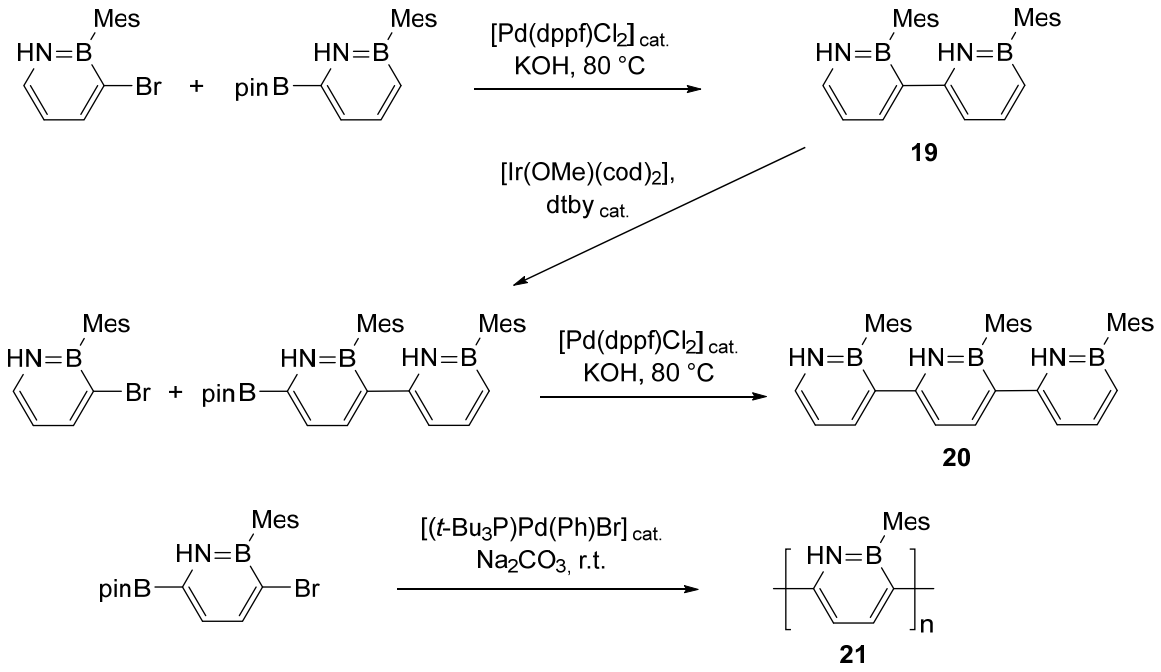

Scheme 3.1.10. Synthesis of **19**, **20**, and polymer **21** (cod = 1,5-cyclooctadiene, dppf = 1,1'-bis(diphenylphosphino)-ferrocene, dtbpy = 4,4'-di-*tert*-butyl-2,2'-bipyridine, pin = pinacolato).[40]

Shortly after this report, two further polymers that contain azaborinine moieties, **23a** and **23b**, were presented by Pei, Wang, and co-workers (Scheme 3.1.11).[41] Here, the B=N unit is embedded in a thiophene-fused polycyclic skeleton. Similar to B-doping of PAHs,[12,14-17] the incorporation of BN into an internal position of a fused ring system also turned out to be general strategy to produce BN PAHs with enhanced stability,[42] and it has been previously demonstrated that this is effective in the case of the framework of **22**.[41a] The synthesis of the polythiophene-type polymers **23a,b** was achieved by Stille coupling polycondensation between **22** and 2,5-bis(trimethylstannyl)thiophene or 5,50-bis(trimethylstannyl)-2,20-bithiophene, respectively. It is supposed that the polymers should be regiorandom in terms of the orientation of the BN units.

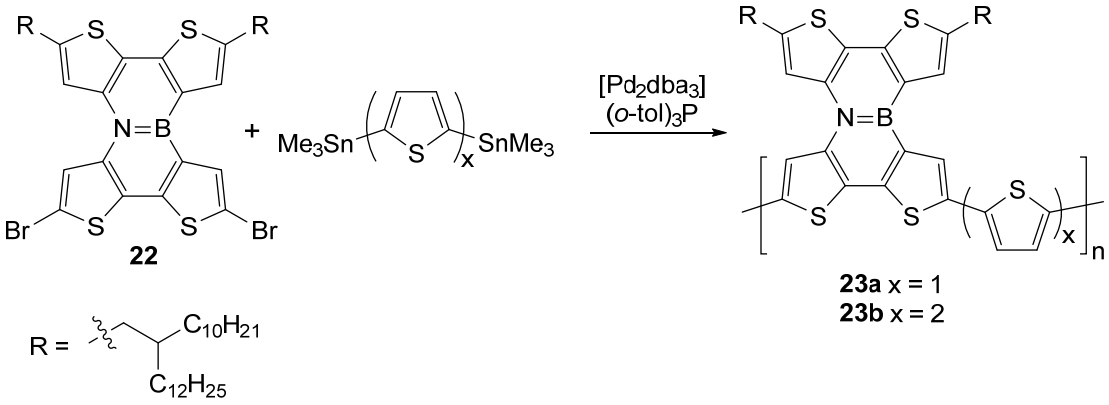

Scheme 3.1.11. Synthesis of polymers **23a,b** (dba = dibenzylideneacetonato, *o*-tol = *ortho*-tolyl).[41c]

The incorporation of 9,10-azaboraphenanthrene moieties into conjugated copolymers **25** and **26** using Suzuki–Miyaura or Stille coupling polycondensation, respectively, was recently explored by He and co-workers (Scheme 3.1.12).[43] The momomer **24** was prepared by an aromaticity-driven ring expansion reaction between mesitylazide and a borafluorene derivative, which has antiaromatic character.

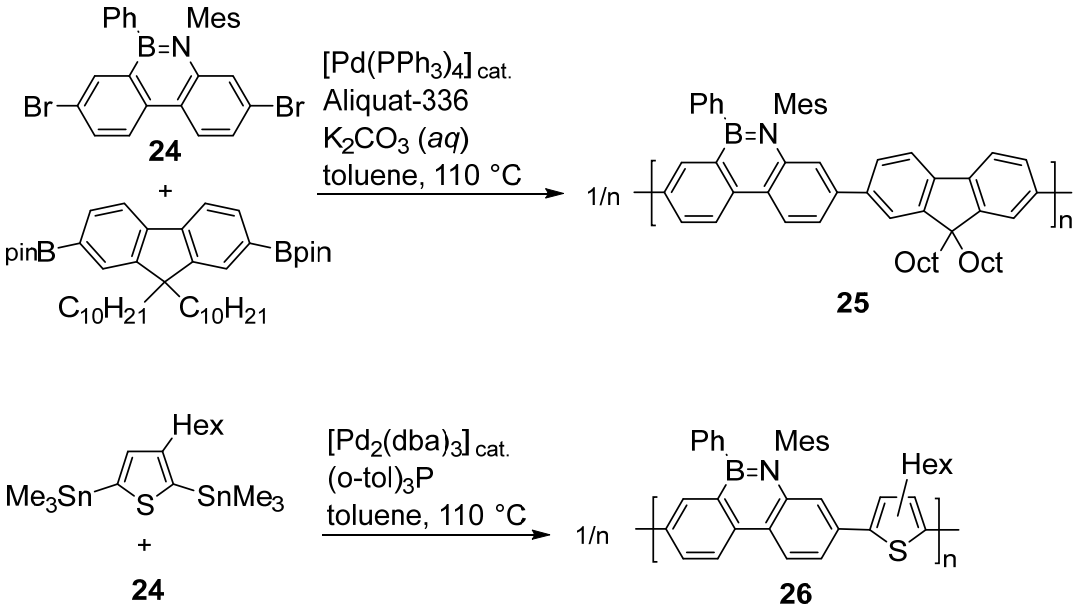

Scheme 3.1.12. Synthesis of 9,10-azaboraphenanthrene-containing copolymers **25** and **26** by Suzuki–Miyaura or Stille-type cross-coupling polycondensation.

3.2 References

[1] a) S. R. Forrest, *Nature* **2004**, *428*, 911–918; b) U. Scherf, A. Gutacker, N. Koenen, *Acc. Chem. Res.* **2008**, *41*, 1086–1097; c) K. Takimiya, I. Osaka, M. Nakano, *Chem. Mater.* **2014**, *26*, 587–593; d) L. Dou, Y. Liu, Z. Hong, G. Li, Y. Yang, *Chem. Rev.* **2015**, *115*, 12633–12665; e) T. M. Swager, *Macromolecules* **2017**, *50*, 4867–4886.

[2] a) A. C. Grimsdale, K. L. Chan, R. E. Martin, P. G. Jokisz, A. B. Holmes, *Chem. Rev.* **2009**, *109*, 897–1091; b) J. Liang, L. Ying, F. Huang, Y. Cao, *J. Mater. Chem. C* **2016**, *4*, 10993–11006.

[3] a) S. Allard, M. Forster, B. Souharce, H. Thiem, U. Scherf, *Angew. Chem. Int. Ed.* **2008**, *47*, 4070–4098; *Angew. Chem.* **2008**, *120*, 4138–4167; b) P. M. Beaujuge, J. M. J. Fréchet, *J. Am. Chem. Soc.* **2011**, *133*, 20009–20029; c) C. Wang, H. Dong, W. Hu, Y. Liu, D. Zhu, *Chem. Rev.* **2012**, *112*, 2208–2267; d) J. Mei, Y. Diao, A. L. Appleton, L. Fang, Z. Bao, *J. Am. Chem. Soc.* **2013**, *135*, 6724–6746; e) H. Sirringhaus, *Adv. Mater.* **2014**, *26*, 1319–1335.

[4] a) C. Li, M. Liu, N. G. Pschirer, M. Baumgarten, K. Müllen, *Chem. Rev.* **2010**, *110*, 6817–6855; b) P.-L. T. Boudreault, A. Najari, M. Leclerc, *Chem. Mater.* **2011**, *23*, 456–469; c) H. Zhou, L. Yang, W. You, *Macromolecules* **2012**, *45*, 607–632; d) L. Dou, J. You, Z. Hong, Z. Xu, G. Li, R. A. Street, Y. Yang, *Adv. Mater.* **2013**, *25*, 6642–667; e) Y. Cai, L. Huo, Y. Sun, *Adv. Mater.* **2017**, *29*, 1605437.

[5] C. Zhu, L. Liu, Q. Yang, F. Lv, S. Wang, *Chem. Rev.* **2012**, *112*, 4687–4735.

[6] S. W. Thomas III, G. D. Joly, T. M. Swager, *Chem. Rev.* **2007**, *107*, 1339–1386.

[7] a) J. F. Mike, J. L. Lutkenhaus, *J. Polym. Sci., Part B: Polym. Phys.* **2013**, *51*, 468–480; b) Z. Song, H. Zhou, *Energy Environ. Sci.* **2013**, *6*, 2280–2301.

[8] a) X. He, T. Baumgartner, *RSC Adv.* **2013**, *3*, 11334–11350; b) A. M. Priegert, B. W. Rawe, S. C. Serin, D. P. Gates, *Chem. Soc. Rev.* **2016**, *45*, 922–953; c) H. Helten, *"Conjugated Inorganic–Organic Hybrid Polymers"*, in *Encyclopedia of Inorganic and Bioinorganic Chemistry* (Ed.: R. A. Scott), John Wiley, Chichester, **2017**.

[9] For reviews, see: a) C. D. Entwistle, T. B. Marder, *Angew. Chem. Int. Ed.* **2002**, *41*, 2927–2931; *Angew. Chem.* **2002**, *114*, 3051–3056; b) C. D. Entwistle, T. B. Marder, *Chem. Mater.* **2004**, *16*, 4574–4585; c) S. Yamaguchi, K. Tamao, *Chem. Lett.* **2005**, *34*, 2–7; d) S. Yamaguchi, A. Wakamiya, *Pure Appl. Chem.* **2006**, *78*, 1413–1424; e) N. Matsumi, Y. Chujo, *Polym. J.* **2008**, *40*, 77–89; f) T. W. Hudnall, C.-W. Chiu, F. P. Gabbaï, *Acc. Chem. Res.* **2009**,

42, 388–397; g) Z. M. Hudson, S. Wang, *Acc. Chem. Res.* **2009**, *42*, 1584–1596; h) C. R. Wade, A. E. J. Broomsgrove, S. Aldridge, F. P. Gabbaï, *Chem. Rev.* **2010**, *110*, 3958–3984; i) F. Jäkle, *Chem. Rev.* **2010**, *110*, 3985–4022; j) Z. M. Hudson, S. Wang, *Dalton Trans.* **2011**, *40*, 7805–7816; k) A. Lorbach, A. Hübner, M. Wagner, *Dalton Trans.* **2012**, *41*, 6048–6063; l) K. Tanaka, Y. Chujo, *Macromol. Rapid Commun*. **2012**, *33*, 1235–1255; m) H. Zhao, L. A. Leamer, F. P. Gabbaï, *Dalton Trans.* **2013**, *42*, 8164–8178; n) A. Wakamiya, S. Yamaguchi, *Bull. Chem. Soc. Jpn.* **2015**, *88*, 1357–1377; o) F. Jäkle, *Top. Organomet. Chem.* **2015**, *49*, 297–325; p) Y. Ren, F. Jäkle, *Dalton Trans.* **2016**, *45*, 13996–14007; q) L. Ji, S. Griesbeck, T. B. Marder, *Chem. Sci.* **2017**, *8*, 846–863; r) S.-Y. Li, Z.-B. Sun, C.-H. Zhao, *Inorg. Chem.* **2017**, *56*, 8705–8717.

[10] Selected examples: a) S. Yamaguchi, T. Shirasaka, S. Akiyama, K. Tamao, *J. Am. Chem. Soc.* **2002**, *124*, 8816–8817; b) X. Y. Liu, D. R. Bai, S. Wang, *Angew. Chem. Int. Ed.* **2006**, *45*, 5475–5478; *Angew. Chem.* **2006**, *118*, 5601–5604; c) Y. Kim, F. P. Gabbaï, *J. Am. Chem. Soc.* **2009**, *131*, 3363–3369; d) A. G. Crawford, A. D. Dwyer, Z. Liu, A. Steffen, A. Beeby, L.-O. Pålsson, D. J. Tozer, T. B. Marder, *J. Am. Chem. Soc.* **2011**, *133*, 13349–13362; e) Y. Kim, H.-S. Huh, M. H. Lee, I. L. Lenov, H. Zhao, F. P. Gabbaï, *Chem. Eur. J.* **2011**, *17*, 2057–2062; f) H. Braunschweig, A. Damme, J. O. C. Jimenez-Halla, C. Hörl, I. Krummenacher, T. Kupfer, L. Mailänder, K. Radacki, *J. Am. Chem. Soc.* **2012**, *134*, 20169–20177; g) Z. M. Hudson, C. Sun, M. G. Helander, Y.-L. Chang, Z.-H. Lu, S. Wang, *J. Am. Chem. Soc.* **2012**, *134*, 13930–1393; h) M. Steeger, C. Lambert, *Chem. Eur. J.* **2012**, *18*, 11937–11948; i) H. Braunschweig, V. Dyakonov, B. Engels, Z. Falk, C. Hörl, J. H. Klein, T. Kramer, H. Kraus, I. Krummenacher, C. Lambert, C. Walter, *Angew. Chem. Int. Ed.* **2013**, *52*, 12852–12855; *Angew. Chem.* **2013**, *125*, 13088–13092; j) K. Matsuo, S. Saito, S. Yamaguchi, *J. Am. Chem. Soc.* **2014**, *136*, 12580–12583; k) L. Ji, R. M. Edkins, A. Lorbach, I. Krummenacher, C. Bruckner, A. Eichhorn, H. Braunschweig, B. Engels, P. J. Low, T. B. Marder, *J. Am. Chem. Soc.* **2015**, *137*, 6750–6753; l) Z. Zhang, R. M. Edkins, J. Nitsch, K. Fucke, A. Eichhorn, A. Steffen, Y. Wang, T. B. Marder, *Chem. Eur. J.* **2015**, *21*, 177–190; m) Z. Zhang, R. M. Edkins, M. Haehnel, M. Wehner, A. Eichhorn, L. Mailänder, M. Meier, J. Brand, F. Brede, K. Müller-Buschbaum, H. Braunschweig, T. B. Marder, *Chem. Sci.* **2015**, *6*, 5922–5927; n) H. Hirai, K. Nakajima, S. Nakatsuka, K. Shiren, J. Ni, S. Nomura, T. Ikuta, T. Hatakeyama, *Angew. Chem. Int. Ed.* **2015**, *54*, 13581–13585; *Angew. Chem.* **2015**, *127*, 13785–13789; o) K. Suzuki, S. Kubo, K. Shizu, T. Fukushima, A. Wakamiya, Y. Murata, C. Adachi, H. Kaji, *Angew. Chem. Int. Ed.* **2015**, *54*, 15231–15235; *Angew. Chem.* **2015**, *127*, 15446–15450.

[11] a) A. J. Mannix, X.-F. Zhou, B. Kiraly, J. D. Wood, D. Alducin, B. D. Myers, X. Liu, B. L. Fisher, U. Santiago, J. R. Guest, M. J. Yacaman, A. Ponce, A. R. Oganov, M. C. Hersam, N. P. Guisinger, *Science* **2015**, *350*, 1513–1516; b) R. D. Dewhurst, R. Claessen, H. Braunschweig, *Angew. Chem. Int. Ed.* **2016**, *55*, 4866–4868; *Angew. Chem.* **2016**, *128*, 4948–4950.

[12] a) A. Narita, X.-Y. Wang, X. Feng, K. Müllen, *Chem. Soc. Rev.* **2015**, *44*, 6616–6643; b) M. Stępień, E. Gońka, M. Żyła, N. Sprutta, *Chem. Rev.* **2017**, *117*, 3479–3716.

[13] a) V. M. Hertz, M. Bolte, H.-W. Lerner, M. Wagner, *Angew. Chem. Int. Ed.* **2015**, *54*, 8800–8804; *Angew. Chem.* **2015**, *127*, 8924–8928; b) V. M. Hertz, H.-W. Lerner, M. Wagner, *Org. Lett.* **2015**, *17*, 5240–5243; c) A. John, M. Bolte, H.-W. Lerner, M. Wagner, *Angew. Chem. Int. Ed.* **2017**, *56*, 5588–5592; *Angew. Chem.* **2017**, *129*, 5680–5684; d) S. Kirschner, J.-M. Mewes, M. Bolte, H.-W. Lerner, A. Dreuw, M. Wagner, *Chem. Eur. J.* **2017**, *23*, 5104–5116; e) K. Schickedanz, J. Radtke, M. Bolte, H.-W. Lerner, M. Wagner, *J. Am. Chem. Soc.* **2017**, *139*, 2842–2851.

[14] a) Z. Zhou, A. Wakamiya, T. Kushida, S. Yamaguchi, *J. Am. Chem. Soc.* **2012**, *134*, 4529–4532; b) S. Saito, K. Matsuo, S. Yamaguchi, *J. Am. Chem. Soc.* **2012**, *134*, 9130–9133; c) C. Dou, S. Saito, K. Matsuo, I. Hisaki, S. Yamaguchi, *Angew. Chem. Int. Ed.* **2012**, *51*, 12206–12210; *Angew. Chem.* **2012**, *124*, 12372–12376; d) T. Kushida, Z. Zhou, A. Wakamiya, S. Yamaguchi, *Chem. Commun.* **2012**, *48*, 10715–10717; e) T. Kushida, C. Camacho, A. Shuto, S. Irle, M. Muramatsu, T. Katayama, S. Ito, Y. Nagasawa, H. Miyasaka, E. Sakuda et al., *Chem. Sci.* **2014**, *5*, 1296–1304; f) T. Kushida, A. Shuto, M. Yoshio, T. Kato, S. Yamaguchi, *Angew. Chem. Int. Ed.* **2015**, *54*, 6922–6925; *Angew. Chem.* **2015**, *127*, 7026–7029; g) S. Osumi, S. Saito, C. Dou, K. Matsuo, K. Kume, H. Yoshikawa, K. Awaga, S. Yamaguchi, *Chem. Sci.* **2016**, *7*, 219–227; h) K. Matsuo, S. Saito, S. Yamaguchi, *Angew. Chem. Int. Ed.* **2016**, *55*, 11984–11988; *Angew. Chem.* **2016**, *128*, 12163–12167.

[15] J. F. Araneda, B. Neue, W. E. Piers, *Angew. Chem. Int. Ed.* **2012**, *51*, 9977–9979; *Angew. Chem.* **2012**, *124*, 10117–10119.

[16] V. M. Hertz, N. Ando, M. Hirai, M. Bolte, H.-W. Lerner, S. Yamaguchi, M. Wagner, *Organometallics*, **2017**, *36*, 2512–2519.

[17] K. Schickedanz, T. Trageser, M. Bolte, H.-W. Lerner, M. Wagner, *Chem. Commun.* **2015**, *51*, 15808–15810.

[18] R. J.-P. Corriu, T. Deforth, W. E. Douglas, G. Guerrero, W. S. Siebert, *Chem. Commun.* **1998**, 963–964

[19] a) N. Matsumi, K. Naka, Y. Chujo, *J. Am. Chem. Soc.* **1998**, *120*, 5112–5113; b) N. Matsumi, M. Miyata, Y. Chujo, *Macromolecules* **1999**, *32*, 4467–4469; c) Y. Chujo, Y. Sasaki, N. Kinomura, N. Matsumi, *Polymer* **2000**, *41*, 5047–5051; d) A. Nagai, T. Murakami, Y. Nagata, K. Kokado, Y. Chujo, *Macromolecules* **2009**, *42*, 7217–7220.

[20] M. Miyata, N. Matsumi, Y. Chujo, *Polym. Bull.* **1999**, *42*, 505–510.

[21] A. Lorbach, M. Bolte, H. Li, H.-W. Lerner, M. C. Holthausen, F. Jäkle, M. Wagner, *Angew. Chem. Int. Ed.* **2009**, *48*, 4584–4588; *Angew. Chem.* **2009**, *121*, 4654–4658.

[22] J. Chai, C. Wang, L. Jia, Y. Pang, M. Graham, S. Z. Cheng, *Synth. Met.* **2009**, *159*, 1443–1449.

[23] N. Matsumi, K. Naka, Y. Chujo, *J. Am. Chem. Soc.* **1998**, *120*, 10776–10777.

[24] N. Matsumi, T. Umeyama, Y. Chujo, *Polym. Bull.* **2000**, *44*, 431–436.

[25] a) A. Sundararaman, M. Victor, R. Varughese, F. Jäkle, *J. Am. Chem. Soc.* **2005**, *127*, 13748–13749; b) H. Li, F. Jäkle, *Angew. Chem. Int. Ed.* **2009**, *48*, 2313–2316; *Angew. Chem.* **2009**, *121*, 2349–2352; c) H. Li, F. Jäkle, *Macromol. Rapid Commun.* **2010**, *31*, 915–920.

[26] X. Yin, F. Guo, R. A. Lalancette, F. Jäkle, *Macromolecules* **2016**, *49*, 537–546.

[27] a) A. Lik, L. Fritze, L. Müller, H. Helten, *J. Am. Chem. Soc.* **2017**, *139*, 5692–5695; b) A. Lik, S. Jenthra, L. Fritze, L. Müller, K.-N. Truong, H. Helten, *Chem. Eur. J.* **2018**, *24*, 11961–11972.

[28] X. Yin, J. Chen, R. A. Lalancette, T. B. Marder, F. Jäkle, *Angew. Chem. Int. Ed.* **2014**, *53*, 9761–9765; *Angew. Chem.* **2014**, *126*, 9919–9923.

[29] C. Reus, F. Guo, A. John, M. Winhold, H.-W. Lerner, F. Jäkle, M. Wagner, *Macromolecules* **2014**, *47*, 3727–3735.

[30] Bonifácio, Vasco D. B., J. Morgado, U. Scherf, *J. Polym. Sci., Part A: Polym. Chem.* **2008**, *46*, 2878–2883.

[31] I. A. Adams, P. A. Rupar, *Macromol. Rapid Commun.* **2015**, *36*, 1336–1340.

[32] Stille cross-coupling was recently applied for the synthesis of electron acceptor-functionalized triarylboranes: X. Yin, K. Liu, Y. Ren, R. A. Lalancette, Y.-L. Loo, F. Jäkle, *Chem. Sci.* **2017**, *8*, 5497–5505.

[33] H. Helten, *Chem. Eur. J.* **2016**, *22*, 12972–12982.

[34] J. E. Mulvaney, J. J. Bloomfield, C. S. Marvel, *J. Polym. Sci.* **1962**, *62*, 59–72.

[35] I. Yamaguchi, T. Tominaga, M. Sato, *Polym. Int.* **2009**, *58*, 17–21.

[36] I. Yamaguchi, B.-J. Choi, T.-a. Koizumi, K. Kubota, T. Yamamoto, *Macromolecules* **2007**, *40*, 438–443.

[37] S. Hayashi, T. Koizumi, *Polym. Chem.* **2012**, *3*, 613–616.

[38] N. Matsumi, Y. Chujo, *Macromolecules* **1998**, *31*, 3802–3806.

[39] a) N. Matsumi, K. Kotera, K. Naka, Y. Chujo, *Macromolecules* **1998**, *31*, 3155–3157; b) N. Matsumi, K. Kotera, Y. Chujo, *Macromolecules* **2000**, *33*, 2801–2806.

[40] A. W. Baggett, F. Guo, B. Li, S.-Y. Liu, F. Jäkle, *Angew. Chem. Int. Ed.* **2015**, *54*, 11191–11195; *Angew. Chem.* **2015**, *127*, 11343–11347.

[41] a) X.-Y. Wang, H.-R. Lin, T. Lei, D.-C. Yang, F.-D. Zhuang, J.-Y. Wang, S.-C. Yuan, J. Pei, *Angew. Chem. Int. Ed.* **2013**, *52*, 3117–3120; *Angew. Chem.* **2013**, *125*, 3199–3202; b) X.-Y. Wang, F.-D. Zhuang, X. Zhou, D.-C. Yang, J.-Y. Wang, J. Pei, *J. Mater. Chem. C* **2014**, *2*, 8152–8161; c) X.-Y. Wang, F.-D. Zhuang, J.-Y. Wang, J. Pei, *Chem. Commun.* **2015**, *51*, 17532–17535.

[42] M. J. D. Bosdet, W. E. Piers, T. S. Sorensen, M. Parvez, *Angew. Chem. Int. Ed.* **2007**, *46*, 4940–4943; *Angew. Chem.* **2007**, *119*, 5028–5031.

[43] W. Zhang, G. Li, L. Xu, Y. Zhuo, W. Wan, N. Yan, G. He, *Chem. Sci.* **2018**, *9*, 4444–4450.

4 Results and Discussion

4.1 Dehydrocoupling and Silazane Cleavage Routes to Organic-Inorganic Hybrid Polymers with NBN Units

The following section is slightly modified and reproduced from published article[1] with permission from Wiley-VCH.

Despite the great potential of both π-conjugated organoboron polymers and BN-containing polycyclic aromatic hydrocarbons for application in organic optoelectronics, the knowledge about conjugated polymers having B–N bonds in their main chain is scarce. Herein, the first examples of a new class of organic–inorganic hybrid polymers are presented which are comprised of alternating NBN and para-phenylene units. Polycondensation with B–N bond formation provides facile access to soluble materials under mild conditions. Photophysical data for the polymer and for molecular model systems of different chain lengths revealed a low extent of π-conjugation across the NBN units, which is supported by DFT calculations. The applicability of the new polymers as macromolecular poly-ligands is demonstrated by a cross-linking reaction via Zr^{IV}.

4.1.1 Introduction

Boron-containing π-conjugated polymers and oligomers are currently attracting considerable attention owing to their great potential for application in organic electronics and optoelectronics, for example, in (polymer-based) organic light-emitting diodes (OLEDs/PLEDs), photovoltaics (OPV), and organic field-effect transistors (OFETs), or as sensory or imaging materials.[1] In such polymers which feature in the main chain tricoordinate boron atoms linked to organic π-systems (A, Scheme 4.1.1) the conjugation path may be extended via the vacant p_π orbital on boron.[2]

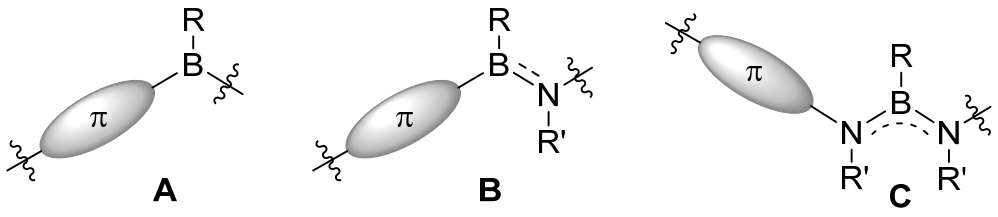

Scheme 4.1.1. Generalized structural units of boron-containing π-conjugated polymers or oligomers (π = organic π-system, R, R' = organic substituents).

[1] T. Lorenz, A. Lik, F. A. Plamper, H. Helten, *Angew. Chem. Int. Ed.* **2016**, *55*, 7236—7241; *Angew. Chem.* **2016**, *128*, 7352—7357.

The replacement of CC units by isoelectronic and isosteric BN units, primarily applied to mono- and polycyclic aromatic hydrocarbons (PAHs), has emerged as a viable strategy to produce novel organic–inorganic hybrid compounds, which show structural similarities to their all-carbon congeners, but in many cases fundamentally altered electronic properties.[3,4] This has led to molecular materials with intriguing properties such as BN-doped nanographenes.[3,4] Linear polymers with main chain B–N linkages involving tricoordinate boron centers (**B**, **C**), however, are relatively undeveloped.[5,6] Theoretical studies predict that (partial) substitution of CC by BN units in semiconducting organic polymers should result in an increase of the electronic band gap of the materials.[7–9] It has been proposed that this concept may be employed as an effective way of band gap tuning.[7b] Chujo and co-workers have devised a synthetic protocol that uses a haloboration–phenylboration polymerization sequence for the preparation of polymers of type **B** which feature acyl groups at nitrogen.[10a,c] For the polymers obtained, however, poorly extended conjugation was deduced from UV–vis absorption measurements. This was attributed to the presence of cross-links[10c] or the *meta*-phenylene linkages[1b] present in the polymer chains. Very recently, Liu, Jäkle, and co-workers reported the synthesis of 1,2-azaborine oligomers and a corresponding conjugated polymer, which may be regarded as a derivative of a cyclolinear version of type **B** polymer.[11] Poly(boronic carbamate)s,[10b] poly(boronic carbamoylchloride)s,[10a,c] and related copolymers, reported by Chujo and co-workers, to date are the only known examples of organoboron polymers that clearly fall into category **C**. The derivatives prepared have the NBN units[12] bridged by *meta*-phenylene groups. A few examples of conjugated polymers have been prepared comprising 1,3,2-benzodiazaboroline units. This building block was incorporated into polymer chains via either the benzo core[13] or via the benzo core and the boron center;[14] chain-linking through the N atoms has not been investigated, so far.

We are interested in the development of mild and environmentally benign methods for the construction of extended molecular architectures. Polymerization via B–N bond formation processes may provide an elegant access to B–N-containing macromolecules. The incorporation of diaminoborane functional groups appeared as an attractive target because its dianionic form, $[RB(NR')_2]^{2-}$, is a versatile bidentate ligand system.[15] Diaminoboryl units may also be coordinated to a metal via the boron atom.[16] Herein, we report on the exploration of two conceivable routes to poly[*N*-(*p*-phenylene)diimidoborane(3)]s (PPP-DIBs): dehydrocoupling[5,17,18] and silazane cleavage with Si/B exchange, the latter of which led to the first soluble derivatives of this class of polymers, which can function as macromolecular poly-ligands, as demonstrated by cross-linking via Zr^{IV}.

4.1.2 Results and Discussion

Manners and co-workers recently showed that aniline–borane (**1**) undergoes spontaneous dehydrocoupling with aniline (**2**) in solution at ambient temperature to selectively afford dianilinoborane (**3**, Scheme 4.1.2).[19] The phenyl rings of **3** adopt a largely coplanar arrangement with the N-B-N moiety in the solid state, thus pointing to potential extended π-conjugation across the NBN unit. We repeated the reported synthesis in order to obtain photophysical data for **3** (Table 4.1-1). The lowest-energy absorption in the UV–vis spectrum of **3** in CH_2Cl_2 showed a maximum at 272 nm. Fluorescence was detected at λ_{max} = 325 nm. We then targeted the synthesis of an extended molecular system having two diaminoborane units connected via a *para*-phenylene linkage.[20] Therefore, the bisborane adduct of *para*-phenylenediamine (**4**) was reacted with excess aniline, which afforded compound **5** in 82 % isolated yield. The UV–vis spectrum of **5** displayed an absorption band at λ_{max} = 290 nm. This bathochromic shift with respect to **3**, though being moderate, however, evidences some degree of extension of π-conjugation due to elongation of the chain length.

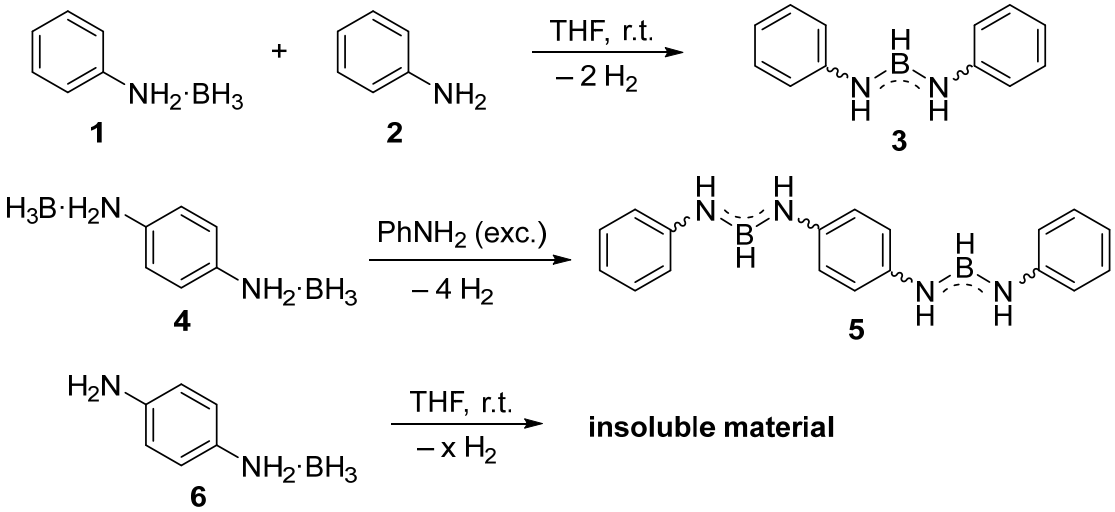

Scheme 4.1.2. Synthesis of **3**[19] and **5**, and attempted dehydropolymerization of **6**.

We anticipated that the monoborane adduct of *para*-phenylenediamine (**6**), which contains both a BH_3-coordinated and a free amino group within the same molecule, should undergo spontaneous dehydrocoupling with itself in the same manner. This would provide access to the parent derivative of a new class of organic–inorganic hybrid polymers featuring alternating *para*-phenylene and diaminoborane groups in the main chain: poly[*N*-(*p*-phenylene)diimidoborane(3)]s (PPP-DIBs). Upon treating **6** with THF it dissolved with vigorous bubbling, thus pointing to H_2 production. However, in the further course of the reaction the formation of a colorless precipitate was observed, and the product obtained after work-up was found to be insoluble in common organic solvents. The

insoluble product obtained was not further analyzed. Rigid conjugated polymers and oligomers, as it is assumed to be the case with the expected product, often show poor solubility if no solubilizing side groups are attached.

With a view to enhance the solubility of the target polymers, we decided to incorporate organic side groups through the introduction of substituents at boron. For this purpose, we found it more convenient to use a different strategy for B–N bond formation: silazane Si–N bond cleavage by chloroboranes. We chose 2,4,6-trimethylphenyl (mesityl, Mes) as the substituent at boron, and we first explored the feasibility of our approach in the synthesis of two molecular model compounds, i.e. **7** and **8** (Scheme 4.1.3).

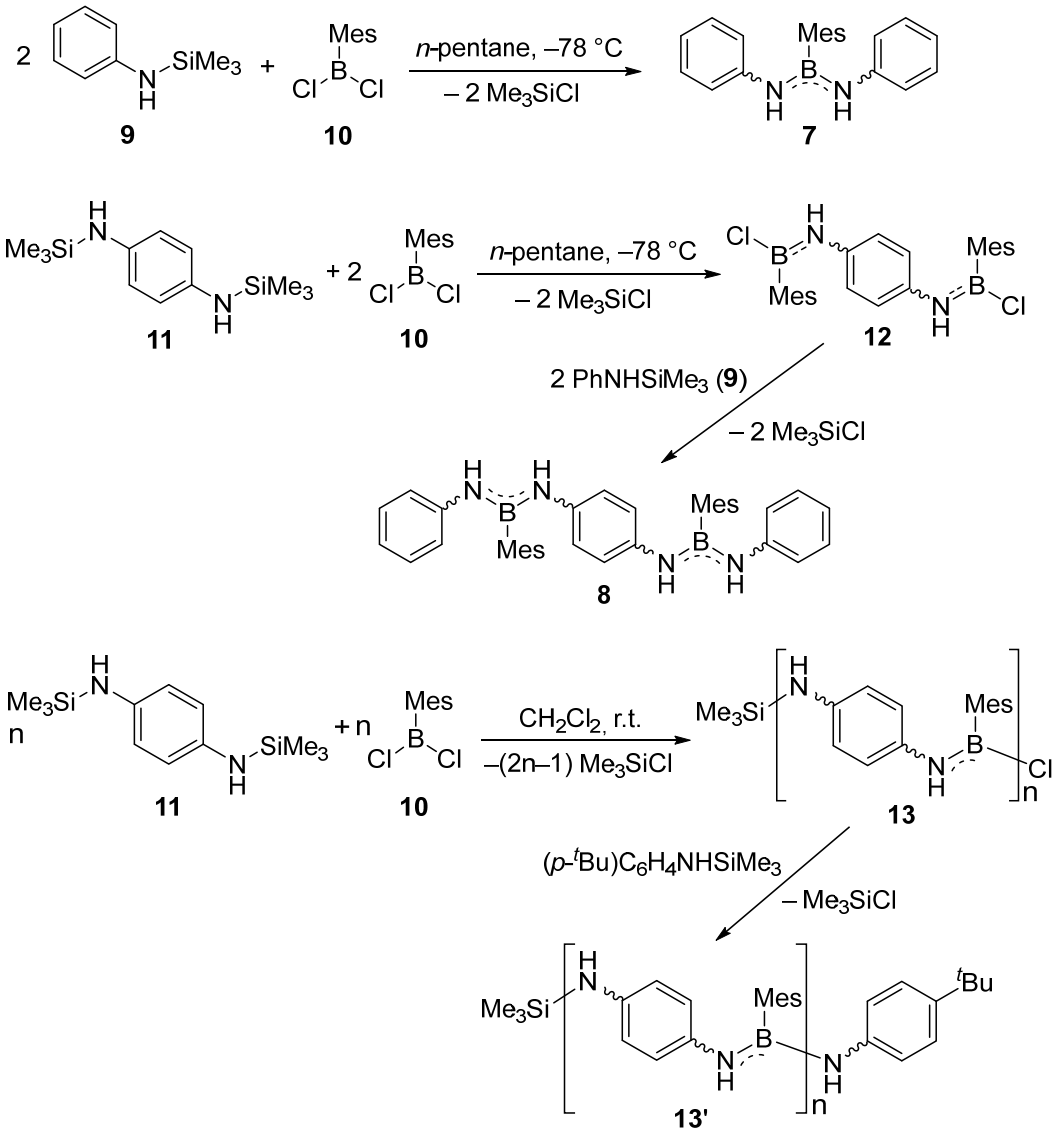

Scheme 4.1.3. Synthesis of **7**, **8**, and polymers **13** and **13'**.

Compound **7** was prepared by condensation 2 equiv. of *N*-trimethylsilylaniline (**9**) and dichloro(mesityl)borane (**10**). In the same manner, reaction of *N,N'*-bis(trimethylsilyl)-*para*-phenylenediamine (**11**) with 2 equiv. of **10** and subsequent reaction of the intermediate, **12**, with 2 equiv. of **9** afforded the extended system **8** having two diaminoborane building blocks. Both model compounds were isolated in excellent yields, 95 (**7**) and 92 % (**8**). Their identity was unambiguously ascertained by NMR spectroscopy and mass spectrometry; the molecular structure of **7** was determined by single-crystal X-ray diffractometry (Figure 4.1.1). In the solid state, compound **7** displays *E,Z* configuration, as observed in other structurally characterized *B,N,N'*-trisubstituted diaminoboranes.[21] While the *N*-phenyl substituent at the *E*-configured B1–N2 bond of **7** adopts a largely coplanar arrangement with the N–B–N plane (twist angle 3.8(3)°), the phenyl group at N1 is twisted out of that plane by 46.5(3)°.[2]

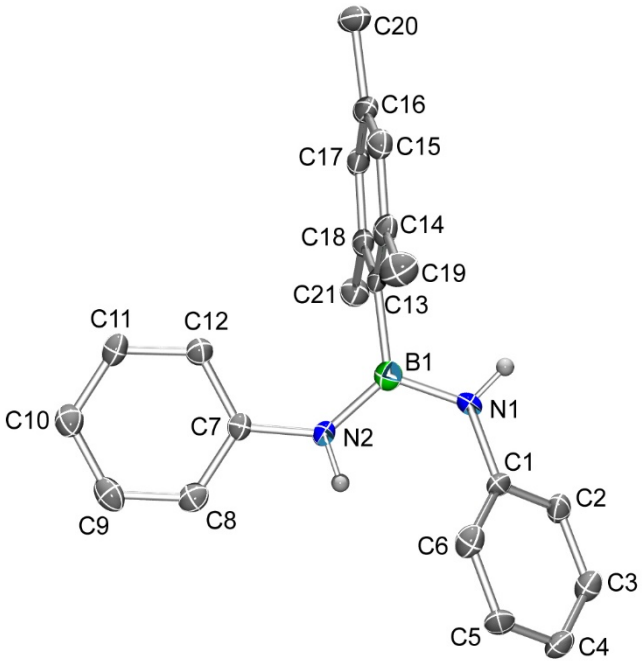

Figure 4.1.1. Molecular structure of **7** in the solid state with thermal ellipsoids at the 50% probability level (only one of two independent molecules with similar structural data shown; C-bonded hydrogen atoms omitted for clarity).

NMR spectroscopy provided evidence that the *E,Z* configuration persists in solution. In the ^{1}H NMR spectra of **7** the phenyl and the NH proton resonances showed dynamic line broadening. Upon lowering the temperature the signals split into two well-resolved resonance sets of equal intensity. An analysis of 2D ^{1}H COSY and NOESY spectra at –40 °C allowed to assign the resonances to the substituents at the *E*- and the *Z*-configured B–N bond, respectively. Analysis of ^{1}H NMR spectra

[2] The Ph / N-B-N twist angles of the other molecule of the asymmetric unit are 9.8(3) and 52.0(3)°.

obtained at varying temperatures revealed that the dynamic process is assigned to simultaneous rotation about both B–N bonds, thus equilibrating two degenerate states with interchanged configuration (*E,Z* ⇌ *Z,E*). The activation parameters for this process were estimated from an Eyring plot as $\Delta H^{\ddagger}$ = 60 kJ mol^{-1} and $\Delta S^{\ddagger}$ = –47 J mol^{-1} K^{-1} (Figure 4.1.5). Similar dynamic line broadening effects were also observed in the case of **8**. In the UV–vis spectra the lowest-energy absorption band was detected at λ_{max} = 267 nm (**7**) and 280 nm (**8**), respectively, which points to some degree of extension of the conjugation length with chain elongation. Both compounds showed fluorescence with a large Stokes shift (Table 4.1-1). Also for polymers featuring 1,3,2-benzodiazaboroline units unusually large Stokes shifts have been found, which was attributed to intramolecular charge transfer processes.[14b] Large Stokes shifts in aminoboranes have been attributed to the emission from twisted intramolecular charge transfer (TICT) states.[22]

Table 4.1-1. Photophysical data for **3**, **5**, **7**, **8**, and polymer **13'**, and calculated vertical singlet excitations for **3**, **5**, **7**, and **8** (by TD-DFT, B3LYP/6-31G(d,p)).

	3[a]	**5**[a]	**7**[b]	**8**[b]	**13'**[b]
$\lambda_{abs,max}$ / nm	272	290	267	280	295
$\lambda_{abs,TD\text{-}DFT}$ / nm	272	308	275	293	–
$\lambda_{em,max}$ / nm[c]	325	365	420	465	455

[a] In THF. [b] In CH_2Cl_2. [c] Irradiated at the absorption maxima.

With the aim to synthesize polymer **13**, compound **11** was reacted with **10** in 1:1 ratio in CH_2Cl_2 at ambient temperature (Scheme 4.1.3). An $^{11}B\{^1H\}$ NMR spectrum of the reaction mixture obtained after 15 min. revealed that **10** was already consumed, and a resonance at δ = 31 ppm indicated the formation of diaminoborane groups. Concomitant formation of the volatile condensation byproduct, Me_3SiCl, was evidenced by detection of its ^1H NMR resonance at δ = 0.45 ppm. After the mixture was stirred for 18 h at room temperature, 10 mol% of (*p*-^{t}Bu)$C_6H_4NHSiMe_3$ was added, in order to destroy the reactive B–Cl end groups of **13**. The product was purified by precipitation (successively twice) with *n*-pentane. This afforded the end-capped PPP-DIB **13'** as a white solid in 83% yield, which proved to be soluble in solvents of moderate polarity such as CH_2Cl_2, $CHCl_3$, and THF. The polymer was characterized by multinuclear NMR, UV–vis, and fluorescence spectroscopy, mass spectrometry, and in terms of molecular weight by gel permeation chromatography (GPC) and dynamic light scattering (DLS). The $^{11}B\{^1H\}$ NMR spectrum of **13'** in $CDCl_3$ displayed a broad resonance at δ = 31 ppm. Like the model systems **7** and **8**, the ^1H NMR spectrum of **13'** at 25 °C showed well-resolved mesityl resonances and broad signals for the phenylene and NH protons and

also for the $SiMe_3$ end groups. At –40 °C the signals decoalesced to give sets of multiple closely spaced peaks (Figure 7.1.17), likely due to the large number of possible relative configurations at the B–N bonds along the polymer chain. The ratio of integrals of the ^1H resonances of the $SiMe_3$ (δ = 0.00–0.30 ppm) and the *tert*-butyl end groups (δ = 1.31 ppm) was 1:1, which indicates quantitative end-capping. Despite prolonged exposure to a vacuum (ca. 10^{-2} mbar) residual *n*-pentane solvent was still detectable, which suggests that it is confined by the polymer chains.

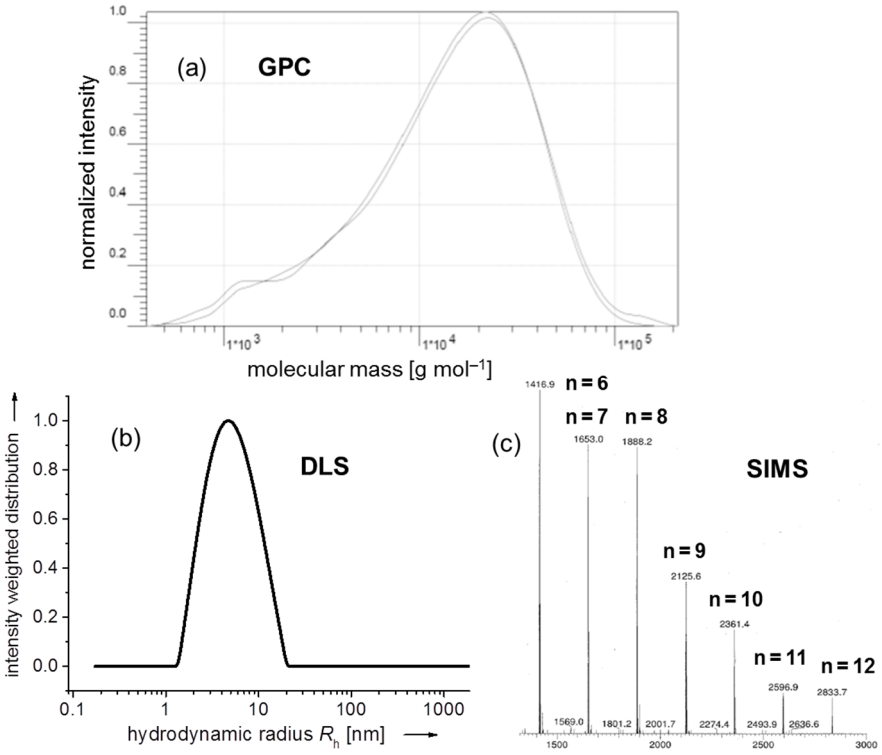

Figure 4.1.2. (a) Molecular mass distribution of **13'** by GPC (in THF, vs. polystyrene standards). (b) Intensity weighted size distribution of particles of **13'** in THF by DLS (θ = 90°). (c) SIMS spectrum of **13'**.

The macromolecular nature of **13'** was confirmed by GPC (Figure 4.1.2a). This revealed an average molecular mass of M_w = 20 400 Da and M_n = 7 900 Da, respectively, according to a number average degree of polymerization (DP_n) of 33, and a fairly large polydispersity index (PDI) of 2.6, typical of a polymer formed via a step-growth process. The GPC trace showed a tail with a shoulder pointing to the presence of a fraction of lower molecular mass species, which could not be separated by repeated precipitation. Evidence for the presence of macrocycles of 6–12 repeat units in the sample of **13'** was obtained from secondary ion mass spectrometry (SIMS, Figure 4.1.2c). This may also explain why the concentration of end groups estimated by ^1H NMR spectroscopy was actually lower than expected from the GPC-derived M_n value. Accurate ^1H NMR end group analysis was hampered by the above-mentioned line broadening caused by dynamic processes and, additionally, by an overlap of the proton resonances of the *t*-Bu end groups with those of residual *n*-pentane in the sample.

A rough estimate yielded $DP_n \approx 90$, which is, in view of the presence of cyclic molecular species, considered as an overestimation. DLS measurements revealed a hydrodynamic radius (R_h) of 5.1 nm for particles of **13'** in THF solution (Figure 4.1.2b). The lowest-energy absorption maximum in the UV–vis spectrum of **13**, $\lambda_{abs,max}$ = 295 nm, is slightly red-shifted with respect to that of the molecular model compounds, which evidences further extension of the conjugation length to some degree upon polymer formation. The fluorescence spectrum of **13** showed a maximum at 455 nm. In order to get more insight into the geometric and electronic structures of PPP-DIBs, DFT calculations[3] were carried out at the B3LYP/6-31+G(d,p) level of theory on the molecular model compounds **3**, **5**, **7**, and **8**. This revealed that the preferred diastereomer of **3** and **5**, respectively, displays *E*-configuration at each B–N unit. In both (*E,E*)-**3** and (*E*,*E*,*E*,*E*)-**5** the aromatic rings and the N-B-N planes adopt an almost perfectly coplanar arrangement (maximum twist angle: 0.19°). For compound **7** our calculations confirm the preference of the *E,Z* configuration, as observed in the crystal. For **8** we found three diastereomers of comparable free energy content, with differing configurations at every two adjacent B–N bonds. The wavelengths of the lowest-energy vertical singlet excitations of **3**, **5**, **7**, and **8** calculated by TD-DFT are in fairly good agreement with their experimental UV–vis absorption maxima (Table 1). The transitions correspond to HOMO → LUMO processes. In (*E*,*E*)-**3** and (*E*,*E*,*E*,*E*)-**5** these MOs are clearly identified as π orbitals, which are extended over the whole molecule (Figure 4.1.3 and Figure 7.1.42). It is furthermore noteworthy that the boron p_π orbitals show significant contribution to the LUMOs but not to the HOMOs of **3** and **5**. Therefore, the HOMO–LUMO transitions are unambiguously characterized as being of π–π* type, with some degree of charge transfer to boron. In compounds **7** and **8** a definite classification of molecular orbitals into σ- or π-type is not possible due to the deviation of the aromatic rings and the N-B-N units from coplanarity (Figure 4.1.3 and Figure 7.1.46–Figure 7.1.48). However, the frontier orbitals clearly show their largest contributions above and below the planes of the phenyl (and, in the case of **8**, the phenylene) rings and the N-B-N units, whereas the constituting nuclei are located in a nodal plane of the orbitals. Therefore, we conclude that a classification of these MOs as being of predominantly π-type is reasonable, and that the corresponding transitions should be characterized as π–π* excitations, despite the noted deviation from coplanarity.

[3] Calculations were performed using the Gaussian 09 suite of programs (Gaussian 09, Revision A.02, M. J. Frisch, et al., Gaussian, Inc., Wallingford CT, **2009**).

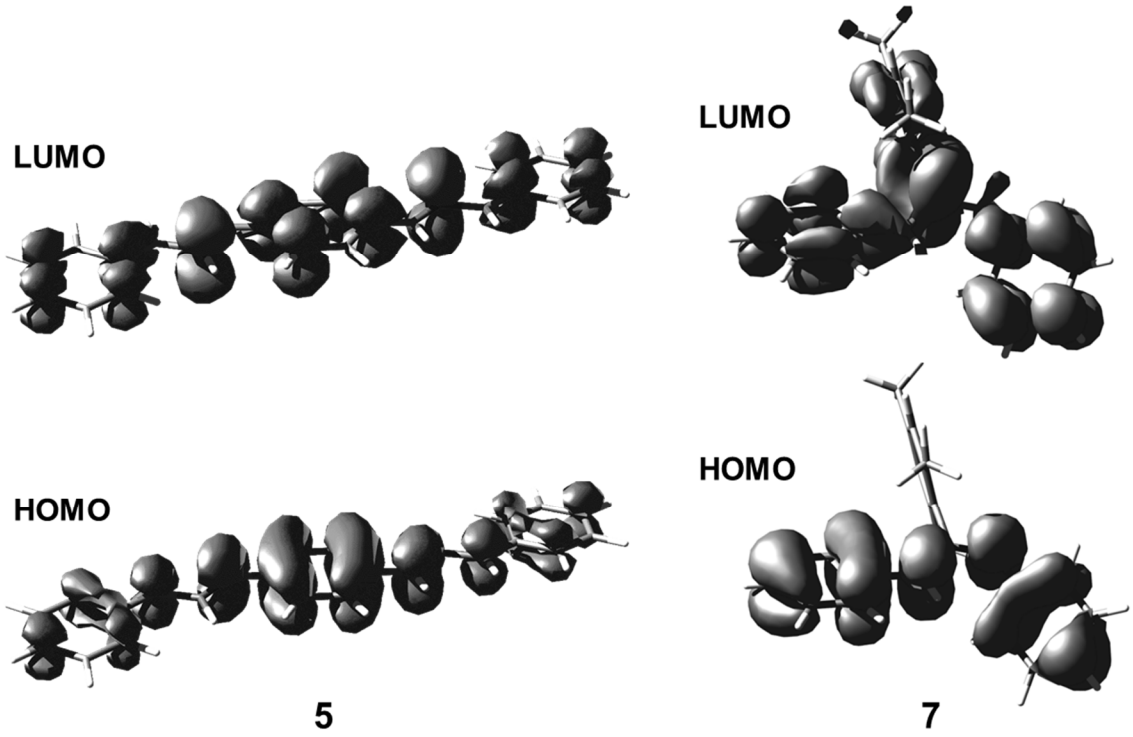

Figure 4.1.3. Calculated frontier orbitals (isovalue 0.022 a.u.) of **5** and **7**.

We then explored the potential of PPP-DIBs to function as macromolecular polyligand framework; we chose polymer **13'** and Zr^{IV} to proof the concept.[23] Heating of **13'** and substoichiometric amounts of $Zr(NMe_2)_4$ in the presence of THF in 1,2-dichlorobenzene at 120 °C yielded a yellow solid which is swollen by solvents (Figure 7.1.43), characteristic of a cross-linked polymer (Figure 4.1.4). The volatile by-product, Me_2NH, was separated by distillation during the reaction and was subsequently identified by ^1H NMR. The solid product obtained was characterized by FTIR spectroscopy. Analysis by NMR spectroscopy, however, was precluded by its insolubility in common organic solvents. Even with very low amounts of $Zr(NMe_2)_4$ (4 mol%) the product obtained was insoluble. Additionally, we carried out a model reaction using **7**, 0.5 equiv. of $Zr(NMe_2)_4$, and THF under conditions comparable to those used for the cross-linking of **13'**. By $^{11}B\{^1H\}$ NMR reaction monitoring a resonance at 37 ppm was detected (Appendix 7.1, Figure 7.1.20), which is 5–6 ppm downfield from the resonance of **7**. A downfield shift of the same magnitude (4.7 ppm) was observed by Manke and Nocera upon the formation of the related complex (^{t}BuN-B(Ph)-N^{t}Bu)$_2$Zr(THF).[23b] Therefore, **14** is given as a tentative structural proposal for the cross-linked material.

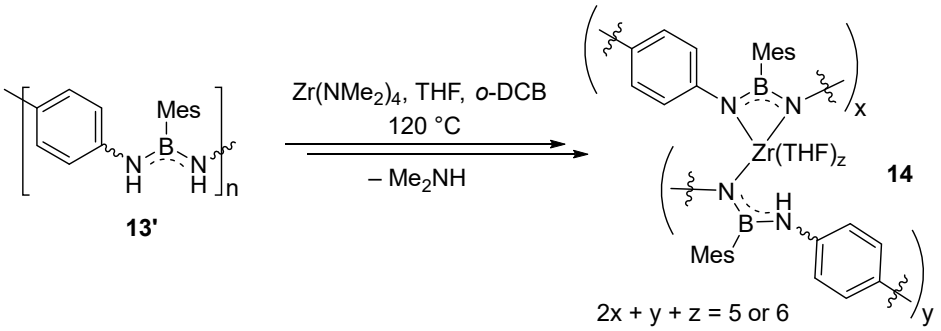

Figure 4.1.4. Cross-linking of **13'**.

4.1.3 Conclusion

In conclusion, the first derivatives of a new class of organic–inorganic hybrid polymers, poly[*N*-(*p*-phenylene)diimidoborane(3)]s (PPP-DIBs), **13** and **13'**, and a series of related model compounds have been prepared. Polycondensation with B–N bond formation through silazane cleavage with Si/B exchange was shown to proceed smoothly under mild conditions and provided facile access to soluble macromolecular materials. Comparison of the photophysical data for polymer **13'** and its molecular model systems revealed moderate π-conjugation across the NBN units with some degree of extension of the conjugation path with increasing chain length. DFT calculations provided deeper insight into this effect. The possibility of metal coordination by the polymer is expected to lead to broad applicability of the new materials.

4.1.4 Experimental Section

General procedures. All manipulations were performed under an atmosphere of dry argon using standard Schlenk techniques or in an MBraun glovebox. Solvents (dichloromethane, *n*-pentane, and tetrahydrofuran) were dried and degassed by means of an MBraun SPS-800 solvent purification system. Deuterated solvents for NMR spectroscopy were dried and degassed at reflux over Na (C_6D_6) or CaH_2 ($CDCl_3$ and DMSO-d_6) and freshly distilled prior to use. Tetrakis(dimethylamino)zirconium(IV), dimethylamine hydrochloride, borane dimethyl sulfide complex, and boron trichloride solution (1 M in hexanes) were commercially purchased and used as received. Triethylamine and *n*-hexane were dried and degassed at reflux over Na and freshly distilled prior to use. Aniline and 1,2-dichlorobenzene were dried and degassed by inert-gas distillation from CaH_2. 1,4-Phenylenediamine was recrystallized from THF. Compounds **1**,[24] **3**,[24] **9**,[25] **10a**,[26] **10b**,[27] **11**[28] and (*p*-^{t}Bu)$C_6H_4NHSiMe_3$[25] were prepared according to methods described in the literature. Borane complexes **4**[29] and **6**[29] were prepared by a procedure adapted from the synthesis of complex **1**.[24] NMR spectra were recorded at 25 °C on a Bruker AVANCE II-400 spectrometer or on a Bruker Advance III HD spectrometer operating at 400 MHz.

Chemical shifts were referenced to residual protic impurities in the solvent (^{1}H) or the deuterio solvent itself (^{13}C) and reported relative to external $SiMe_4$ (^{1}H, ^{13}C) or $BF_3{\cdot}OEt_2$ (^{11}B) standards. Mass spectra were obtained with the use of a Finnigan MAT95 spectrometer employing electron ionisation (EI) using a 70 eV electron impact ionisation source or secondary ionisation (SIMS). Elemental analysis was performed with a CHN-O-Rapid VarioEL by Heraeus. UV/VIS-spectra were obtained using a Jasco V-630 spectrophotometer. Fluorescence spectra were obtained with a Jasco FP-6500 spectrofluorometer (excited at the absorption maxima). Melting points (uncorrected) were obtained using a SMP3 melting point apparatus by Stuart in 0.5 mm (o.d.) glass capillaries, which were sealed under argon. GPC chromatograms were recorded on a Agilent 1100 Series, using a flow rate of 1 mL / min in THF at 25 °C, calibrated for polystyrene standards. Infrared spectra were recorded on KBr pellets with an Avatar 360 FTIR spectrometer from Nicolet.

Spectra. All spectra and other result figures are shown in Appendix 7.1.

Synthesis

Synthesis of 5. To neat aniline (**2**, 40 mL, 420 mmol) was added *p*-phenylenediamine–diborane (**4**, 200 mg, 1.47 mmol) in small portions at room temperature, which dissolved with vigorous bubbling. After the mixture was stirred for 17 h at ambient temperature, all volatiles were removed *in vacuo*. The crude product was washed with *n*-pentane (3 x 15 mL) and, subsequently, dried *in vacuo*, which gave **5** as a colorless solid. Yield: 380 mg (1.21 mmol, 82 %). m.p. 214 °C; ^{1}H NMR (400 MHz, DMSO-d_6): δ = 7.13–7.21 (m, 3H; Ar-CH), 6.95–7.05 (m, 4H; Ar-CH), 6.75–6.90 (m, 5 H; Ar-CH), 6.71 (br, 1H; NH), 6.58 (br, 1H; NH), 6.52–6.56 (m, 1H; Ar-CH), 6.45–6.50 (m, 1H; Ar-CH), 4.97 (br, 2H; NH), ppm; $^{11}B\{^{1}H\}$ NMR (128 MHz, DMSO-d_6): δ = 25.7 ppm (s); $^{13}C\{^{1}H\}$ NMR (101 MHz, DMSO-d_6): δ = 148.5 (s; Ar-C), 145.4 (s; Ar-C), 145.1 (s; Ar-C), 138.6 (s; Ar-C), 138.3 (s; Ar-C), 138.0 (s; Ar-C), 129.1 (s; Ar-CH), 128.1 (s; Ar-CH), 120.0 (s; Ar-CH), 119.7 (s; Ar-CH), 117.6 (br; Ar-CH), 116.7 (s; Ar-CH), 116.6 (s; Ar-CH), 115.7 (s; Ar-CH), 115.3 (br; Ar-CH), 113.9 ppm (s; Ar-CH); MS (EI, 70 eV): *m/z* (%) = 314.4 (M^+, 2), 211.3 ([M-PhNBH]$^+$, 4), 196.3 ([M-PhNHBHNH]$^+$, 100), 118.3 ([M-PhNHBHNHPh]$^+$, 10), 93.3 ($PhNH_2^+$, 91), 77.3 (Ph^+, 16); elem. anal. calcd (%) for $C_{18}H_{20}B_2N_4$: C 68.85, H 6.42, N 17.84, found: C 68.10, H 6.40, N 17.29; UV–vis (CH_2Cl_2): λ_{max} = 290 nm; fluorescence (CH_2Cl_2, λ_{ex} = 290 nm): λ_{max} = 365 nm.

Synthesis of 7. To a stirred solution of dichloro(mesityl)borane (**10**, 510 mg, 2.54 mmol) in *n*-pentane (5 mL) was added dropwise $PhNHSiMe_3$ (**9**, 839 mg, 5.08 mmol) at –78 °C. During the addition,

immediately a white suspension was formed. After 1 h at –78 °C the mixture was warmed to room temperature and stirred for further 2 h. All volatiles were removed *in vacuo*, and **7** was obtained as a colorless solid. Yield: 760 mg (2.42 mmol, 95 %), m.p. 95 °C; ^{1}H NMR (400 MHz, C_6D_6): δ = 6.40–7.15 (br, 10H; Ph-CH), 6.84 (s, 2H, Mes-CH), 5.83 (s, 1H; NH), 4.47 (s, 1H; NH), 2.35 (s, 6H; *o*-Mes-CH_3), 2.22 ppm (s, 3H; *p*-Mes-CH_3); ^{11}B{^{1}H} NMR (128 MHz, C_6D_6): δ = 31.4 ppm (s); ^{13}C{^{1}H} NMR (101 MHz, C_6D_6): δ = 144.8 (br s; *ipso*-Ph-C), 140.2 (s; *o*-Mes-C), 138.3 (s; *p*-Mes-C), 137.0 (br s; *ipso*-Mes-C), 129.8 (br; *m*-Ph-CH), 128.3 (s; *m*-Mes-CH), 122.1 (br; *o*-Ph), 119.3 (br; *p*-Ph), 22.3 (s; *o*-Mes-CH_3), 21.8 ppm (s; *p*-Mes-CH_3); MS (EI, 70 eV): *m/z* (%) = 314.1 (M^+, 78), 221.2 ([M–$PhNH_2$]$^+$, 46), 93.1 ($PhNH_2^+$, 100); elem. anal. calcd (%) for $C_{21}H_{23}BN_2$: C 80.27, H 7.38, N 8.91, found: C 79.59, H 7.37, N 8.85; UV–vis (CH_2Cl_2): λ_{max} = 267 nm (ε = 1.5·10^5 L cm^{-1} mol^{-1}); fluorescence (CH_2Cl_2, λ_{ex} = 267 nm): λ_{max} = 420 nm; IR (cm^{-1}): 3382 (s, ν(N-H)), 3369 (m, ν(N-H)), 3049 (w, ν(C-H-Ar)), 2914 (w, ν(C-H-Ar)), 1601 (m, ν(C-C-Ar)), 1591 (m, ν(C-C-Ar)), 1512 (s, ν(B-N)), 1497 (s, ν(B-N)), 1429 (m, ν(B-C-Ar)), 1319 (m, ν(C-N-Ar)).

^{1}H NMR (400 MHz, $CDCl_3$, *T* = –40°C): δ = 7.41 (t, *J* = 7.5 Hz; 2H; *m*-Ph*(Z)*, 7.19 (d, *J* = 7.3 Hz; 2H; *o*-Ph*(Z)*), 7.03–7.12 (m; 3H, *p*-Ph*(Z), m*-Ph*(E)*) 6.90 (s; 2H; Mes-Ar-H), 6.84 (t, *J* = 7.3 Hz; 1H; *p*-Ph*(E)*), 6.60 (d; *J* = 7.5 Hz; 2H; *o*-Ph*(E)*); 6.03 (s; 1H; NH(*E*)), 5.09 (s; 1H; NH(*Z*)) ppm.

^{1}H NMR (400 MHz, $CDCl_3$, *T* = 50°C): δ = 6.40–7.50 (m; 12H; Ar-H), 5.42 (br; 2H; NH) ppm.

Synthesis of 8. To a stirred solution of dichloro(mesityl)borane (**10**, 1.615 g, 8.04 mmol) in *n*-pentane (8 mL) was added dropwise a solution of **11** (1.015 g, 4.02 mmol) in *n*-pentane (16 mL) at –78°C. During the addition, immediately a white suspension was formed. After the mixture was stirred at –78 °C for 3 h, a solution of $PhNHSiMe_3$ (**9**, 1.329 mg, 8.04 mmol) in *n*-pentane (20 mL) was added dropwise. The mixture was warmed to room temperature within 14 h. Then all volatiles were removed *in vacuo*, and **8** was obtained as colorless solid. Yield: 2.030 g (3.69 mmol, 92 %). m.p. 74 °C; ^{1}H NMR (400 MHz, C_6D_6): δ = 6.05–7.15 (br, 14H; Ar-CH), 6.8 (s, 4H, Mes-CH), 5.72 (br, 2H; NH), 4.33 (br, 2H; NH), 2.34 (br, 12H; *o*-Mes-CH_3), 2.23 ppm (s, 6H; *p*-Mes-CH_3); ^{11}B{^{1}H} NMR (128 MHz, C_6D_6): δ = 31.4 ppm (s); ^{13}C{^{1}H} NMR (101 MHz, C_6D_6): δ = 145.2 (br; *ipso*-Ar-C), 144.6 (br; *ipso*-Ar-C), 140.2 (s; *o*-Mes-C), 138.1 (br; *p*-Mes-C), 137.1 (br; *ipso*-Mes), 129.7 (br; Ar-CH), 128.2 (s; *m*-Mes-CH), 124.2 (br; Ar-CH), 121.9 (br; Ar-CH), 120.3 (br; Ar-CH), 119.1 (br; Ar-CH), 22.4 (s; *o*-Mes-CH_3), 21.8 ppm (s; *p*-Mes-CH_3); MS (EI, 70 eV): *m/z* (%) = 550,2 (M^+, 3), 314.1 ([$(PhNH)_2BMes$]$^+$, 100), 195.1 ($(PhNH)_2B^+$, 18), 221.2 ([PhNBMes]$^+$, 65), 93.1 ($PhNH_2^+$, 18); UV–vis (CH_2Cl_2): λ_{max} = 280 nm (ε = 9.8 · 10^5 L cm^{-1} mol^{-1}); fluorescence (CH_2Cl_2, λ_{ex} = 280 nm): λ_{max}

= 465 nm; IR (cm^{-1}): 3383 (m, ν(N-H)), 2916 (w, ν(C-H-Ar)), 1603 (m, ν(C-C-Ar)), 1582 (m, ν(C-C-Ar)), 1497 (s, ν(B-N)), 1446 (m, ν(B-C-Ar)), 1303 (m, ν(C-N-Ar)).

Synthesis of 13'. The polymerisation was carried out in a glovebox and the glassware was treated with Me_3SiCl prior to use. To a stirred solution of **11** (506 mg, 2.00 mmol) in CH_2Cl_2 (4 mL) was added dichloro(mesityl)borane (**10**, 402 mg, 2.00 mmol) at r.t. and stirred for further 18 h. (*p*-^{t}Bu)$C_6H_4NHSiMe_3$ (44.0 mg, 0.20 mmol) was added and stirred for 2 h. Subsequently, the mixture was first precipitated into cooled (–40 °C) *n*-pentane (40 mL). The supernatant liquid was removed by filtration and the product was dried *in vacuo*. The product was further purified by a second precipitation into cooled (–78 °C) *n*-pentane (40 mL). The supernatant liquid was removed by filtration and the product was dried *in vacuo* to give **13'** as a white solid. Yield: 391 mg (83 %); ^{1}H NMR (400 MHz, $CDCl_3$): δ = 6.00–7.26 (br; 4H; phenylene-CH), 6.86 (s; 2H, Mes-CH), 5.62 (br; 1H; NH), 4.71 (br; 1H; NH), 3.56 (NH-end group). 3.32 (NH end group), 2.35 (br; 9H; *o*-/*p*-Mes-CH_3), 1.34 (s, ^{t}Bu-end group) 0.00–0.30 ppm (br; $Si(CH_3)_3$ end groups); $^{11}B\{^1H\}$ NMR (128 MHz, $CDCl_3$): δ = 31 ppm (s); $^{13}C\{^1H\}$ NMR (101 MHz, $CDCl_3$): δ = 139.8 (s; *ipso*-Ar-C). 137.5 (br; *p*-Mes-C), 136.3 (br; *o*-Mes-C), 127.2 (s; m-Mes-CH), 123,7 (br; Ar-H), 119.2 (br; Ar-CH), 21.8 (s; *o*-Mes-CH_3), 21.2 ppm (s; *p*-Mes-CH_3) ppm; *m/z* (%) = 2833.7 $[(C_6H_4NHBMesNH)_{12}]^+$, 10), 2596.9 $([(C_6H_4NHBMesNH)_{11}]^+$, 12), 2361.4 $([(C_6H_4NHBMesNH)_{10}]^+$, 30), 2125.6 $([(C_6H_4NHBMesNH)_9]^+$, 44), 1888.2 $([(C_6H_4NHBMesNH)_8]^+$, 83), 1653.0 $([(C_6H_4NHBMesNH)_7]^+$, 84), 416.9 $([(C_6H_4NHBMesNH)_6]^+$, 100), 1180.8 $([(C_6H_4NHBMesNH)_5]^+$, 5), 944.5 $([(C_6H_4NHBMesNH)_3]^+$, 3), 236.2 $([(C_6H_4NHBMesNH)_1]^+$, 53); UV–vis (CH_2Cl_2): λ_{max} = 295 nm (ε = $4.7 \cdot 10^3$ L cm^{-1} mol^{-1}); fluorescence (CH_2Cl_2, λ_{ex} = 295 nm): λ_{max} = 455 nm; IR (cm^{-1}): 3384 (m, ν(N-H)), 2916 (w, ν(C-H-Ar)), 2855 (w, ν(C-H-Ar)), 1610 (m, ν(C-C-Ar)), 1507 (s, ν(B-N)), 1448 (m, ν(B-C-Ar)), 1303 (m, ν(C-N-Ar)); GPC (THF, vs. polystyrene): M_n = 7900 Da; M_w = 20400 Da; DLS (THF): R_h = 5.1 nm.

Reaction of 7 with $Zr(NMe_2)_4$. To a stirred solution of **7** (47 mg, 0.15 mmol) in 1,2-dichlorobenzene (0.5 mL) and THF (12 mg) was added $Zr(NMe_2)_4$ (20 mg, 0.08 mmol) in 1,2-dichlorobenzene (0.4 mL) at room temperature. The colorless solution was stirred at 120 °C for 45 min. During heating a yellow solution was formed. An $^{11}B\{^1H\}$ NMR spectrum (128 MHz, $CDCl_3$) of the reaction mixture showed a broad resonance at δ = 37 ppm.

Cross-linking of 13'. To a stirred solution of **13'** (39 mg) in 1,2-dichlorobenzene (0.5 mL) and THF (12 mg) was added $Zr(NMe_2)_4$ (2 mg, 20 mg, or 40 mg) in 1,2-dichlorobenzene (0.4 mL) at room temperature. During the addition a yellow gel was formed (see Figure 7.1.41). The mixture was heated at 120 °C for 1 h during which volatile products passing the reflux condenser were condensed at –78 °C. The collected by-product was identified as Me_2NH by ^1H NMR spectroscopy in $CDCl_3$: δ = 2.42 (s; CH_3) (see Figure 7.1.22), which was confirmed by an independent synthesis of Me_2NH from $[Me_2NH_2]Cl$ and KOH in water, ^1H NMR ($CDCl_3$): δ = 1.28 (s, 1H; N*H*), 2.39 (s, 6H; C*H*$_3$) (see Figure S.23); IR (cm^{-1}): 3383 (m, ν(N-H)), 2914 (w, ν(C-H-Ar)), 1610 (m, ν(C-C-Ar)), 1505 (s, ν(B-N)), 1455 (m, ν(B-C-Ar)), 1300 (m, ν(C-N-Ar)).

X-ray crystallographic analysis of 7. Suitable colorless single crystals of **7** (2 $C_{21}H_{23}BN_2$, M = 628.48 g mol^{-1}) were obtained from a concentrated *n*-hexane solution upon decreasing the temperature from ambient temperature to +5 °C. Data were collected on a Bruker SMART APEX CCD detector on a D8 goniometer equipped with an Oxford Cryostream 700 temperature controller at 100(2) K using graphite monochromated Mo-K_α radiation (λ = 0.71073 Å). An absorption correction was carried out semi-empirically using SADABS[30] (min./max. transmissions = 0.6453). The structure was solved with Olex2[31] using Direct Methods (ShelXS[32a]) and refined with the ShelXL[32b] refinement package by full-matrix least squares on F^2. All non-hydrogen atoms were refined anisotropically. The hydrogen atoms were included isotropically and treated as riding. Crystal size 0.35 x 0.27 x 0.2 mm, orthorhombic, $P2_12_12$ (No. 18), a = 16.074(3), b = 20.326(4), c = 11.135(2) Å, V = 3637.9(11) $Å^3$, Z = 4, ρ_{calc} = 1.147 Mg · m^{-3}, 4.00° ≤ 2θ ≤ 53.14°, collected (independent) reflections = 33683 (7566), R_{int} = 0.1354, μ = 0.062 mm^{-1}, 439 refined parameters, 0 restraints, $R1$ (I > 2σ(I)) = 0.0625, $R1$ (all data) = 0.1036, $wR2$ (I > 2σ(I)) = 0.1294, $wR2$ (all data) = 0.1479, S = 1.025, max./min. residual electron density = 0.226/–0.226 e · $Å^{-3}$. CCDC-1443357 contains the supplementary crystallographic data for the structure of **7**. This data can be obtained free of charge from The Cambridge Crystallographic Data Centre via www.ccdc.cam.ac.uk/data_request/cif.

Dynamic light scattering (DLS) of 13'. The light scattering measurements on **13'** were performed in THF (c = 4 mg mL^{-1}) with an ALV 5000 E autocorrelator equipped with a red laser (λ = 633 nm). The time-resolved signal of two Single Photon Counting Modules (SPCM-CD 2969; Perkin Elmer) was cross-correlated. Hereby, the CONTIN analysis was performed in an angular dependent way. For each measurement (sampling time 90 s), the intensity-weighted decay-time τ distributions (as obtained from the field autocorrelation function obtained by use of the Siegert relation)[33] were

analyzed in respect to multimodality, where for each diffusive mode its (intensity-) average decay rate $\Gamma\,(1/\tau)$ was extracted (if necessary, the probability factor of the CONTIN algorithm was adjusted in order to increase resolution). Then, the decay rates were plotted against the squared length of the scattering vector q^2 (Figure 7.1.2). The slope gave the diffusion coefficient, D = (86294 ± 804) nm^2 ms^{-1}, and its value was transformed to the hydrodynamic radius R_h (5.1 nm) by the Stokes-Einstein equation.

Determination of the activation parameters for the interchange of configurations (*E,Z* ⇌ *Z,E*) in 7

The rate constants (k_c) at the temperatures for coalescence of the signals for the NH, the *ortho*-, the *meta*-, and the *para*-phenyl protons were calculated from equation (1).[34]

$$k_c = \frac{\pi \Delta \nu_0}{\sqrt{2}} \qquad (1)$$

The coalescence temperatures (T_c) were determined from the ^{1}H NMR spectra of **7** at variable temperature, and the no-exchange chemical shift differences ($\Delta\nu_0$) were obtained from a ^{1}H NMR spectrum recorded at –40 °C (Table 4.1-2). The activation parameters were subsequently obtained from an analysis of an Eyring plot of $\ln(k_c/T_c)$ against T_c^{-1} (Figure 4.1.5). Down to –60 °C no evidence was obtained for a hindered rotation about the C1–N1 or the C7–N2 bond.

Table 4.1-2. Coalescence temperatures (T_c), chemical shift differences ($\Delta\nu_0$), and rate constants (k_c) associated with the dynamic process in **7**.

	T_c / K	$\Delta\nu_0$ / Hz	k_c / s^{-1}
para-Ph-CH	298	107.92	239.74
meta-Ph-CH	303	134.83	299.52
ortho-Ph-CH	313	236.29	524.90
NH	318	374.69	832.35

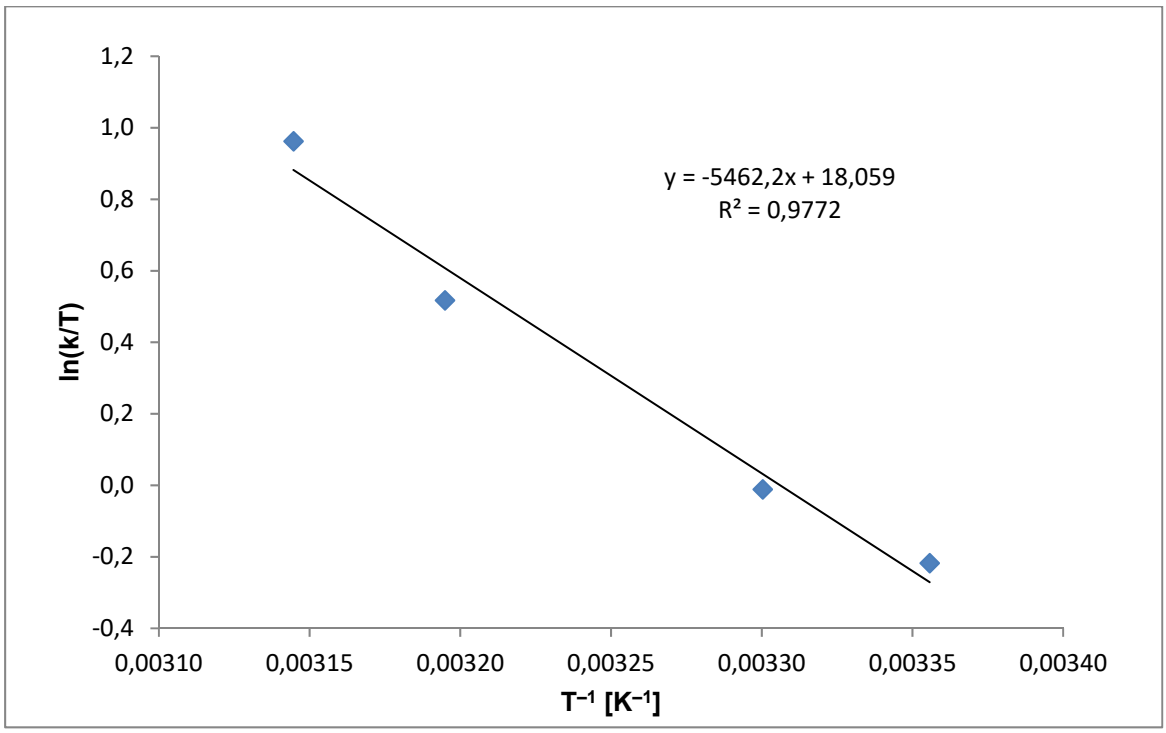

Figure 4.1.5. Eyring plot of ln(k_c/T_c) against T_c^{-1} for the configuration interchange of **7**.

Computational Information

Computational methods. DFT calculations were carried out with the Gaussian 09 program package.[35] Optimizations were performed with Becke's Three Parameter Hybrid Functional Becke3 (B3)[36] in combination with the gradient corrected correlation functional by Lee, Yang, and Parr (LYP),[37] and the valence-double-ζ basis set 6-31G(d,p).[38] All stationary points were characterized as minima by analytical vibrational frequency calculations (NImag = 0). Vertical singlet excitations were calculated by means of Time-dependent DFT[39] using the same density functional–basis set combination as specified above.

Computational results. We optimized several diastereomeric forms of **3**, **5**, **7**, and **8**, shown in Figure 4.1.6 – Figure 4.1.9, which differ in their configurations at the partial B–N double bonds. For compound **3** all three possible *E/Z*-isomers were computed (Figure 4.1.6). This revealed that (*E,E*)-**3** – i.e., the isomer which has been found in the solid state structure[1] – is also expected to be the thermodynamically most stable form of **3** in the gas phase. The favored diastereomer of **5** is predicted to feature *E* configuration at each B–N bond as well (Figure 4.1.7). Additionally, three isomers were calculated with differing configurations at each adjacent B–N bonds (involving the same B atom), as such arrangements have been found to be the most stable forms of the *B*-mesityl substituted compounds **7** and **8** (*vide infra*). However, in the case of **5**, the isomer (*E*,*E*,*E*,*E*)-**5** was clearly

preferred. In both (*E,E*)-**3** and (*E*,*E*,*E*,*E*)-**5** the aromatic rings and the N-B-N units are almost perfectly coplanar (maximum twist angle: 0.19°). For compound **7**, the calculations confirmed the preference of the *E,Z* configuration (Figure 4.1.8), consistent with the result of our crystallographic study. While the phenyl ring at the *E*-configured B–N bond of (*E,Z*)-**7** is twisted out of the N-B-N plane by 20.56°, the other phenyl group is twisted out of that plane by 36.75°. Due to the definite preference of the *E,Z* configuration in **7**, in the case of **8** only such isomers were considered that have differing configurations at every two adjacent B–N bonds, i.e. (*E*,*Z*,*Z*,*E*)-**8**, (*E*,*Z*,*E*,*Z*)-**8**, and (*Z*,*E*,*E*,*Z*)-**8** (Figure 4.1.9). The differences in calculated free energies between these diastereomers are rather small; the lowest value was obtained for (*E*,*Z*,*Z*,*E*)-**8**.

Vertical singlet excitations were calculated via TD-DFT for the most stable isomer of **3**, **5**, and **7**, respectively, as well as for the three optimized isomeric forms of **8**. For each compound the excitation wavelength of the lowest-energy absorption having an oscillator strength $f \geq 0.1000$ is given in Figure 7.1.42–Figure 7.1.48, together with the orbitals that are relevant for the respective transition. In each case this was the first excitation, corresponding to a HOMO → LUMO process, except for (*E*,*Z*,*Z*,*E*)-**8**, in which case it was the second lowest-energy excitation, to which two acceptor orbitals contribute in 60 and 34 % ratio, respectively (Figure 7.1.46).

In both (*E*,*E*)-**3** and (*E*,*E*,*E*,*E*)-**5** the respective HOMO and LUMO are unambiguously characterized as π orbitals, which are extended over the whole molecule (Figure 7.1.42 and Figure 7.1.43). It is furthermore noteworthy that the boron p_π orbitals show significant contributions to the LUMOs but not to the HOMOs. Therefore, in both cases the HOMO–LUMO transitions are unambiguously characterized as being of π–π* type, with some degree of charge transfer to boron. In compounds **7** and **8**, a definite classification of molecular orbitals as σ- or π-type is not possible due to the lack of a mirror plane resulting from the deviation of the aromatic rings and the N-B-N units from coplanarity. However, the orbitals relevant for the calculated excitations clearly show their largest contributions (lobes) above and below the planes of the phenyl (and, in the case of **8**, the phenylene) rings and the N-B-N units, whereas the constituting nuclei appear to situate in a nodal plane of the orbitals. Therefore, we conclude that a classification of these MOs as being of predominantly π-type is reasonable, and that the corresponding transitions should be characterized as π–π* transitions. Furthermore, all relevant orbitals are largely extended over the N-B-N, the phenyl and, in **8**, the phenylene units. The LUMO and the LUMO+1 of (*E*,*Z*,*Z*,*E*)-**8** show some extent of localization at the phenylene group (Figure 7.1.46), and in (*E*,*Z*,*E*,*Z*)-**8** one of the phenyl groups (on the right hand side, Figure 7.1.47) shows less significant contribution. The LUMO of (*E*,*Z*)-**7** displays an additional contribution of the mesityl group.

Because of the noted deviation of the calculated gas phase structure of (*E*,*Z*)-**7** and its molecular structure in the solid state with respect to the twist angles between the N-B-N unit and the phenyl groups, the influence of the degree of a phenyl rotation was further investigated. Therefore, a further calculation was performed, in which the torsion angle of the phenyl ring at the *Z*-configured B–N bond with respect to the N-B-N plane was adopted from the crystal structure (44.50°) and frozen during geometry optimization, while all other coordinates were allowed to relax (Figure 7.1.45). Actually, applying this constraint did not cause a significant qualitative effect on the shape of the frontier orbitals of (*E*,*Z*)-**7**. Regarding the lowest-energy absorption, the enforced torsion was associated with a slight decrease of the excitation wavelength as well as the oscillator strength (cf. Figure 7.1.44 and Figure 7.1.45).

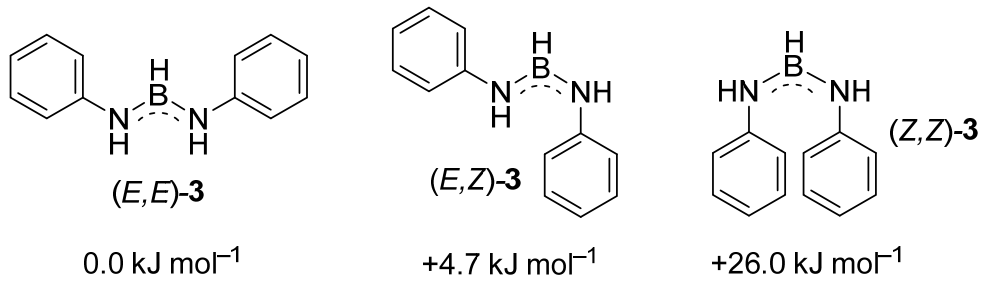

Figure 4.1.6. Calculated diastereomeric forms of **3**, and relative free energies (ΔG_{298}). The free energy of the most stable isomer was arbitrarily chosen as the reference.

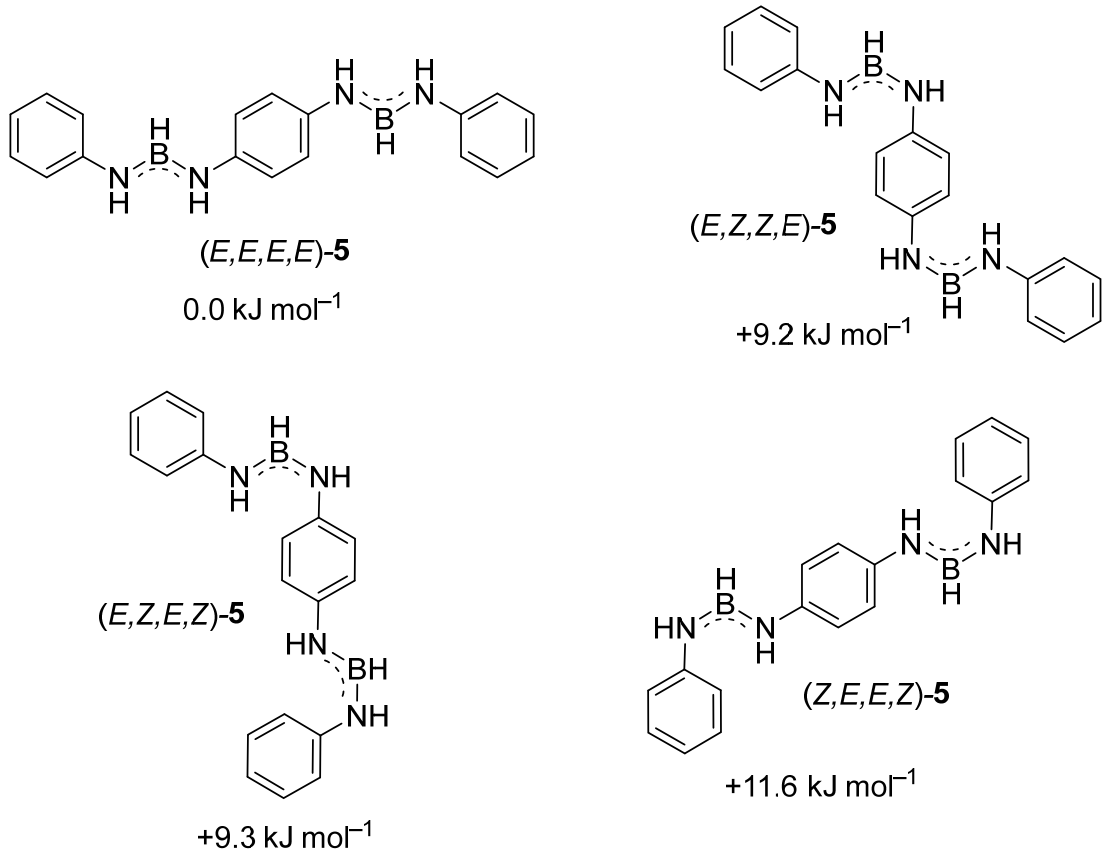

Figure 4.1.7. Calculated diastereomeric forms of **5**, and relative free energies (ΔG_{298}). The free energy of the most stable isomer was arbitrarily chosen as the reference.

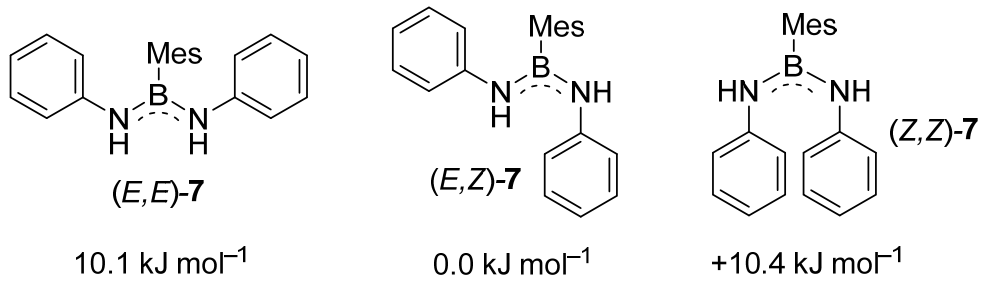

Figure 4.1.8. Calculated diastereomeric forms of **7**, and relative free energies (ΔG_{298}). The free energy of the most stable isomer was arbitrarily chosen as the reference.

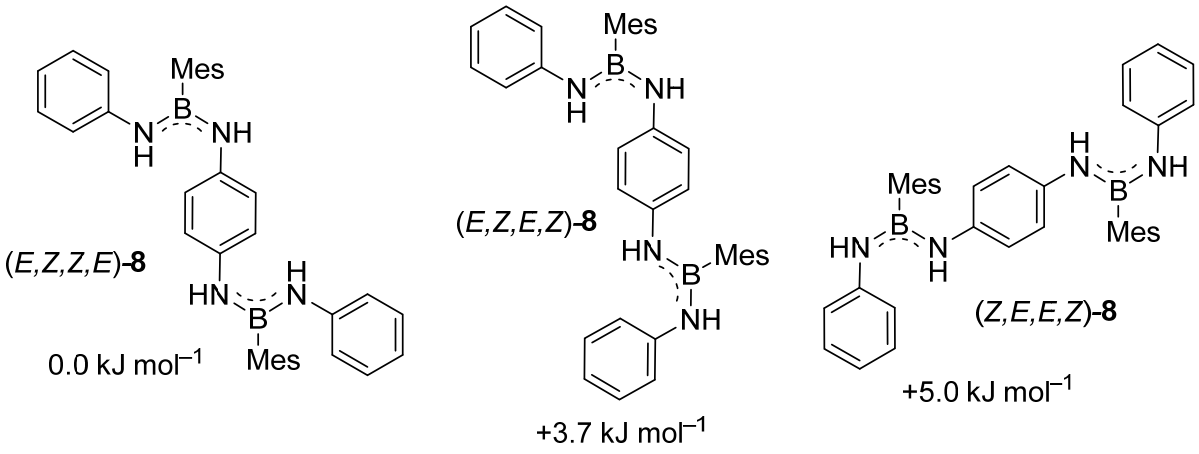

Figure 4.1.9. Calculated diastereomeric forms of **8**, and relative free energies (ΔG_{298}). The free energy of the most stable isomer was arbitrarily chosen as the reference.

4.1.5 References

[1] a) C. D. Entwistle, T. B. Marder, *Angew. Chem. Int. Ed.* **2002**, *41*, 2927–2931; *Angew. Chem.* **2002**, *114*, 3051–3056; b) F. Jäkle, *Chem. Rev.* **2010**, *110*, 3985–4022; c) K. Tanaka, Y. Chujo, *Macromol. Rapid Commun.* **2012**, *33*, 1235–1255; d) F. Jäkle, *Top. Organomet. Chem.* **2015**, *49*, 297–325.

[2] Selected examples: a) N. Matsumi, K. Naka, Y. Chujo, *J. Am. Chem. Soc.* **1998**, *120*, 5112–5113; b) A. Sundararaman, M. Victor, R. Varughese, F. Jäkle, *J. Am. Chem. Soc.* **2005**, *127*, 13748–13749; c) V. D. B. Bonifácio, J. Morgado, U. Scherf, *J. Polym. Sci., Part A: Polym. Chem.* **2008**, *46*, 2878–2883; d) A. Lorbach, M. Bolte, H. Li, H.-W. Lerner, M. C. Holthausen, F. Jäkle, M. Wagner, *Angew. Chem. Int. Ed.* **2009**, *48*, 4584–4588; *Angew. Chem.* **2009**, *121*, 4654–4658; e) A. Nagai, T. Murakami, Y. Nagata, K. Kokado, Y. Chujo, *Macromolecules* **2009**, *42*, 7217–7220; f) C. Reus, F. Guo, A. John, M. Winhold, H.-W. Lerner, F. Jäkle, M. Wagner, *Macromolecules* **2014**, *47*, 3727–3735; g) X. Yin, J. Chen, R. A. Lalancette, T. B. Marder, F. Jäkle, *Angew. Chem. Int. Ed.* **2014**, *53*, 9761–9765; *Angew. Chem.* **2014**, *126*, 9919–9923; h) I. A. Adams, P. A. Rupar, *Macromol. Rapid Commun.* **2015**, *36*, 1336–1340; i) X. Yin, F. Guo, R. A. Lalancette, F. Jäkle, *Macromolecules* **2016**, *49*, 537–546.

[3] a) Z. Liu, T. B. Marder, *Angew. Chem. Int. Ed.* **2008**, *47*, 242–244; *Angew. Chem.* **2008**, *120*, 248–250; b) M. J. D. Bosdet, W. E. Piers, *Can. J. Chem.* **2009**, *87*, 8–29; c) P. G. Campbell, A. J. V. Marwitz, S.-Y. Liu, *Angew. Chem. Int. Ed.* **2012**, *51*, 6074–6092; *Angew. Chem.* **2012**, *124*, 6178–6197; d) X.-Y. Wang, J.-Y. Wang, J. Pei, *Chem. Eur. J.* **2015**, *21*, 3528–3539.

[4] Selected examples: a) M. J. D. Bosdet, W. E. Piers, T. S. Sorensen, M. Parvez, *Angew. Chem. Int. Ed.* **2007**, *46*, 4940–4943; *Angew. Chem.* **2007**, *119*, 5028–5031; b) T. Hatakeyama, S. Hashimoto, S. Seki, M. Nakamura, *J. Am. Chem. Soc.* **2011**, *133*, 18614–18617; c) S. Xu, L. N. Zakharov, S.-Y. Liu, *J. Am. Chem. Soc.* **2011**, *133*, 20152–20155; d) H. Braunschweig, A. Damme, J. O. C. Jimenez-Halla, B. Pfaffinger, K. Radacki, J. Wolf, *Angew. Chem. Int. Ed.* **2012**, *51*, 10034–10037; *Angew. Chem.* **2012**, *124*, 10177–10180; e) B. Neue, J. F. Araneda, W. E. Piers, M. Parvez, *Angew. Chem. Int. Ed.* **2013**, *52*, 9966–9969; *Angew. Chem.* **2013**, *125*, 10150–10153; f) X. Wang, F. Zhang, J. Liu, R. Tang, Y. Fu, D. Wu, Q. Xu, X. Zhuang, G. He, X. Feng, *Org. Lett.* **2013**, *15*, 5714–5717; g) H. Braunschweig, K. Geetharani, J. O. C. Jimenez-Halla, M. Schäfer, *Angew. Chem. Int. Ed.* **2014**, *53*, 3500–3504; *Angew. Chem.* **2014**, *126*, 3568–3572; h) H. Braunschweig, C. Hörl, L. Mailänder, K. Radacki, J. Wahler, *Chem. Eur. J.* **2014**, *20*, 9858–9861; i) S. A. Couchman, T. K. Thompson, D. J. D. Wilson, J. L. Dutton, C. D. Martin, *Chem. Commun.* **2014**, *50*, 11724–11726; j) M. Müller, C. Maichle-Mössmer, H. F. Bettinger, *Angew. Chem. Int. Ed.* **2014**, *53*, 9380–9383; *Angew. Chem.* **2014**, *126*, 9534–9537; k) H. Braunschweig, M. A. Celik, F. Hupp, I. Krummenacher, L. Mailänder, *Angew. Chem. Int. Ed.* **2015**, *54*, 6347–6351; *Angew. Chem.* **2015**, *127*, 6445–6449; l) X.-Y. Wang, A. Narita, X. Feng, K. Müllen, *J. Am. Chem. Soc.* **2015**, *137*, 7668–7671; m) X.-Y. Wang, F.-D. Zhuang, X.-C. Wang, X.-Y. Cao, J.-Y. Wang, J. Pei, *Chem. Commun.* **2015**, *51*, 4368–4371.

[5] For (non-conjugated) polymers having exclusively B–N units in the main chain see: a) R. Komm, R. A. Geanangel, R. Liepins, *Inorg. Chem.* **1983**, *22*, 1684–1686; b) A. Staubitz, A. Presa Soto, I. Manners, *Angew. Chem. Int. Ed.* **2008**, *47*, 6212–6215; *Angew. Chem.* **2008**, *120*, 6308–6311; c) A. Staubitz, M. E. Sloan, A. P. M. Robertson, A. Friedrich, S. Schneider, P. J. Gates, J. Schmedt auf der Günne, I. Manners, *J. Am. Chem. Soc.* **2010**, *132*, 13332–13345; d) W. C. Ewing, A. Marchione, D. W. Himmelberger, P. J. Carroll, L. G. Sneddon, *J. Am. Chem. Soc.* **2011**, *133*, 17093–17099; e) A. P. M. Robertson, E. M. Leitao, T. Jurca, M. F. Haddow, H. Helten, G. C. Lloyd-Jones, I. Manners, *J. Am. Chem. Soc.* **2013**, *135*, 12670–12683; f) A. N. Marziale, A. Friedrich, I. Klopsch, M. Drees, V. R. Celinski, J. Schmedt auf der Günne, S. Schneider, *J. Am. Chem. Soc.* **2013**, *135*, 13342–13355; g) H. C. Johnson, E. M. Leitao, G. R. Whittell, I. Manners, G. C. Lloyd-Jones, A. S. Weller, *J. Am. Chem. Soc.* **2014**, *136*, 9078–9093.

[6] For polyboramines used for transfer hydrogenation, see: A. Ledoux, P. Larini, C. Boisson, V. Monteil, J. Raynaud, E. Lacôte, *Angew. Chem. Int. Ed.* **2015**, *54*, 15744–15749; *Angew. Chem.* **2015**, *127*, 15970–15975.

[7] a) A. Abdurahman, M. Albrecht, A. Shukla, M. Dolg, *J. Chem. Phys.* **1999**, *110*, 8819–8824; b) M. Côté, P. D. Haynes, C. Molteni, *Phys. Rev. B* **2001**, *63*, 125207.

[8] The degree of aromaticity of borazine is still a topic of debate. See, e.g.: a) R. Islas, E. Chamorro, J. Robles, T. Heine, J. C. Santos, G. Merino, *Struct. Chem.* **2007**, *18*, 833–839; b) D. E. Bean, P. W. Fowler, *J. Phys. Chem. A* **2011**, *115*, 13649–13656; c) W. Wu, X. Li, L. Meng, S. Zheng, Y. Zeng, *J. Phys. Chem. A* **2015**, *119*, 2091–2097.

[9] For investigations on the aromaticity of the 1,2-azaborine system see: P. G. Campbell, E. R. Abbey, D. Neiner, D. J. Grant, D. A. Dixon, S.-Y. Liu, *J. Am. Chem. Soc.* **2010**, *132*, 18048–18050.

[10] a) N. Matsumi, K. Kotera, K. Naka, Y. Chujo, *Macromolecules* **1998**, *31*, 3155–3157; b) N. Matsumi, Y. Chujo, *Macromolecules* **1998**, *31*, 3802–3806; c) N. Matsumi, K. Kotera, Y. Chujo, *Macromolecules* **2000**, *33*, 2801–2806.

[11] A. W. Baggett, F. Guo, B. Li, S.-Y. Liu, F. Jäkle, *Angew. Chem. Int. Ed.* **2015**, *54*, 11191–11195; *Angew. Chem.* **2015**, *127*, 11343–11347.

[12] For molecular optoelectronic materials featuring NBN units, see, e.g.: a) T. Riehm, G. de Paoli, H. Wadepohl, L. de Cola, L. H. Gade, *Chem. Commun.* **2008**, 5348–5350; b) J.-i. Nishida, T. Fujita, Y. Fujisaki, S. Tokito, Y. Yamashita, *J. Mater. Chem.* **2011**, *21*, 16442–16447; c) E. R. Abbey, S.-Y. Liu, *Org. Biomol. Chem.* **2013**, *11*, 2060–2069.

[13] a) I. Yamaguchi, B.-J. Choi, T.-a. Koizumi, K. Kubota, T. Yamamoto, *Macromolecules* **2007**, *40*, 438–443; b) S. Hayashi, T. Koizumi, *Polym. Chem.* **2012**, *3*, 613–616; c) J. H. Son, G. Jang, T. S. Lee, *Polymer* **2013**, *54*, 3542–3547.

[14] a) J. E. Mulvaney, J. J. Bloomfield, C. S. Marvel, *J. Polym. Sci.* **1962**, *62*, 59–72; b) I. Yamaguchi, T. Tominaga, M. Sato, *Polym. Int.* **2009**, *58*, 17–21.

[15] a) C. Fedorchuk, M. Copsey, T. Chivers, *Coord. Chem. Rev.* **2007**, *251*, 897–924; b) S. Harder, D. Naglav, *Eur. J. Inorg. Chem.* **2010**, 2836–2840.

[16] a) H. Braunschweig, C. Kollann, D. Rais, *Angew. Chem. Int. Ed.* **2006**, *45*, 5254–5274; *Angew. Chem.* **2006**, *118*, 5380–5400; b) L. Dang, Z. Lin, T. B. Marder, *Chem. Commun.* **2009**, 3987–3995; c) H. Braunschweig, R. D. Dewhurst, A. Schneider, *Chem. Rev.* **2010**, *110*, 3924–3957; d) M. Asay, C. Jones, M. Driess, *Chem. Rev.* **2011**, *111*, 354–396.

[17] a) A. Staubitz, A. P. M. Robertson, I. Manners, *Chem. Rev.* **2010**, *110*, 4079–4124; b) H. C. Johnson, T. N. Hooper, A. S. Weller, *Top. Organomet. Chem.* **2015**, 49, 153–220.

[18] Selected examples: a) C. A. Jaska, K. Temple, A. J. Lough, I. Manners, *J. Am. Chem. Soc.* **2003**, *125*, 9424–9434; b) M. E. Bluhm, M. G. Bradley, R. Butterick, U. Kusari, L. G. Sneddon, *J. Am. Chem. Soc.* **2006**, *128*, 7748–7749; c) M. Käß, A. Friedrich, M. Drees, S. Schneider, *Angew. Chem. Int. Ed.* **2009**, *48*, 905–907; *Angew. Chem.* **2009**, *121*, 922–924; d) A. B. Chaplin, A. S. Weller, *Angew. Chem. Int. Ed.* **2010**, *49*, 581–584; *Angew. Chem.* **2010**, *122*, 591–594; e) W. R. H. Wright, E. R. Berkeley, L. R. Alden, R. T. Baker, L. G. Sneddon, *Chem. Commun.* **2011**, *47*, 3177–3179; f) E. M. Leitao, N. E. Stubbs, A. P. M. Robertson, H. Helten, R. J. Cox, G. C. Lloyd-Jones, I. Manners, *J. Am. Chem. Soc.* **2012**, *134*, 16805–16816; g) L. J. Sewell, G. C. Lloyd-Jones, A. S. Weller, *J. Am. Chem. Soc.* **2012**, *134*, 3598–3610; h) P. Cui, T. P. Spaniol, L. Maron, J. Okuda, *Chem. Eur. J.* **2013**, *19*, 13437–13444; i) H. Helten, B. Dutta, J. R. Vance, M. E. Sloan, M. F. Haddow, S. Sproules, D. Collison, G. R. Whittell, G. C. Lloyd-Jones, I. Manners, *Angew. Chem. Int. Ed.* **2013**, *52*, 437–440; *Angew. Chem.* **2013**, *125*, 455–458; j) G. Chen, L. N. Zakharov, M. E. Bowden, A. J. Karkamkar, S. M. Whittemore, E. B. Garner, T. C. Mikulas, D. A. Dixon, T. Autrey, S.-Y. Liu, *J. Am. Chem. Soc.* **2015**, *137*, 134–137.

[19] H. Helten, A. P. M. Robertson, A. Staubitz, J. R. Vance, M. F. Haddow, I. Manners, *Chem. Eur. J.* **2012**, *18*, 4665–4680.

[20] For a dinuclear bis(diaminoboryl) complex bridged by a *para*-phenylene group, see: H. Braunschweig, T. Kupfer, K. Radacki, A. Schneider, F. Seeler, K. Uttinger, H. Wu, *J. Am. Chem. Soc.* **2008**, *130*, 7974–7983.

[21] a) N. Niederprüm, R. Boese, G. Schmid, *Z. Naturforsch. B* **1991**, *46*, 84–96; b) T. Chivers, C. Fedorchuk, M. Parvez, *Inorg. Chem.* **2004**, *43*, 2643–2653; c) M. L. Buil, M. A. Esteruelas, K. Garcés, E. Oñate, *J. Am. Chem. Soc.* **2011**, *133*, 2250–2263; d) A. M. Corrente, T. Chivers, *New J. Chem.* **2010**, *34*, 1751–1759.

[22] a) J. Wang, Y. Wang, T. Taniguchi, S. Yamaguchi, S. Irle, *J. Phys. Chem. A* **2012**, *116*, 1151–1158; b) T. Taniguchi, J. Wang, S. Irle, S. Yamaguchi, *Dalton Trans.* **2013**, *42*, 620–624.

[23] For *bam* complexes of Zr^{IV}, see: a) D. Fest, C. D. Habben, A. Meller, G. M. Sheldrick, D. Stalke, F. Pauer, *Chem. Ber.* **1990**, *123*, 703–706; b) D. R. Manke, D. G. Nocera, *Inorg. Chem.* **2003**, *42*, 4431–4436.

[24] H. Helten, A. P. M. Robertson, A. Staubitz, J. R. Vance, M. F. Haddow, I. Manners, *Chem. Eur. J.* **2012**, *18*, 4665–4680.

[25] M. J. Fuchter, C. J. Smith, M. W. S. Tsang, A. Boyer, S. Saubern, J. H. Ryan, A. B. Holmes, *Chem.Commun.* **2008**, 18, 2152–2154.

[26] A. Sundararaman, F. Jäkle, *J. Organomet. Chem.* **2003**, *681*, 134–142.

[27] R. Soundararajan, D. S. Matteson, *Organometallics*, **1995,** *14*, 4157–4166.

[28] H. Bock, J. Meuret, C. Näther, U. Krynitz, *Chem. Ber.* **1994**, *127*, 55–65.

[29] C. Camacho, M. A. Paz-Sandoval, R. Contreras, *Polyhedron* **1986**, *5*, 1723–1732.

[30] SADABS: Area-Detector Absorption Correction; Siemens Industrial Automation, Inc.: Madison, WI, **1996**.

[31] O. V. Dolomanov, L. J. Bourhis, R. J. Gildea, J. A. K. Howard, H. Puschmann, *J. Appl. Cryst.* **2009**, *42*, 339–341.

[32] a) G. M. Sheldrick, *Acta Crystallogr., Sect. A*, **2008**, *64*, 112–122; b) G. M. Sheldrick, *Acta Crystallogr., Sect. C*, **2015**, *71*, 3–8.

[33] A. J. F. Siegert, *MIT Rad Lab Rep No 465* **1943**.

[34] J. Sandström, Dynamic NMR Spectroscopy, Academic Press Inc. (London) Lt., London, New York, **1982**, p. 79.

[35] Gaussian 09, Revision **A.02**, M. J. Frisch, G. W. Trucks, H. B. Schlegel, G. E. Scuseria, M. A. Robb, J. R. Cheeseman, G. Scalmani, V. Barone, B. Mennucci, G. A. Petersson, H. Nakatsuji, M. Caricato, X. Li, H. P. Hratchian, A. F. Izmaylov, J. Bloino, G. Zheng, J. L. Sonnenberg, M. Hada, M. Ehara, K. Toyota, R. Fukuda, J. Hasegawa, M. Ishida, T. Nakajima, Y. Honda, O. Kitao, H. Nakai, T. Vreven, J. A. Montgomery, Jr., J. E. Peralta, F. Ogliaro, M. Bearpark, J. J. Heyd, E. Brothers, K. N. Kudin, V. N. Staroverov, R. Kobayashi, J. Normand, K. Raghavachari, A. Rendell, J. C. Burant, S. S. Iyengar, J. Tomasi, M. Cossi, N. Rega, J. M. Millam, M. Klene, J. E. Knox, J. B. Cross, V. Bakken, C. Adamo, J. Jaramillo, R. Gomperts, R. E. Stratmann, O. Yazyev, A. J. Austin, R. Cammi, C. Pomelli, J. W. Ochterski, R. L. Martin, K. Morokuma, V. G. Zakrzewski, G. A. Voth, P. Salvador, J. J. Dannenberg, S. Dapprich, A. D. Daniels, Ö. Farkas, J. B. Foresman, J. V. Ortiz, J. Cioslowski, and D. J. Fox, Gaussian, Inc., Wallingford CT, **2009**.

[36] A. D. Becke, *J. Chem. Phys.* **1993**, *98*, 5648–5652.

[37] a) C. Lee, W. Yang, R. G. Parr, *Phys. Rev. B* **1988**, *37*, 785–789; b) B. Miehlich, A. Savin, H. Stoll, H. Preuss, *Chem. Phys. Lett.* **1989**, *157*, 200–206.

[38] a) R. Ditchfield, W. J. Hehre, J. A. Pople, *J. Chem. Phys.* **1971**, *54*, 724; b) W. J. Hehre, R. Ditchfield, J. A. Pople, *J. Chem. Phys.* **1972**, *56*, 2257; c) P. C. Hariharan, J. A. Pople, *Theor. Chem. Acc.* **1973**, *28*, 213–222; d) P. C. Hariharan, J. A. Pople, *Mol. Phys.* **1974**, *27*, 209–214; e) M. S. Gordon, *Chem. Phys. Lett.* **1980**, *76*, 163–168; f) M. M. Francl, W. J. Pietro, W. J. Hehre, J. S. Binkley, D. J. DeFrees, J. A. Pople, M. S. Gordon, *J. Chem. Phys.* **1982**, *77*, 3654–3665; g) M. J. Frisch, J. A. Pople, J. S. Binkley, *J. Chem. Phys.* **1984**, *80*, 3265–3269.

[39] a) R. Bauernschmitt, R. Ahlrichs, *Chem. Phys. Lett.* **1996**, *256*, 454–464; b) M. E. Casida, C. Jamorski, K. C. Casida, D. R. Salahub, *J. Chem. Phys.* **1998**, *108*, 4439–4449; c) R. E. Stratmann, G. E. Scuseria, M. J. Frisch, *J. Chem. Phys.* **1998**, *109*, 8218–8224; d) C. Van Caillie, R. D. Amos, *Chem. Phys. Lett.* **1999**, *308*, 249–255; e) C. Van Caillie, R. D. Amos, *Chem. Phys. Lett.* **2000**, *317*, 159–164; f) F. Furche, R. Ahlrichs, *J. Chem. Phys.* **2002**, *117*, 7433–7447; g) G. Scalmani, M. J. Frisch, B. Mennucci, J. Tomasi, R. Cammi, V. Barone, *J. Chem. Phys.* **2006**, *124*, 094107: 1–15.

.

4.2 Poly(*p*-phenylene iminoborane): A Boron–Nitrogen Analogue of Poly(*p*-phenylene vinylene)

The following section is slightly modified and reproduced from published article[4] with permission from Wiley-VCH.

Substitution of selected CC units in π-conjugated organic frameworks by their isoelectronic and isosteric BN units (BN/CC isosterism) has proven to be a successful concept for the development of BN-doped polycyclic aromatic hydrocarbons (PAHs) with intriguing properties and functions. First examples have just demonstrated the applicability of this approach to polymer chemistry. Herein, we present the synthesis and comprehensive characterization of the first poly(p-phenylene iminoborane). This novel inorganic–organic hybrid polymer can be regarded as a BN-analog of the well-known poly(p-phenylene vinylene) (PPV). Photophysical investigations on the polymer and a series of model oligomers provide clear-cut evidence for some π-conjugation across the B=N bonds and extension of the conjugation path with increasing chain length. TD-DFT calculations provide deeper insight into the electronic structure of the new materials.

4.2.1 Introduction

π-Conjugated polymers continue to attract tremendous research attention, owing to their use as cost-effective, lightweight materials for electronic and optoelectronic device applications, such as (polymer-based) organic light-emitting diodes (OLEDs/PLEDs),[1a] organic field-effect transistors (OFETs),[1b] and organic photovoltaic cells (OPV),[1c] or as imaging or sensory materials.[1d] In recent years, the focus has shifted towards the functionalization of conjugated polymers with inorganic main group elements.[2–4] Particularly, the incorporation of boron has led to various novel hybrid macromolecules with intriguing properties and functions.[5,6] Substitution of selected CC units by their isoelectronic and isosteric BN units in π-conjugated organic frameworks has emerged as a viable strategy to produce new materials with structural similarities to their all-carbon congeners but in many cases fundamentally altered electronic features.[5d,7-9] This "BN/CC isosterism" approach has been primarily used to develop BN-doped polycyclic aromatic hydrocarbons (PAHs) with tailored properties. Recently, we and others have started to utilize this concept for conjugated polymers.[5d,9–17] Liu and Jäkle and co-workers presented a 1,2-azaborinine polymer, which is formally derived from

[4] T. Lorenz, M. Crumbach, T. Eckert, A. Lik, H. Helten, *Angew. Chem. Int. Ed.* **2017**, *56*, 2780—2784; *Angew. Chem.* **2017**, *129*, 2824—2828.

poly(*p*-phenylene) (Scheme 4.2.1). Detailed investigations revealed that the electronic structure of this effectively conjugated polymer resembles that of poly(cyclohexadiene) more than poly(*p*-phenylene).[11] Shortly after this report, Wang and Pei and co-workers presented polythiophene-type polymers with a fused azaborinine-containing polycyclic skeleton, which showed favorable charge transport characteristics in OFET devices.[12]

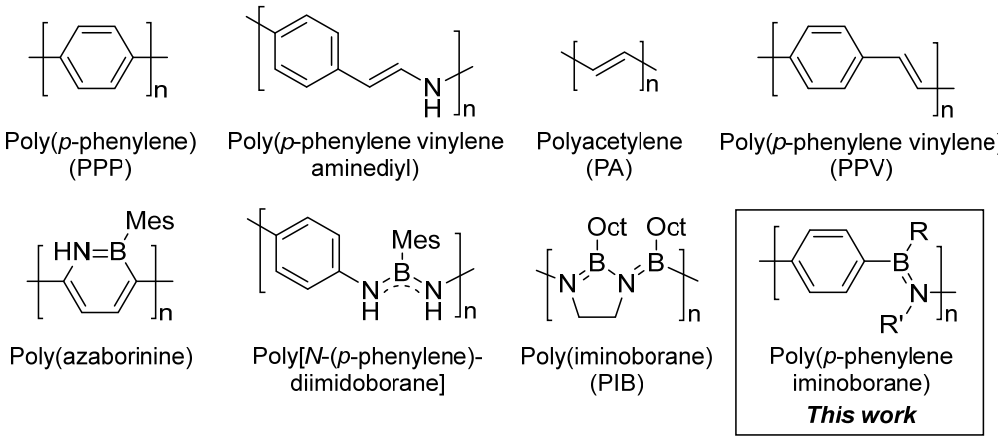

Scheme 4.2.1. Representative examples of π-conjugated organic polymers and BN isosteres thereof (Mes = 2,4,6-trimethylphenyl, mesityl; Oct = *n*-C_8H_{17}; R, R' = organic substituents or H).

A common observation is that the conjugation along the backbone of such polymers occurs preferentially via the carbon chain rather than via the BN moieties, consistent with a lower π contribution in B=N bonds compared to analogous C=C bonds.[18] Therefore, we became interested in developing such polymers with essentially linear B=N linkages in which π-conjugation – if present – must occur via this unit, as no alternative conjugation pathways exist.[14,15] Recently, we developed a novel silicon/boron exchange polycondensation approach to prepare a polymer composed of NBN and *para*-phenylene building blocks (i.e., a poly[*N*-(*p*-phenylene)diimidoborane]).[16,19] Complete replacement of the carbon atoms in polyacetylene by alternating boron and nitrogen atoms leads to poly(iminoborane)s (PIBs). Such species had been previously unknown. We succeeded in the synthesis of a linear oligo(iminoborane) comprised of on average 12–14 BN units.[17]

Poly(*p*-phenylene vinylene)s (PPVs) are among the most widely studied semiconducting organic polymers.[1] Phosphorus analogs thereof containing P=C or P=P linkages were presented by Gates and Protasiewicz and their respective co-workers.[3,4] Boron–nitrogen analogs of PPV, however, are unknown thus far.

4.2.2 Results and Discussion

Herein, we present the first derivative of this class of compounds with bridging B=N linkages, i.e. a poly(*p*-phenylene iminoborane), as well as a series of molecular model compounds for the polymer. Our studies reveal clear-cut evidence for moderate π-conjugation across the B=N bonds. We initiated our investigations by preparing the model oligomers **3**, **5**, and **7**, featuring one or two B=N units, respectively, via selective silicon/boron exchange reactions (Scheme 4.2.2). 2,4,6-Triisopropylphenyl (Tip) was chosen as the substituent at boron in order to provide kinetic stabilization. The oligomers **5** and **7** differ in the sequence of their BN units along the chain, whereby both species contain subunits of the targeted polymer, which has the sequence BBNNBBNN (see below). The air-stable products were isolated in good yields. Compounds **3** and **5** were purified by column chromatography on silica, with no special precautions to exclude air and moisture, and pure **7** was obtained upon re-crystallization. Their identity was unambiguously ascertained by NMR spectroscopy and mass spectrometry. The molecular structures of **5** and **7** were additionally determined by single-crystal X-ray diffraction (Figure 4.2.1).

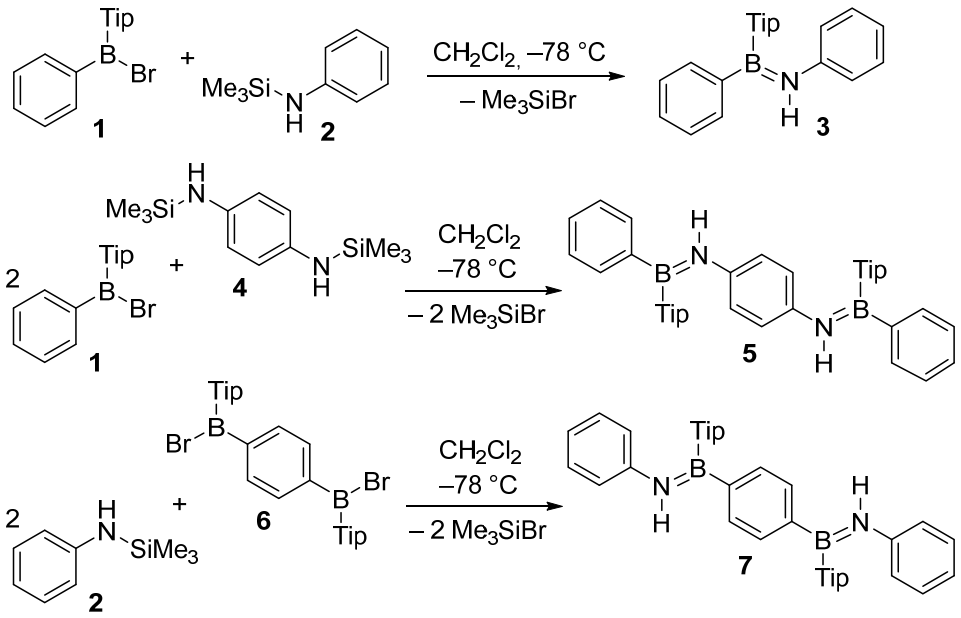

Scheme 4.2.2. Synthesis of molecular model compounds **3**, **5**, and **7** (Tip = 2,4,6-triisopropylphenyl).

The B–N bond lengths of **5** (B1–N1: 1.429(7) Å, B2–N2: 1.443(8) Å) and **7** (B1–N1: 1.409(6) Å) in the solid state are in a similar range with those of $PhNHBMes_2$ (1.407(2) Å)[20a] and $MesNHBMes_2$ (1.406(3) Å).[20b] In both oligomers the phenyl and the phenylene groups adopt *trans* positions at each B=N unit. Variable-temperature NMR measurements revealed that this configuration persists at room temperature in solution. In the solid state, the planes of these rings are slightly twisted with respect to each other and with respect to the planes of the adjacent BN moieties (defined by C_2BNC). In **5**,

the angles between the planes are: 20.2(3)° (between phenyl at B2 and the B2N2 moiety), 18.9(2)° (between B2N2 and the phenylene group), 11.6(2)° (between the latter and the B1N1 moiety), and 27.2(3)° (between B1N1 and the phenyl group at B1). As the phenyl and the phenylene groups at the B2N2 moiety both are twisted in the same direction, the two rings are almost coplanar (twist angle: 4.7(3)°). At the B1N1 moiety, on the other hand, the substituents are twisted in different directions, resulting in a torsion angle of 38.7(3)° between the two ring systems. Centrosymmetric **7** features twist angles of 16.0(1)° between the phenyl group and the BN unit, and 25.3(2)° between BN and the plane of the phenylene group. With respect to each other both rings are twisted by 40.9(2)°.

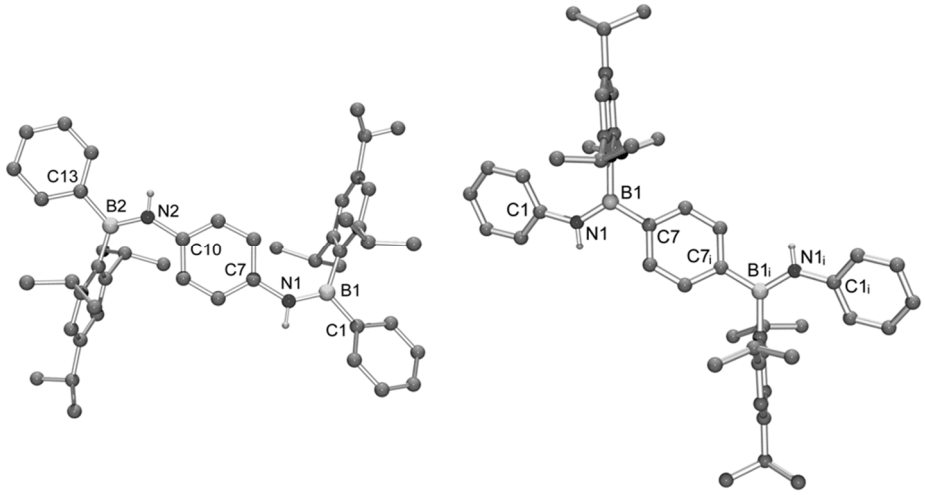

Figure 4.2.1. Molecular structures of **5** (left) and **7** (right) in the solid state (C-bonded H-atoms omitted for clarity).

The synthesis of the desired poly(p-phenylene iminoborane) 8 was achieved by Si/B exchange co-polycondensation of **4** and 6 (1:1 ratio) in CH_2Cl_2 at ambient temperature (Scheme 4.2.3). Upon mixing a solution of **4** with a suspension of **6** in CH_2Cl_2, instantaneously, a clear solution was formed. Monitoring of the reaction by $^{11}B\{^1H\}$ NMR spectroscopy showed that **6** (δ = 73.6 ppm) was immediately consumed. A spectrum recorded after 20 min displayed a small, broad resonance at $\delta \approx$ 45 ppm, which is in the same range with the ^{11}B resonances of **3** (δ = 44.0 ppm), **5** (δ = 43.4 ppm), and **7** (δ = 44.5 ppm), i.e. in the expected range for aminoborane structural units, thus pointing to the formation of **8**. This signal further broadened during the reaction and was no longer detected after 20 h. The formation of the condensation byproduct, Me_3SiBr, was evidenced by ^1H NMR spectroscopy (δ = 0.58 ppm). During the reaction a marked increase in the viscosity of the solution was observed. After the mixture had been stirred for 20 h at room temperature, Me_3SiNMe_2 (10 mol%) was added to deactivate the B–Br end groups of **8**. The end-capped poly(p-phenylene iminoborane) **8'** was purified by precipitation with cold *n*-pentane and was obtained as a pale yellow solid in 85% yield. The soluble polymer was characterized by NMR and UV–vis spectroscopy, and

in terms of molecular weight and shape and size distribution by gel permeation chromatography (GPC), dynamic light scattering (DLS), and small-angle X-ray scattering (SAXS).

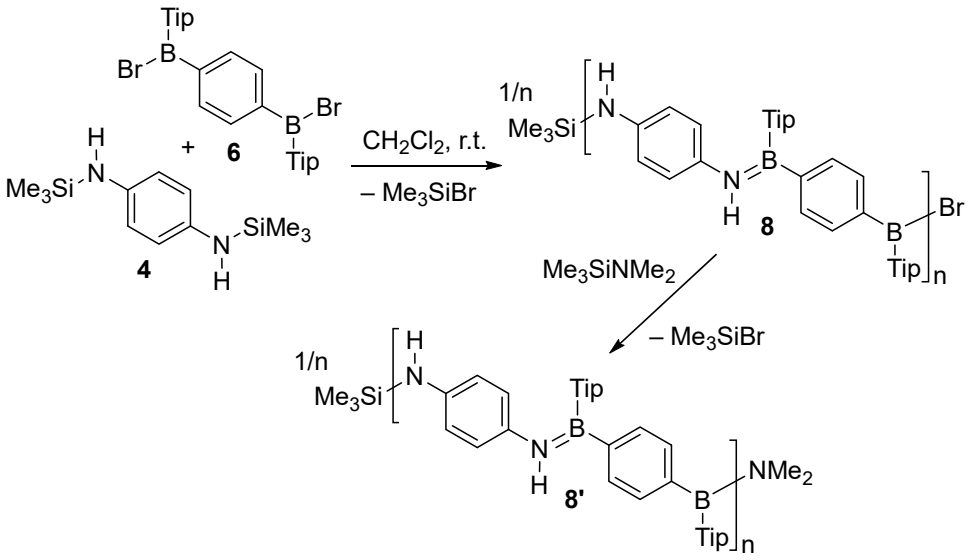

Scheme 4.2.3. Synthesis of polymer **8** and end-capped derivative **8'** (Tip = 2,4,6-triisopropylphenyl).

The ^{1}H and $^{13}C\{^{1}H\}$ NMR spectra of **8'** were easily assigned via comparison with the corresponding data for the model compounds. Distinct ^{1}H and ^{13}C resonances were detected for the nuclei of the bis-amino- and the bis-boryl-substituted phenylene rings. The NH proton resonates at $\delta = 6.80$ ppm, and the isopropyl-CH_3 groups in *ortho*-position at the Tip substituent show clearly separated signals in the $^{13}C\{^{1}H\}$ NMR spectrum, as a result of the hindered rotation about the C^{Tip}–B bond. A proton resonance at $\delta = 2.76$ ppm for the NMe_2 end group confirmed successful end-capping. Residual *n*-pentane was still detectable even after prolonged evacuation (ca. 10^{-2} mbar), which suggests that it is confined by the polymer chains.

The GPC analysis revealed molecular weight averages of M_n = 11 440 Da and M_w = 46 870 Da, respectively, according to a number average degree of polymerization of $DP_n = 19$, and a fairly large polydispersity index of PDI = $M_w/M_n = 4.1$. DLS measurements gave a hydrodynamic radius of R_h = 5.4 nm for particles of **8'** in THF solution. The SAXS measurements revealed that **8'** adopts an anisotropic structure in THF with an aspect ratio of 10:1 and a radius of gyration of $R_g = 3.6$ nm. The data is consistent with a rod-like helical structure with a translation of 3–4 repeat units and dimensions of 10 × 1 nm.

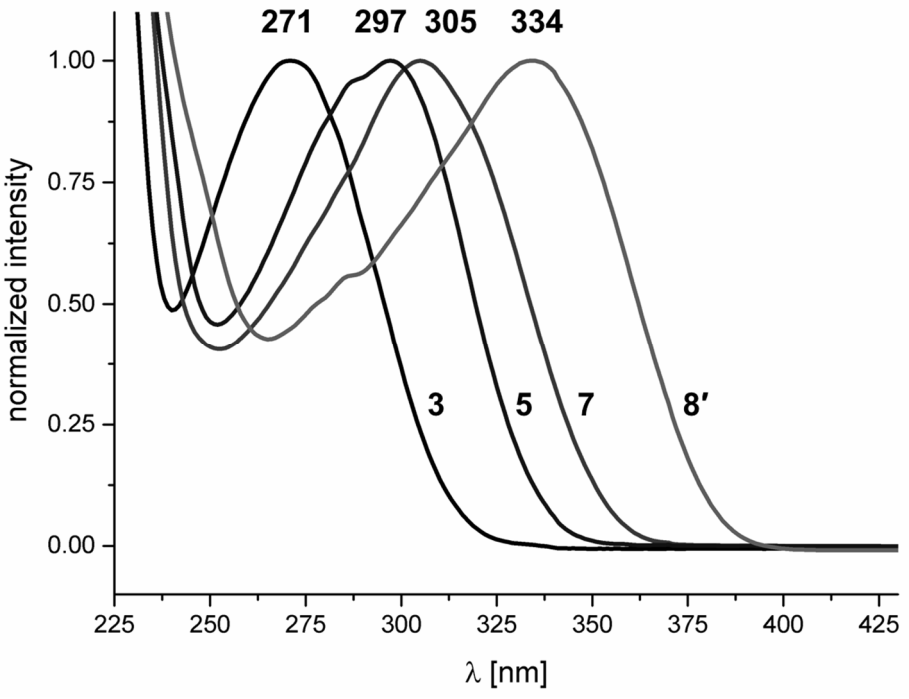

Figure 4.2.2. UV–vis absorption spectra of **3**, **5**, **7**, and **8'** in CH_2Cl_2 (λ_{max} in nm).

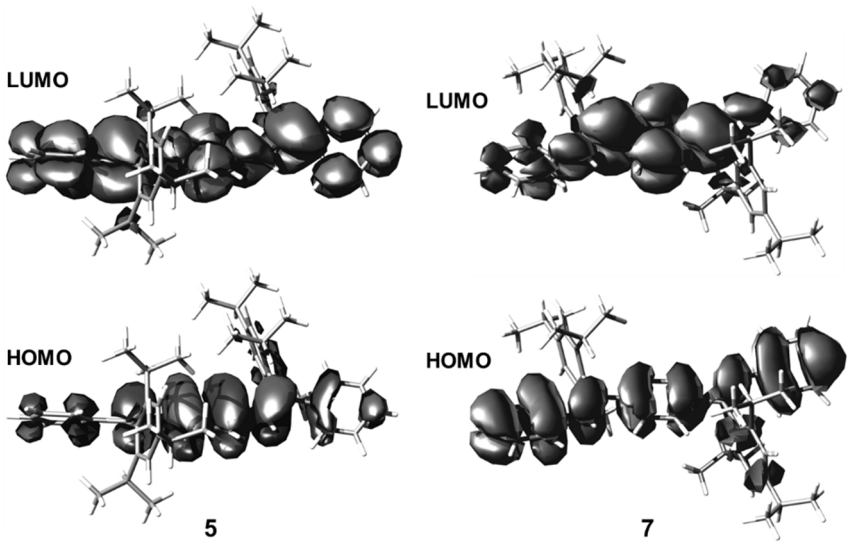

Figure 4.2.3. Calculated frontier orbitals of **5** and **7** (isovalue: 0.015; B3LYP-D3(BJ)/def2-SV(P)).

Comparison of the UV–vis spectra of **3**, **5**, **7**, and **8'** in CH_2Cl_2 (Figure 4.2.2) revealed that the lowest-energy absorption band shows a systematic red-shift with increasing number of B=N units, i.e., in the order **3** (λ_{max} = 271 nm) < **5** (297 nm), **7** (305 nm) < **8'** (334 nm). To gain deeper insight into the electronic structure of these species, we optimized the structures of **3**, **5**, and **7** by means of DFT calculations (B3LYP-D3(BJ)/def2-SV(P)) and calculated their vertical singlet excitations via TD-DFT. This showed that the lowest-energy absorptions correspond to HOMO→LUMO excitations. As these orbitals orbitals are unambiguously characterized as π-orbitals extended over the phenyl and

phenylene rings and the B=N units, the respective transitions are classified as π–π* processes (Figure 4.2.3).

In agreement with theoretical predictions for related systems,[18] π-conjugation in **8'** along the polymer backbone is less pronounced than in the parent all-carbon PPV.[1,21a] The unsubstituted PPV, however, is insoluble, intractable, and infusible. Its standard synthesis proceeds via a polymer precursor from which the C=C double bonds are formed in a subsequent elimination step, usually performed at high temperatures.[21b] For the synthesis of soluble, substituted PPV derivatives, various routes have been developed, and the properties of the materials obtained are highly dependent on the applied method.[1] Structural defects are often difficult to control,[21c] and some approaches require *Z*→*E* isomerizations in the final step.[1,21a] Notably, our synthetic approach to BN-PPV **8'** is characterized by a facile procedure that affords the polymer in the preferred *trans* configuration of the phenylene moieties under mild conditions.

4.2.3 Conclusion

In this study, we presented a poly(p-phenylene iminoborane), which is the first derivative of a novel class of inorganic–organic hybrid polymers that can be regarded as BN analogs of poly(p-phenylene vinylene) (PPV). Photophysical investigations combined with TD-DFT calculations afforded clear-cut evidence for π-conjugation across the B=N units along the polymer backbone and extension of the conjugation path with increasing chain length. Our study also demon-strates the broader applicability of silicon/boron exchange polycondensation as a versatile synthetic approach to access high-molecular-weight organoboron polymers. Currently, we are further exploring the concept of BN-doping of conjugated polymers towards applications in organic electronics.

4.2.4 Experimental Section

General procedures. All manipulations were performed under an atmosphere of dry argon using standard Schlenk techniques or in an MBraun glovebox. Solvents (dichloromethane, n-pentane, and tetrahydrofuran) were dried and degassed by means of an MBraun SPS-800 solvent purification system. Deuterated solvents for NMR spectroscopy were dried and degassed at reflux over Na (C_6D_6) or CaH_2 ($CDCl_3$) and freshly distilled prior to use. Boron tribromide was commercially purchased and used as received. Aniline and N,N-Dimethyltrimethylsilylamine were dried and degassed by inert-gas distillation from CaH_2. 1,4-Phenylenediamine was recrystallized from THF. TipLi,[22] PhBBr2,[23] **2**,[24] **4**,[25] 1,4-bis(dibromoboryl)benzene,[26] were prepared according to methods

described in the literature. For column chromatography SiO_2 with a pore diameter between (0.2-0.5 mm) was used. NMR spectra were recorded at 25 °C on a Bruker AVANCE II-400 spectrometer or on a Bruker Advance III HD spectrometer operating at 400 MHz. Chemical shifts were referenced to residual protic impurities in the solvent (^1H) or the deuterio solvent itself (^{13}C) and reported relative to external $SiMe_4$ (^1H, ^{13}C) or $BF_3 \cdot OEt_2$ (^{11}B) standards. Mass spectra were obtained with the use of a Finnigan MAT95 spectrometer employing electron ionisation (EI) using a 70 eV electron impact ionisation source. UV/VIS-spectra were obtained using a Jasco V-630 spectrophotometer. Melting points (uncorrected) were obtained using a SMP3 melting point apparatus by Stuart in 0.5 mm (o.d.) glass capillaries, which were sealed under argon. GPC chromatograms were recorded on a Agilent 1100 Series, using a flow rate of 1 mL min-1 in THF at 25 °C, calibrated for polystyrene standards. X-ray crytallographic data were collected on a Bruker SMART APEX CCD detector on a D8 goniometer equipped with an Oxford Cryostream 700 temperature controller at 100(2) K using graphite monochromated Mo-Kα radiation (λ = 0.71073 Å ;**5**) or Cu-Kα radiation (λ = 1.54178 Å ; **7**). An absorption correction was carried out semi-empirically using SADABS[27] (min./max. transmissions = 0.3502/0.7454 (**5**), 0.9408/1.0000 (**7**)). The structure was solved with Olex2[28] using Direct Methods (ShelXS[29a]) and refined with the ShelXL[29b] refinement package by full-matrix least squares on F2. All non-hydrogen atoms were refined anisotropically. The hydrogen atoms were included isotropically and treated as riding. The SAXS measurements were carried out at 10 °C on an S-Max3000 system with a MicroMaxTM-002+ X-ray microfocus generator (Rigaku) and an out-of-center beam stop to increase the q range to higher q values. The Bayesian weighted distance distribution function p(r) was calculated from the angle dependent scattering using a fit routine included in the manufacturer supplied software.[30]

Spectra. All spectra and other result figures are shown in Appendix 7.2.

Synthesis

Synthesis of 1. To a stirred suspension of TipLi (1.054 g, 5.01 mmol) in toluene (10 mL) was added dropwise a solution of $PhBBr_2$ (1.239 g, 5.00 mmol) in toluene (10 mL) at –78 °C. Subsequently, the mixture was warmed to room temperature and stirred overnight. The solid was filtered off and all volatiles were removed *in vacuo*. The colorless solid was washed with cooled pentane (3x5 mL). All volatiles were removed *in vacuo* and **1** was obtained as colorless solid. Yield: 1.559 g (4.20 mmol, 84 %). ^1H NMR (400 MHz, C_6D_6): δ = 7.88 (d, 2H; *o*-Ph-*H*), 7.53 (t, 1H, *J* = 7.4 Hz, *p*-Ph-*H*), 7.36 (d, 2H; *m*-Ph-*H*), 6.93 (s, 2H; Tip-H_{Ar}), 2.84 (sept, 1H, *J* = 7.03 Hz, *p*-Tip-C*H*), 2.42 (sept, 2H, *J* =

6.66 Hz, *o*-Tip-C*H*), 1.22 (d, 6H, *J* = 7.03 Hz, *p*-Tip-CH_3), 1.15 (d, 6H, *J* = 6.78 Hz, *o*-Tip-CH_3), 1.22 (d, 6H, *J* = 6.53 Hz, *o*-Tip-CH_3); $^{11}B\{^1H\}$ NMR (128 MHz, $CDCl_3$): δ = 71.0 ppm (s).

Synthesis of 3. To a stirred solution of **1** (1.840 g, 4.97 mmol) in dichloromethane (5 mL) was added dropwise **2** (826 mg, 5.00 mmol) at –78 °C. During the addition, immediately a white-grey suspension was formed. Subsequently, the mixture was warmed to room temperature and stirred overnight. All volatiles were removed *in vacuo*. The beige-colored solid was purified via column chromatography (hexane/ DCM (10:1)). **3** was obtained as colorless solid. Yield: 1.545 g (4.03 mmol, 81 %). m.p. 96 °C; ^1H NMR (400 MHz, $CDCl_3$): δ = 7.64 (m, 2H; *o*-B-Ph-*H*), 7.42 (m, 3H; *m*/*p*-B-Ph-*H*), 7.09 (m, 2H; *m*-N-Ph-*H*), 7.03 (s, 2H; Tip-H_{Ar}), 6.99 (s, 1H; N*H*), 6.91 (tt, ^3J(H,H) = 7.41 Hz, ^4J(H,H) = 1.38 Hz, 1H; *p*-N-Ph-*H*), 6.82 (m, 2H; *o*-N-Ph-*H*), 2.97 (sept, ^3J(H,H) = 6.91 Hz, 1H; *p*-Tip-C*H*), 2.72 (sept, ^3J(H,H) = 6.91 Hz, 2H; *o*-Tip-C*H*), 1.34 (d, ^3J(H,H) = 7.03 Hz, 6H; *p*-Tip-CH_3), 1.02 (d, ^3J(H,H) = 6.78 Hz, 6H; *o*-Tip-CH_3), 0.99 (d, ^3J(H,H) = 6.78 Hz, 6H; *o*-CH_3); $^{11}B\{^1H\}$ NMR (128 MHz, $CDCl_3$): δ = 44.0 ppm (s); $^{13}C\{^1H\}$ NMR (101 MHz, $CDCl_3$): δ = 149.6 (s, *o*-C_{Tip}), 148.9 (s, *p*-C_{Tip}), 143.7 (s, N-C-Ph), 140.4 (br s, B-C-Ph), 135.7 (br s, B-*ipso*-C_{Tip}), 133.1 (s, m-C-B-Ph), 130.2 (s, B-*p*-C-B-Ph), 128.7 (s, *m*-C-B-Ph), 127.9 (s, *o*-C-Ph-NH), 122.4 (s, *p*-C-Ph-NH), 120.4 (s, C_{Tip}-Ar-CH), 120.3 (s, *o*-C-Ph-NH), 34.7 (s, *p*-Tip-CH), 34.3 (s, *o*-Tip-CH), 24.6 (s, *o*-Tip-CH_3), 24.2 (s, *o/p*-Tip-CH_3), 24.1 (s, *o/p*-Tip-CH_3), MS (EI, 70 eV): *m/z* (%) = 383.5 (M^+, 25), 308.4 ([PhB(Tip)NH]$^+$, 89), 215.3 ([PhNHBTip]$^+$,100), 180.2 ([PhBNHPh]$^+$, 28); HRMS: found *m/z* = 383.2785, theo. mass for $^{12}C_{27}{}^1H_{34}{}^{14}N_1{}^{11}B_1$ = 383.2779; UV–vis (CH_2Cl_2): λ_{max} = 271 nm (ε = 1.1 · 10^4 L cm^{-1} mol^{-1}).

Synthesis of 5. To a stirred solution of **4** (757 mg, 3.00 mmol) in dichloromethane (5 mL) was added dropwise a solution of **1** (2.264 g, 6.10 mmol) in DCM (18 mL) at –78 °C. Subsequently, the mixture was warmed to room temperature and stirred overnight. All volatiles were removed *in vacuo*. The beige-colored solid was purified via column chromatography (hexane/DCM 5:1 to 2:1, R_f = 0.55). The product was obtained as colorless solid. Yield: 1.632 g (2.37 mmol, 79%). m.p. 223 °C; ^1H NMR (400 MHz, $CDCl_3$): δ = 7.60 (m, 4H; *o*-Ph-*H*), 7.41 (m, 6H; *m/p*-Ph-*H*), 6.98 (s, 4H; Tip-H_{Ar}), 6.83 (br, 2H; NH), 6.48 (s, 4H; N_2-C_6H_4), 2.94 (sept, ^3J(H,H) = 6.91 Hz, 2H; *p*-Tip-C*H*), 2.66 (sept, ^3J(H,H) = 6.91 Hz, 4H; *o*-Tip-C*H*), 1.33 (d, ^3J(H,H) = 7.03 Hz, 12H; *p*-Tip-CH_3), 1.00 (d, ^3J(H,H) = 6.78 Hz, 12H; *o*-Tip-CH_3), 0.93 (d, ^3J(H,H) = 6.78 Hz, 12H; *o*-Tip-CH_3); $^{11}B\{^1H\}$ NMR (128 MHz, $CDCl_3$): δ = 43.4 ppm (s); $^{13}C\{^1H\}$ NMR (101 MHz, $CDCl_3$): δ = 149.6 (s, *o*-C_{Tip}), 148.8 (s, *p*-C_{Tip}), 140.3 (br s, B-C_{ispo}-Ph), 138.7 (s, C_{ispo}-Ph-NH), 135.8 (br s, B-C_{ispo}-Tip), 133.0 (s, B-*o*-Ph-CH), 130.1

(s, B-*p*-Ph), 127.8 (s, B-*m*-Ph), 120.5 (s, C_{Ar}Tip), 120.3 (s, *o*-Ph-CNH), 34.6 (s, *o*-Tip-CH), 34.3 (s, *p*-Tip-CH), 24.6 (s, *o*-Tip-CH_3), 24.2 (s, *p*-Tip-CH_3), 24.1 (s, *o*-Tip-CH_3); MS (EI, 70 eV): *m/z* (%) = 688.7 (M^+, 100), 485.5 ([M -Tip]$^+$, 2), 398.5 ([PhB(Tip)NHC_6H_4NH)]$^+$, 8), 247.3 ([PhBDip)]$^+$, 5); HRMS: found *m/z* = 688.5106, theo. mass for $^{12}C_{48}{}^{1}H_{62}{}^{14}N_2{}^{11}B_2$ = 688.5094; UV–vis (CH_2Cl_2): λ_{max} = 297 nm ($\varepsilon = 1.2 \cdot 10^4$ L cm^{-1} mol^{-1}).

Synthesis of 6. To a stirred suspension of TipLi (1.180 g, 5.61 mmol) in toluene (30 mL) was added dropwise a solution of 1,4-bis(dibromoboryl)benzene (1.148 g, 2.75 mmol) in toluene (10 mL) at –78 °C. Subsequently, the mixture was warmed to room temperature and stirred overnight. The colorless dispersion was filtered through a G4 glass filter and washed with toluene (1x10 mL). All volatiles were removed *in vacuo*. The colorless solid was washed with pentane (3x5 mL) and **6** was obtained as colorless solid. Yield: 1.463 g (2.21 mmol, 80 %); ^{1}H NMR (400 MHz, C_6D_6): δ = 8.00 (s, 4H; *o*-B_2-C_6H_4), 7.12 (s, 4H; Tip-H_{Ar}), 2.84 (sept, *J* = 6.78 Hz, 2H; *p*-Tip-C*H*), 2.56 (sept, *J* = 6.53 Hz, 4H; *o*-Tip-C*H*), 1.27 (d, *J* = 6.78 Hz, 12H; *p*-Tip-CH_3), 1.25 (d, *J* = 6.53 Hz, 12H; *o*-Tip-CH_3); 1.01 (d, *J* = 6.53 Hz, 12H; *o*-Tip-CH_3); ^{11}B{^{1}H} NMR (128 MHz, $CDCl_3$): δ = 73.6 ppm (s); ^{13}C{^{1}H} NMR (101 MHz, $CDCl_3$): δ = 151.2 (s, *p*-C_{Tip}),149.6 (s, *o*-C_{Tip}), 144.7 (br s,C_{ipso}-B_2-C_6H_4), 138.1 (br s, C_{ipso}-Tip), 137.9 (s, *o*-C-B_2-C_6H_4)), 121.4 (s, C_{Ar}-Tip), 36.6 (s, *o*-Tip-*C*H), 35.3 (s, *p*-Tip-*C*H), 24.9 (s, *o*/*p*-Tip-CH_3), 24.7 (s, *o*/*p*-Tip-CH_3), 24.1 (s, *p*-Tip-CH_3); MS (EI, 70 eV): *m/z* (%) = 189.2 ([($C_{14}H_{21}$)]$^+$, 34), 203.2 ([Tip]$^+$, $C_{15}H_{23}$, 31), 259.2 ([$C_6H_2BC_6H_4BC_7H_3$]$^+$, 29), 293.1 ([TiPBBr]$^+$, 19), 664.1 ([M^+], 100); HRMS: found *m/z* = 664.2413, theo. mass for $^{12}C_{36}{}^{1}H_{50}{}^{11}B_2{}^{79}Br_1{}^{81}Br_1$ = 664.2439.

Synthesis of 7. To a stirred solution of **6** (1.292 g, 1.94 mmol) in dichloromethane (25 mL) was added dropwise $PhNHSiMe_3$ (0.696 g, 4.21 mmol) at –78 °C. Subsequently, the mixture was warmed to room temperature and stirred overnight. All volatiles were removed *in vacuo*, and the colorless solid was identified as **7**. Yield: (1.215 g, 1.76 mmol, 91 %). m.p. 229 °C; ^{1}H NMR (400 MHz, $CDCl_3$): δ = 7.64 (s, 4H; B_2-C_6H_4), 7.11 (m, 4H; *m*-Ph-*H*), 7.03 (s br, 4H; Tip-H_{Ar}), 7.03 (br, 2H; N*H*), 6.93 (tt, 2H; *p*-Ph-*H*, ^3J(H,H) = 7.40 Hz, ^4J(H,H) = 1.21 Hz; *p*-Ph-H), 6.85 (m, 4H; *o*-Ph-*H*), 2.97 (sept, ^3J(H,H) = 6.78 Hz, 2H; *p*-Tip-C*H*), 2.73 (sept, ^3J(H,H) = 6.78 Hz, 4H; *o*-Tip-C*H*), 1.34 (d, ^3J(H,H) = 7.03 Hz, 12H; *p*-Tip-CH_3), 1.00 (d, ^3J(H,H) = 7.03 Hz, 24H; *o*-Tip-CH_3); ^{11}B{^{1}H} NMR (128 MHz, $CDCl_3$): δ = 44.5 ppm (s); ^{13}C{^{1}H} NMR (101 MHz, $CDCl_3$): δ = 149.6 (s, *o*-C_{Tip}), 148.9 (s, *p*-C_{Tip}), 143.7 (s, C_{ipso}-Ph-NH), 142.5 (br s, C_{ipso}-B-C_6H_4), 135.8 (br s, C_{ipso}-Tip), 132.6 (s, *o*-C-B_2-C_6H_4), 128.7 (s, *m*-Ph-C(NH)), 122.5 (s, *p*-Ph-C(NH)), 120.4 (s, C_{Ar}Tip), 120.3 (s, *o*-Ph-C(NH)), 34.8 (s, *p*-

Tip-CH), 34.3 (s, *o*-Tip-CH), 24.5 (s, *o*-Tip-CH_3), 24.2 (s, *o*/*p*-Tip-CH_3), 24.1 (s, *o*/*p*-Tip-CH_3); MS (EI, 70 eV): *m/z* (%) = 93.2 ($[PhNH_2)]^+$, C_6H_7N, 100), 189.2 ($[(C_{14}H_{21})]^+$, 47], $C_{14}H_{20}$, 47), 262.2 ($[PhNBTip]^+$, $C_{18}H_{21}BN$, 25), 485.4 ($[M^+ - Tip]^+$, 6), 688.5 ($[M^+]$, 16), HRMS: found *m/z* = 688.5087, theo. mass for $^{12}C_{48}{}^{1}H_{62}{}^{14}N_2{}^{11}B_2$ = 688.5094; UV–vis (CH_2Cl_2): λ_{max} = 305 nm ($\varepsilon = 1.4 \cdot 10^4$ L cm^{-1} mol^{-1}).

Synthesis of polymer 8'. To a stirred suspension of **6** (664.4 mg, 1.0 mmol) in dichloromethane (10 mL) was added dropwise a solution of **4** (252.5 mg, 1.0 mmol) in dichloromethane (1.0 mL). During addition the solution turned light yellow and the solid was dissolved. The yellow color disappeared after a few minutes. The mixture was stirred for 20h. TMS-NMe_2 (12 mg, 0.1 mmol, 10 mol%) was added and the mixture was stirred for 2h. Subsequently, the mixture was precipitated into cooled (–40 °C) *n*-pentane (40 mL). The supernatant liquid was removed by filtration and the product was dried *in vacuo* to give **8'** as pale yellow solid. Yield: 519 mg (85%); ^{1}H NMR (400 MHz, $CDCl_3$): δ = 7.51 (br s, 4H; B_2-C_6H_4), 6.92 (s br, 4H; Tip-H_{Ar}), 6.80 (br, 2H; N*H*), 6.45 (br, 4H; N_2-C_6H_4), 2.89 (m, 2H; *p*-Tip-C*H*), 2.76 (N(CH_3)$_2$ end groups), 2.60 (m, 4H; *o*-Tip-C*H*), 1.27 (m, 12H; *p*-Tip-CH_3), 1.00 (m, 24H; *o*-Tip-CH_3), 0.08–0.27 (Si(CH_3)$_3$ end groups); 11B {1H} NMR (128 MHz, $CDCl_3$): δ = 45 ppm (br); ^{13}C{^{1}H} NMR (101 MHz, $CDCl_3$): δ = 149.5 (s, *o*-C-Tip), 148.7 (s, *p*-C-Tip), 142.2 (br s, C_{ipso}-B_2-C_6H_4), 138.6 (br s, C_{ipso}-N-C_6H_4), 135.8 (br s, C_{ipso}-Tip), 132.4 (s, o-B_2-C_6H_4), 120,5 (s, *o*-C-$N_2C_6H_4$), 120.2 (s. C_{ArH}-Tip), 34.6 (s, *o*-Tip-CH), 34.3 (*p*-Tip-CH), 24.5 (*o*-Tip-CH_3), 24.2 (*o*/*p*-Tip-CH_3), 24.1 (*o*/*p*-Tip-CH_3). UV–vis (CH_2Cl_2): λ_{max} = 334 nm, ($\varepsilon = 7.2 \cdot 10^3$ L cm^{-1} mol^{-1}); GPC (THF, vs. polystyrene, detection by UV signal): M_n = 11 400 Da; M_w = 46 900 Da; DLS (THF): R_h = 5.4 nm.

X-ray crystallographic analysis of 5 and 7. Suitable colorless single crystals of **5** and **7** ($C_{48}H_{62}B_2N_2$, M = 688.66 g mol^{-1}) were obtained from a concentrated *n*-hexane by slow evaporation of the solvent at room temperature.

5: Crystal size 0.27 x 0.22 x 0.2 mm, triclinic, P-1 (No. 2), a = 10.573(8), b = 14.446(11), c = 15.573(12) Å, V = 2196(3) Å^3, Z = 2, ρ_{calc} = 1.041 Mg · m^{-3}, 3.46° ≤ 2θ ≤ 52.78°, collected (independent) reflections = 14995 (8903), R_{int} = 0.1110, μ = 0.059 mm^{-1}, 489 refined parameters, 0 restraints, $R1$ ($I > 2\sigma(I)$) = 0.0945, $R1$ (all data) = 0.2410, $wR2$ ($I > 2\sigma(I)$) = 0.2663, $wR2$ (all data) = 0.2985, max./min. residual electron density = 0.26/–0.26 e · Å^{-3}. CCDC-1524185 contains the

supplementary crystallographic data for the structure of **7**. This data can be obtained free of charge from The Cambridge Crystallographic Data Centre via www.ccdc.cam.ac.uk/data_request/cif.

7: Crystal size 0.48 x 0.2 x 0.03 mm, triclinic, P-1 (No. 2), a = 9.4011(8), b = 10.2329(9), c = 11.1918(11) Å, V = 1010.34(16) Å^3, Z = 1, ρ_{calc} = 1.132 Mg · m^{-3}, 8.38° ≤ 2θ ≤ 135.56°, collected (independent) reflections = 9204 (3381), R_{int} = 0.1063, μ = 0.474 mm^{-1}, 241 refined parameters, 0 restraints, $R1$ ($I > 2\sigma(I)$) = 0.0894, $R1$ (all data) = 0.1217, $wR2$ ($I > 2\sigma(I)$) = 0.2596, $wR2$ (all data) = 0.2824, max./min. residual electron density = 0.43/–0.36 e · Å^{-3}. CCDC-1524186 contains the supplementary crystallographic data for the structure of **7**. This data can be obtained free of charge from The Cambridge Crystallographic Data Centre via www.ccdc.cam.ac.uk/data_request/cif.

Dynamic light scattering (DLS) of 8'. The light scattering measurements on **8'** were performed in THF (5 mg mL^{-1}) at 20 °C with an ALV 5000 E autocorrelator equipped with a red laser (λ = 633 nm). The time-resolved signal of two Single Photon Counting Modules (SPCM-CD 2969; Perkin Elmer) was cross-correlated. Hereby, the CONTIN analysis was performed in an angular dependent way (30° to 150°). For each measurement (sampling time 90 s), the intensity-weighted decay-time τ distributions (as obtained from the field autocorrelation function obtained by use of the Siegert relation)[31] were analyzed in respect to multimodality, where for each diffusive mode its (intensity-) average decay rate $\Gamma(1/\tau)$ was extracted. Then, the decay rates were plotted against the squared length of the scattering vector q^2 (Figure 7.2.2). The slope gave the diffusion coefficient, D = 8.23 · 10^{-11} m^2 s^{-1}, and its value was transformed to the hydrodynamic radius R_h (5.4 nm) by the Stokes-Einstein equation.

Computational methods. DFT calculations were carried out with the TURBOMOLE V7.0.1 program package.[32] Optimizations were performed with Becke's three parameter exchange-correlation hybrid functional B3LYP[33] in combination with the valence-double-ζ basis set def2-SV(P).[34] The empirical dispersion correction DFT-D3 by Grimme was used including the three-body term and with Becke-Johnson (BJ) damping.[35] The stationary points were characterized as minima by analytical vibrational frequency calculations,[36] which revealed the absence of imaginary frequencies. Vertical singlet excitations were calculated by means of time-dependent DFT[37] using the same density functional–basis set combination as specified above.

4.2.5 References

[1] a) A. C. Grimsdale, K. L. Chan, R. E. Martin, P. G. Jokisz, A. B. Holmes, *Chem. Rev.* **2009**, *109*, 897–1091; b) C. Wang, H. Dong, W. Hu, Y. Liu, D. Zhu, *Chem. Rev.* **2012**, *112*, 2208–2267; c) C. Li, M. Liu, N. G. Pschirer, M. Baumgarten, K. Müllen, *Chem. Rev.* **2010**, *110*, 6817–6855; d) S. W. Thomas III, G. D. Joly, T. M. Swager, *Chem. Rev.* **2007**, *107*, 1339–1386.

[2] a) X. He, T. Baumgartner, *RSC Adv.* **2013**, *3*, 11334–11350; b) E. I. Carrera, D. S. Seferos, *Macromolecules* **2015**, *48*, 297–308; c) D. Joly, P.-A. Bouit, M. Hissler, *J. Mater. Chem. C* **2016**, *4*, 3686–3698; d) A. M. Priegert, B. W. Rawe, S. C. Serin, D. P. Gates, *Chem. Soc. Rev.* **2016**, *45*, 922–953; e) K. L. Chan, M. J. McKiernan, C. R. Towns, A. B. Holmes, *J. Am. Chem. Soc.* **2005**, *127*, 7662–7663; f) M. Heeney, W. Zhang, D. J. Crouch, M. L. Chabinyc, S. Gordeyev, R. Hamilton, S. J. Higgins, I. McCulloch, P. J. Skabara, D. Sparrowe, S. Tierney, *Chem. Commun.* **2007**, 5061–5063; g) G. He, Le Kang, W. Torres Delgado, O. Shynkaruk, M. J. Ferguson, R. McDonald, E. Rivard, *J. Am. Chem. Soc.* **2013**, *135*, 5360–5363; h) J. Linshoeft, E. J. Baum, A. Hussain, P. J. Gates, C. Näther, A. Staubitz, *Angew. Chem. Int. Ed.* **2014**, *53*, 12916–12920; *Angew. Chem.* **2014**, *126*, 13130–13134; i) T. Matsumoto, Y. Onishi, K. Tanaka, H. Fueno, K. Tanaka, Y. Chujo, *Chem. Commun.* **2014**, *50*, 15740–15743.

[3] V. A. Wright, D. P. Gates, *Angew. Chem. Int. Ed.* **2002**, *41*, 2389–2392; *Angew. Chem.* **2002**, *114*, 2495–2498; V. A. Wright, B. O. Patrick, C. Schneider, D. P. Gates, *J. Am. Chem. Soc.* **2006**, *128*, 8836–8844.

[4] R. C. Smith, X. F. Chen, J. D. Protasiewicz, *Inorg. Chem.* **2003**, *42*, 5468–5470; R. C. Smith, J. D. Protasiewicz, *J. Am. Chem. Soc.* **2004**, *126*, 2268–2269.

[5] a) C. D. Entwistle, T. B. Marder, *Angew. Chem. Int. Ed.* **2002**, *41*, 2927–2931; *Angew. Chem.* **2002**, *114*, 3051–3056; b) F. Jäkle, *Chem. Rev.* **2010**, *110*, 3985–4022; c) F. Jäkle, *Top. Organomet. Chem.* **2015**, *49*, 297–325; d) H. Helten, *Chem. Eur. J.* **2016**, *22*, 12972–12982.

[6] For selected examples, see: a) A. Sundararaman, M. Victor, R. Varughese, F. Jäkle, *J. Am. Chem. Soc.* **2005**, *127*, 13748–13749; b) C.-H. Zhao, A. Wakamiya, S. Yamaguchi, *Macromolecules* **2007**, *40*, 3898–3900; c) A. Nagai, J. Miyake, K. Kokado, Y. Nagata, Y. Chujo, *J. Am. Chem. Soc.* **2008**, *130*, 15276–15278; d) A. Lorbach, M. Bolte, H. Li, H.-W. Lerner, M. C. Holthausen, F. Jäkle, M. Wagner, *Angew. Chem. Int. Ed.* **2009**, *48*, 4584–4588; *Angew. Chem.* **2009**, *121*, 4654–4658; e) M. Scheibitz, H. Li, J. Schnorr, A. Sánchez Perucha, M. Bolte, H.-W. Lerner, F. Jäkle, M. Wagner, *J. Am. Chem. Soc.* **2009**, *131*, 16319–16329; f) X. Yin, J. Chen, R. A. Lalancette, T. B. Marder, F. Jäkle, *Angew. Chem. Int. Ed.* **2014**, *53*,

9761–9765; *Angew. Chem.* **2014**, *126*, 9919–9923; g) I. A. Adams, P. A. Rupar, *Macromol. Rapid Commun.* **2015**, *36*, 1336–1340; h) X. Yin, F. Guo, R. A. Lalancette, F. Jäkle, *Macromolecules* **2016**, *49*, 537–546; i) S. Novoa, J. A. Paquette, S. M. Barbon, R. R. Maar, J. B. Gilroy, *J. Mater. Chem. C* **2016**, 4, 3987–3994.

[7] a) Z. Liu, T. B. Marder, *Angew. Chem. Int. Ed.* **2008**, *47*, 242–244; *Angew. Chem.* **2008**, *120*, 248–250; b) M. J. D. Bosdet, W. E. Piers, *Can. J. Chem.* **2009**, *87*, 8–29; c) P. G. Campbell, A. J. V. Marwitz, S.-Y. Liu, *Angew. Chem. Int. Ed.* **2012**, *51*, 6074–6092; *Angew. Chem.* **2012**, *124*, 6178–6197; d) M. M. Morgan, W. E. Piers, *Dalton Trans.* **2016**, *45*, 5920–5924.

[8] For selected examples, see: a) M. J. D. Bosdet, W. E. Piers, T. S. Sorensen, M. Parvez, *Angew. Chem. Int. Ed.* **2007**, *46*, 4940–4943; *Angew. Chem.* **2007**, *119*, 5028–5031; b) S. Xu, L. N. Zakharov, S.-Y. Liu, *J. Am. Chem. Soc.* **2011**, *133*, 20152–20155; c) H. Braunschweig, A. Damme, J. O. C. Jimenez-Halla, B. Pfaffinger, K. Radacki, J. Wolf, *Angew. Chem. Int. Ed.* **2012**, *51*, 10034–10037; *Angew. Chem.* **2012**, *124*, 10177–10180; d) H. Braunschweig, K. Geetharani, J. O. C. Jimenez-Halla, M. Schäfer, *Angew. Chem. Int. Ed.* **2014**, *53*, 3500–3504; *Angew. Chem.* **2014**, *126*, 3568–3572; e) H. Braunschweig, M. A. Celik, F. Hupp, I. Krummenacher, L. Mailänder, *Angew. Chem. Int. Ed.* **2015**, *54*, 6347–6351; *Angew. Chem.* **2015**, *127*, 6445–6449; f) K. Edel, S. A. Brough, A. N. Lamm, S.-Y. Liu, H. F. Bettinger, *Angew. Chem. Int. Ed.* **2015**, *54*, 7819–7822; *Angew. Chem.* **2015**, *127*, 7930–7933; g) X.-Y. Wang, A. Narita, X. Feng, K. Müllen, *J. Am. Chem. Soc.* **2015**, *137*, 7668–7671; h) S. Wang, D.-T. Yang, J. Lu, H. Shimogawa, S. Gong, X. Wang, S. K. Mellerup, A. Wakamiya, Y.-L. Chang, C. Yang, Z.-H. Lu, *Angew. Chem. Int. Ed.* **2015**, *54*, 15074–15078; *Angew. Chem.* **2015**, *127*, 15289–15293; i) M. Krieg, F. Reicherter, P. Haiss, M. Ströbele, K. Eichele, M.-J. Treanor, R. Schaub, H. F. Bettinger, *Angew. Chem. Int. Ed.* **2015**, *54*, 8284–8286; *Angew. Chem.* **2015**, *127*, 8402–8404; j) X. Wang, F. Zhang, K. S. Schellhammer, P. Machata, F. Ortmann, G. Cuniberti, Y. Fu, J. Hunger, R. Tang, A. A. Popov, R. Berger, K. Müllen, X. Feng, *J. Am. Chem. Soc.* **2016**, *138*, 11606–11615.

[9] For azaborinine oligomers and PAHs containing multiple azaborinine moieties, see: a) T. Agou, J. Kobayashi, T. Kawashima, *Chem. Commun.* **2007**, 3204–3206; b) C. A. Jaska, W. E. Piers, R. McDonald, M. Parvez, *J. Org. Chem.* **2007**, *72*, 5234–5243; c) O. Lukoyanova, M. Lepeltier, M. Laferrière, D. F. Perepichka, *Macromolecules* **2011**, *44*, 4729–4734; d) T. Hatakeyama, S. Hashimoto, S. Seki, M. Nakamura, *J. Am. Chem. Soc.* **2011**, *133*, 18614–18617; e) Marwitz, Adam J. V., A. N. Lamm, L. N. Zakharov, M. Vasiliu, D. A. Dixon, S.-Y. Liu, *Chem. Sci.* **2012**, *3*, 825–829; f) B. Neue, J. F. Araneda, W. E. Piers, M. Parvez, *Angew. Chem. Int. Ed.* **2013**, *52*, 9966–9969; *Angew. Chem.* **2013**, *125*, 10150–10153; g) X.

Wang, F. Zhang, J. Liu, R. Tang, Y. Fu, D. Wu, Q. Xu, X. Zhuang, G. He, X. Feng, *Org. Lett.* **2013**, *15*, 5714–5717; h) H. Braunschweig, C. Hörl, L. Mailänder, K. Radacki, J. Wahler, *Chem. Eur. J.* **2014**, *20*, 9858–9861; i) X.-Y. Wang, F.-D. Zhuang, X.-C. Wang, X.-Y. Cao, J.-Y. Wang, J. Pei, *Chem. Commun.* **2015**, *51*, 4368–4371; j) X. Wang, F. Zhang, J. Gao, Y. Fu, W. Zhao, R. Tang, W. Zhang, X. Zhuang, X. Feng, *J. Org. Chem.* **2015**, *80*, 10127–10133; k) M. Schäfer, N. A. Beattie, K. Geetharani, J. Schäfer, W. C. Ewing, M. Krahfuß, C. Hörl, R. D. Dewhurst, S. A. Macgregor, C. Lambert, H. Braunschweig *J. Am. Chem. Soc.* **2016**, *138*, 8212–8220.

[10] For polymers containing 1,3,2-benzodiazaboroline building blocks, see: a) I. Yamaguchi, B.-J. Choi, T.-a. Koizumi, K. Kubota, T. Yamamoto, *Macromolecules* **2007**, *40*, 438–443; b) I. Yamaguchi, T. Tominaga, M. Sato, *Polym. Int.* **2009**, *58*, 17–21; c) S. Hayashi, T. Koizumi, *Polym. Chem.* **2012**, *3*, 613–616.

[11] A. W. Baggett, F. Guo, B. Li, S.-Y. Liu, F. Jäkle, *Angew. Chem. Int. Ed.* **2015**, *54*, 11191–11195; *Angew. Chem.* **2015**, *127*, 11343–11347.

[12] X.-Y. Wang, F.-D. Zhuang, J.-Y. Wang, J. Pei, *Chem. Commun.* **2015**, *51*, 17532–17535.

[13] For non-conjugated polymers containing azaborinine moieties in side chains, see: a) W.-M. Wan, A. W. Baggett, F. Cheng, H. Lin, S.-Y. Liu, F. Jäkle, *Chem. Commun.* **2016**, *52*, 13616–13619; b) B. Thiedemann, P. J. Gliese, J. Hoffmann, P. G. Lawrence, F. D. Sönnichsen, A. Staubitz, *Chem. Commun.*, DOI: 10.1039/c6cc08599g.

[14] Matsumi and Chujo have presented poly(boronic carbamate)s. Investigation of possible π-conjugation, however, was not mentioned by the authors: N. Matsumi, Y. Chujo, *Macromolecules* **1998**, *31*, 3802–3806.

[15] Polymers with *meta*-phenylene-linked aminoborane B=N units in the backbone and acyl groups at nitrogen showed poorly extended conjugation. This was attributed to the presence of cross-links in the polymer chains. See: a) N. Matsumi, K. Kotera, K. Naka, Y. Chujo, *Macromolecules* **1998**, *31*, 3155–3157; b) N. Matsumi, K. Kotera, Y. Chujo, *Macromolecules* **2000**, *33*, 2801–2806.

[16] T. Lorenz, A. Lik, F. A. Plamper, H. Helten, *Angew. Chem. Int. Ed.* **2016**, *55*, 7236–7241; *Angew. Chem.* **2016**, *128*, 7352–7357.

[17] O. Ayhan, T. Eckert, F. A. Plamper, H. Helten, *Angew. Chem. Int. Ed.* **2016**, *55*, 13321–13325; *Angew. Chem.* **2016**, *128*, 13515–13519.

[18] Theoretical studies predict that the (partial) substitution of CC by BN units in conjugated organic polymers should result in an increase in the electronic band gap of these materials: a) A. Abdurahman, M. Albrecht, A. Shukla, M. Dolg, *J. Chem. Phys.* **1999**, *110*, 8819–8824; b) M. Côté, P. D. Haynes, C. Molteni, *Phys. Rev. B* **2001**, *63*, 125207.

[19] Their organic congeners exist as copolymers with both enamine and imine functional groups in the backbone: S. Greenberg, D. W. Stephan, *Polym. Chem.* **2010**, *1*, 1332–1338.

[20] a) R. A. Bartlett, X. Feng, M. M. Olmstead, P. P. Power, K. J. Weese, *J. Am. Chem. Soc.* **1987**, *109*, 4851–4854; b) H. Chen, R. A. Bartlett, M. M. Olmstead, P. P. Power, S. C. Shoner, *J. Am. Chem. Soc.* **1990**, *112*, 1048–1055.

[21] a) R. Schenk, H. Gregorius, K. Meerholz, J. Heinze, K. Müllen, *J. Am. Chem. Soc.* **1991**, *113*, 2634–2647; b) P. L. Burn, D. D. C. Bradley, R. H. Friend, D. A. Halliday, A. B. Holmes, R. W. Jackson, A. Kraft, *J. Chem. Soc., Perkin Trans. 1* **1992**, 3225–3231; c) H. Becker, H. Spreitzer, W. Kreuder, E. Kluge, H. Schenk, I. Parker, Y. Cao, *Adv. Mater.* **2000**, *12*, 42–48.

[22] K. Ruhlandt-Senge, J. Ellison, R. Wehmschulte, F. Pauer, P. Power, *J. Am. Chem. Soc.*, **1993**, *115*, 11353-11357.

[23] D. Kaufmann, *Chem. Ber.*, **1987**, *120*, 853-854.

[24] M. Fuchter, C. Smith, M. Tsang, A. Boyer, S. Saubern, J. Ryan, A. Holmes, *Chem.Comm.*, **2008**, *18*, 2152-2154.

[25] H. Bock, J. Meuret, C. Näther, U. Krynitz, *Chem. Ber.*, **1994**, *127*, 55-65.

[26] M. C. Haberecht, J. B. Heilmann, A. Haghiri, M. Bolte, J. W. Bats, H.-W. Lerner, M. C. Holthausen, M. Wagner, *Z. Anorg. Allg. Chem.*, **2004**, *630*, 904–913.

[27] SADABS: Area-Detector Absorption Correction; Siemens Industrial Automation, Inc.: Madison, WI, **1996**.

[28] O. V. Dolomanov, L. J. Bourhis, R. J. Gildea, J. A. K. Howard, H. Puschmann, *J. Appl. Cryst.* **2009**, *42*, 339–341.

[29] a) G. M. Sheldrick, *Acta Crystallogr., Sect. A*, **2008**, *64*, 112–122; b) G. M. Sheldrick, *Acta Crystallogr., Sect. C*, **2015**, *71*, 3–8.

[30] B. Vestergaard, S. Hansen, *J. Appl. Crystallogr.* **2006,** *39*, 797–804.

[31] A. J. F. Siegert, *MIT Rad Lab Rep No 465* **1943**.

[32] R. Ahlrichs, M. Bär, M. Häser, H. Horn, C. Kölmel, *Chem. Phys. Lett.* **1989**, *162*, 165–169.

[33] a) P. A. M. Dirac, *Proc. R. Soc. London, Ser. A* **1929**, *123*, 714–733; b) J. C. Slater, *Phys. Rev.* **1951**, *81*, 385–390; c) A. D. Becke, *Phys. Rev. A.* **1988**, *38*, 3098–3100; d) C. Lee, W. Yang, R. G. Parr, *Phys. Rev. B* **1988**, *37*, 785–789; e) A. D. Becke, *J. Chem. Phys.* **1993**, *98*, 5648–5652.

[34] A. Schäfer, H. Horn, R. Ahlrichs*, J. Chem. Phys.* **1992**, *97*, 2571–2577.

[35] a) S. Grimme, J. Antony, S. Ehrlich, H. Krieg, *J. Chem. Phys.* **2010**, *132*, 154104; b) S. Grimme, S. Ehrlich, L. Goerigk, *J. Comput. Chem.* **2011**, *32*, 1456–1465.

[36] P. Deglmann, F. Furche, R. Ahlrichs, *Chem. Phys. Lett.* **2002**, *362*, 511–518; b) P. Deglmann, F. Furche, *J. Chem. Phys.* **2002**, *117*, 9535–9538.

[37] a) R. Bauernschmitt, R. Ahlrichs, *Chem. Phys. Lett.* **1996**, *256*, 454–464; b) R. Bauernschmitt, R. Ahlrichs, *J. Chem. Phys.* **1996**, *104*, 9047–9052; c) F. Furche, D. Rappoport, *Density functional methods for excited states: equilibrium structure and electronic spectra.* In M. Olivucci, Ed., *Computational Photochemistry*, Vol. 16 of *Computational and Theoretical Chemistry*, ch. III., Elsevier, Amsterdam, **2005**.

4.3 BN- and BO-Doped Inorganic–Organic Hybrid Polymers With Sulfoximine Core Units

The following section is slightly modified and reproduced from published article[5] with permission from Wiley-VCH.

While polysulfones constitute a class of well-established, highly valuable applied materials, knowledge about polymers based on the related sulfoximine group is very limited. We have employed functionalized diaryl sulfoximines and a p-phenylene bisborane as building blocks for unprecedented BN- and BO-doped alternating inorganic–organic hybrid copolymers. While the former were accessed by a facile silicon/boron exchange protocol, the synthesis of polymers with main-chain B–O linkages was achieved by salt elimination.

4.3.1 Introduction

Polysulfones are a family of plastic materials that are noted for their high thermal and oxidative stability.[1] They are being used within fluid handling components, steam sterilisable biomedical moldings as well as in a range of chemical process and automotive applications.[2] Some of us recently reported a series of BN-doped inorganic–organic hybrid polymers,[3-6] including the first poly(p-phenylene iminoborane), which can be regarded as a BN-analogue of poly(p-phenylene vinylene) (PPV).[3d] A dapson-type diaryl sulfone was also incorporated into a polymeric material.[3e]

Formal exchange of a sulfonyl oxygen by a nitrogen atom converts a sulfone into a sulfoximine. The latter compounds are relevant in asymmetric synthesis[7] and applications in medicinal[8] and crop protection chemistry.[9] Functionalising the sulfoximine nitrogen allows a fine-tuning of physicochemical properties, which proved useful in drug design and bioactivity adjustment.[10] Surprisingly, sulfoximines have only once been applied as building blocks in polymers.[11] In that study, Takata et al. used Friedel–Crafts reactions to prepare polysulfoximines with molecular weights (Mn) of approximately 13 000. Herein, we describe the synthesis and characterization of the first inorganic–organic hybrid polysulfoximines.

[5] F. Brosge, T. Lorenz, H. Helten, C. Bolm, *Chem. Eur. J.*, **2019**, *25*, 12708–12711.

4.3.2 Results and Discussion

In light of previous work [12] sulfoximines **1** and **2** were identified as suitable organic starting materials. Both compounds were *N*-methylated, thereby confining the reactive anchor sites of the molecules to the free arylic amino and hydroxyl groups. With the vision to allow future variations of the *N*-substituent, phthalimid- and benzyl-protected *N*H-sulfoximines **4** and **6**, respectively, were targeted first. The synthetic sequences are shown in Scheme 4.3.1. The preparation of **1** started from known diarylsulfide **3**,[12] which was imidated and oxidized by adopting a protocol reported by Luisi, Bull, and others[13] to give **4** in 62% yield. Noteworthy, we applied aqueous ammonia as nitrogen source instead of the originally suggested ammonium carbamate. N-Methylation under standard Eschweiler-Clark conditions afforded sulfoximine **5** (21%), which was deprotected with hydrazine in ethanol to give **1** in 61% yield. Following an analogous reaction sequence, sulfoximine **2** was prepared by imidation/oxidation of **6**[14] to give **7** (64%) followed by N-methylation with MeI in KOH/DMSO[15] providing **8** in 48% yield and sequential debenzylation with BBr_3 (98%).

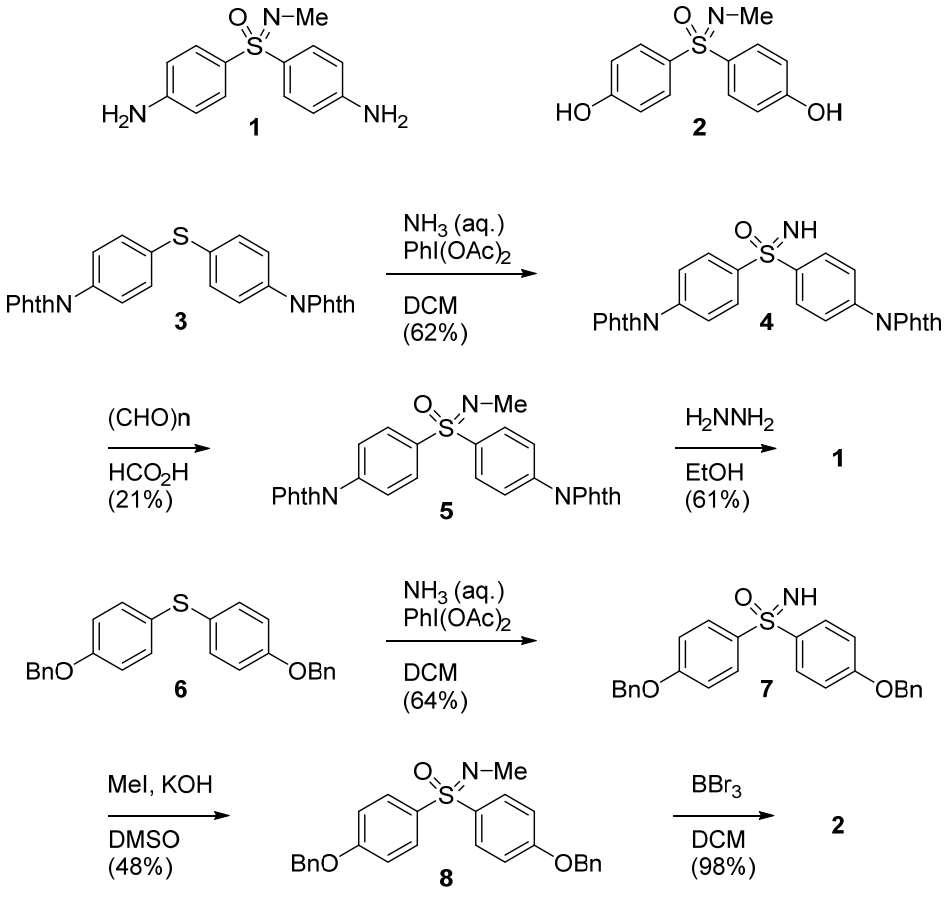

Scheme 4.3.1. Syntheses of key intermediates **1** and **2**.

Targeting a polymer formation by silicon/boron exchange, bis(silylated) sulfoximine **9** was prepared, in analogy of literature precedence,[16] by treatment of **1** with a mixture of Me_3SiCl and Et_3N in THF at 45 °C for 24 h. The coupling partner for **9** was bis(bromoborane) **10**[3d] (Tip = 2,4,6-triisopropylphenyl). Two co-polycondensation reactions were performed (Scheme 4.3.2). In both cases, a 1:1 ratio of **9** and **10** was applied. In the first experiment (trial 1), the mixture was kept in dichloromethane for 3 days at ambient temperature. Trial 2 involved *o*-difluorobenzene (*o*-DFB) as the solvent and heating of the mixture to 80 °C for 24 h. The resulting alternating copolymers **11** were then purified by precipitation from concentrated solutions with hexane and subsequent drying in vacuo.

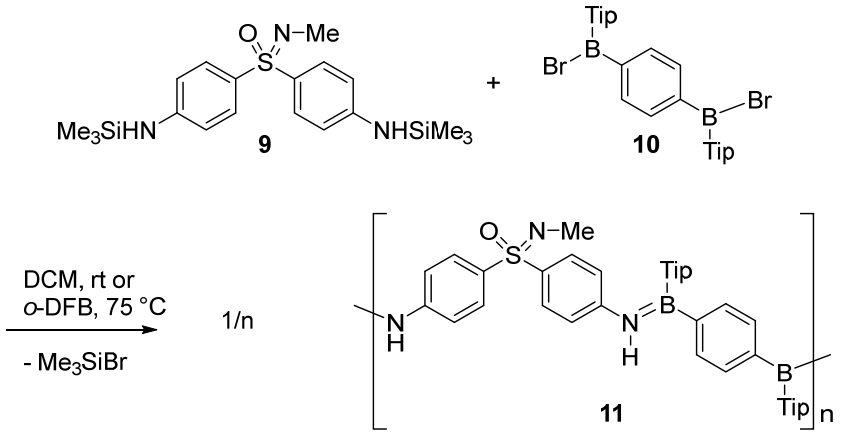

Scheme 4.3.2. Polycondensation reaction of sulfoximine **9** and bisborane **10** to give alternating copolymer **11**.

The identities of copolymers **11**, which were obtained as off-white solids, were unambiguously ascertained by multinuclear NMR spectroscopy. Their molecular mass distributions were determined by gel permeation chromatography (GPC, Table 4.3-1). For both samples, the ^1H NMR spectrum showed a shift of the N*H*-signal from $\delta = 3.77$ ppm in **9** to the aromatic region in **11** (7.25 ppm), which was also observed in previously prepared related BN polymers.[3d] The GPC analyses revealed number average molecular weights of M_n = 9 750 Da (trial 1) and 11 830 Da (trial 2), according to polymerization degrees of $DP_n = 13$ and 15, respectively. The polydispersity indices were close to 2, as expected for step-growth polycondensation processes.

Table 4.3-1. GPC data of polymers **11** and **15** (against polystyrene standards)

	M_n/Da	M_w/Da	PDI	DP_n
11 (trial 1)[a]	9 750	18 600	1.91	13
11 (trial 2)[b]	11 830	28 900	2.44	15
15 (trial 1)[a]	2400	2970	1.52	3
15 (trial 2)[b]	5300	9740	1.84	7

[a] Prepared in dichloromethane (DCM), rt, 3 d. [b] Prepared in o-difluorobenzene (o-DFB), 80 °C, 24 h.

Next, copolymers with main chain B–O linkages[17] were targeted. Hypothesising that such products could be accessed by analogous Si/B exchange reactions as applied before in the synthesis of **11**, organic starting materials with silylated phenolic hydroxyl groups became of interest. In order to get an estimate of the feasibility of such an approach, a prior model reaction between **10** and trimethylsilylated phenol **12** was performed (Scheme 4.3.3).

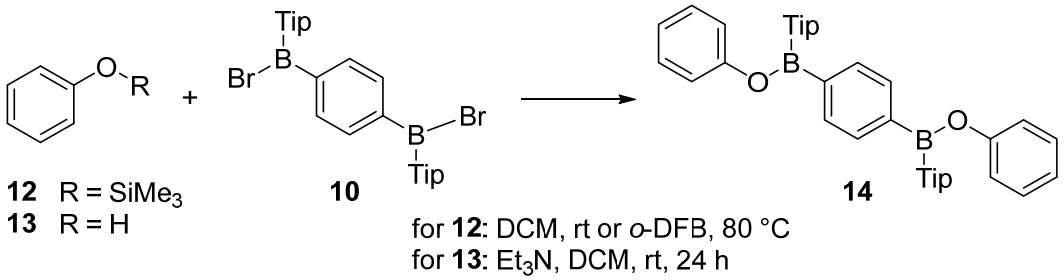

Scheme 4.3.3. Model reactions testing the feasibility of Si/B exchange and salt elimination reactions in the formation of alternating copolymers with B–O linkages.

In the first experiment, the reaction was run in dichloromethane at room temperature. As hypothesised, product **14** was indeed formed as revealed by ^{1}H and ^{11}B NMR spectroscopy. The initial presence of two doublets (8.04 ppm and 7.88 ppm) in the ^{1}H NMR spectrum suggested a stepwise formation of **14**. However, the entire process was very slow, and even after 4 weeks the conversion was not yet complete. A similar outcome resulted when *o*-difluorobenzene was used as solvent at a reaction temperature of 80 °C. Also in this case, the conversion was slow, taking 5 weeks in total. Although these results showed that a Si/B exchange could, in principle, be applied to accomplish a B–O bond formation starting from **10**, the slow rate of this process proved unfavourable for its application to co-polycondensation reactions. Therefore, we decided to investigate B–O bond formation between **10** and the parent free phenol (**13**). While initial attempts without base remained unsatisfying, the presence of triethylamine had a tremendously positive effect, leading to a clean and quantitative coupling

providing **14** within 24 hours at room temperature. Compound **14** was then isolated by filtration and characterized by multinuclear NMR spectroscopy. The $^{11}B\{^{1}H\}$ NMR spectrum showed a resonance at $\delta = 47.3$ ppm, which is in the expected range for the suggested constitution.

Encouraged by this result, the aforementioned conditions were applied in the copolymerization of sulfoximine **2** with bisborane **10** (Scheme 4.3.4). Within 3 days in the presence of Et_3N, the dichloromethane solution became highly viscous (trial 1). However, after work-up the GPC analysis revealed that the product was of relatively low molecular weight (M_n = 2 400 Da, DP_n = 3; Table 4.3-1). Consequently, in the next experiment (trial 2) the solvent was changed to *o*-DFB, and the reaction temperature was raised to 80 °C. Pleasingly, in this manner, after 24 h the molecular weight (M_n) of the resulting polymer **15** was increased to 5 300 Da, revealing an average chain length of DP_n = 7 (Table 1).[6]

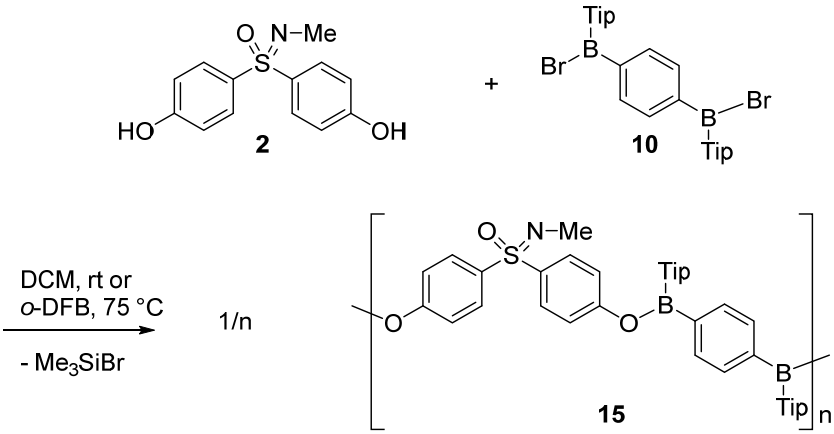

Scheme 4.3.4. Polycondensation reaction of sulfoximine **2** and bisborane **10** to give alternating copolymer **15**.

4.3.3 Conclusion

In summary, we have prepared the first inorganic–organic hybrid sulfoximine-containing polymers as alternating copoly mers with B=N and B–O linkages. While our Si/B exchange polycondensation protocol was successful in the former case, for the synthesis of polymers with B–O linkages in the main chain a salt elimination approach proved to be favorable. In view of the recently demonstrated advantageous effect of the formulation of dapsone-type drugs into polymer conjugates for anti-inflammatory purposes[18] on the one hand, and the well-established biomedical activity of many boron-containing polymers[19] on the other hand, we are currently exploring the biomedical potential of our novel sulfoximine-B=N/B–O hybrids in detail.

[6] The product obtained still contained some amount of [Et3NH]Br by-product, which could not be fully separated after repeated precipitation.

4.3.4 Experimental Section

General procedures. Unless otherwise stated, all reagents were purchased from commercial suppliers and used without further purification. All solvents were distilled prior to using. When required, solvents were dried according to general purification methods. Reactions were tracked by thin layer chromatography using aluminum foil backed silica TLC plates with a fluorescent indicator from Merck. UV-active compounds were detected with a UV lamp (λ = 254 nm). For flash column chromatography (FCC), silica gel 60 (63–200 μm) was used as stationary phase. ^{1}H and ^{13}C NMR spectra were recorded either on a Varian V-NMRS 600, Varian V-NMRS 400 or Varian Mercury 300 in deuterated solvents. The chemical shifts (δ) are given in ppm relative to the residual peak of the non-deuterated solvent as internal standard (^{1}H: $CDCl_3$, 7.26 ppm; DMSO-*d*$_6$, 2.50 ppm; MeCN-*d*$_3$, 1.94 ppm; acetone-*d*$_6$, 2.05 ppm; ^{13}C: $CDCl_3$, 77.16 ppm; DMSO-*d*$_6$, 39.52 ppm; MeCN-*d*$_3$, 118.26 ppm; acetone-*d*$_6$, 29.84 ppm) or external $BF_3 \cdot OEt_2$ (^{11}B). ^{13}C{^{1}H} NMR spectra were recorded at 100 or 151 MHz with complete proton decoupling and will be stated as ^{13}C for simplification. Spin-spin coupling constants (*J*) are given in Hz. Coupling patterns are given as br s (broad singlet), s (singlet), t (triplet), q (quartet), sept (septet) and m (multiplet). Data are reported as follows: Chemical shift, multiplicity and integration. The IR spectra were recorded on a PerkinElmer Spectrum 100 spectrometer with an attached UATR device Diamond KRS-5. All IR data were collected by attenuated total reflectance (ATR) and wave numbers ν are given in cm^{-1}. Mass spectra were recorded on a Finnigan SSQ 7000 spectrometer (EI, 70 eV). High resolution mass spectra (HRMS) were recorded on a Thermo Scientific LTQ Orbitrap XL spectrometer. Melting points (mp) were measured on a Büchi B-560 melting point apparatus.

Spectra. All spectra and other result figures are shown in Appendix 7.3.

Synthesis

Synthesis of 3. To a solution of 4,4'-thiodianiline (6.00 g, 27.7 mmol) in AcOH (111 mL) phthalic anhydride (9.04 g, 61.0 mmol) was added. The reaction mixture was heated to reflux overnight. After cooling to room temperature the solvent was removed under reduced pressure. The title compound **3** (12.4 g, 25.8 mmol, 93%) was isolated after purification by FCC (1–2% EtOAc in DCM) as a white solid. ^{1}H NMR (600 MHz, DMSO-*d*$_6$) δ = 8.00–7.97 (m, 4H), 7.93–

7.90 (m, 4H), 7.55–7.50 (m, 8H) ppm. $^{13}C\{^{1}H\}$ NMR (151 MHz, DMSO-d_6) δ = 166.9, 134.8, 134.3, 131.5, 131.3, 131.2, 128.4, 123.5 ppm.

The NMR data is in accordance with the literature.[20]

Synthesis of 6. To an ice cold solution of 4,4'-thiodiphenol (5.00 g, 22.9 mmol) in dry THF (90 mL) was added NaH (60% in petrol oil, 2.29 g, 57.3 mmol). The reaction mixture was stirred for 30 min at 0 °C. Then benzyl bromide (10.9 mL, 91.7 mmol) was added. The reaction mixture was stirred overnight at room temperature. Ice was added and the aqueous phase was extracted three times with DCM. The combined organic phases were washed with water, dried over $MgSO_4$ and filtered. The solvent was removed under reduced pressure. The title compound **6** (8.46 g, 21.2 mmol, 93%) was isolated after purification by FCC (10–50% DCM in pentane) as a white solid. ^{1}H NMR (400 MHz, $CDCl_3$) δ = 7.43–7.27 (m, 14H), 6.93–6.90 (m, 4H), 5.04 (s, 4H) ppm. $^{13}C\{^{1}H\}$ NMR (101 MHz, $CDCl_3$) δ = 158.3, 136.9, 132.9, 128.8, 128.2, 127.8, 127.6, 115.8, 70.3 ppm.

The NMR data is in accordance with the literature.[21]

General procedure for the synthesis of *N*H sulfoximines from sulfides (GP 1): The sulfide (**3** or **6**, 1.0 equiv.) was dissolved in DCM (5 mL/mmol). An aqueous solution of NH_3 (13.5 M, 4.0 equiv.) and (diacetoxyiodo)benzene (2.5 equiv.) were added at room temperature, and the reaction mixture was stirred overnight. The solvent was either removed under reduced pressure (**4**, variant A) or water was added to the reaction mixture and it was extracted three times with DCM. The combined organic layers were washed with water and dried over $MgSO_4$, filtered and then the solvent was removed under reduced pressure (**7**, variant B). The corresponding product (**4** or **7**) was isolated after purification by FCC (5–15% EtOAc in DCM).

Synthesis of 4. Prepared according to GP 1 (variant A) from 2,2′-[4,4′-thiobis(1,4-phenylene)]diisoindoline-1,3-dione (**3**) (5.50 g, 11.5 mmol), (diacetoxyiodo)benzene (9.26 g, 28.8 mmol) and aqueous NH_3 solution (3.41 mL, 46.0 mmol). The title compound **4** (3.61 g, 7.11 mmol, 62%) was isolated after purification by FCC as a white solid; mp: 274–275 °C. ^{1}H NMR (600 MHz, DMSO-d_6) δ = 8.16–8.15 (m, 4H), 8.00–7.97 (m, 4H), 7.93–7.92 (m, 4H), 7.69–7.68 (m, 4H) ppm. $^{13}C\{^{1}H\}$ NMR (151 MHz, DMSO-d_6) δ = 166.5, 142.7, 135.6, 134.9,

131.5, 128.5, 127.6, 123.6 ppm. IR (ATR): ν = 3477, 3265, 3067, 2925, 2852, 2680, 2323, 2106, 1996, 1922, 1708, 1590, 1493, 1373, 1222, 1083, 1013, 948, 885, 836, 796, 716, 669. MS (EI): *m/z* = 145 (14), 143 (39), 108 (23), 91 (100), 77 (21), 65 (13). MS (CI): *m/z* = 192 (10), 178 (11), 123 (78), 114 (11), 101 (16), 89 (75), 87 (63), 85 (100), 83 (94), 75 (18), 73 (31), 71 (12), 61 (79). HRMS (ESI): *m/z* calcd. for $C_{28}H_{18}O_5N_3S$: 508.0962; found: 508.0953.

Synthesis of 7. Prepared according to GP 1 (variant B) from bis[4-(benzyloxy)phenyl]sulfide (**6**) (7.50 g, 18.8 mmol), (diacetoxyiodo)benzene (15.1 g, 47.0 mmol) and aqueous NH_3 solution (5.57 mL, 75.2 mmol). The title compound **7** (5.18 g, 12.1 mmol, 64%) was isolated after purification by FCC as a white solid; mp: 159–161 °C. ^{1}H NMR (600 MHz, $CDCl_3$) δ = 7.95–7.94 (m, 4H), 7.39–7.32 (m, 10H), 7.01–7.00 (m, 4H), 5.08 (s, 4H) ppm. $^{13}C\{^1H\}$ NMR (151 MHz, $CDCl_3$) δ = 162.0, 135.9, 135.3, 129.8, 128.7, 128.3, 127.4, 115.1, 70.3 ppm. IR (ATR): ν = 3459, 3319, 3025, 2937, 2294, 2101, 1985, 1909, 1739, 1583, 1489, 1376, 1303, 1224, 1093, 977, 828, 747, 699. MS (EI): *m/z* = 429 ($[M]^+$, 10), 198 (17), 91 (100). MS (CI): *m/z* = 458 (22), 431 (26), 430 ($[M+H]^+$, 91), 248 (40), 246 (11), 185 (13), 107 (28), 104 (12), 93 (18), 92 (24), 91 (100). HRMS (ESI): *m/z* calcd. for $C_{26}H_{23}O_3NNaS$: 452.1291; found: 452.1282.

Synthesis of 8. To a solution of bis[4-(benzyloxy)phenyl](imino)-λ^6-sulfanone (**7**) (4.00 g, 9.31 mmol) in dry DMSO (14 mL) was added KOH (1.04 g, 18.6 mmol). The reaction mixture was stirred for 30 min at room temperature. Afterwards MeI (0.868 mL, 14.0 mmol) was added and the reaction mixture was stirred overnight. Upon completion of the reaction, water was added and the aqueous phase was extracted three times with DCM. The combined organic layers were washed with water, dried over $MgSO_4$ and filtered. The solvent was removed under reduced pressure. The title compound **8** (1.98 g, 4.45 mmol, 48%) was isolated after purificaion by FCC (1–5% EtOAc in DCM) as a white solid; mp: 109–111 °C. ^{1}H NMR (600 MHz, $CDCl_3$) δ = 7.91–7.89 (m, 4H), 7.39–7.33 (m, 10H), 7.07–7.04 (m, 4H), 5.09 (s, 4H), 2.82 (s, 3H) ppm. $^{13}C\{^1H\}$ NMR (151 MHz, $CDCl_3$) δ = 162.6, 135.9, 130.7, 128.9, 128.5, 127.6, 115.7, 115.7, 70.5, 29.2 ppm. IR (ATR): ν = 3066, 3035, 2922, 2875, 2804, 2322, 2105, 1907, 1736, 1654, 1584, 1491, 1461, 1386, 1301, 1235, 1174, 1140, 1098, 995, 919, 865, 835, 750, 697. MS (EI): *m/z* = 91 (100). MS (CI): *m/z* = 444 ($[M+H]^+$, 14), 252 (15), 225 (16), 224 (100). HRMS (ESI): *m/z* calcd. for $C_{27}H_{26}O_3NS$: 444.1628; found: 444.1625.

Synthesis of 1. To a solution of 2,2'-[(methylsulfonimidoyl)bis(1,4-phenylene)]bis(isoindoline-1,3-dione) (**5**) (346 mg, 0.663 mmol) in EtOH (7 mL) was added an aqueous hydrazine monohydrate solution (60%, 3.30 mL, 0.66 mmol). The reaction mixture was stirred overnight. Upon completion of the reaction, water was added and the aqueous phase was extracted five times with EtOAc. The combined organic phases were dried over $MgSO_4$, filtered and the solvent was removed under reduced pressure. The title compound **1** (106 mg, 0.404 mmol, 61%) was isolated after purification by FCC (1–5% MeOH in DCM + 0.5% NEt_3) as a white solid; mp: 175–176 °C. ^{1}H NMR (600 MHz, MeCN-*d*$_3$) δ = 7.54–7.52 (m, 4H), 6.65–6.63 (m, 4H), 4.69 (s, 4H), 2.61 (s, 3H) ppm. ^{13}C{^{1}H} NMR (151 MHz, MeCN-*d*$_3$) δ =152.6, 130.7, 129.3, 114.5, 29.7 ppm. IR (ATR): ν = 3558, 3478, 3427, 3361, 3312, 3184, 3063, 2967, 2929, 2875, 2805, 2666, 2322, 2169, 2114, 1990, 1911, 1742, 1625, 1590, 1497, 1462, 1400, 1337, 1307, 1258, 1206, 1144, 1070, 993, 940, 912, 861, 809, 753, 716, 696, 660. MS (EI): *m/z* = 261 ([M]$^+$, 4), 122 (10), 121 (100), 94 (16), 93 (24), 92 (16), 65 (36). MS (CI): *m/z* = 290 (15), 263 (11), 262 ([M+H]$^+$, 100), 140 (26), 121 (57). HRMS (ESI): *m/z* calcd. for $C_{13}H_{16}ON_3S$: 262.1009; found: 262.1008.

Synthesis of 2. To an ice cold solution of bis[4-(benzyloxy)phenyl](methylimino)-λ^6-sulfanone (**8**) (1.33 g, 5.19 mmol) in dry DCM (60 mL) was added BBr_3 (1 M in DCM, 10.4 mL, 10.4 mmol). The reaction mixture was stirred at room temperature for 30 min. Upon completion of the reaction, ice was added and the solvent was removed under reduced pressure. The title compound **2** (1.33 g, 5.07 mmol, 98%) was isolated after purification by FCC (3–10% MeOH in DCM + 0.1% NEt_3) as a white solid; mp: 60 °C. ^{1}H NMR (600 MHz, Acetone-*d*$_6$) δ = 9.23 (br s, 2H), 7.78–7.76 (m, 4H), 6.95–6.93 (m, 4H), 2.66 (s, 3H) ppm. ^{13}C{^{1}H} NMR (151 MHz, Acetone-*d*$_6$) δ = 161.7, 132.9, 131.4, 116.5, 29.5 ppm. IR (ATR): ν = 3275, 2924, 2803, 2671, 2577, 2473, 2178, 2103, 1985, 1911, 1699, 1577, 1492, 1443, 1376, 1283, 1222, 1141, 1087, 831, 718, 691. MS (EI): *m/z* = 263 ([M]$^+$, 6), 182 (27), 142 (15), 141 (18), 123 (10), 122 (100), 93 (31), 82 (46), 81 (13), 80 (47), 79 (17), 65 (42), 63 (15), 55 (11), 53 (12). MS (CI): *m/z* = 242 (16), 241 (100), 214 (11), 213 (60), 182 (34), 156 (23), 141 (55), 125 (13), 111 (11), 79 (13). HRMS (ESI): *m/z* calcd. for $C_{13}H_{14}O_3NS$: 264.0689; found: 264.0679.

Synthesis of 9. To a solution of **1** (21.4 mg, 0.08 mmol) in THF (0.7 mL) was added Et_3N (0.2 mL) and TMSCl (0.04 mL, 0.32 mmol). The reaction mixture was heated at 45 °C for 24 h. The solvent was removed in vacuo. The product was extracted with hexane (3 x 3 mL) and the solvent was removed in vacuo. **9** was isolated as white solid (27.6 mg, 0.068 mmol, 85%). ^{1}H-NMR (400 MHz, $CDCl_3$) δ = 7.68–7.66 (m, 4H), 6.64–6.2 (m, 4H), 3.77 (s, 2H, N*H*), 2.78 (s, 3H, NC*H*$_3$), 0.27 (s, 18H, Si(C*H*$_3$)$_3$) ppm.

Synthesis of polymer 11 (trial 2). To a suspension of **9** (40.5 mg, 0.10 mmol) in *o*-DFB (0.5 mL) was added a solution of **10**[22] (66.5 mg, 0.10 mmol) in *o*-DFB (0.5 mL). The mixture was heated to 80 °C for 24 h. Then the product was precipitated with hexane. All volatiles were removed, and the product was dried in vacuo. ^{1}H-NMR (400 MHz, $CDCl_3$) δ = 7.61 (s, 4H), 7.59 (s, 4H), 7.25 (br s, 2H, N*H*), 6.97 (s, 4H), 6.91 (d, 4H), 2.92 (sept, 2H), 2.68 (s, 3H, NC*H*$_3$), 2.53 (sept, 4H), 1.30 (d, 12H), 0.92 (d, 12H), 0.87 (m, 12H) ppm.

Synthesis of 14. To a solution of **10**[22] (166 mg, 0.25 mmol) in DCM (1.5 mL) was added Et_3N (0.1 mL) and a solution of trimethyl(phenoxy)silane (83 mg, 0.50 mmol) in DCM (0.5 mL). The mixture was stirred for 24 h. Then the solvent was removed in vacuo. The product was extracted with hexane (3 x 2 mL) and the solvent was removed in vacuo. **14** was isolated as a white solid (126 mg, 0.18 mmol, 73 %). ^{1}H-NMR (400 MHz, $CDCl_3$) δ = 7.82 (s, 4H, B-C$_6$*H*$_4$), 7.21–7.17 (m, 4H, Ph), 7.05–6.94 (m, 6H, Ph), 6.89 (s, 4H, C$_6$*H*$_2$), 2.92–2.79 (sept, 2H, C*H*-*i*Pr), 2.66–2.55 (sept, 4H, C*H*-*i*Pr), 1.24 (d, 12H, C*H*$_3$-*i*Pr), 1.01 (d, 24H, C*H*$_3$-*i*Pr) ppm. ^{11}B{^{1}H} NMR (128 MHz, $CDCl_3$): δ = 47.3 ppm (s).

Synthesis of polymer 15 (trial 2). To a solution of **10**[22] (65 mg, 0.10 mmol) in *o*-DFB (1.5 mL), was added Et_3N (0.1 mL) and **2** (26 mg, 0.10 mmol). The mixture was heated to 80 °C for 24 h. The solvent was removed and the product was dried in vacuo. ^{1}H-NMR (400 MHz, $CDCl_3$) δ = 10.87 (br s, 2H, (CH$_3$CH$_2$)$_3$N·*H*Br), 7.76 (s, 4H), 7.67 (d, 4H), 6.98 (d, 4H), 6.83 (s, 4H), 3.12 (q, 12H, (CH$_3$C*H*$_2$)$_3$N·HBr), 2.89–2.75 (m 2H), 2.63 (s, 3H, NC*H*$_3$), 2.50–2.38 (m, 4H), 1.41 (t, 18H, (C*H*$_3$CH$_2$)$_3$N·HBr), 1.21 (m, 12H), 0.92 (br d, 12H) ppm. ^{11}B{^{1}H} NMR (128 MHz, $CDCl_3$): δ = 47.9 ppm (s).

4.3.5 References

[1] J. B. Rose, *Polymer,* **1974**, *15*, 456–465.

[2] D. Parker, J. Bussink, H. T. van de Grampel, G. W. Wheatley, E. Dorf, E. Ostlinning and K. Reinking, (Eds.) Polymers, High-Temperature. In *Ullmann's Encyclopedia of Industrial Chemistry*, **2000**.

[3] (*a*) T. Lorenz, A. Lik, F. A. Plamper and H. Helten, *Angew. Chem. Int. Ed.*, **2016**, *55*, 7236–7241; (*b*) O. Ayhan, T. Eckert, F. A. Plamper and H. Helten, *Angew. Chem. Int. Ed.*, **2016**, *55*, 13321–13325; (*c*) concept: H. Helten, *Chem. Eur. J.*, **2016**, *22*, 12972–12982; (*d*) T. Lorenz, M. Crumbach, T. Eckert, A. Lik and H. Helten, *Angew. Chem. Int. Ed.*, **2017**, *56*, 2780–2784; (*e*) N. A. Riensch, A. Deniz, S. Kühl, L. Müller, A. Adams, A. Pich and H. Helten, *Polym. Chem.*, **2017**, *8*, 5264–5268; (*f*) O. Ayhan, N. A. Riensch, C. Glasmacher and H. Helten, *Chem. Eur. J.*, **2018**, *24*, 5883–5894; (*g*) review: H. Helten, *Chem. Asian J.,* **2019**, ***14***, 919–935.

[4] Examples from other groups: (a) A. W. Baggett, F. Guo, B. Li, S.-Y. Liu and F. Jäkle, *Angew. Chem. Int. Ed.*, **2015**, *54*, 11191–11195; (b) X.-Y. Wang, F.-D. Zhuang, J.-Y. Wang and J. Pei, *Chem. Commun.*, **2015**, *51*, 17532–17535; (c) W.-M. Wan, A. W. Baggett, F. Cheng, H. Lin, S.-Y. Liu and F. Jäkle, *Chem. Commun.*, **2016**, *52*, 13616–13619; (d) D. Marinelli, F. Fasano, B. Najjari, N. Demitri and D. Bonifazi, *J. Am. Chem. Soc.*, **2017**, *139*, 5503–5519; (e) W. Zhang, G. Li, L. Xu, Y. Zhuo, W. Wan, N. Yan and G. He, *Chem. Sci.*, **2018**, *9*, 4444–4450; (f) H. L. van de Wouw, J. Young Lee, E. C. Awuyah and R. S. Klausen, *Angew. Chem. Int. Ed.*, **2018**, *57*, 1673–1677; Angew. Chem. 2018, 130, 1689–1693.

[5] For polymers with B–N single bond linkages, see, e.g.: (a) A. Staubitz, A. Presa Soto and I. Manners, *Angew. Chem. Int. Ed.*, **2008**, *47*, 6212–6215; (b) A. Staubitz, M. E. Sloan, A. P. M. Robertson, A. Friedrich, S. Schneider, P. J. Gates, J. Schmedt auf der Günne and I. Manners, *J. Am. Chem. Soc.*, **2010**, *132*, 13332–13345; (c) W. C. Ewing, A. Marchione, D. W. Himmelberger, P. J. Carroll and L. G. Sneddon, *J. Am. Chem. Soc.,* **2011**, *133*, 17093–17099; (d) A. N. Marziale, A. Friedrich, I. Klopsch, M. Drees, V. R. Celinski, J. Schmedt auf der Günne and S. Schneider, *J. Am. Chem. Soc.*, **2013**, *135*, 13342–13355; (e) A. P. M. Robertson, E. M. Leitao, T. Jurca, M. F. Haddow, H. Helten, G. C. Lloyd-Jones and I. Manners, *J. Am. Chem. Soc.*, 2013, *135*, 12670–12683; (f) A. Kumar, H. C. Johnson, T. N. Hooper, A. S.

Weller, A. G. Algarra and S. A. Macgregor, *Chem. Sci.*, **2014**, *5*, 2546–2553; (g) H. C. Johnson, E. M. Leitao, G. R. Whittell, I. Manners, G. C. Lloyd-Jones and A. S. Weller, *J. Am. Chem. Soc.*, **2014**, *136*, 9078–9093; (h) H. C. Johnson and A. S. Weller, *Angew. Chem. Int. Ed.*, **2015**, *54*, 10173–10177; (i) A. Ledoux, P. Larini, C. Boisson, V. Monteil, J. Raynaud and E. Lacôte, *Angew. Chem. Int. Ed.*, **2015**, *54*, 15744–15749; (j) F. Anke, D. Han, M. Klahn, A. Spannenberg and T. Beweries, *Dalton Trans.*, **2017**, *46*, 6843–6847.

[6] For organoborane hybrid polymers with B–C linkages, see, e.g.: (a) A. Lik, L. Fritze, L. Müller and H. Helten, *J. Am. Chem. Soc.*, **2017**, *139*, 5692–5695; (b) A. Lik, S. Jenthra, L. Fritze, L. Müller, K.-N. Truong and H. Helten, *Chem. Eur. J.*, **2018**, *24*, 11961–11972.

[7] (*a*) H. Okamura and C. Bolm, *Chem. Lett.,* **2004**, *33*, 482–487; (*b*) T. Toru and C. Bolm, *Organosulfur Chemistry in Asymmetric Synthesis*, Wiley-VCH, Weinheim, **2008**; (*c*) V. Bizet, C. M. M. Hendriks and C. Bolm, *Chem. Soc. Rev.*, **2015**, *44*, 3378–3390; (*d*) V. Bizet, R. Kowalczyk and C. Bolm, *Chem. Soc. Rev.*, **2014**, *43*, 2426-2438; (*e*) X. Shen and J. Hu, *Eur. J. Org. Chem.*, **2014**, 4437-4451; (*f*) J. A. Bull, L. Degennaro and R. Luisi, *Synlett*, **2017**, *28*, 2525–2538.

[8] (*a*) U. Lücking, *Angew. Chem. Int. Ed.*, **2013**, *52*, 9399–9408; (*b*) M. Frings, C. Bolm, A. Blum and C. Gnamm, *Eur. J. Med. Chem.*, **2017**, *126*, 225–245; (c) U. Lücking, *Org. Chem. Front*., **2019**, *6*, 1319–1324.

[9] K. E. Arndt, D. C. Bland, N. M. Irvine, S. L. Powers, T. P. Martin, J. R. McConnell, D. E. Podhoerz, J. M. Renga, R. Ross, G. A. Roth, B. D. Scherzer and T. W. Toyzan, *Org. Process. Res. Dev*., **2015**, *19*, 454–462.

[10] (*a*) F. W. Goldberg, J. G. Kettle, J. Xiong and D. Lin, *Tetrahedron,* **2014**, *70*, 6613–6622; (*b*) K. M. Foote, J. W. M. Nissik, T. McGuire, P. Turner, S. Guichard, J. W. T. Yates, A. Lau, K. Blades, D. Heathcote, R. Odedra, G. Wilkinson, Z. Wilson, C. M. Wood and P. J. Jewsbury, *J. Med. Chem*., **2018**, *61*, 9889–9907.

[11] T. Takata, K. Namakura, T. Endo, *Macromolecules* **1996**, *29*, 2696–2697.

[12] (*a*) X. Y. Chen, H. Buschmann and C. Bolm, *Synlett*, **2012**, *23*, 2808–2810; (*b*) G. Karpel-Massler, R. E. Kast, M. D. Siegelin, A. Dwucet, E. Schneider, M.-A.

Westhoff, C. R. Wirtz, X. Y. Chen, M.-E. Halatsch and C. Bolm, *Neurochem. Res.*, **2017**, *42*, 3382–3389.

[13] (*a*) A. Tota, M. Zenzola, S. J. Chawner, S. St John-Campbell, C. Carlucci, G. Romanazzi, L. Degennaro, J. A. Bull and R. Luisi, *Chem. Commun.*, **2017**, *53*, 348–351; (*b*) J.-F. Lohier, T. Glachet, H. Marzag, A.-C. Gaumont and V. Reboul, *Chem. Commun.*, **2017**, *53*, 2064–2067; (*c*) Y. Xie, B. Zhou, S. Zhou, S. Zhou, W. Wei, J. Liu, Y. Zhan, D. Cheng, M. Chen, Y. Li, B. Wang, X.-S. Xue and Z. Li, *ChemSelect*, **2017**, *2*, 1620–1624; (d) T. Glachet, X. Franck and V. Reboul, *Synthesis*, **2019**, *51*, 971–975.

[14] K. H. V. Reddy, V. P. Reddy, J. Shanar, B. Madhav, B. S. P. A. Kumar and Y. V. D. Nageswar, *Tetrahedron Lett.*, **2011**, *52*, 2679–2682.

[15] C. M. M. Hendriks, R. A. Bohmann, M. Bohlem and C. Bolm, *Adv. Synth. Catal.*, **2014**, *356*, 1847–1852.

[16] X. Lin, Z. Zhang, L. Chen, F. Zeng, Y. Luo and C. Xu, *J. Organomet. Chem.,* **2014**, *749*, 251–254.

[17] For polymers with B–O linkages, see: (a) W. Niu, M. D. Smith and J. J. Lavigne, *J. Am. Chem. Soc.*, **2006**, *128*, 16466–16467; (b) N. Christinat, E. Croisier, R. Scopelliti, M. Cascella, U. Röthlisberger and K. Severin, *Eur. J. Inorg. Chem.*, **2007**, 5177–5181; (c) W. Liu, M. Pink and D. Lee, *J. Am. Chem. Soc.*, **2009**, *131*, 8703–8707.

[18] L. Rojo, M. Fernandez-Gutierrez, S. Deb, M. M. Stevens, J. San Roman, *Acta Biomater*. **2015**, *27*, 32–41.

[19] J. N. Cambre, B. S. Sumerlin, *Polymer* **2011**, *52*, 4631–4643.

[20] X. Y. Chen, H. Buschmann and C. Bolm, *Synlett*, **2012**, *23*, 2808–2810.

[21] K. H. V. Reddy, V. P. Reddy, J. Shankar, B. Madhav, B. S. P. Anil Kumar and Y. V. D. Nageswar, *Tetrahedron Lett.*, **2011**, *52*, 2679–2682.

[22] T. Lorenz, M. Crumbach, T. Eckert, A. Lik and H. Helten, *Angew. Chem. Int. Ed.*, 2017, **56**, 2780–2784; for the synthesis of the precursor, 1,4-bis(dibromoboryl)-benzene, see: M. C. Haberecht, J. B. Heilmann, A. Haghiri, M. Bolte, J. W. Bats,

H.-W. Lerner, M. C. Holthausen and M. Wagner, *Z. Anorg. Allg. Chem.*, 2004, **630**, 904–913.

4.4 Conjugated Oligomers with BP-Linkages

4.4.1 Introduction

The concept of replacing C=C units with isoelectronic and isosteric BN units in π-conjugated organic frameworks continues to attract considerable interest due to the utility of the resulting materials for electronic and biomedical applications.[1],[2] In contrast the implementation of BP units instead of their valence isoelectronic CC or BN counterparts has been studied significantly less extensively,[3] although the potential of including phosphorus in π-conjugated materials for electronic applications has been recognized in recent years.[4]

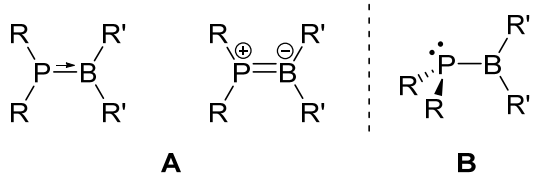

Figure 4.4.1. Structures of R_2PBR_2' compounds.[3c]

Aminoboranes, $R_2NBR'_2$, show a trigonal planar structure at B and N, while for their unhindered borylphosphine (phosphanylborane) congeners, $R_2PBR'_2$, a pyramidal structure is observed at the phosphorus center, due to the lone pair´s higher s-character (**B**, Figure 4.4.1).[3c] However, the π-bond character of the B–P unit can be increased by using sterically demanding substituents at the P-center or by incorporation of the BP-moiety into a cyclic system. The resulting compounds can be described with structure **A** (Figure 4.4.1). The strongest B–P π-bond can be obtained by maximizing the planarity at P with sterically very demanding substituents, so that the sum of angles at P advances to 360°. One of the smallest B–P bond lengths of 1.762(4) Å with a sum of angles at P of 359.8° was found in Cy_2P-$B(C_6F_5)_2$.[5] Pringle proposed that, if the B–P bond length in $R_2PBR'_2$ is smaller than 1.88 Å and the sum of angles around P is higher than 330°, they are called phosphinoboranes and have a distinctive B=P double bond character. Are the values of bond length and sum of angles smaller than that they are referred to as borylphosphines and they predominantly exhibit a B-P single bond.[3c] The stability of R_2NBR_2' compounds can also be influenced by the electronic environment at P and B with Lewis basic or acidic substituents.[3c]

For the synthesis of known BP-compounds different strategies have been established. A very common pathway is the salt elimination by the reaction of P-nucleophilic lithium phosphides

with haloboranes (Scheme 4.4.1, **I**).[5-6] In addition, if boron is incorporated in electron rich systems other routes are accessible, i.e. using B-nucleophiles derived from diazaboroles (Scheme 4.4.1, **II**).[7] In aromatic BN-containing heterocycles silicon/boron (Si/B) exchange via elimination of Me_3SiCl is a possible pathway (Scheme 4.4.1, **III**).[8] Another strategy is the use of Pd complexes as catalysts for catalytic B-P coupling reactions.[9] (Scheme 4.4.1, **IV**).

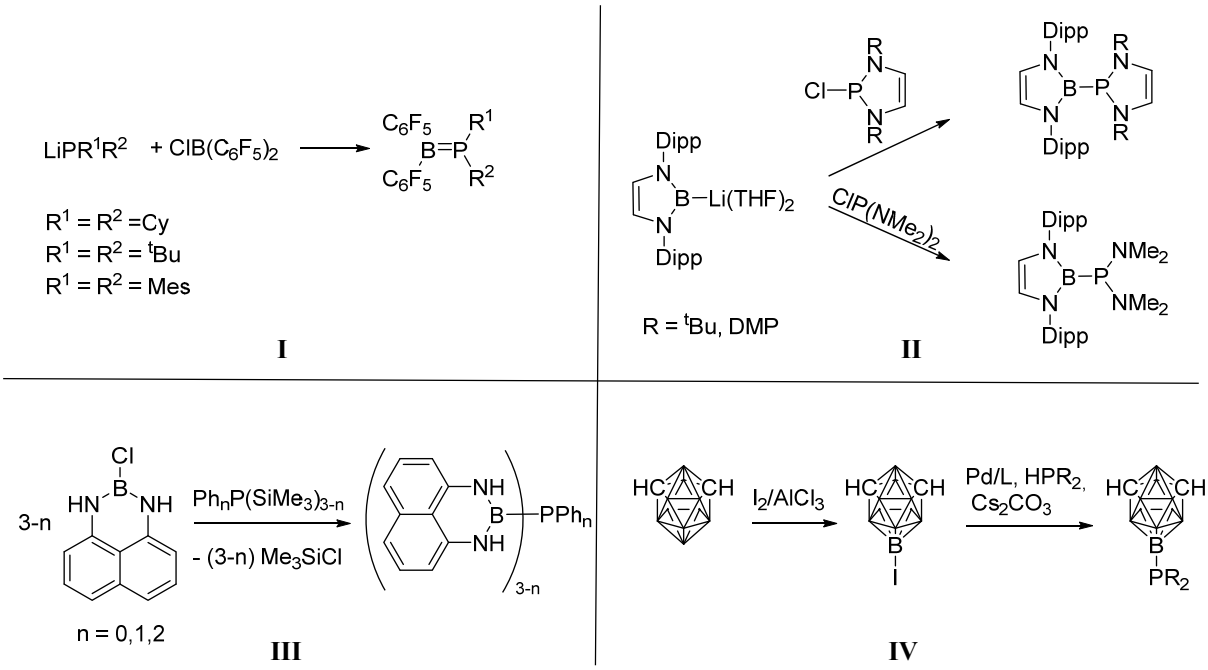

Scheme 4.4.1. General pathways for the synthesis of BP-compounds.[5-9]

4.4.2 Synthesis

Herein, we investigate conjugated BP compounds and the effect of different steric demanding substituents at P on the BP bond characteristics. This study gives preliminary insight for future syntheses of conjugated polymers with B=P linkages. As reaction pathway for the B–P-bond formation we applied the Si/B exchange reaction, which was reported for B-P bond formation by Pringle et al.[8] They prepared borylphosphines by the reaction of heterocyclic haloboranes with silylphosphines under mild conditions. In our case, the corresponding silylphosphines **4a-c** were prepared similar to the approach of Lutz[10] by reaction of dichlorophenylphosphine (**1**) with different aryl lithium compounds (**a** Mes = 2,4,6-trimethylphenyl, **b** Tip = 2,4,6-triisopropylphenyl, **c** Mes* = 2,4,6-tri-*tert*-butylphenyl) yielding chlorodiarylphophines **2a-c**. Exchange of the chloride in **2** by hydride with $LiAlH_4$ and subsequent lithiation/silylation afforded **4a-c** (Scheme 4.4.2).

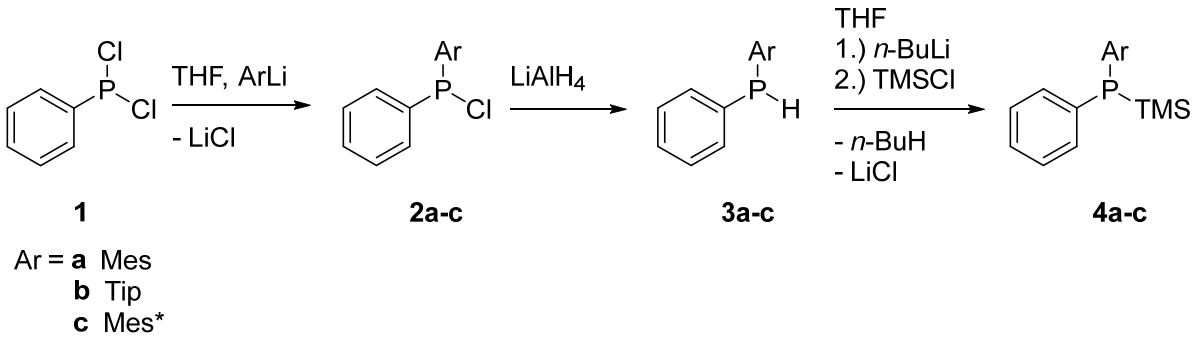

Scheme 4.4.2. Synthesis of diarylsilylphosphines **4a-c**.
Mes = 2,4,6-trimethylphenyl, Tip = 2,4,6-triisopropylphenyl, Mes* = 2,4,6-tri-*tert*-butylphenyl.

We prepared compounds **6a** and **6b** based on those precursors **4a-c** and bromo-(mesityl)phenylborane (**5**) via Si/B exchange under mild conditions (Scheme 4.4.3). Here we observed that a sterically more demanding Tip-substituent (**6b**) needed considerable more time (15 days) for full conversion in comparison to 3 days for **6a**.

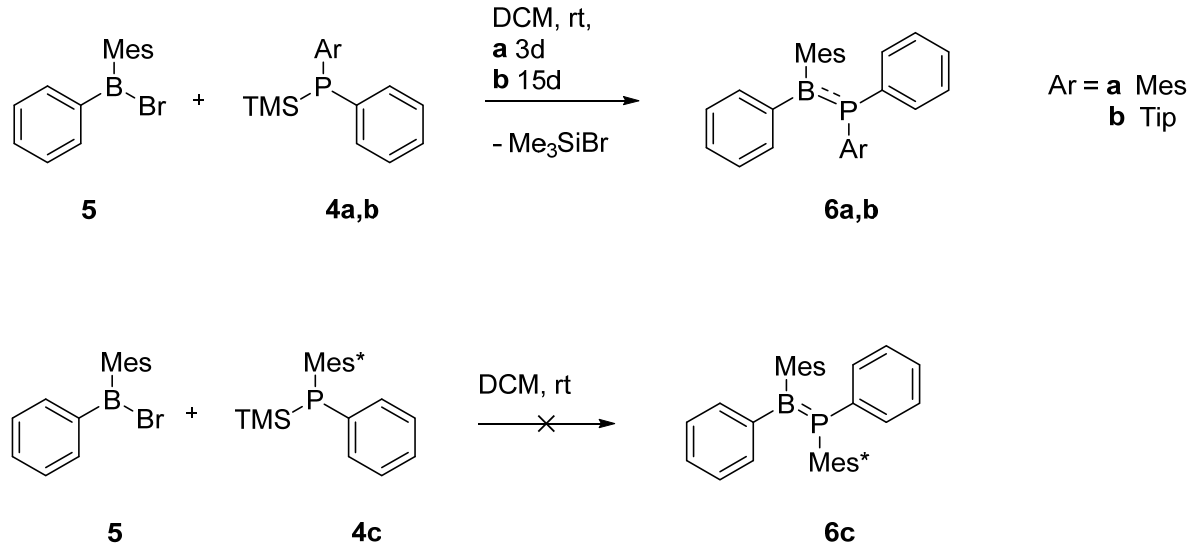

Scheme 4.4.3. Synthesis of compounds **6a** and **6b** and attempted synthesis of **6c** by Si/B exchange.
Mes = 2,4,6-trimethylphenyl, Tip = 2,4,6-triisopropylphenyl.

Compound **6c** was not accessible in this way, probably because of the steric hindrance of the Mes*-group as substituent at the phosphorus (Scheme 4.4.4). Nonetheless, **6c** was successfully obtained by applying the salt elimination strategy using lithiated species **7** with bromodiarylborane **5** (Scheme 4.4.4). The molecular structures of **6c** was determined by single-crystal X-ray diffraction (Figure 4.4.2).

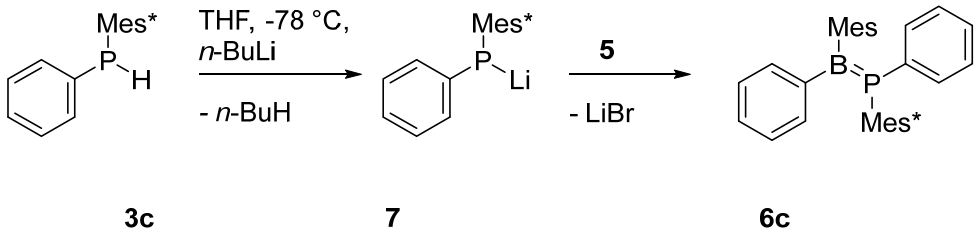

3c **7** **6c**

Scheme 4.4.4. Synthesis of compound **6c**.
Mes = 2,4,6-trimethylphenyl, Mes* = 2,4,6-tri-*tert*-butylphenyl.

Additionally, we were able to prepare oligomer **9**, which contains a BPPB unit along the main chain using the silicon/boron exchange route (Scheme 4.4.5). **9** was characterized with $^{11}B\{^1H\}$ and $^{31}P\ \{^1H\}$ NMR spectroscopy.

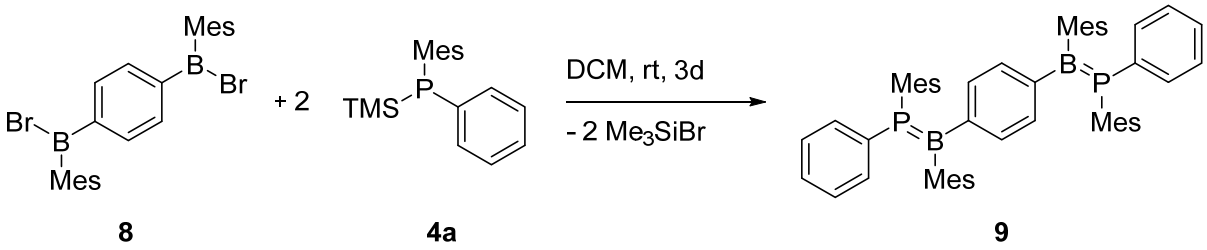

8 **4a** **9**

Scheme 4.4.5. Synthesis of oligomer **9**.
Mes = 2,4,6-trimethylphenyl.

In Table 4.4-1 the $^{31}P\{^1H\}$ NMR and $^{11}B\{^1H\}$ NMR data for **6a**–**c** and **9** are listed. The $^{11}B\{^1H\}$ NMR resonance of **6a-c** shows an upfield shift from 65.0 ppm to 50.0 ppm with increased steric bulk of the substituents. Additionally, the $^{31}P\{^1H\}$ NMR resonance shows an upfield shift from –8.4 ppm (**6a**) to –11.6 ppm (**6b**), though **6c** with a chemical shift of 16.4 ppm does not follow that tendency. The group of Mizuta observed a related exception, where a Mes*-group in iron-substituted phosphinoboranes, as most steric demanding substituent at phosphorus, did not show an upfield shift in the corresponding $^{31}P\{^1H\}$ NMR spectrum in comparison to its counterparts with Ph-, Mes- or Tip substituents.[11] Compound **9** incorporating two BP groups showed a ^{31}P shift of –5.9 ppm and an ^{11}B shift of 62.4 ppm in the NMR (Table 4.4-1), which would fit in the before described tendency.

Table 4.4-1: $^{31}P\{^1H\}$ NMR and $^{11}B\{^1H\}$ NMR Data for **6a**–**c** and **9**.

	6a	6b	6c	9
$^{11}B\{^1H\}$ NMR (δ)	65.0	61.9	50.0	62.4
$^{31}P\{^1H\}$ NMR (δ)	–8.4	–11.6	16.4	–5.4

4.4.3 Molecular structures

The molecular structures of **6a-c** were optimized by DFT calculations (B3LYP/def2-SV(P)). Comparison of the calculated sum of the angles of P in compounds **6a-c** demonstrates the influence of the substituent at P. The value increases with the steric hindrance of the substituent from **6a** (Mes, 337.6°) to **6b** (Tip, 353.5°) to **6c** (Mes *, 360.0°) (Table 4.4-2). The calculated geometry of **6c** is largely consistent with the experimentally determined molecular structure via single-crystal X-ray diffraction (Figure 4.4.2). The experimental value for the sum of the angles at P constitutes 359.8° (Table 4.4-2), which confirms that **6c** has a trigonal planar structure in the solid state. Additionally, the DFT-calculations show that with increasing steric hindrance at the P-atom the Ph/Ph-twist angle decreases significantly from 60.8° (**6a**) > 36.7° (**6b**) > 1.6° (**6c**) (Table 4.4-2), which shows that the π-system may expand over the complete molecule with Mes* at P.

Table 4.4-2: Structural parameters for **6a-c**.

	calculated values			*X-ray structure*
	6a (Ar = Mes)	**6b** (Ar = Tip)	**6c** (Ar = Mes*)	**6c** (Ar = Mes*)
B – P bond length / Å	-	-	-	1.757(8)
Σ∢(angles at P) / °	337.6	353.5	360.0	359.8(4)
Ph/Ph twist angle / °	60.8	36.7	1.6	17.5

Furthermore the B-P bond length 1.757(8) Å in the solid state is in a similar range as those of $Cy_2P\text{-}B(C_6F_5)_2$ (1.762(4) Å)[6] and $^tBu_2P\text{-}B(C_6F_5)_2$ (1.786(4) Å),[5] which have been described to have distinctive B=P-double bond character.

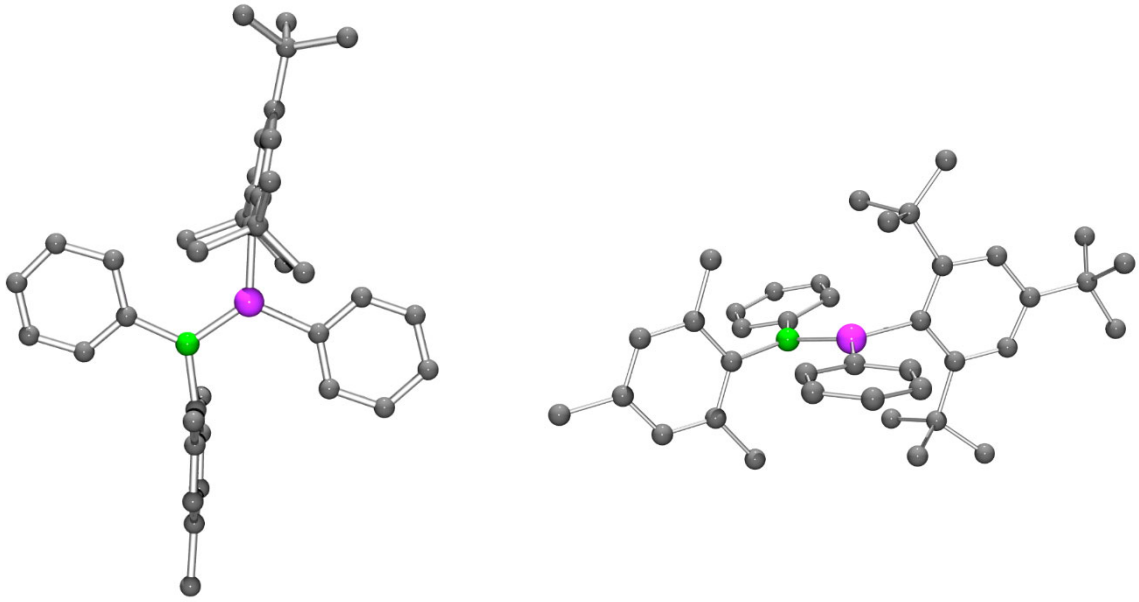

Figure 4.4.2. Molecular structure of **6c** in solid state determined by X-ray crystallographic analysis. C-bonded hydrogen atoms are omitted for clarity. B–P 1.757(8) Å, Σ(angles at P) = 359.8(4)°.

4.4.4 Photophysical Properties

Comparison of the UV/Vis spectra of **6a-c** and **9** in CH_2Cl_2 (Figure 4.4.3) showed a small but systematic red-shift with increasing steric demand of the substiuent at the P, from **6a** (λ = 366 nm, Mes), to **6b** (λ = 372 nm, Tip) and **6c** (λ = 375 nm, Mes*). Furthermore compound **9** shows an even further red-shift to λ = 397 nm. This points to a higher degree of π-conjugation between the two trigonal planar B-atoms (over the phenylene ring). The trends for the absorption maxima are well reproduced by the theoretically predicted values by TD-DFT (Table 4.4-3).

Table 4.4-3: Photophysical data for **6a-c**, oligomer **9** and BN compounds **10**[2c] and **11**.[2c] Calculated excitations for **6a**, **9** and BN compounds **10** and **11** (TD-DFT, B3LYP-D3(BJ)/def2-SV(P)//BP86-D3(BJ)/def2-SV(P)).

	6a	**6b**	**6c**	**9**	**10**[2c]	**11**[2c]
$\lambda_{abs,max}$ [nm]	366	372	375	397	271	305
$\lambda_{abs,TD\text{-}DFT}$ [nm]	370	-	-	432	294	328

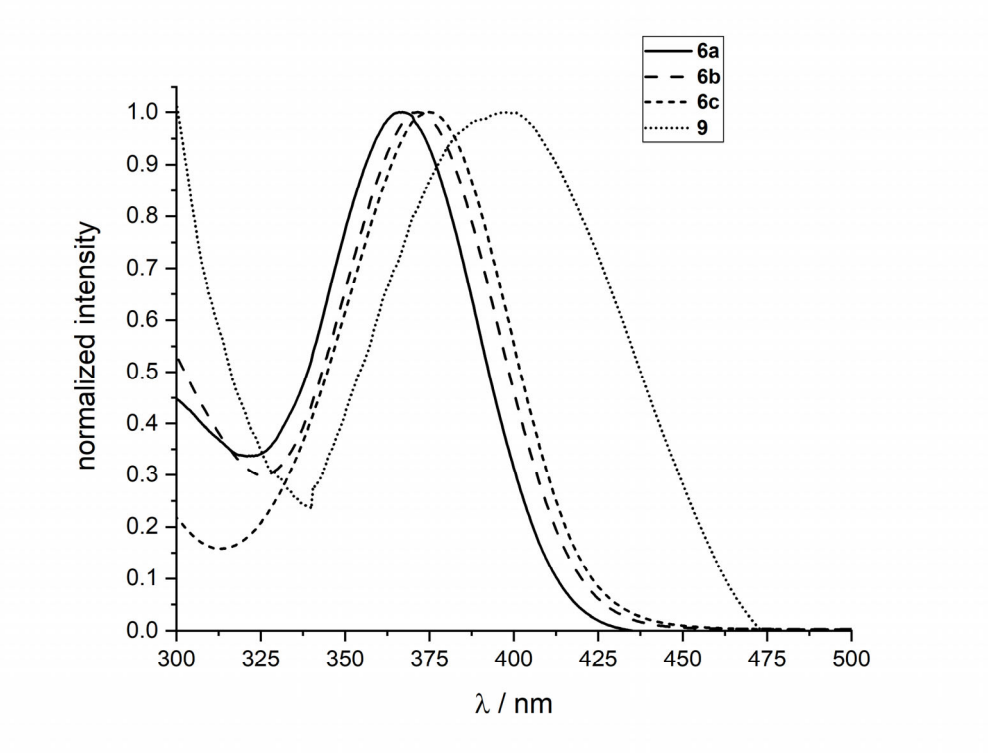

Figure 4.4.3. UV/vis spectra of BP compounds **6a-c**, **9**.

Interestingly, the longest-wavelength absorption maxima of **6a-c** and **9** are significantly further bathochromic shifted compared to their BN analogues[2c] (Figure 4.4.4) **10** (by 95 nm) and **11** (by 97 nm)[2c] (Figure 4.4.3, Table 4.4-3).

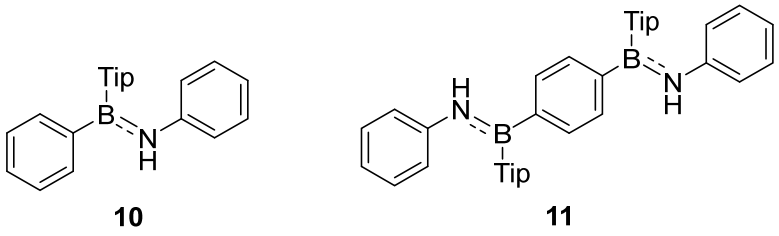

Figure 4.4.4. Compounds **10** and **11**,[2c] the BN-analogues of **6a-c** and **9** for comparison.

The calculated HOMO for **6a** shows major contributions of P and the P-phenyl ring, which points basically to a to lone-pair character, although there is also partial π-character for a B=P π bond evident. The corresponding LUMO has π*-character and shows major contributions of boron and interaction between boron and the phenyl ring. It has predominantly the characteristics of the vacant p-orbital on boron, but to some extend also characteristics of a π-orbital of a B=P π bond. The comparison of **6a-c** shows a stronger delocalization in the LUMO

from **6a** to **6c**. Also the interaction between MOs of boron and phosphorus in the HOMO increases from **6a** < **6b** < **6c**, which indicates a stronger π-character with increased bulk of the substituent at P (Figure 4.4.5).

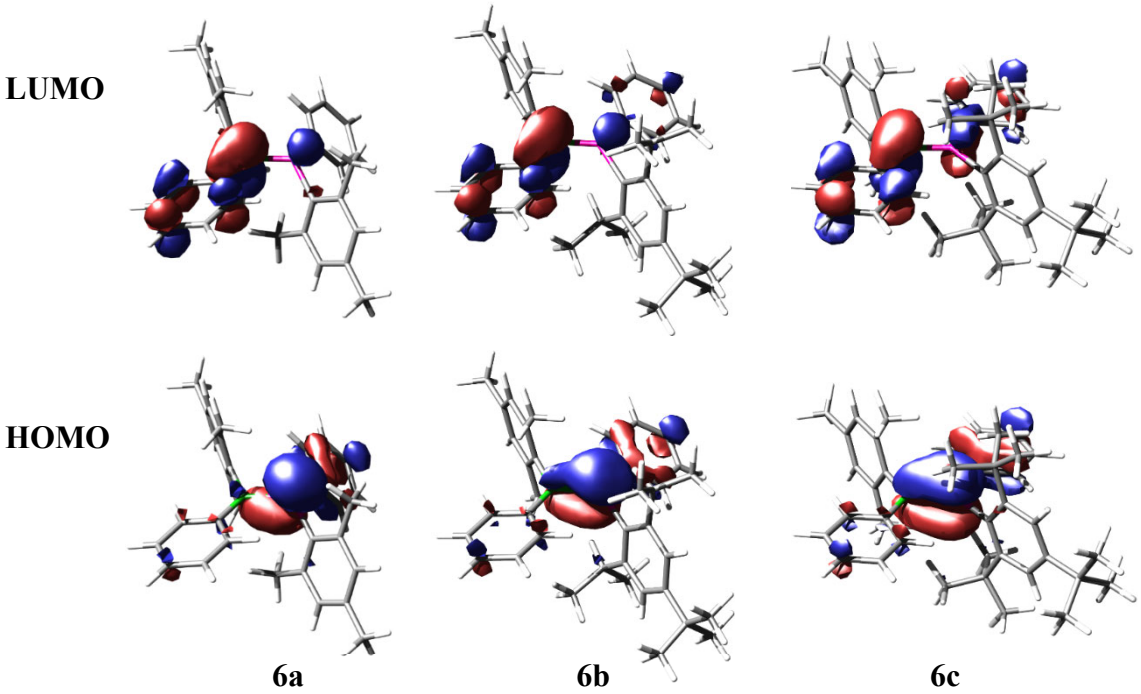

Figure 4.4.5. Calculated frontier orbitals of **6a**, **6b** and **6c** (B3LYP-D3(BJ)/def2-SV(P)).

4.4.5 Conclusion

In this study we presented the synthesis and characterization of BP containing oligomers **6a-c** and **9**. Whilst **6a**,**b** were obtained by Si/B exchange condensation, **6c** was prepared via salt elimination. Photophysical studies and TD-DFT calculations demonstrate the influence of steric effect of the P-substituent on the molecular geometry of the phosphorus and consequently on the characteristics of the BP bond. The partial BP double bond character increases with the steric bulk of the P-substituent. Currently, we investigate the possible synthesis of the corresponding BP-containing polymers.

4.4.6 Experimental Section

General procedures. All manipulations were performed under an atmosphere of dry argon using standard Schlenk techniques or in an MBraun glovebox. Solvents (dichloromethane, Et_2O, *n*-

pentane, toluene and tetrahydrofuran) were dried and degassed by means of an MBraun SPS-800 solvent purification system. Hexane was dried and degassed at reflux over Na. Deuterated solvents for NMR spectroscopy were dried and degassed at reflux over Na (C_6D_6 and THF-d_8) or CaH_2 ($CDCl_3$) and freshly distilled prior to use. Boron tribromide and dichlorophenylphosphine were commercially purchased and used as received. MesCu,[12] TipLi,[13] Mes*Li,[14] $PhBBr_2$,[15] *p*-Br_2B-C_6H_4-BBr_2,[16] were prepared according to methods described in the literature. NMR spectra were recorded at 25 °C on a Bruker AVANCE II-400 spectrometer or on a Bruker Advance III HD spectrometer operating at 400 MHz. Chemical shifts were referenced to residual protic impurities in the solvent (^1H) or the deuterio solvent itself (^{13}C) and reported relative to external $SiMe_4$ (^1H, ^{13}C), $BF_3{\cdot}OEt_2$ (^{11}B) or 85% H_3PO_4 in aqueos solution (^{31}P) standards. UV-vis-spectra were obtained using a Jasco V-630 spectrophotometer.

Spectra. All spectra and other result figures are shown in Appendix 7.4.

Synthesis

Synthesis of 5. To a stirred suspension of MesCu (3.431 g, 18.77 mmol) in toluene (55 ml) was added dropwise a solution of $PhPBr_2$ (4.516 g, 18.23 mmol) in toluene (20 mL) at –78 °C. The mixture was warmed to room temperature and stirred at 60 °C overnight. The suspension was filtered and washed with additional toluene (10 mL). The solvent was removed *in vacuo*. The crude product was purified by destillation *in vacuo* ($2x10^{-2}$ mbar) at 105 °C yielding in **5** as colorless liquid. Yield: 3.941 g (13.73 mmol, 75%). ^1H NMR (400 MHz, C_6D_6): δ = 8.05-8.10 (m, 2H; *o*-C_6H_2), 7.64-7.70 (m, 1H; *p*-C_6H_4), 7.46-7.52 (m, 2H; *m*-C_6H_4), 6.93 (s, 2H; H_{Ar}(Mes)), 2.40 (s, 3H; *p*-Mes-CH_3), 2.21 (s, 6H; *o*-Mes-CH_3) ppm; $^{11}B\{^1H\}$ NMR (128 MHz, $CDCl_3$): δ = 70.4 ppm (s).

Synthesis of 8. To a stirred solution of MesCu (2.343 g, 12.62 mmol) in DCM (32 ml) was added dropwise a solution of *p*-Br_2B-C_6H_4-BBr_2 (2.671 g, 6.40 mmol) in DCM (29 mL) at 0 °C, during which a red-orange suspension was formed. The mixture was warmed to room temperature and stirred overnight. Then, all volatiles were removed *in vacuo* and the residue was dissolved in *n*-pentane (100 mL). The suspension was filtered and washed with additional *n*-pentane (3x10 mL). The solvent was removed *in vacuo* yielding **8** as colorless solid. ^1H NMR (400 MHz, C_6D_6): δ = 7.99 (s, 4H; *o*-B_2-C_6H_4), 6.71 (s, 4H; Mes-H_{Ar}), 2.17 (s, 6H; *p*-Mes-CH_3), 2.05 ppm (s, 12H; *o*-Mes-CH_3); $^{11}B\{^1H\}$ NMR (128 MHz, $CDCl_3$): δ = 72.4 ppm (s).

Synthesis of 6a. To a stirred solution of **5** (0.580 g, 2.02 mmol) in DCM (4 mL) was added neat **4a** (0.617 g, 2.05 mmol) at room temperature. After stirring the reaction mixture for 3 days all volatiles were removed *in vacuo*. The black residue was dissolved in toluene and crystallized at –40 °C. **6a** was yielded as yellow solid. ^{1}H NMR (400 MHz, $CDCl_3$): δ = 7.50-7.42 (m, 3H; Ph-CH_{Ar}), 7.33 (tr, 2H; Ph-H_{Ar}), 7.27 (br s, 2H; Mes-H_{Ar}), 7.25-7.15 (m, 3H; Ph-CH_{Ar}), 7.08 (s, 2H; Mes-H_{Ar}), 6.82 (br tr, 2H; Ph-CH_{Ar}), 2.68 (s, 6H; *o*-Mes-CH_3), 2.59 (s, 3H; *p*-Mes-CH_3), 2.57 (s, 3H; *p*-Mes-CH_3), 2.38 ppm (s, 6H; *o*-Mes-CH_3); ^{11}B{^{1}H} NMR (128 MHz, $CDCl_3$): δ = 65.3 ppm (s); ^{31}P{^{1}H} NMR (162 MHz, $CDCl_3$): δ = –8.2 ppm (s).

Synthesis of 6b. To a stirred solution of **4b** (0.781 g, 2.02 mmol) in DCM (4 mL) was added neat PhB(Mes)Br **5** (0.591 g, 2.06 mmol) at room temperature. After stiring the reaction mixture for 15 days all volatiles were removed *in vacuo*. The crude yellow product was dissolved in hexane and crystallized at –40 °C. **6b** was yielded as yellow solid. ^{1}H NMR (400 MHz, $CDCl_3$): δ = 7.23-7.19 (m, 1H; Ph-CH_{Ar}), 7.17 (d, 2H; SMes-H_{Ar}), 7.16 (m, 2H, Ph-H_{Ar}), 7.10-7.07 (m, 2H; Ph-CH_{Ar}), 7.03-6.95 (m, 3H; Ph-CH_{Ar},) 6.91 (s, 2H; Mes-H_{Ar}), 6.87-6.60 (m, 2H; Ph-CH_{Ar}), 3.86 (sep, *J* = 6.85 Hz, 2H; *o*-C*H*-Tip), 3.00 (sep, *J* = 6.85 Hz, 2H; *p*-C*H*-Tip), 2.39 (s, 3H; *p*-Mes-CH_3), 2.21 (s, 6H; *o*-Mes-CH_3), 1.35 (d, 6H; *J* = 6.85 Hz, *p*-*i*-Pr-CH_3), 1.10 (d, 6H; *J* = 6.85 Hz, *o*-*i*-Pr-CH_3) 1.00 ppm (d, 6H; *J* = 6.85 Hz,*o*-*i*-Pr-CH_3); ^{11}B{^{1}H} NMR (128 MHz, $CDCl_3$): δ = 62.7 ppm (s); ^{31}P{^{1}H} NMR (162 MHz, $CDCl_3$): δ = –11.5 ppm (s).

Synthesis of 6c. To a stirred solution of PhP(SMes)H **3c** (0.521 g, 1.47 mmol) in THF (15 ml) was added dropwise *n*-BuLi (1.6 *M* in hexane, 0.93 mL, 1.49 mmol) at –78 °C, during which the solution turned red. After the mixture was warmed up to –60 °C, it was stirred for another 30 min at this temperature. Then, Ph(Mes)BBr **5** (0.437 g, 1.52 mmol) was added dropwise. During the addition the colour of the mixture turned from red over black to green. Subsequently, the mixture was warmed up to room temperature and stirred overnight. Then, all volatiles were removed *in vacuo* and the residue was dissolved in *n*-pentane (30 mL). The suspension was filtered and the solvent was removed *in vacuo*. The crude product **6c** was crystallized from hexane at –40 °C. ^{1}H NMR (400 MHz, C_6D_6): δ = 7.83 (d, *J* = 3.51 Hz, 2H; *o*-C_6H_2), 7.16-7.08 (m, 3H; Ph-*H*), 7.02-6.97 (m, 2H; Ph-H_{Ar}), 6.95 (br s, 2H; SMes-H_{Ar}), 6.93-6.85 (m, 3H; Ph-H_{Ar}), 6.53-6.46 (m, 2H; Mes-H_{Ar}), 1.53 (s, 18H; *o*-SMes-CH_3), 1.44 ppm (s, 9H; *p*-SMes-CH_3); ^{13}C{^{1}H} NMR (101 MHz, THF-d_8): δ = 158.9 (d, *p*-C_{SMes}), 154.6 (d, *p*-C_{SMes}), 140.5 (d, o-

C_{Mes}), 139.2 (s, C_q), 138.6 (s, C_q), 138.0 (s, *p*-C_{Mes}), 137.0 (d, C_{Ar}-Ph), 130.4 (d, *p*-C-Ph), 130.0 (d, C-Ph), 129.0 (s, *m*-C_{SMes}),128.7 (d, C_{Ar}-Ph), 127.9 (s, *m*-C_{Mes}), 126.8 (d, *p*-C_{Ar}-Ph), 125.6 (d, *o*-B-C_2), 40.7 (s, *o*-*C*-*t*-Bu), 36.3 (s, *p*-*C*-*t*-Bu), 33.8 (s, *o*-(CH_3)$_3$), 31.7 (s, *p*-(CH_3)$_3$), 23.8 (s, *o*-CH_3 (Mes)), 21.6 ppm (s, *p*-CH_3 (Mes)); $^{11}B\{^1H\}$ NMR (128 MHz, $CDCl_3$): δ = 47.1 ppm (s); $^{31}P\{^1H\}$ NMR (162 MHz, $CDCl_3$): δ = 16.4 ppm (s).

Synthesis of 9. To a stirred brownish suspension of **8** (0.995 g, 2.01 mmol) in DCM (8 mL) was added **5** (1.207 g, 4.02 mmol), during which the suspension turned from brown over yellow to black. After stirring for 3 d all volatiles were removed *in vacuo*. The residue was dissolved in toluene. The precipitate was removed by filtration. All volatiles were removed *in vacuo* yielding crude **9** as yellow solid. $^{11}B\{^1H\}$ NMR (128 MHz, $CDCl_3$): δ = 64.4 ppm (s); $^{31}P\{^1H\}$ NMR (162 MHz, $CDCl_3$): δ = –5.9 ppm (s).

4.4.7 References

[1] a) Z. Liu, T. B. Marder, *Angew. Chem. Int. Ed.* **2008**, *47*, 242-244; b) M. J. D. Bosdet, W. E. Piers, *Can. J. Chem.* **2009**, *87*, 8-29; c) P. G. Campbell, A. J. V. Marwitz, S.-Y. Liu, *Angew. Chem. Int. Ed.* **2012**, *51*, 6074-6092; d) D. Bonifazi, F. Fasano, M. M. Lorenzo-Garcia, D. Marinelli, H. Oubaha, J. Tasseroul, *Chem. Commun.* **2015**, *51*, 15222-15236; e) H. Helten, in *Encyclopedia of Inorganic and Bioinorganic Chemistry*, **2017**, pp. 1-27; f) G. Bélanger-Chabot, H. Braunschweig, D. K. Roy, *Eur. J. Inorg. Chem.* **2017**, *2017*, 4353-4368.

[2] a) T. Lorenz, A. Lik, F. A. Plamper, H. Helten, *Angew. Chem. Int. Ed.* **2016**, *55*, 7236-7241; b) O. Ayhan, T. Eckert, F. A. Plamper, H. Helten, *Angew. Chem. Int. Ed.* **2016**, *55*, 13321-13325; c) T. Lorenz, M. Crumbach, T. Eckert, A. Lik, H. Helten, *Angew. Chem. Int. Ed.* **2017**, *56*, 2780-2784; d) O. Ayhan, N. A. Riensch, C. Glasmacher, H. Helten, *Chem. Eur. J.* **2018**, *24*, 5883-5894; e) H. Helten, *Chemistry – An Asian Journal* **2019**, *14*, 919-935; f) F. Brosge, T. Lorenz, H. Helten, C. Bolm, *Chem. Eur. J.* **2019**, *25*, 12708-12711.

[3] a) P. P. Power, *Angew. Chem. Int. Ed.* **1990**, *29*, 449-460; b) R. T. Paine, H. Noeth, *Chem. Rev.* **1995**, *95*, 343-379; c) J. A. Bailey, P. G. Pringle, *Coord. Chem. Rev.* **2015**, *297-298*, 77-90.

[4] a) T. Baumgartner, *Acc. Chem. Res.* **2014**, *47*, 1613-1622; b) D. Joly, P. A. Bouit, M. Hissler, *J. Mater. Chem. C* **2016**, *4*, 3686-3698; c) A. Lik, D. Kargin, S. Isenberg, Z. Kelemen, R. Pietschnig, H. Helten, *Chem. Commun.* **2018**, *54*, 2471-2474.

[5] S. J. Geier, T. M. Gilbert, D. W. Stephan, *Inorg. Chem.* **2011**, *50*, 336-344.

[6] S. J. Geier, T. M. Gilbert, D. W. Stephan, *J. Am. Chem. Soc.* **2008**, *130*, 12632-12633.

[7] M. Kaaz, J. Bender, D. Förster, W. Frey, M. Nieger, D. Gudat, *Dalton Trans.* **2014**, *43*, 680-689.

[8] J. A. Bailey, M. F. Haddow, P. G. Pringle, *Chem. Commun.* **2014**, *50*, 1432-1434.

[9] A. M. Spokoyny, C. D. Lewis, G. Teverovskiy, S. L. Buchwald, *Organometallics* **2012**, *31*, 8478-8481.

[10] J. Brauer David, F. Bitterer, F. Dörrenbach, G. Heßler, O. Stelzer, C. Krüger, F. Lutz, in *Zeitschrift für Naturforschung B, Vol. 51*, **1996**, p. 1183.

[11] K. Kubo, T. Kawanaka, M. Tomioka, T. Mizuta, *Organometallics* **2012**, *31*, 2026-2034.

[12] a) H. Eriksson, M. Håkansson, *Organometallics* **1997**, *16*, 4243-4244; b) S. Gambarotta, C. Floriani, A. Chiesi-Villa, C. Guastini, *J. Chem. Soc., Chem. Commun.* **1983**, 1156-1158; c) E. M. Meyer, S. Gambarotta, C. Floriani, A. Chiesi-Villa, C. Guastini,

Organometallics **1989**, *8*, 1067-1079; d) T. Tsuda, T. Yazawa, K. Watanabe, T. Fujii, T. Saegusa, *J. Org. Chem.* **1981**, *46*, 192-194.

[13] K. Ruhlandt-Senge, J. J. Ellison, R. J. Wehmschulte, F. Pauer, P. P. Power, *J. Am. Chem. Soc.* **1993**, *115*, 11353-11357.

[14] X. Yin, J. Chen, R. A. Lalancette, T. B. Marder, F. Jäkle, *Angew. Chem. Int. Ed.* **2014**, *53*, 9761-9765.

[15] D. Kaufmann, *Chem. Ber.* **1987**, *120*, 853-854.

[16] M. C. Haberecht, J. B. Heilmann, A. Haghiri, M. Bolte, J. W. Bats, H.-W. Lerner, M. C. Holthausen, M. Wagner, *Z. Anorg. Allg. Chem.* **2004**, *630*, 904-913.

5 Conclusion

This work has substantiated silazane cleavage with silicon-boron (Si/B) exchange as simple but effective approach for the synthesis of novel classes of BN-linked polymers. In the first chapter a novel class of inorganic–organic hybrid polymers with discrete N-B-N units in the main chain was presented. First polymerization attempts using dehydrocoupling of a mono BH_3 adduct of *p*phenylenediamine under mild conditions as polycondensation strategy lead to materials insoluble in common organic solvents. The incorporation of solubility enhancing side groups (mesityl) on the boron center proved to be successful to obtain well defined polymers with NBN moieties as main chain component. Therefore, another polycondensation strategy was applied using silicon-boron exchange of silylated *p*-phenylenediamine with dichloro(mesityl)borane (Scheme 5.1) leading to the a new class of inorganic–organic hybrid polymers, poly[*N*-(*para*-phenylene)-diimidoborane(3)]s (PPP-DIBs, **3**).

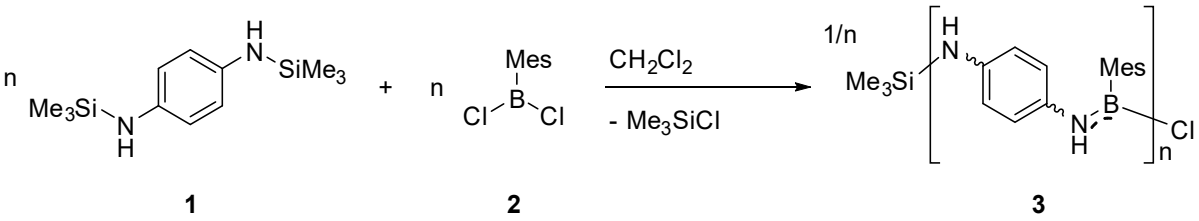

Scheme 5.1. Si/B exchange for NBN-polymer **3**.

Polymer **3** is soluble in common organic solvents and GPC measurements revealed an average molecular weight of $M_n = 7900$, which corresponds to a number average degree of polymerization (DP_n) of 33. The corresponding model compounds with one (**4**) and two NBN moieties (**5**) were also accessible using the Si/B exchange approach (Figure 5.1).

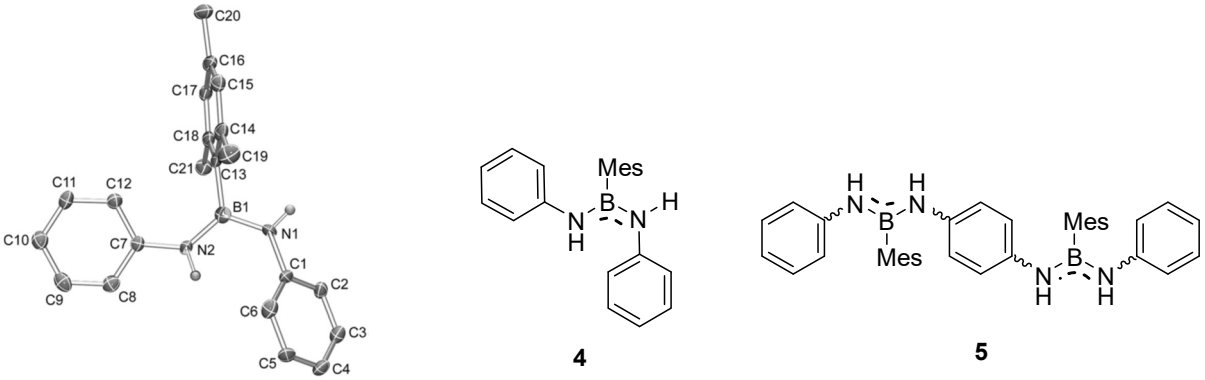

Figure 5.1. NBN-model compounds **4** and **5** and molecular structure of **4** in solid state determined by single-crystal X-ray diffractometry.

Photophysical studies showed moderate π-conjugation across the NBN moieties with a slight red shift with increasing number of NBN units from 267 nm (**4**) to 280 nm (**5**) to 295 nm (polymer **3**). This redshift substantiates the hypothesis that the conjugation length is moderately extended upon polymer formation. It was also possible to use $Zr(NMe_2)_4$ for metal coordination of polymer **3a** yielding in cross-linked polymer **3b** (Scheme 5.2).

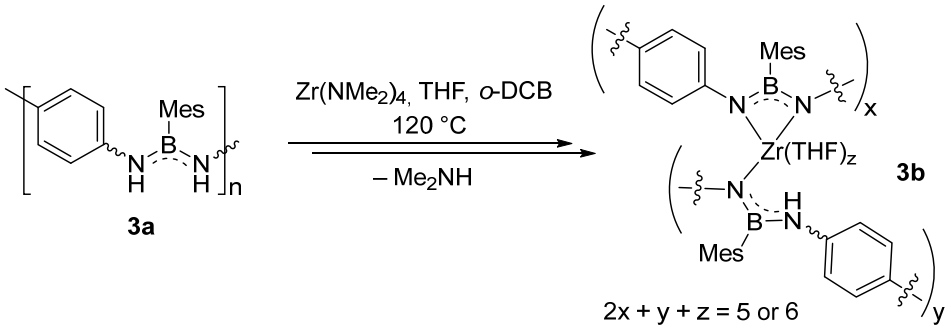

Scheme 5.2. Cross-linking of **3a**.

Furthermore, first derivatives of another novel class of inorganic–organic hybrid polymers, that is poly(*p*-phenylene iminoborane)s, were obtained by using the previously established Si/B exchange for polymer synthesis. These polymers can be described as BN analogues of poly(*p*-phenylene vinylene) (PPV).

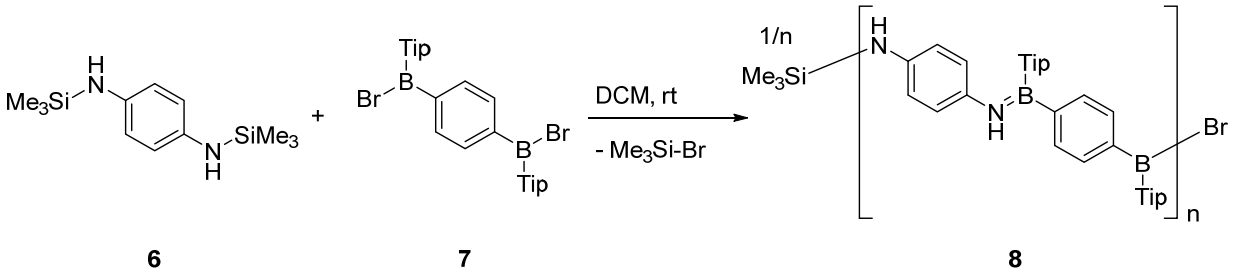

Scheme 5.3. Synthesis of polymer **8** (BN-PPV).

In order to increase the stability at the boron center, a more sterically demanding Tip-group (Tip = 2,4,6-triisopropylphenyl) was used as substituent at B, which lead to polymer **8** showing enhanced air and moisture stability. To get more insight into the molecular structure of those polymers, the corresponding BN-model compounds **9**-**11** were synthesized in addition (Figure 5.2). Molecular structures of compounds **10** and **11** were determined by single-crystal X-ray diffraction. Both oligomers showed a slight twist between *trans* positioned phenyl and phenylene groups at the B=N unit. Photophysical investigations combined with TD-DFT

calculations afforded clear-cut evidence for π-conjugation across the B=N units along the polymer backbone and extension of the conjugation path with increasing chain length.

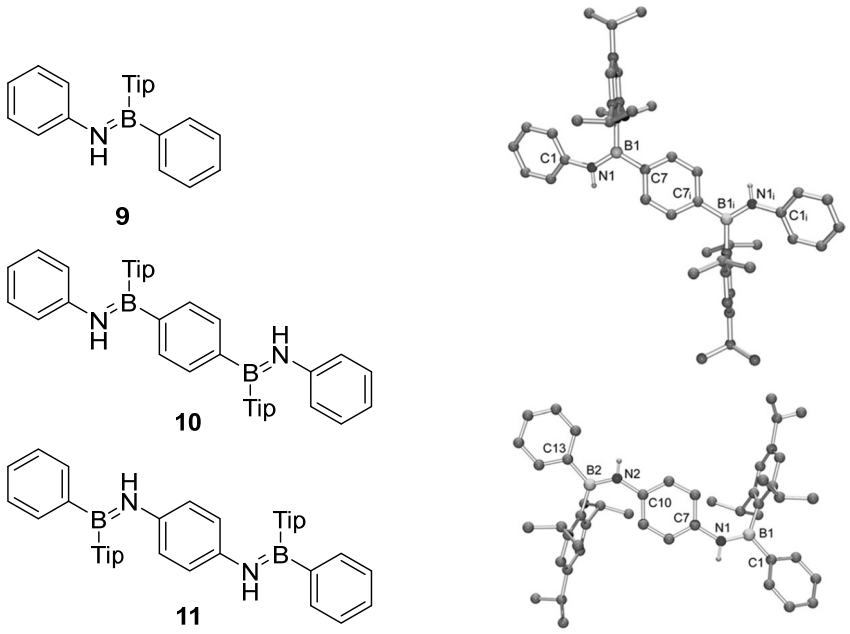

Figure 5.2. Compounds **9-11** and molecular structures of **10** and **11** in solid state.

To explore further application of Si/B exchange as polymerization strategy, sulfoximine **12** was employed as the diamine component. This yielded the first inorganic–organic hybrid sulfoximine-containing polymer **13** as alternating copolymers with B=N linkages (Scheme 5.4) with a number average degree of polymerization (DP_n) of 15 (by GPC analysis).

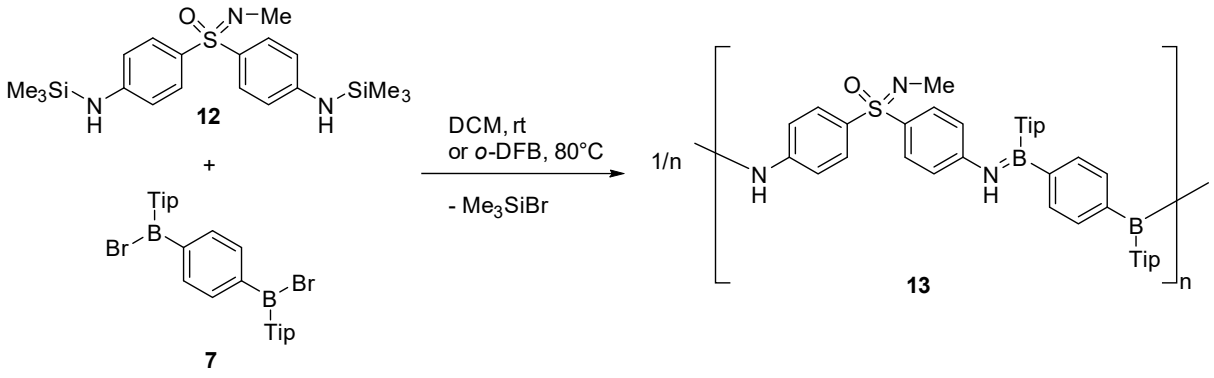

Scheme 5.4. Polycondensation reaction of sulfoximine **12** and bisborane **7** to yield alternating BN-containing polymer **13**.

This Si/B exchange polycondensation protocol was however not applicable for the synthesis of polymers containing B–O linkages in the main chain. To obtain those types of B–O-linked

polymers a salt elimination strategy proved to be more successful, by reaction of bisborane **7** and OH-substituted sulfoximine **14** (Scheme 5.5) leading to BO-linked polymer **15** with a number average degree of polymerization (DP_n) of 7 (by GPC analysis).

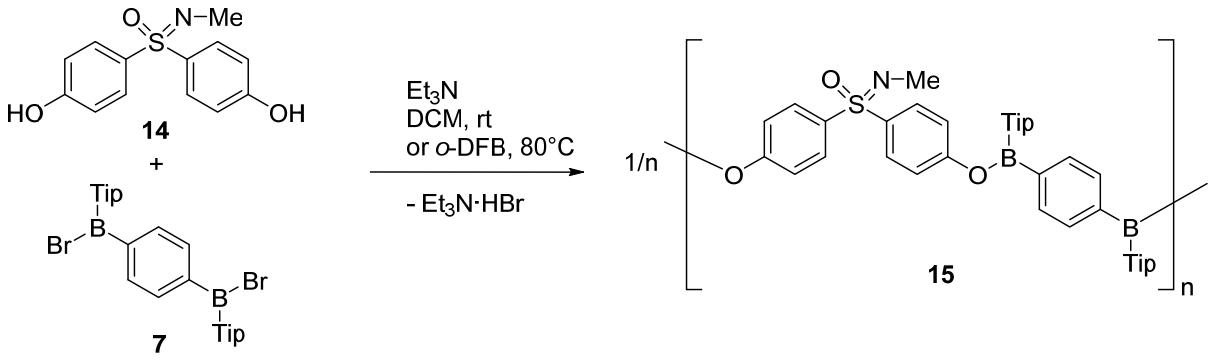

Scheme 5.5. Polycondensation reaction of sulfoximine **14** and bisborane **7** to yield alternating polymer **15**.

The Si/B exchange condensation was also applied for the synthesis of BP-linked oligomers. Oligomers **18a,b** were accessible using this approach (Scheme 5.6). On the other hand, the synthesis of oligomer **18c**, with Mes* (2,4,6-tri-*tert*-butylphenyl) as the sterically most demanding substituent at the P (in comparison to **18a** (Mes-substituent) and **18b** (Tip-substituent)), was not possible using this route. However, a salt elimination pathway proved to be successful (Scheme 5.6).

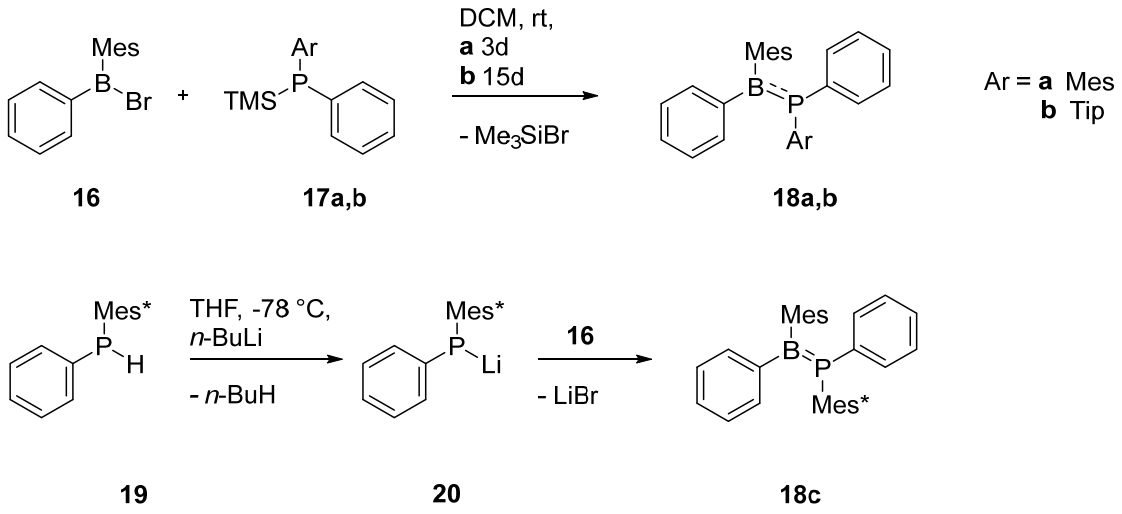

Scheme 5.6. Synthesis of BP-compounds **18a-c**.

Comparison of experimental and TD-DFT calculated data for these oligomers indicates the influence of the P-substituent on the molecular geometry of the phosphorus center and consequently on the characteristics of the BP bond. With the higher steric demand of the P-substituent the planarity at P increases and consequently the partial BP double bond character increases.

6 Zusammenfassung

Diese Arbeit zeigt, dass Silazanspaltung mit Si/B-Austausch eine einfache, aber effektive Synthesemethode zur Herstellung neuartiger anorganisch-organischer Polymere unter BN-Verknüpfung, darstellt. Im ersten Kapitel werden erste Derivate einer neuen Klasse von anorganischen–organisch Hybridpolymeren mit diskreten N-B-N-Einheiten in der Hauptkette vorgestellt. Erste Polymerisationsversuche unter Dehydrokupplung des Mono-boranaddukts von *para*-Phenylendiamin unter milden Bedingungen als Polykondensationsstrategie führte zu Materialien, die sich in gebräuchlichen organischen Lösungsmitteln als unlöslich erwiesen. Der Einbau von löslichkeitssteigernden Seitengruppen (Mesityl) am Boratom stellte sich als erfolgreicher Weg hinaus, um wohldefinierte Polymere mit NBN-Einheiten in der Hauptkette zu erhalten. Dafür wurde eine andere Polykondensationsstrategie genutzt, nämlich der Silizium-Bor-Austausch. Hierbei führte die Reaktion von silyliertem *p*-Phenylendiamin mit Dichlor(mesityl)boran (Schema 6.1) zu einer neuen Klasse von anorganisch-organischen Hybridpolymeren, den Poly[*N*-(*p*-phenylen)diimidoboran(3)]en (PPP-DIBs, **3**).

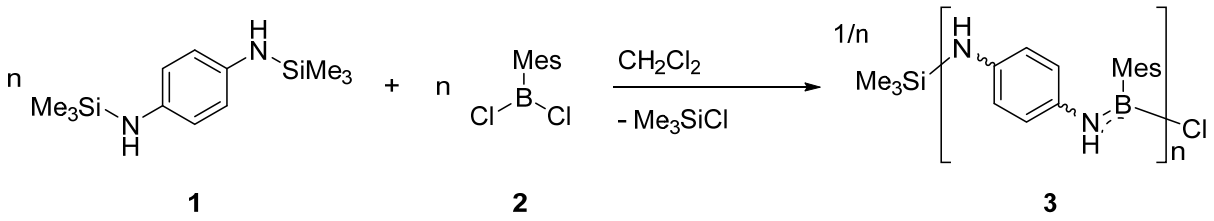

1 **2** **3**

Schema 6.1. Si/B-Austausch für die Synthese von NBN-Polymer **3**.

Das Polymer **3** löst sich in den gebräuchlichen organischen Lösungsmitteln. Die GPC-Analyse zeigte eine mittlere Molmasse von Mn = 7900 Da, was einem Polymerisationsgrad (DP_n) von 33 entspricht. Korrespondierende Modellverbindungen mit einer (**4**) bzw. mit zwei NBN-Einheiten (**5**) konnten ebenso durch Anwendung des Si/B-Austauschkonzepts synthetisiert werden (Abbildung 6.1).

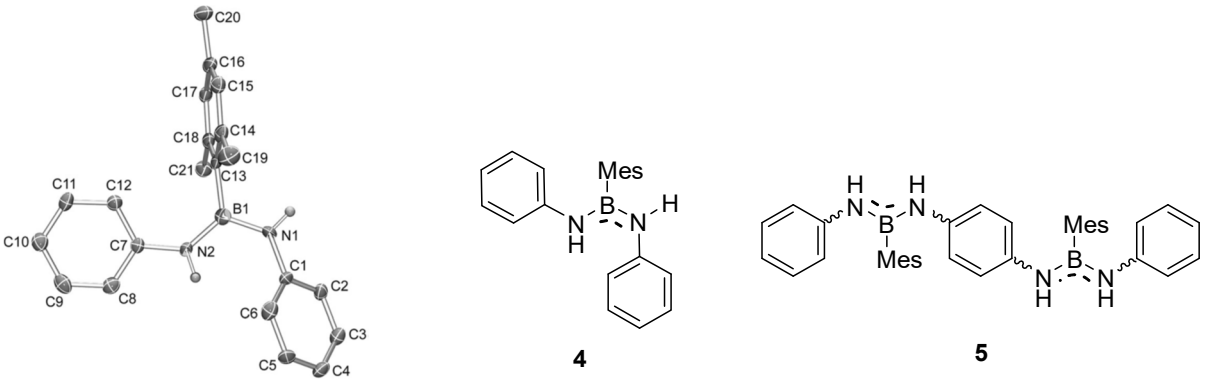

Abbildung 6.1. NBN-Modellverbindungen **4** und **5** und Molekülstruktur von **4** im Festkörper bestimmt durch Einkristall-Röntgendiffraktometrie.

Photophysikalische Untersuchungen zeigten eine moderate π-Konjugation entlang der NBN-Einheit mit einer geringen bathochromen Verschiebung mit steigender Anzahl an NBN-Einheiten von 267 nm (**4**), über 280 nm (**5**) zu 295 nm (Polymer **3**). Diese Rotverschiebung untermauert die Hypothese, dass sich bei Polymerbildung die Konjugationslänge moderat erweitert. Außerdem zeigte Polymer **3a** das Potenzial als Polyligand zu fungieren, indem es unter Metallkoordination (Zr^{4+}) zu Polymer **3b** reagiert (Schema 6.2).

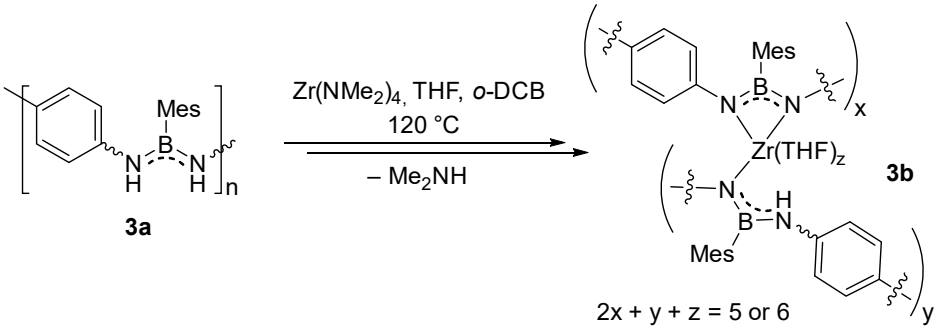

Schema 6.2. Vernetzung von **3a**.

Weiterhin wurden mittels des zuvor etablierten Si/B-Austauschs erste Derivate einer anderen neuen Klasse von anorganisch-organischen Hybridpolymeren, die Poly(*p*-Phenylenimino-borane), synthetisiert (Schema 6.3). Diese Polymere können als BN-Analoga von Poly(*p*-phenylenvinylen) (PPV) bezeichnet werden.

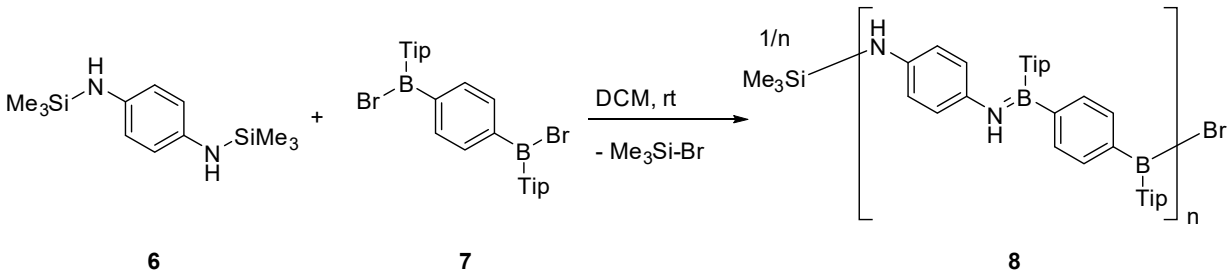

6 **7** **8**

Schema 6.3. Synthese von Polymer **8** (BN-PPV).

Um die Stabilität am Borzentrum zu erhöhen, wurde eine sterisch anspruchsvollerer Tip-Gruppe (Tip = 2,4,6-triisopropylphenyl) als Substituent am B eingebaut, wodurch für das Polymer **8** eine bessere Luft- und Wasserstabilität erreicht wurde. Zusätzlich wurden für einen besseren Einblick in die Molekülstruktur von **8** die entsprechenden BN-Modellverbindungen **9-11** synthetisiert (Abbildung 6.2). Die Molekülstrukturen von Verbindungen **10** und **11** wurden mittels Einkristall-Röntgendiffraktometrie bestimmt. Beide Oligomere wiesen eine leichte Verdrehung zwischen den *trans*-gerichteten Phenyl- und Phenylengruppen an der B=N-Einheit auf. Kombinierte photophysikalische Untersuchungen und TD-DFT-Berechnungen lieferten eindeutige Belege für eine π-Konjugation entlang des Polymerrückgrats über die B=N-Einheiten hinaus und eine Erweiterung der Konjugation mit steigender Kettenlänge.

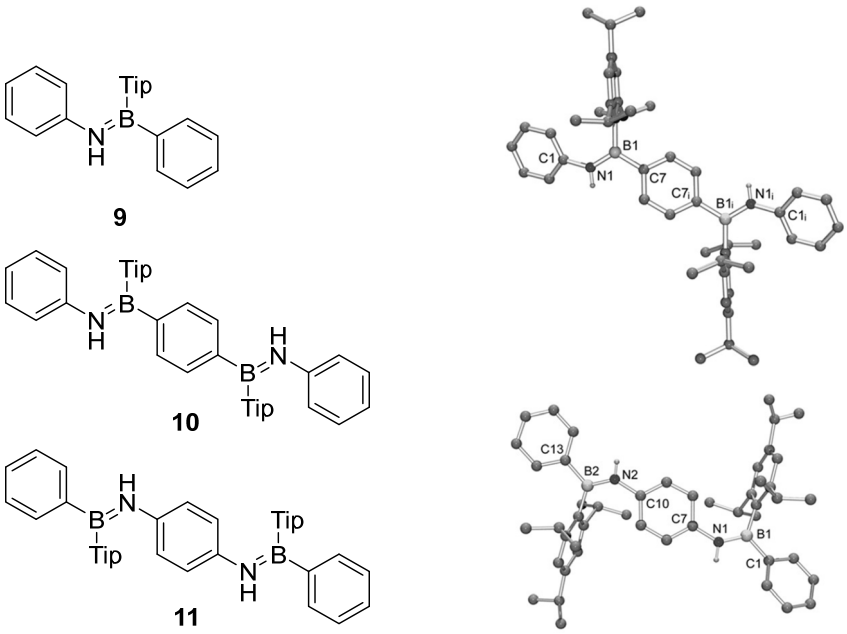

Abbildung 6.2. Modellverbindungen **9-11** und Molekülstrukturen von **10** und **11** im Festkörper.

Um die Übertragbarkeit des Si/B-Austauschs auf weitere Systeme zu untersuchen, wurde Sulfoximin **12** als Diaminmonomer getestet. Dies führte zu den ersten anorganisch-organischen

Hybridpolymeren, die aus alternierenden Sulfoximin-Copolymeren mit B=N Verknüpfungen bestehen (Schema 6.4) und einen Polymerisationsgrad (DP_n) von 15 aufweisen (GPC-Analyse).

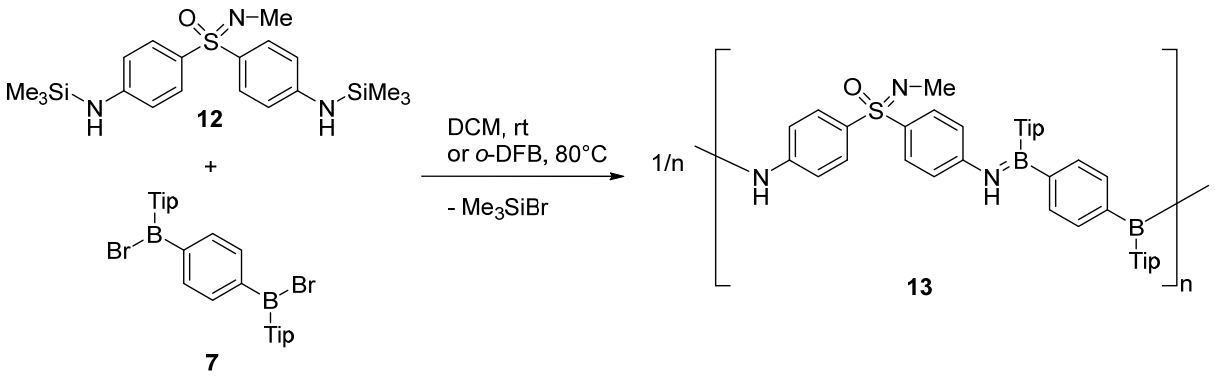

Schema 6.4. Polykondensationsreaktion von Sulfoximin **12** und Bisboran **7** zur Synthese von Polymer **13**.

Allerdings ließ sich das Konzept der Polykondensation unter Si/B-Austausch nicht auf Polymere mit B–O-Bindung in der Hauptkette anwenden. Um diese Art der B–O-verknüpften Polymere zu erhalten, erwies sich eine Salzeliminierung als Synthesestrategie zielführend. Hierbei wurde das Bisboran **7** mit dem OH-substituierten Sulfoximin **14** umgesetzt (Schema 6.5) und das Polymer **15** wurde mit einem Polymerisationsgrad (DP_n) von 7 erhalten.

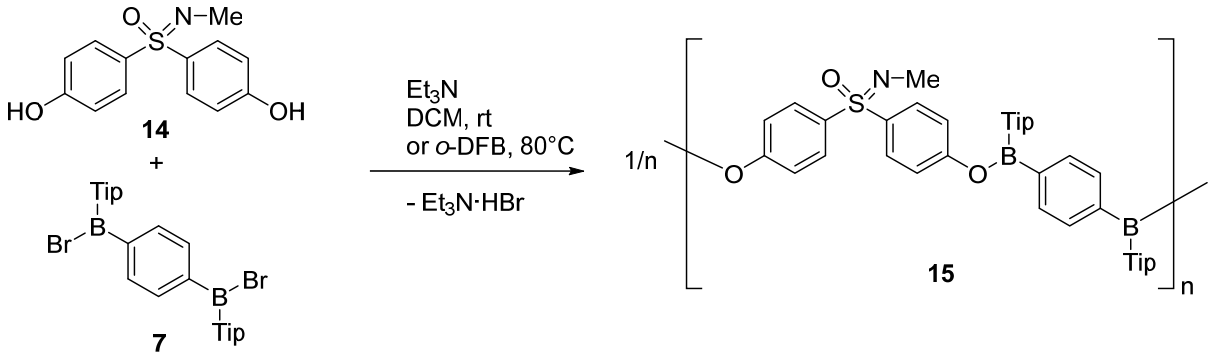

Schema 6.5. Polykondensationsreaktion von Sulfoximin **14** und Bisboran **7** zur Synthese von Polymer **15**.

Das Konzept des Si/B-Austauschs wurde auch zur Synthese von B–P-verknüpften Oligomeren angewendet. Oligomere **18a,b** konnten mittels dieses Ansatzes synthetisiert werden. Dagegen konnte Verbindung **18c**, mit Mes* (2,4,6-tri-*tert*-butylphenyl) als sterisch anspruchsvollster Substituent am Phosphor (im Vergleich zu **18a** (Mes-substituiert) und **18b** (Tip-substituiert)), nicht auf diesem Weg synthetisiert werden. Jedoch erwies sich für die Synthese von **18c** eine Salzeliminierungsroute als zielführend (Schema 6.6).

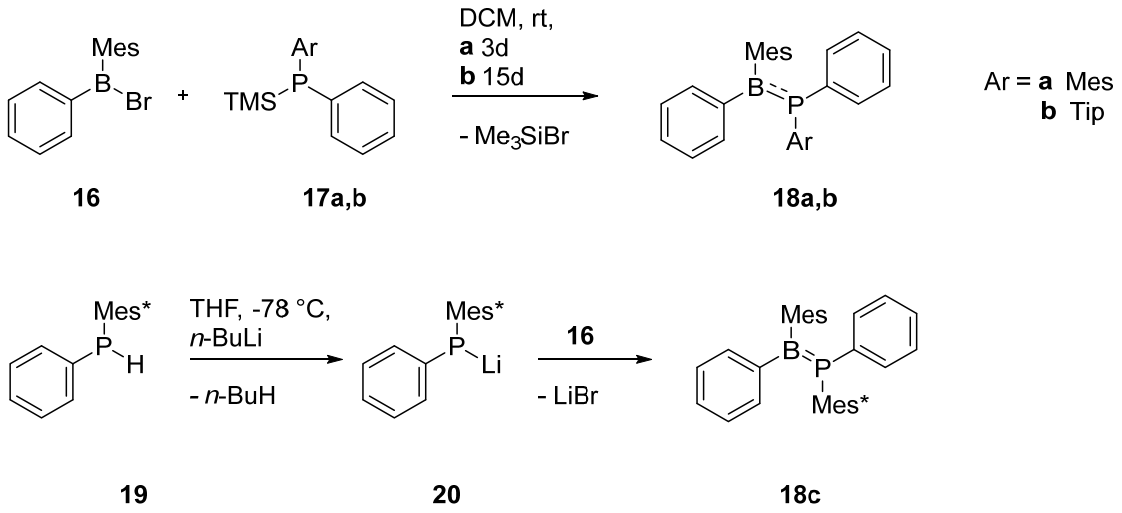

Schema 6.6. Synthese von BP-Verbindungen **18a-c**.

Ein Vergleich der experimentellen und der mittels TD-DFT berechneten Daten für diese Oligomere deuten auf einen Einfluss des P-Substituenten auf die Molekülgeometrie am Phosphorzentrum und somit auch auf die BP-Bindung hin. Mit sterisch anspruchsvolleren P-Substituenten wird die Umgebung am Phosphor planarisiert und infolgedessen wird auch der partielle Doppelbindungscharakter der BP-Bindung vergrößert.

7 Appendix

7.1 Dehydrocoupling and Silazane Cleavage Routes to Organic-Inorganic Hybrid Polymers with NBN Units

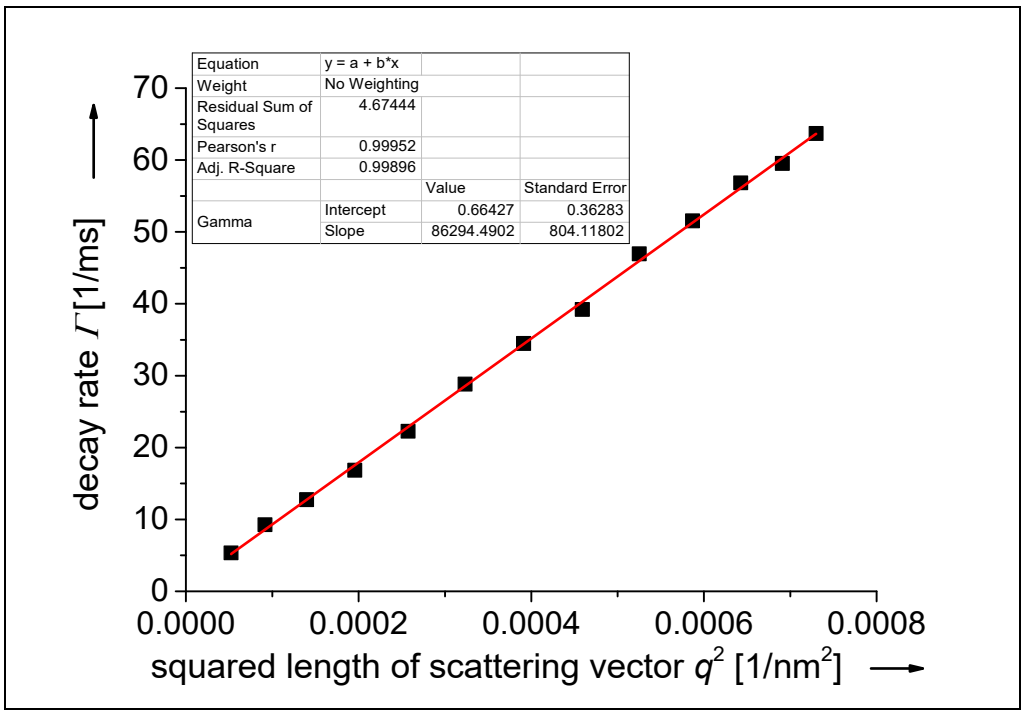

Figure 7.1.1. Plot of decay rates against the squared length of the scattering vector q^2 for the DLS measurement of **13'** in THF.

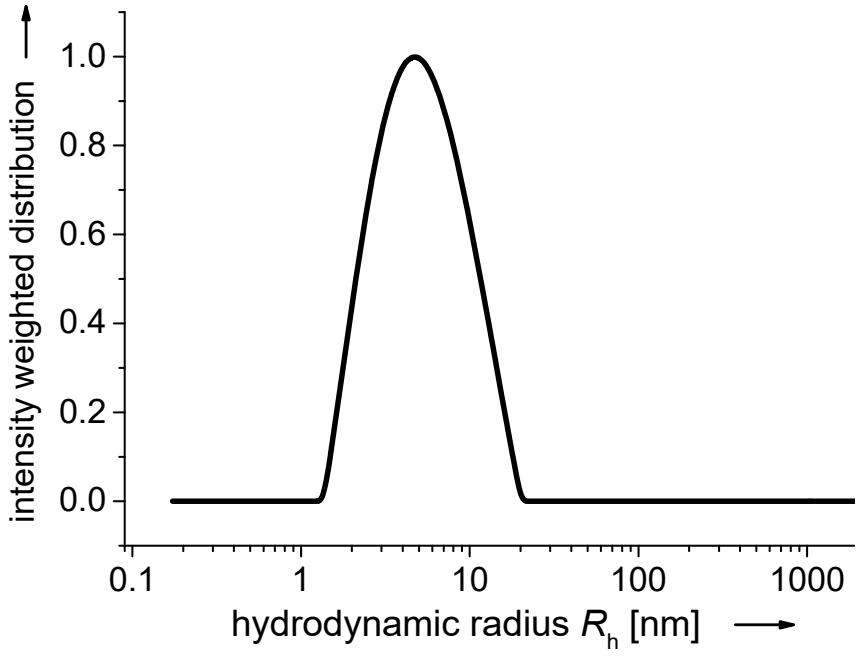

Figure 7.1.2. Intensity weighted size distribution of particles of **13'** in THF by DLS ($\theta = 90°$).

Gel permeation chromatography (GPC) of 13'

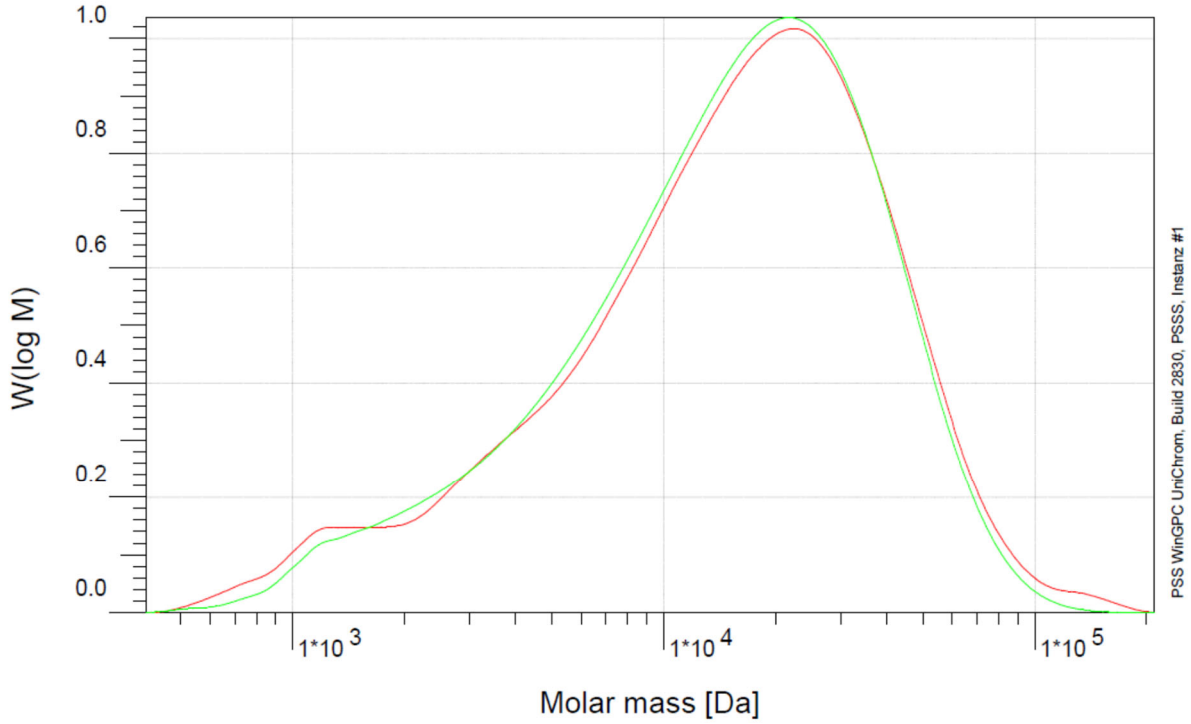

Figure 7.1.3. Gel permeation chromatography (GPC) trace of **13'** (in THF); green line: detection by UV signal; red line: detection by RI signal.

NMR spectra

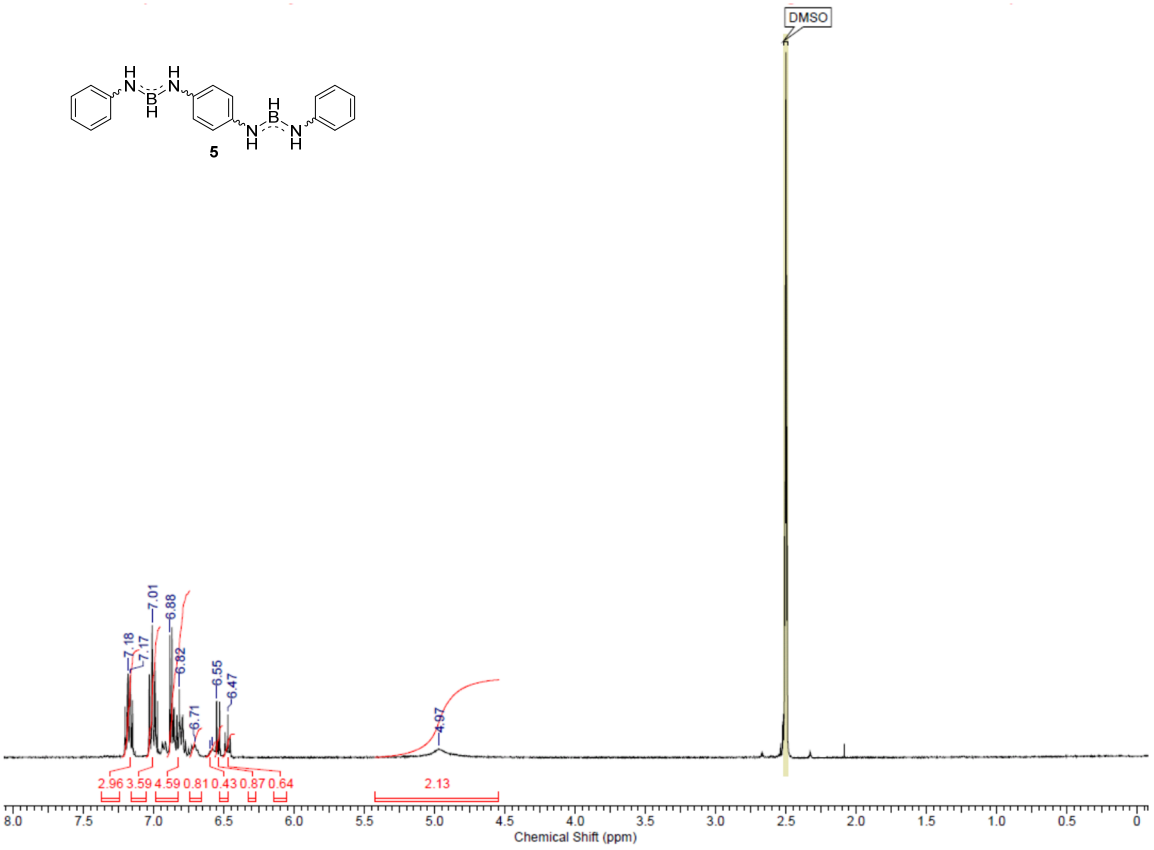

Figure 7.1.4. ^{1}H NMR spectrum of **5** (in DMSO-d_6).

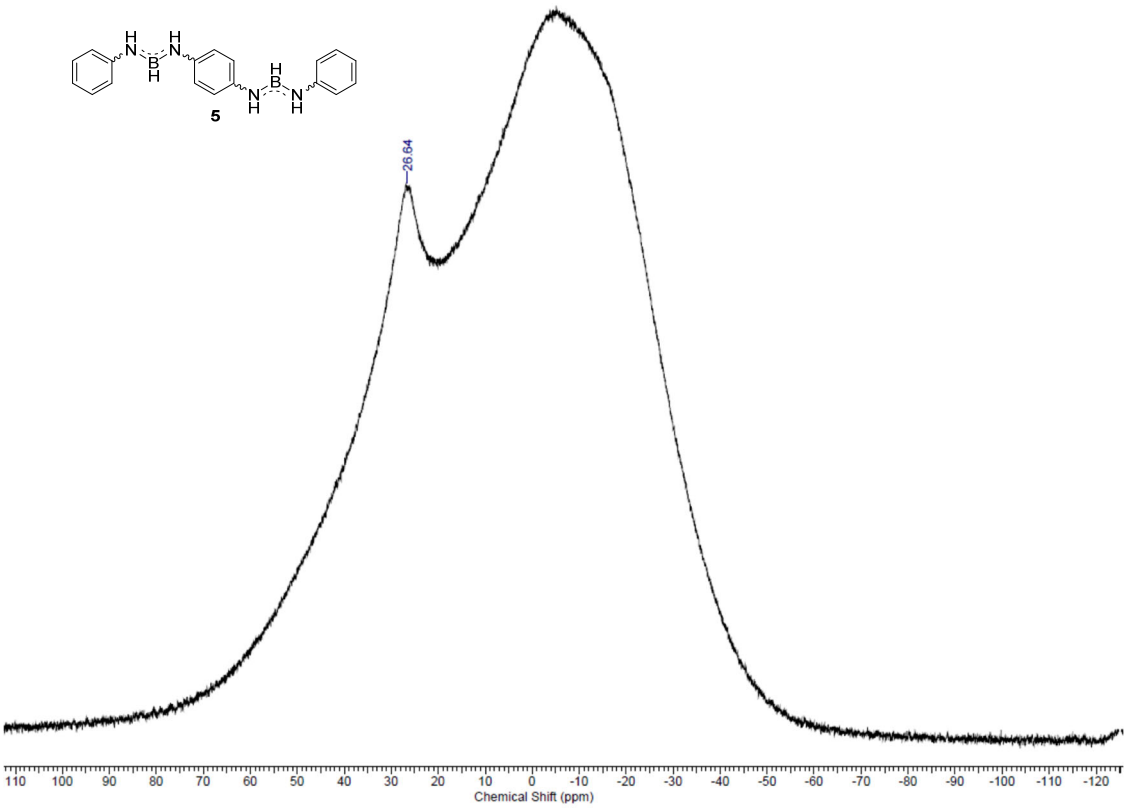

Figure 7.1.5. $^{11}B\{^{1}H\}$ NMR spectrum of **5** (in DMSO-d_6).

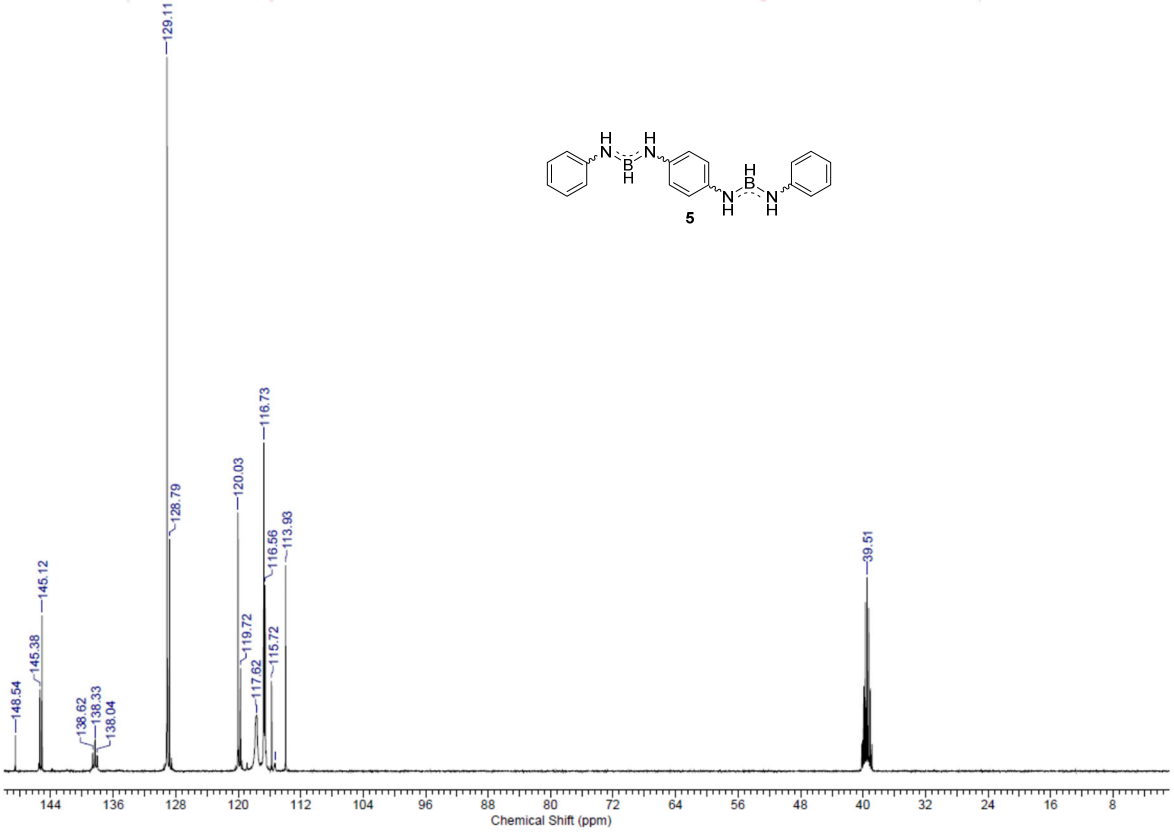

Figure 7.1.6. $^{13}C\{^{1}H\}$ NMR spectrum of **5** (in DMSO-d_6).

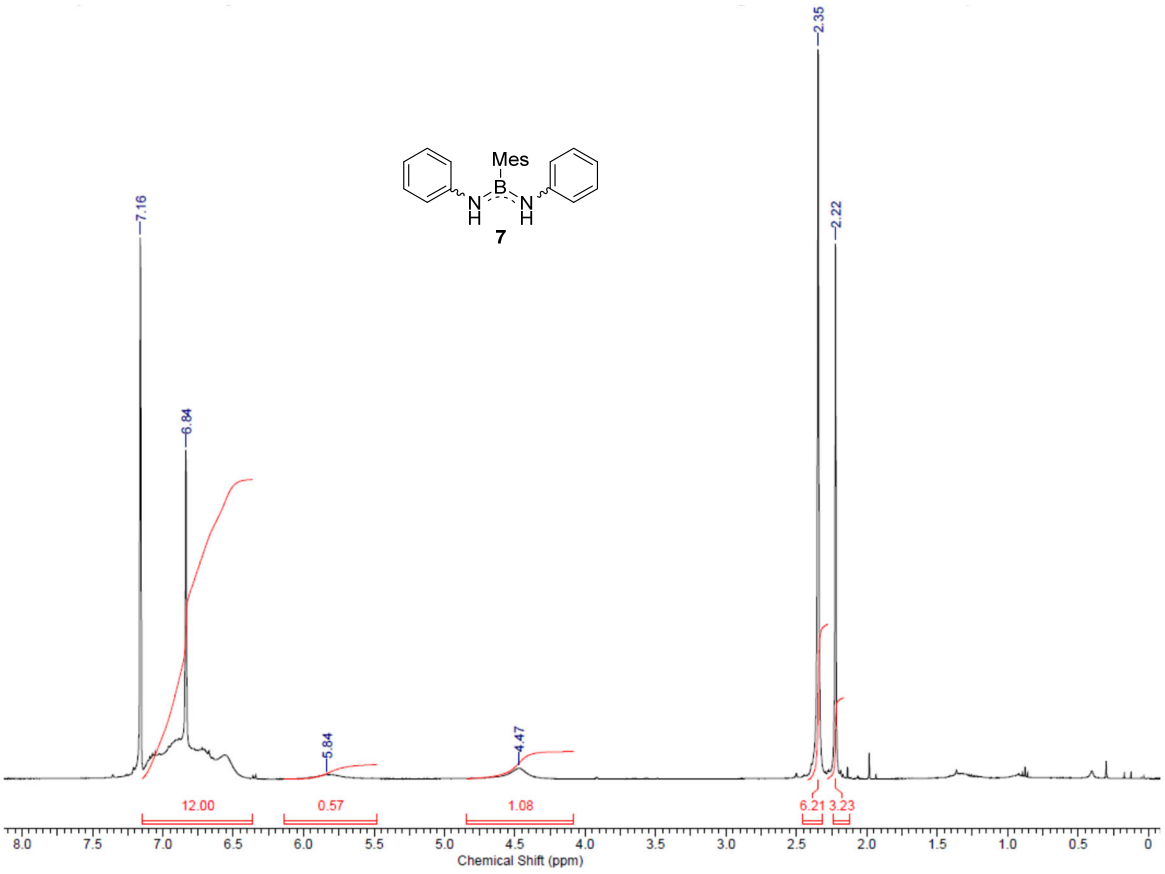

Figure 7.1.7. ^{1}H NMR spectrum of **7** (in C_6D_6).

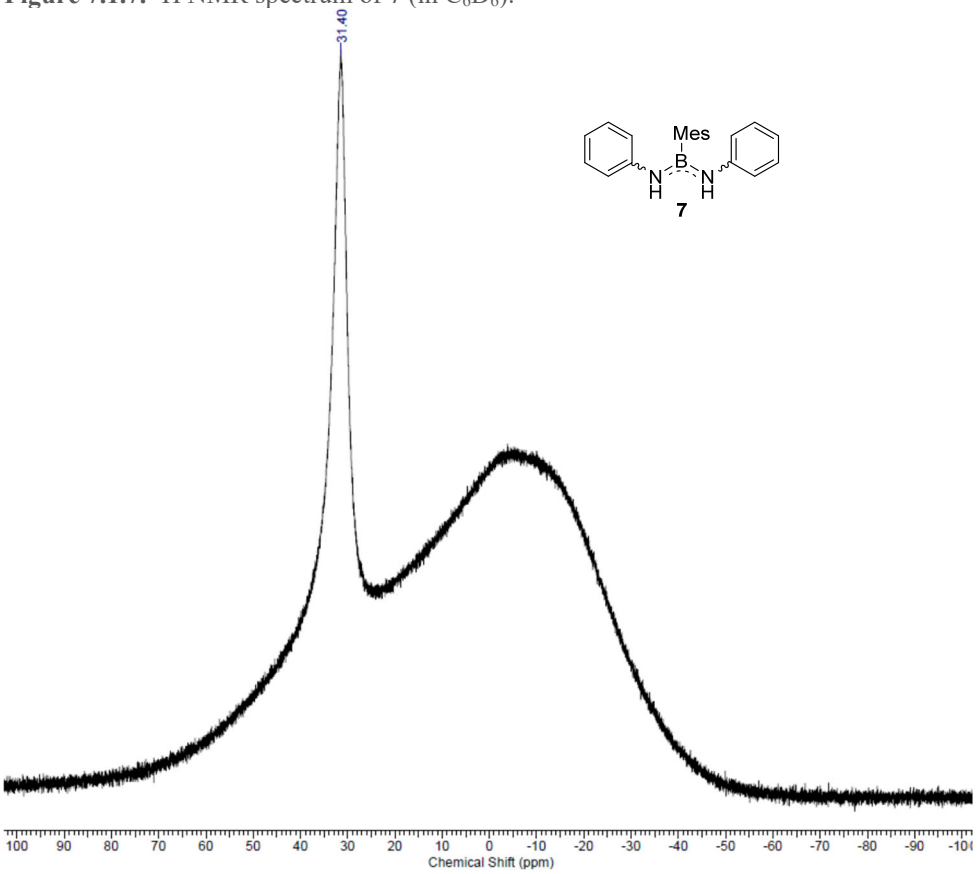

Figure 7.1.8. ^{11}B{^{1}H} NMR spectrum of **7** (in C_6D_6).

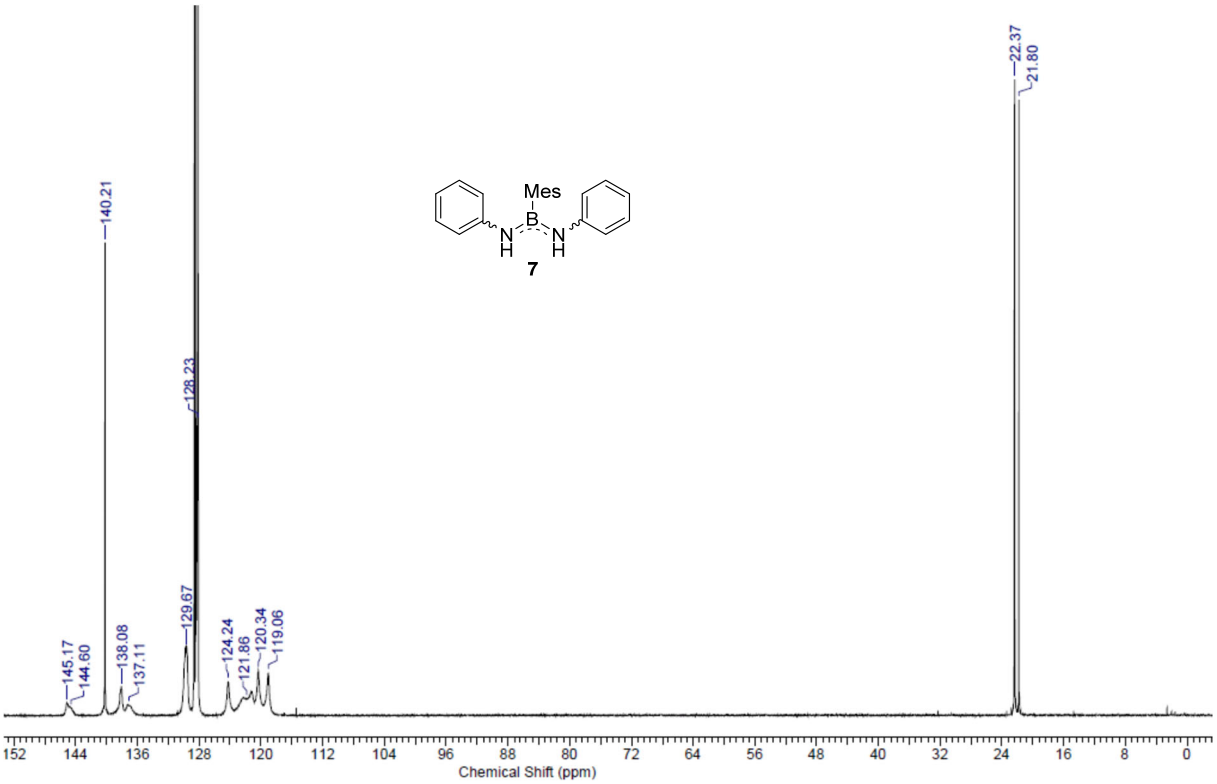

Figure 7.1.9. $^{13}C\{^{1}H\}$ NMR spectrum of **7** (in C_6D_6).

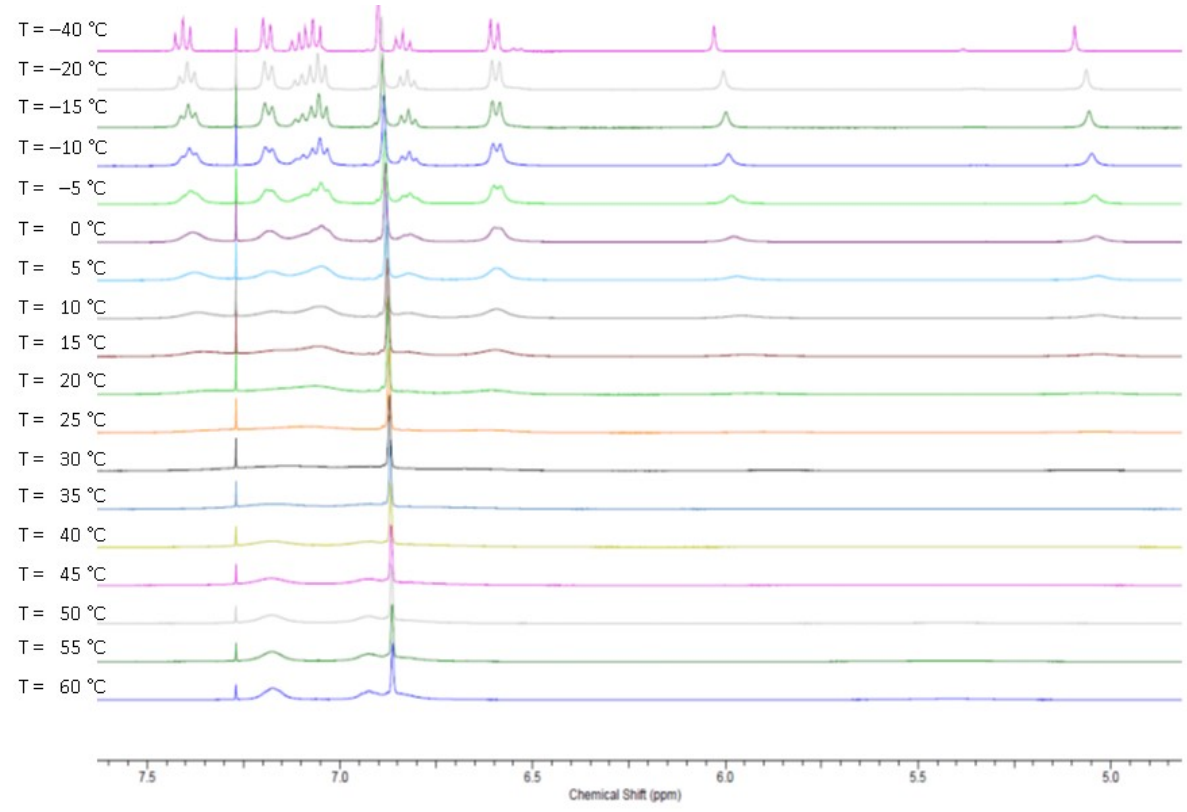

Figure 7.1.10. ^{1}H NMR spectrum of **7** (in $CDCl_3$; T = –40 °C to 60 °C).

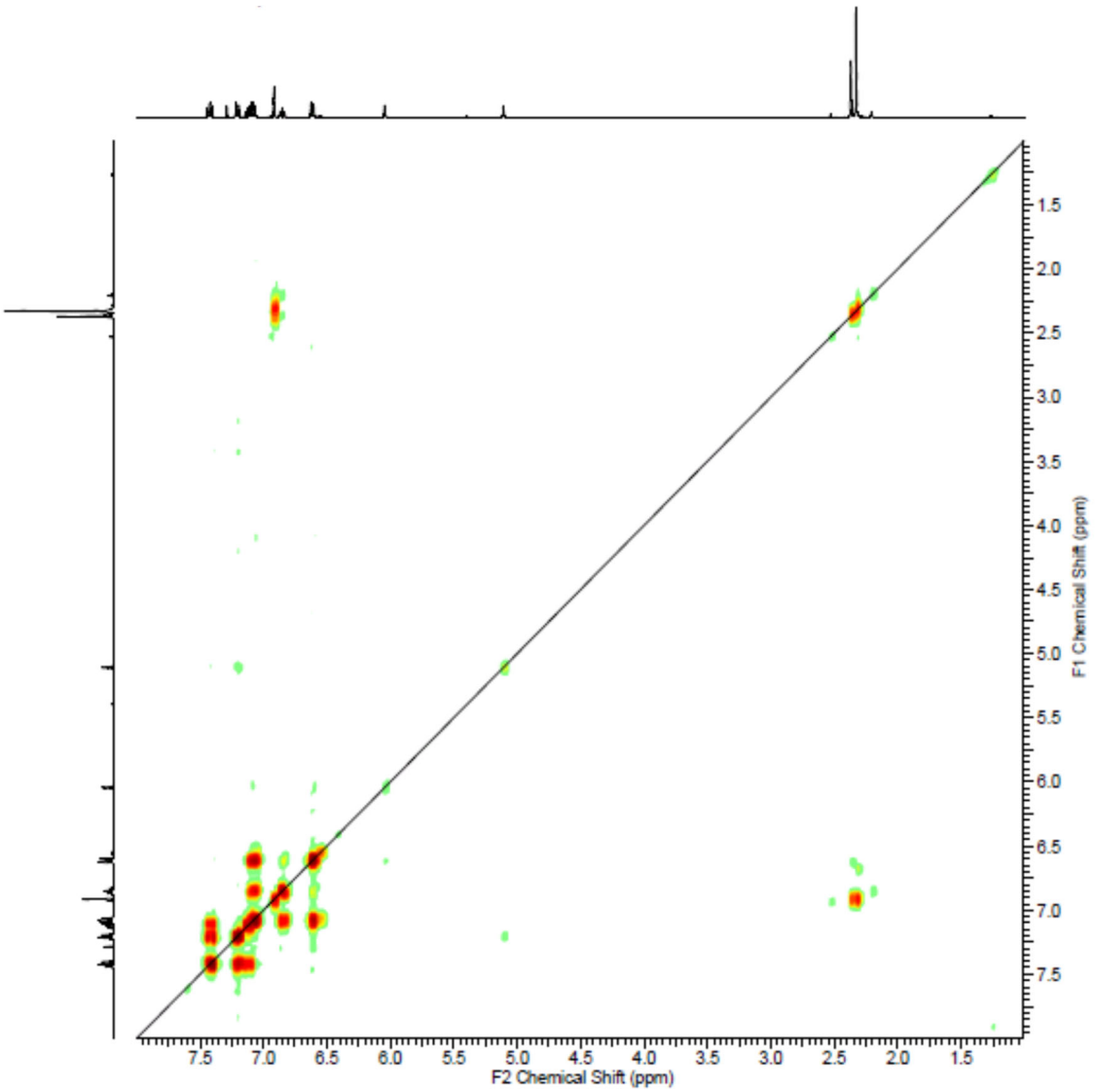

Figure 7.1.11. ^{1}H COSY NMR spectrum of **7** (in $CDCl_3$; T = –40 °C).

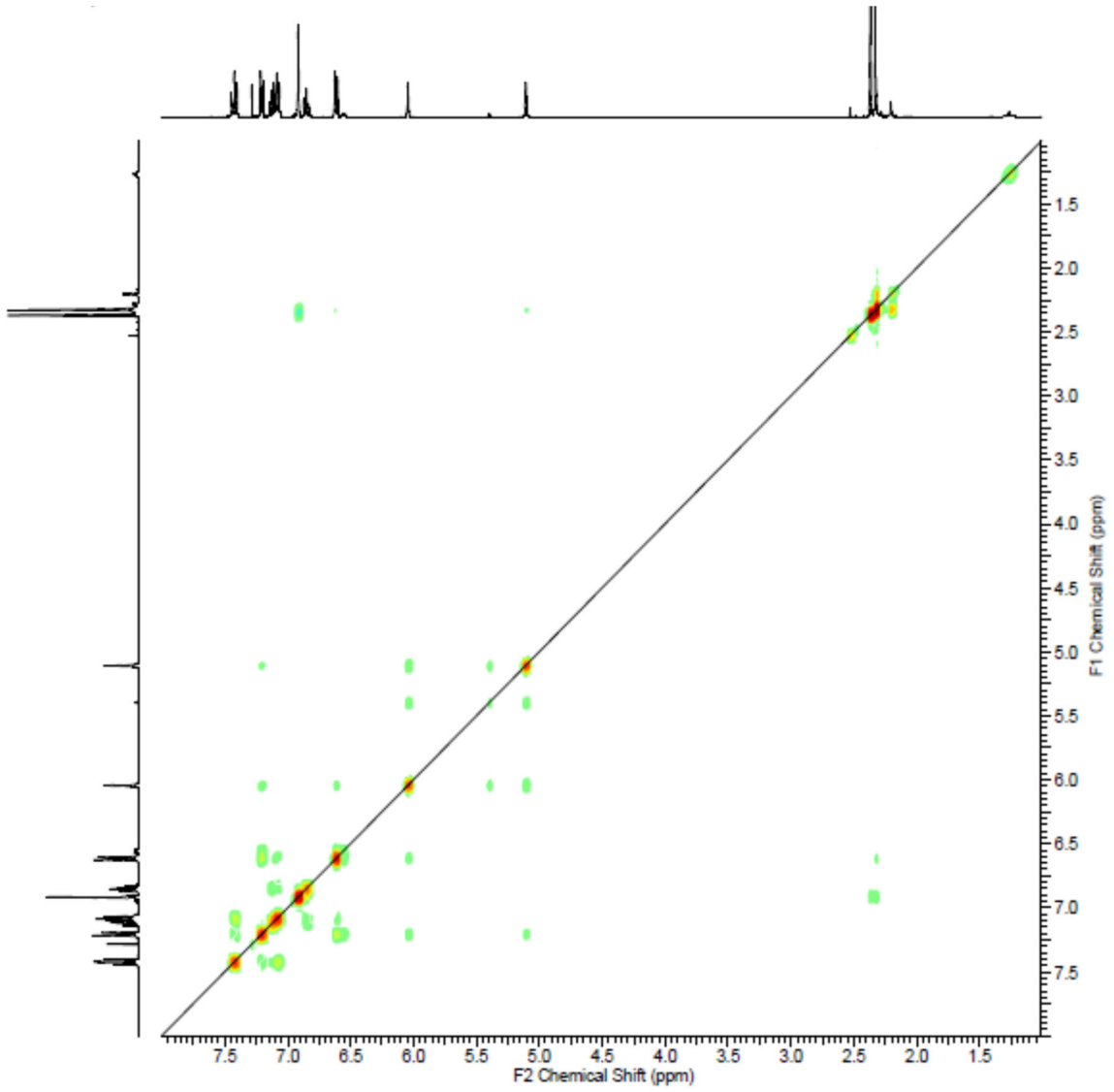

Figure 7.1.12. ^{1}H NOESY NMR spectrum of **7** (in $CDCl_3$; T = –40 °C).

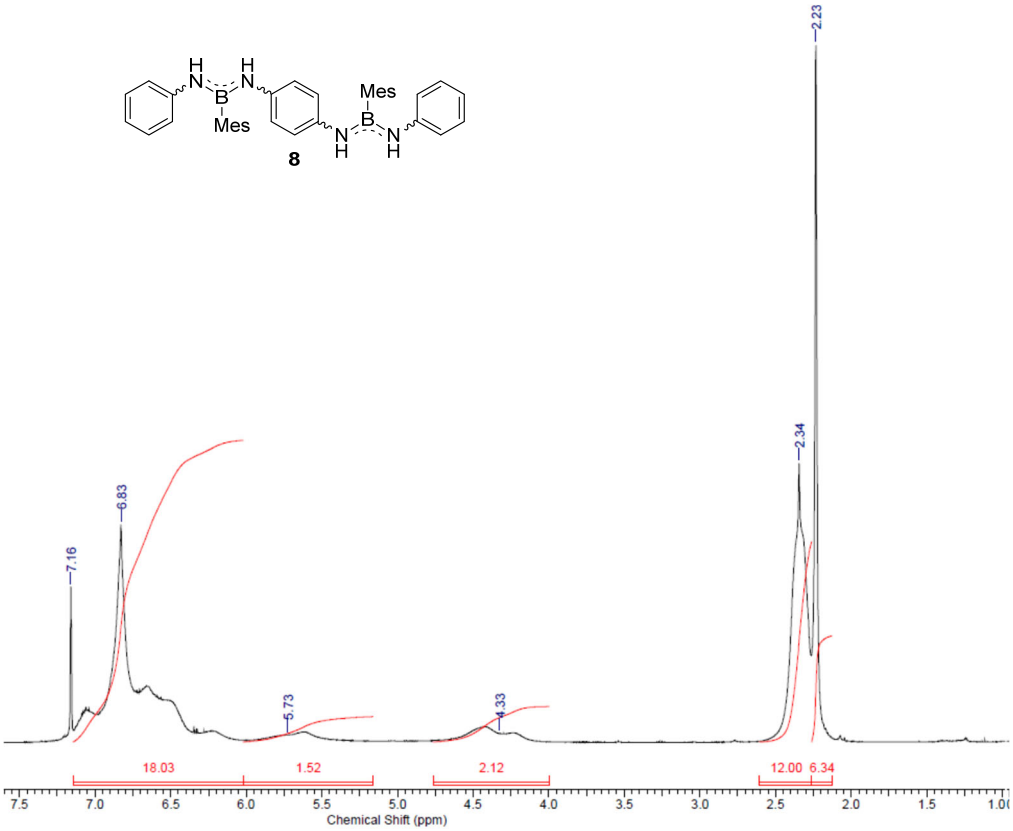

Figure 7.1.13. ^{1}H NMR spectrum of **8** (in C_6D_6).

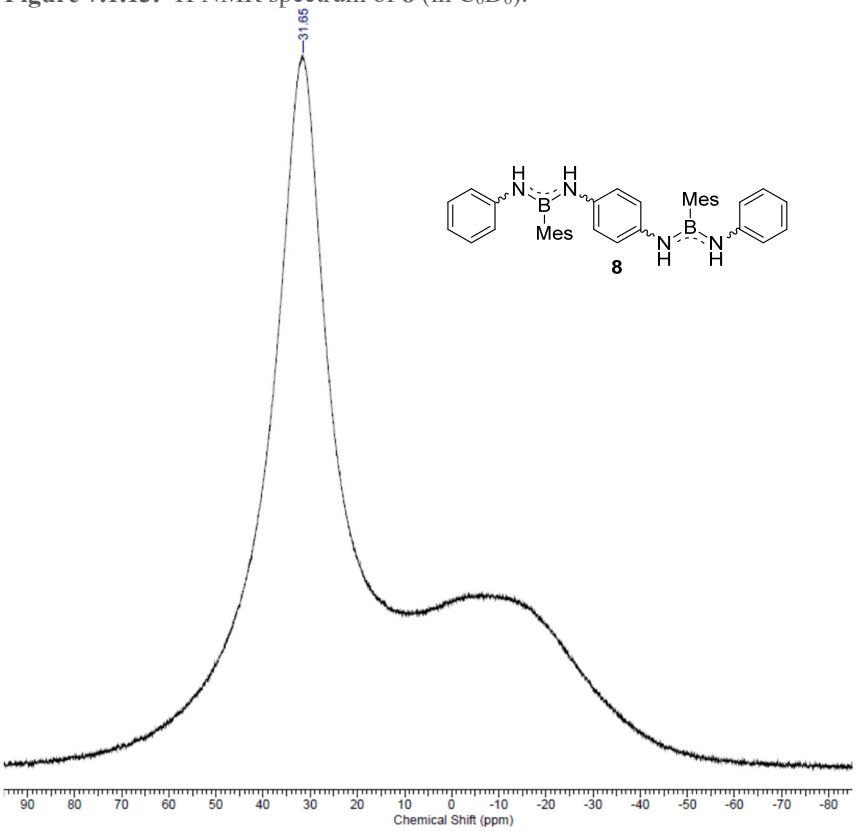

Figure 7.1.14. ^{11}B{^{1}H} NMR spectrum of **8** (in C_6D_6).

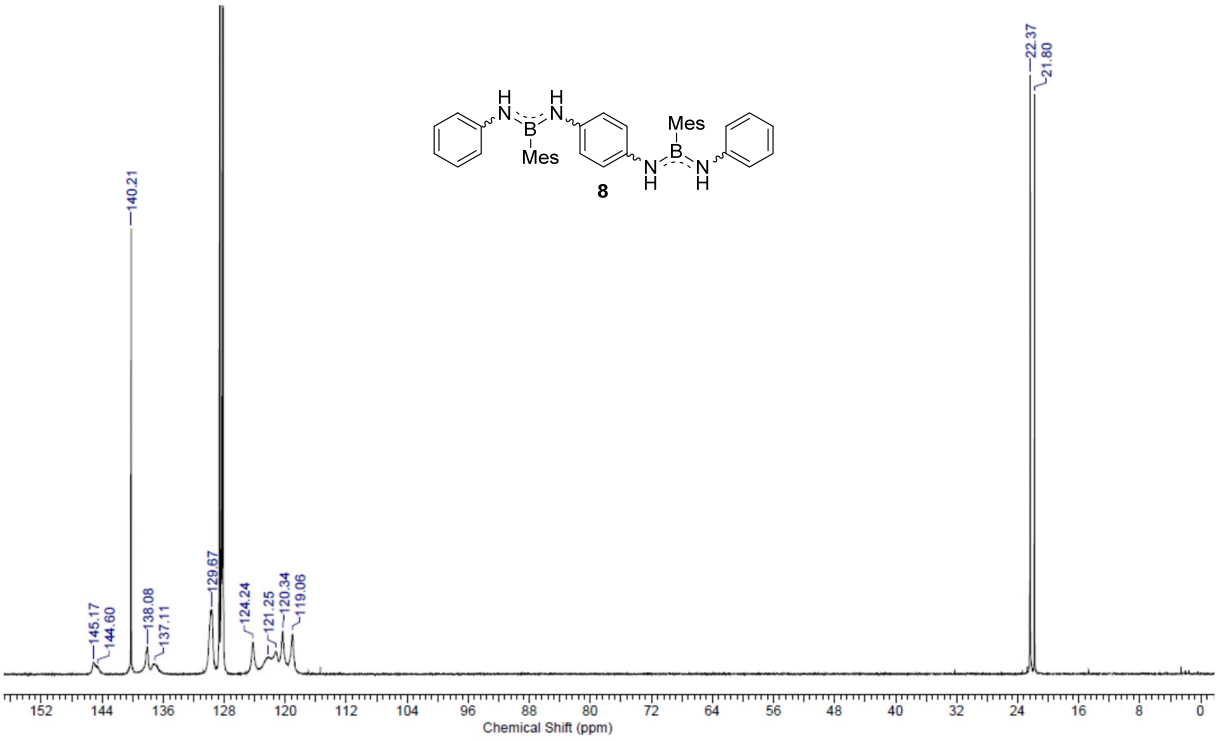

Figure 7.1.15. $^{13}C\{^{1}H\}$ NMR spectrum of **8** (in C_6D_6).

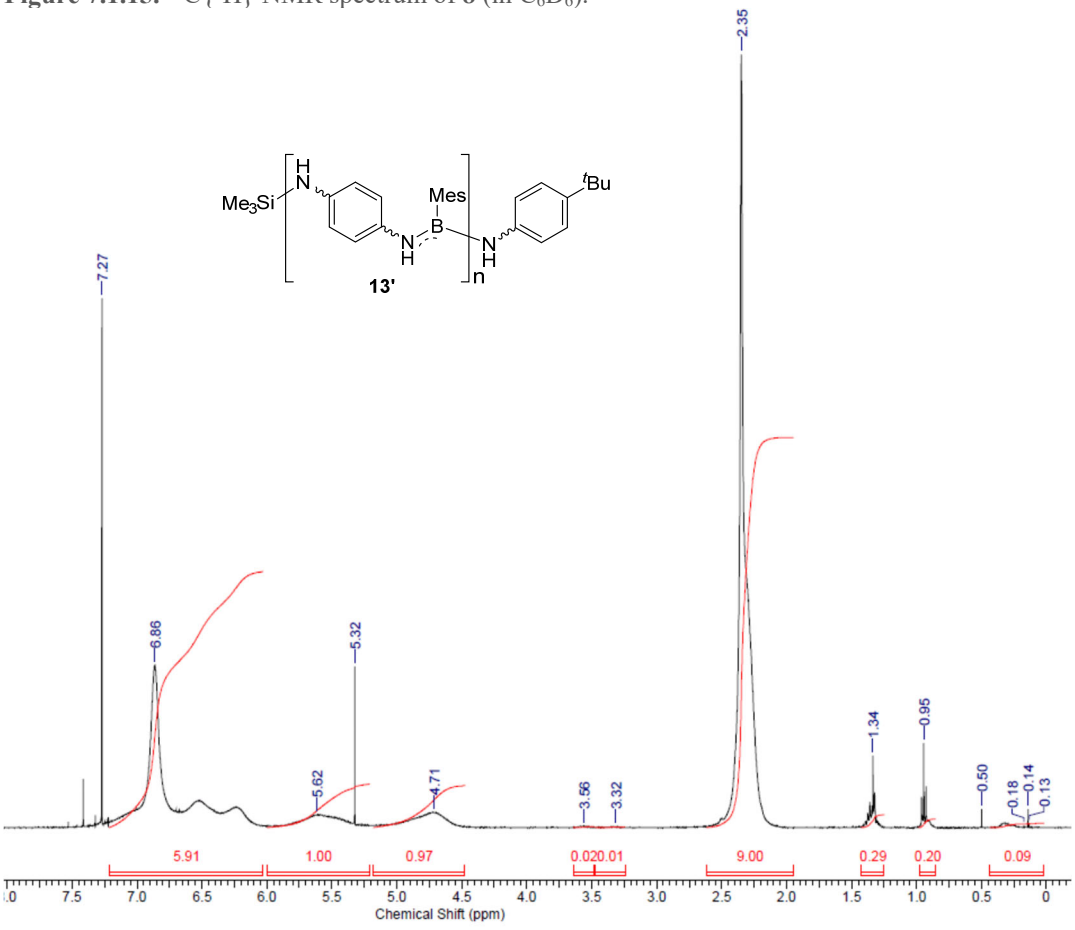

Figure 7.1.16. ^{1}H NMR spectrum of **13'** (in $CDCl_3$).

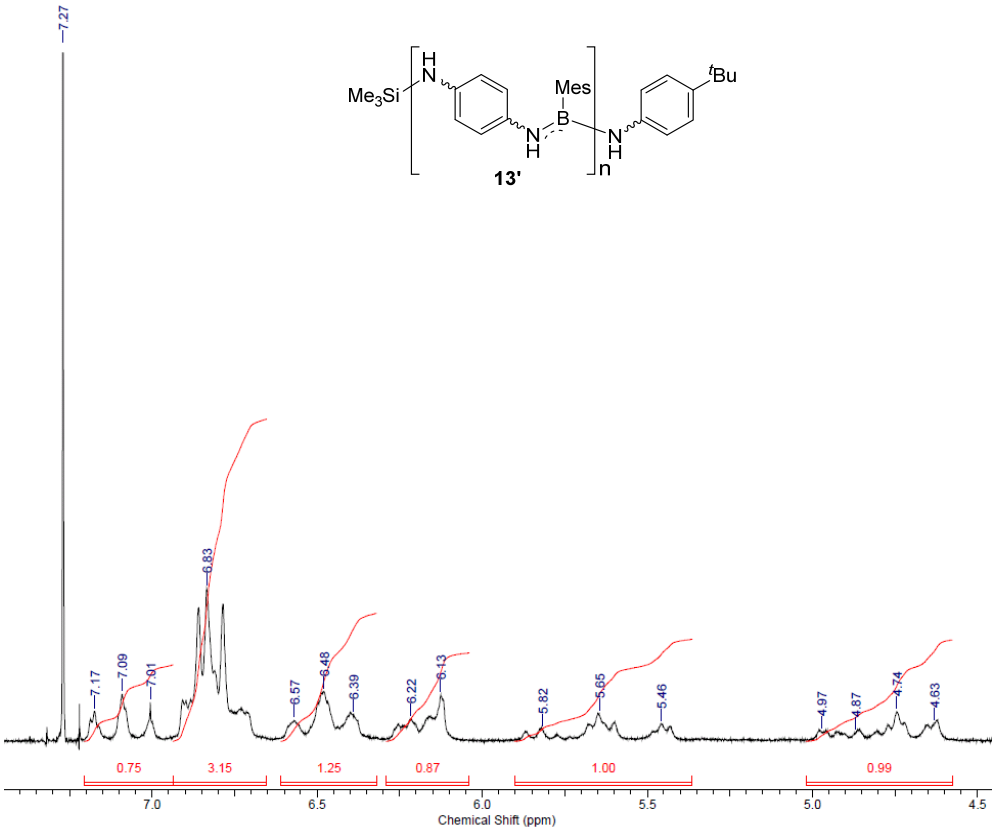

Figure 7.1.17. ^{1}H NMR spectrum (selected region) of **13'** (in $CDCl_3$; T = –40°C).

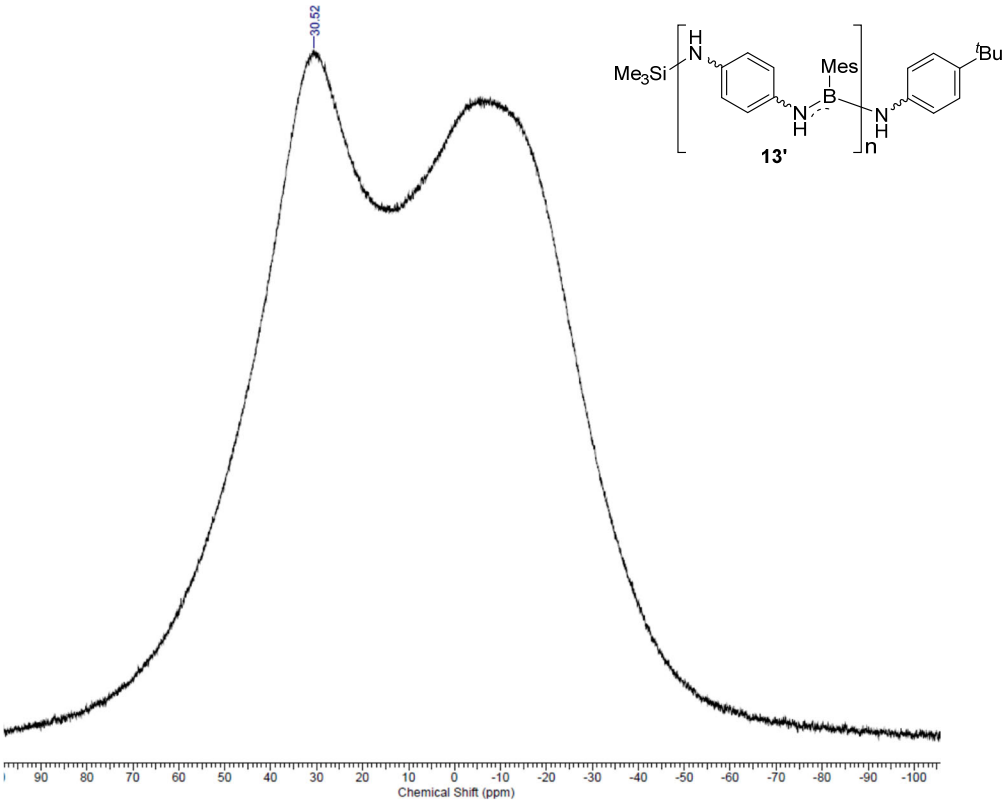

Figure 7.1.18. ^{11}B{^{1}H} NMR spectrum of **13'** (in $CDCl_3$).

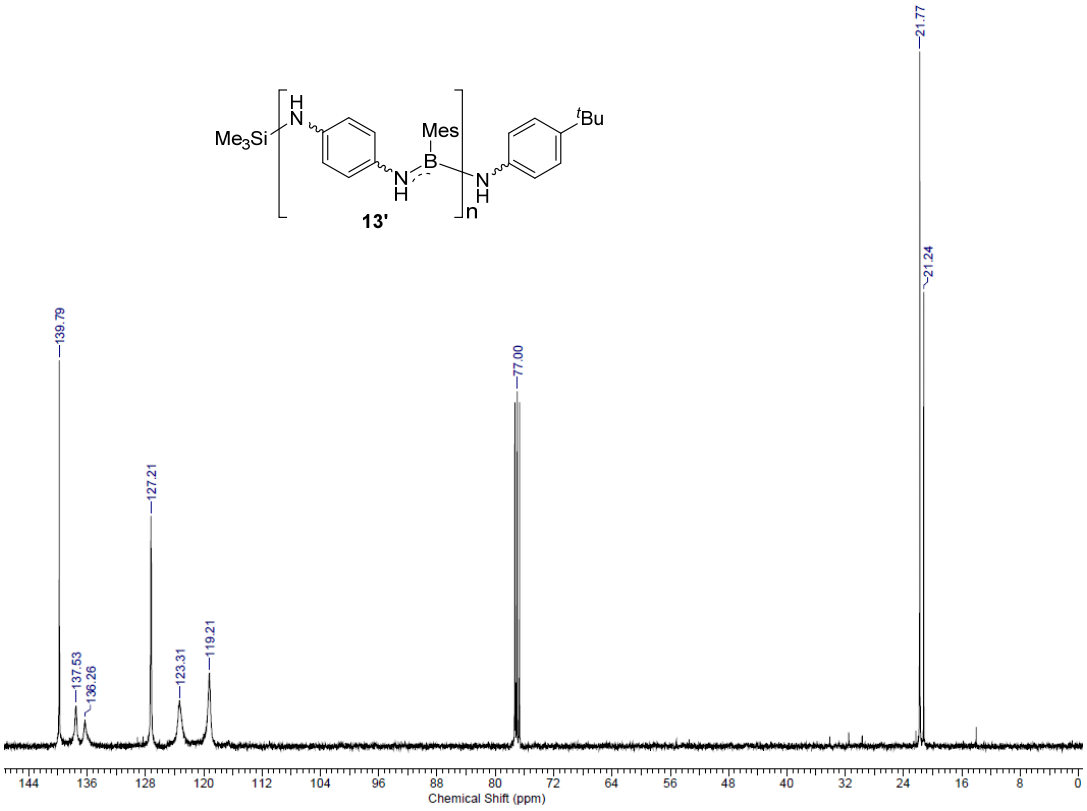

Figure 7.1.19. $^{13}C\{^{1}H\}$ NMR spectrum of **13'** (in $CDCl_3$).

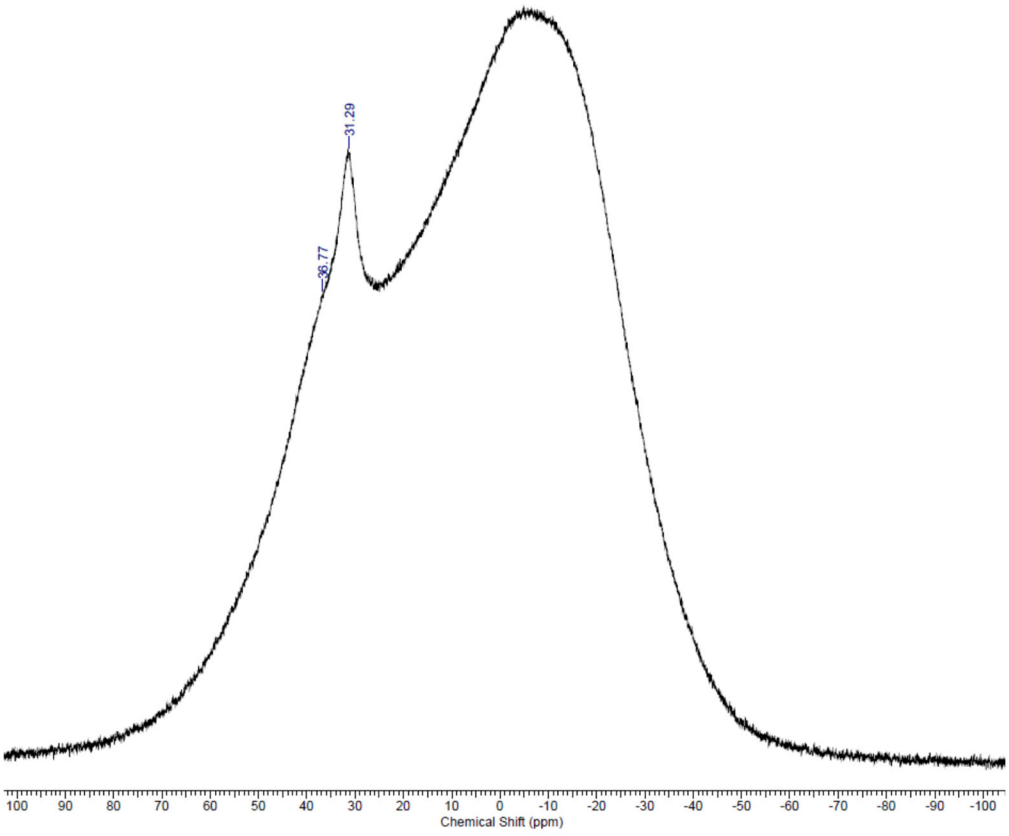

Figure 7.1.20. $^{11}B\{^{1}H\}$ NMR spectrum (in $CDCl_3$) of the reaction mixture of **7** with 0.5 equiv. of $Zr(NMe_2)_4$ and THF heated at 120°C in 1,2-dichlorobenzene for 45 min.

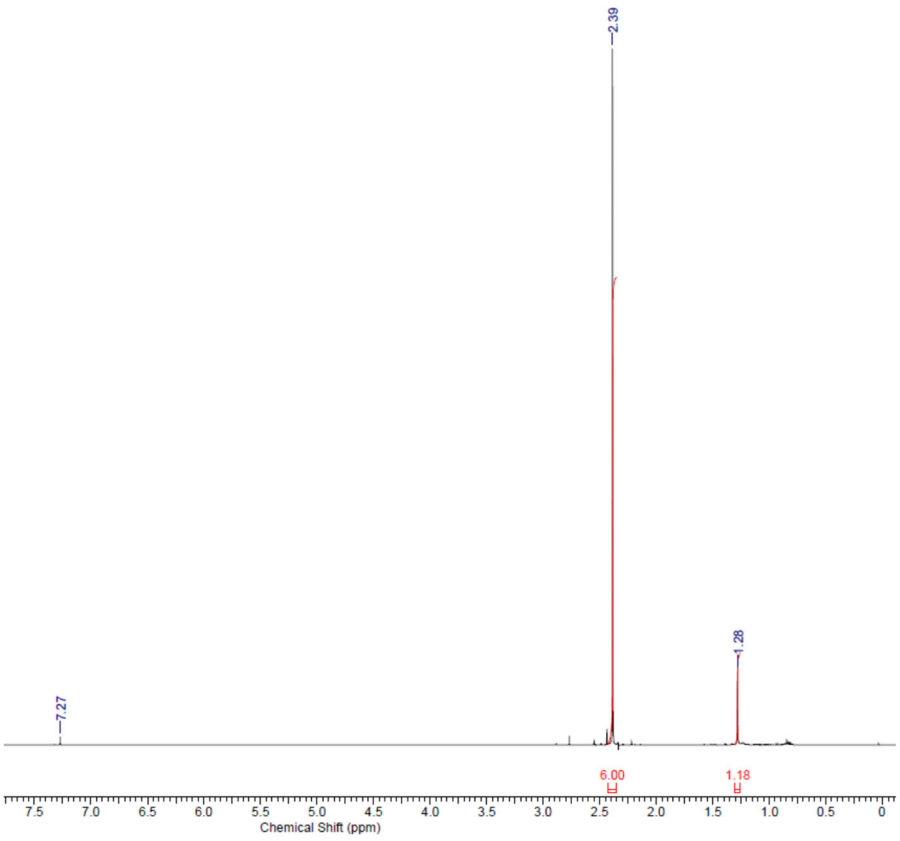

Figure 7.1.21. ^{1}H NMR spectrum of $HNMe_2$ (in $CDCl_3$) obtained by reaction of dimethylamine hydrochloride with KOH in water and subsequent condensation into cooled (–78 °C) $CDCl_3$.

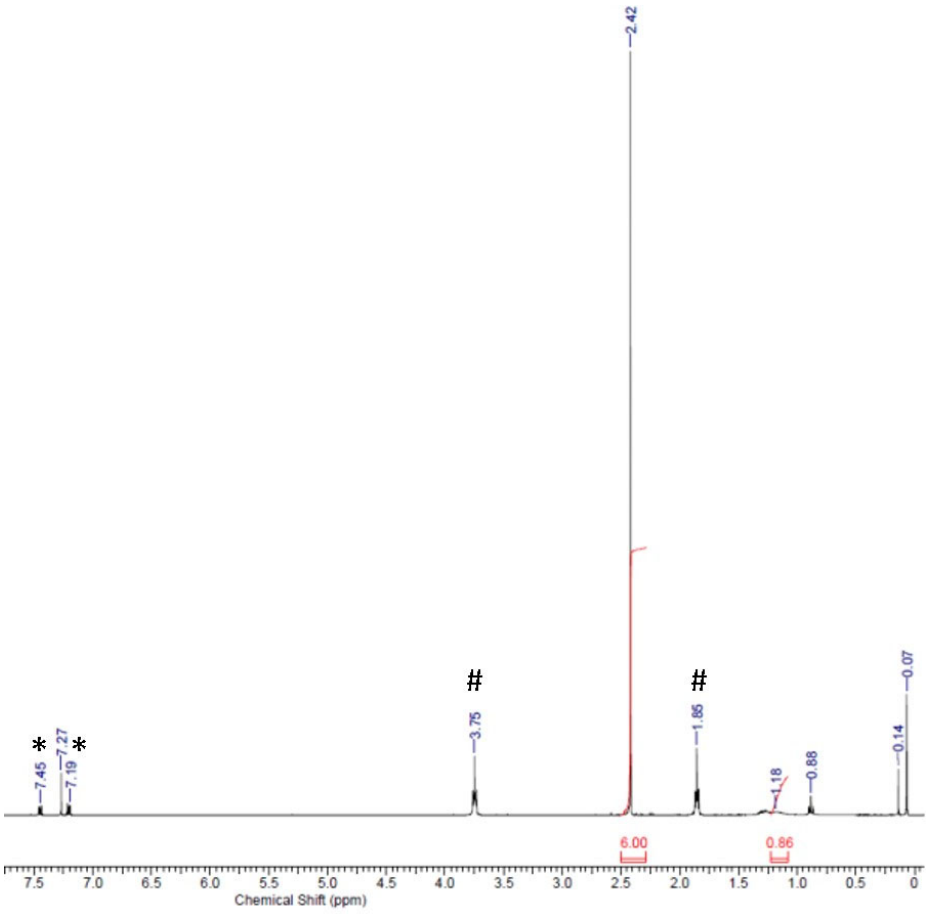

Figure 7.1.22. ^{1}H NMR spectrum of the condensate of the cross-linking of **13'** (in $CDCl_3$). *: *o*-DCB, #: THF

UV-vis spectra

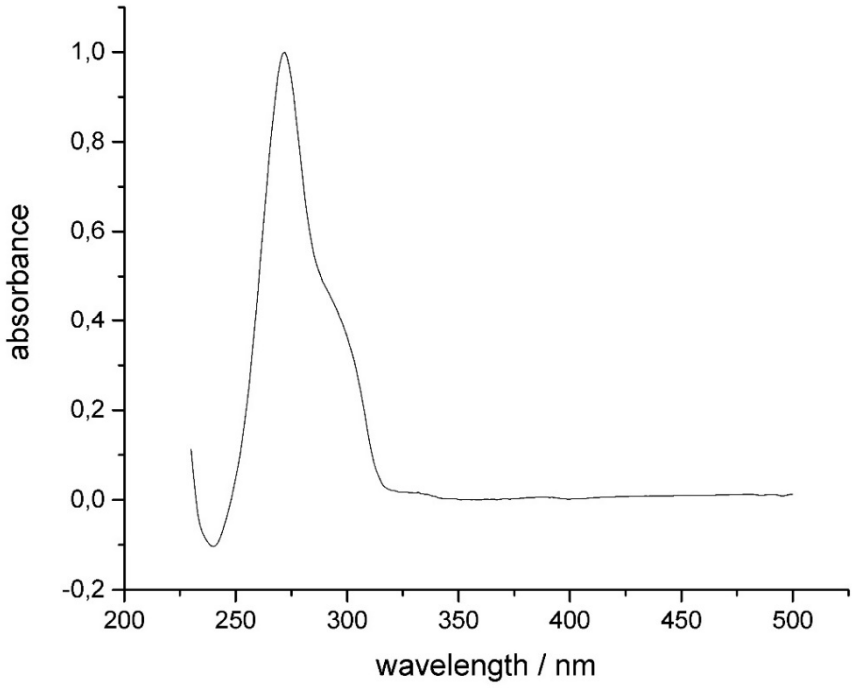

Figure 7.1.23. UV-vis spectrum of **3** (in THF).

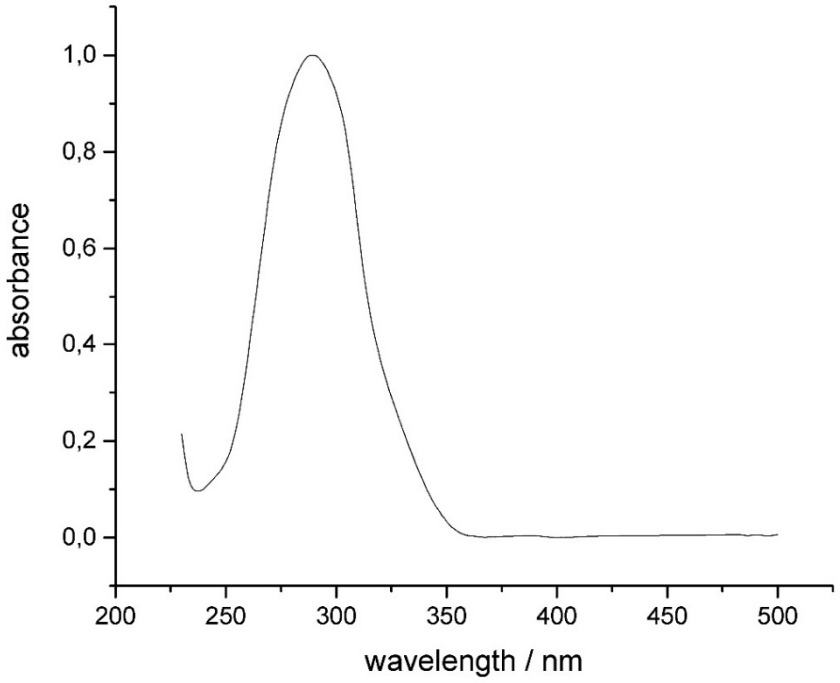

Figure 7.1.24. UV-vis spectrum of **5** (in THF).

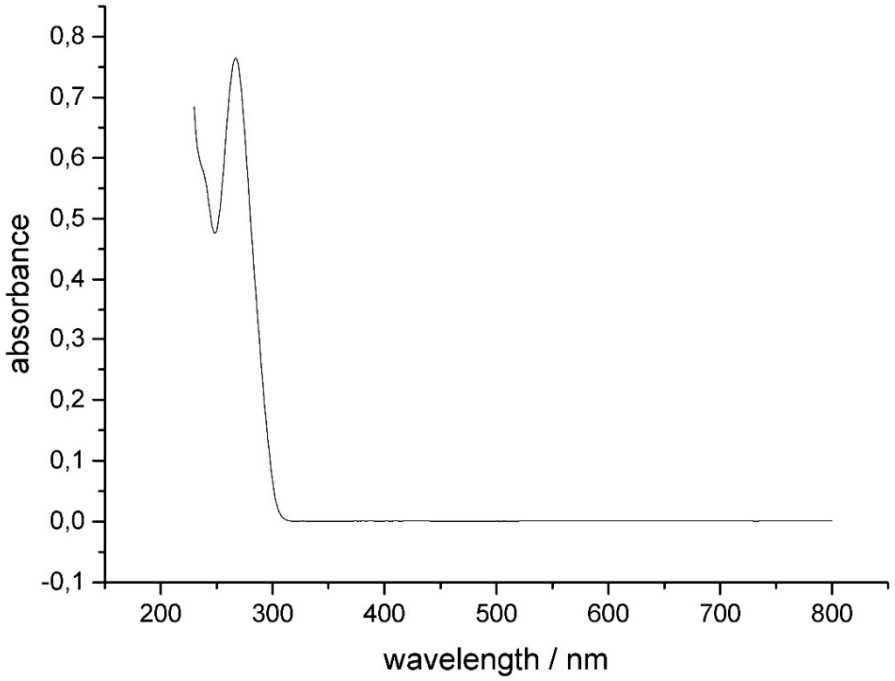

Figure 7.1.25. UV-vis spectrum of **7** (in CH_2Cl_2).

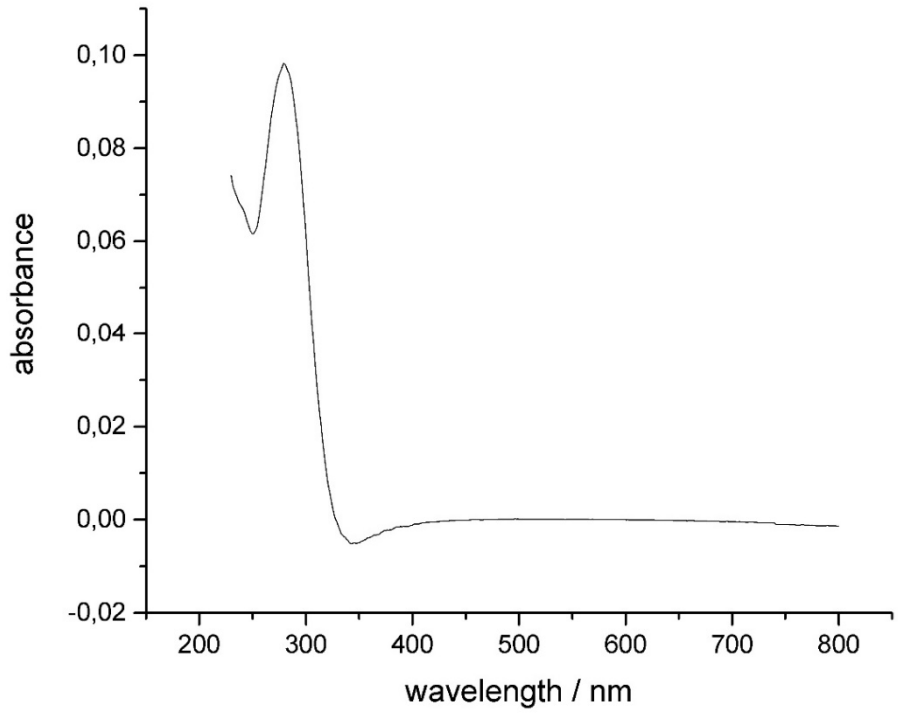

Figure 7.1.26. UV-vis spectrum of **8** (in CH_2Cl_2).

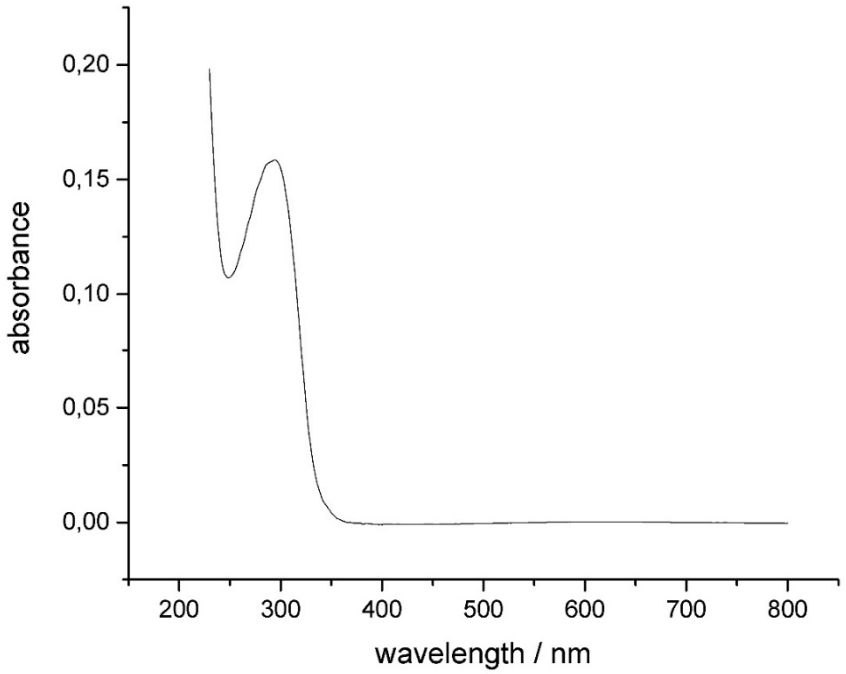

Figure 7.1.27. UV-Vis spectrum of **13'** (in CH_2Cl_2).

Fluorescence spectra

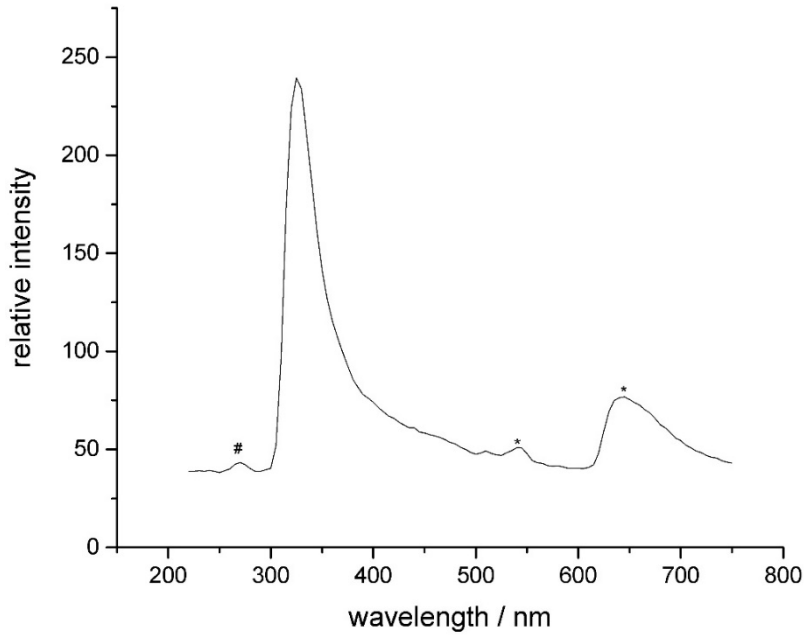

Figure 7.1.28. Fluorescence spectrum of **3** (in CH_2Cl_2; λ_{ex} = 272 nm). #: artifacts of CH_2Cl_2, *: artifact at double wavelength.

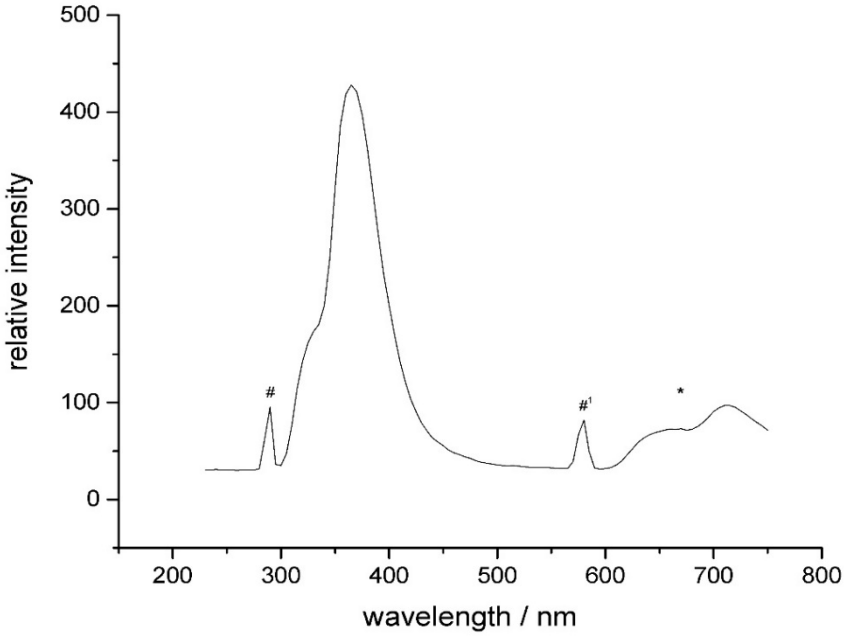

Figure 7.1.29. Fluorescence spectrum of **5** (in CH_2Cl_2; λ_{ex} = 290 nm). #, #[1]: artifacts of CH_2Cl_2,*: artifact at double wavelength.

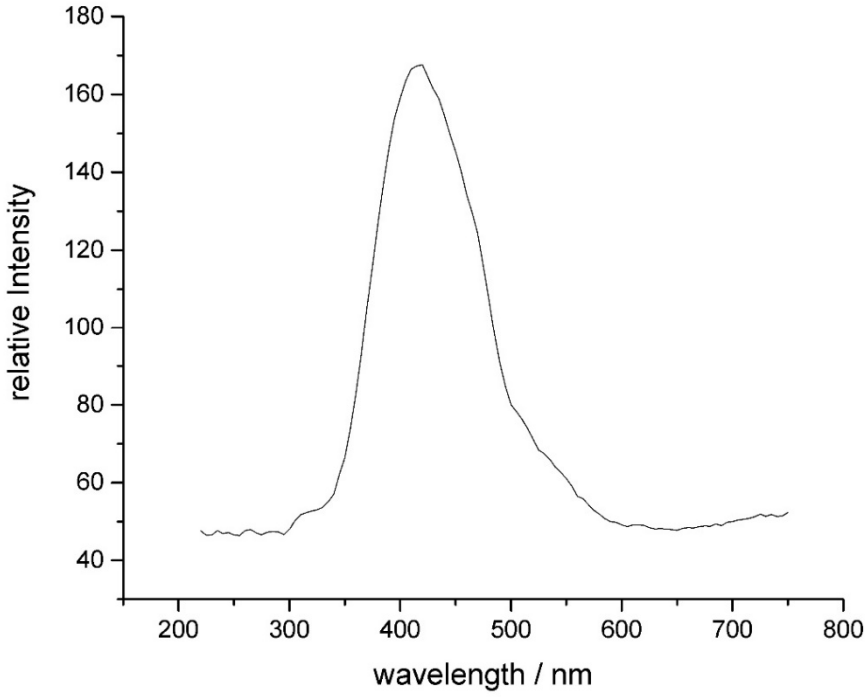

Figure 7.1.30. Fluorescence spectrum of **7** (in CH_2Cl_2; λ_{ex} = 267 nm).

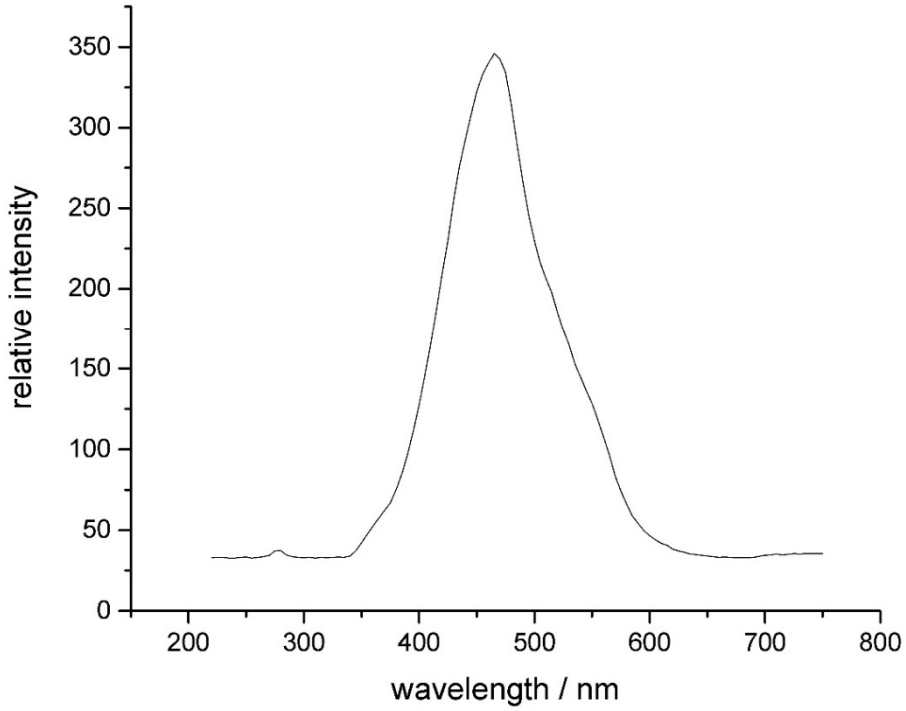

Figure 7.1.31. Fluorescence spectrum of **8** (in CH_2Cl_2; λ_{ex} = 280 nm).

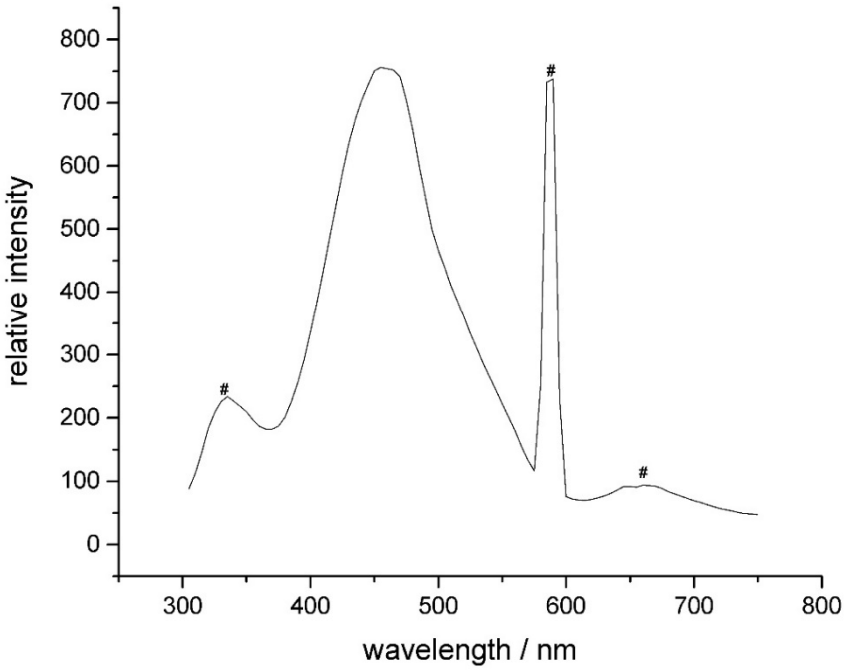

Figure 7.1.32. Fluorescence spectrum of **13'** (in CH_2Cl_2; λ_{ex} = 295 nm). #: artifacts of CH_2Cl_2.

MS spectra

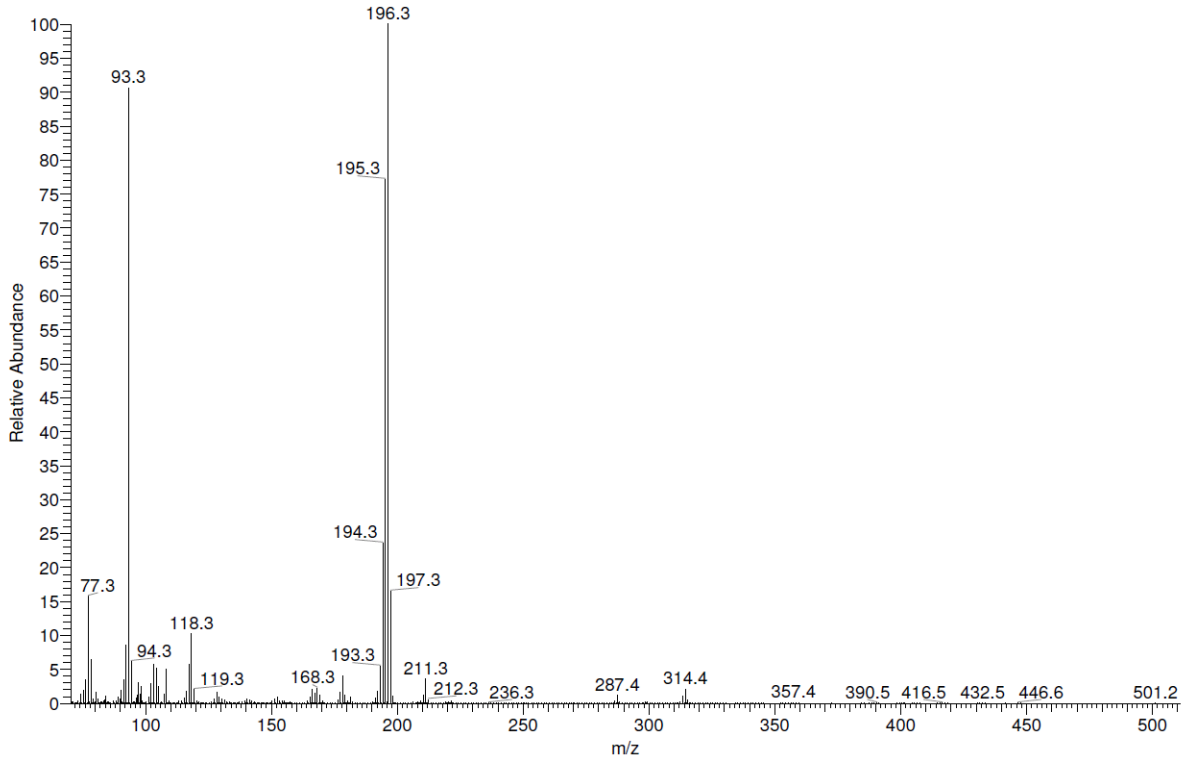

Figure 7.1.33. EI-MS spectrum of **5**.

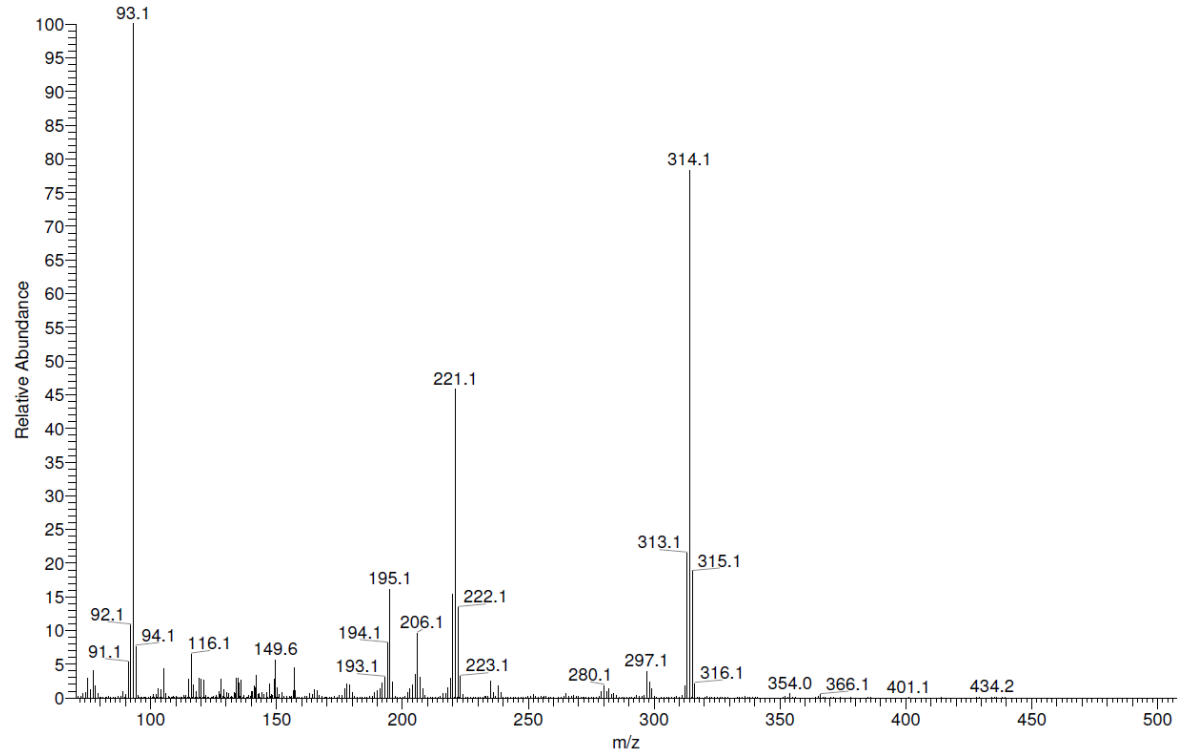

Figure 7.1.34. EI-MS spectrum of **7**.

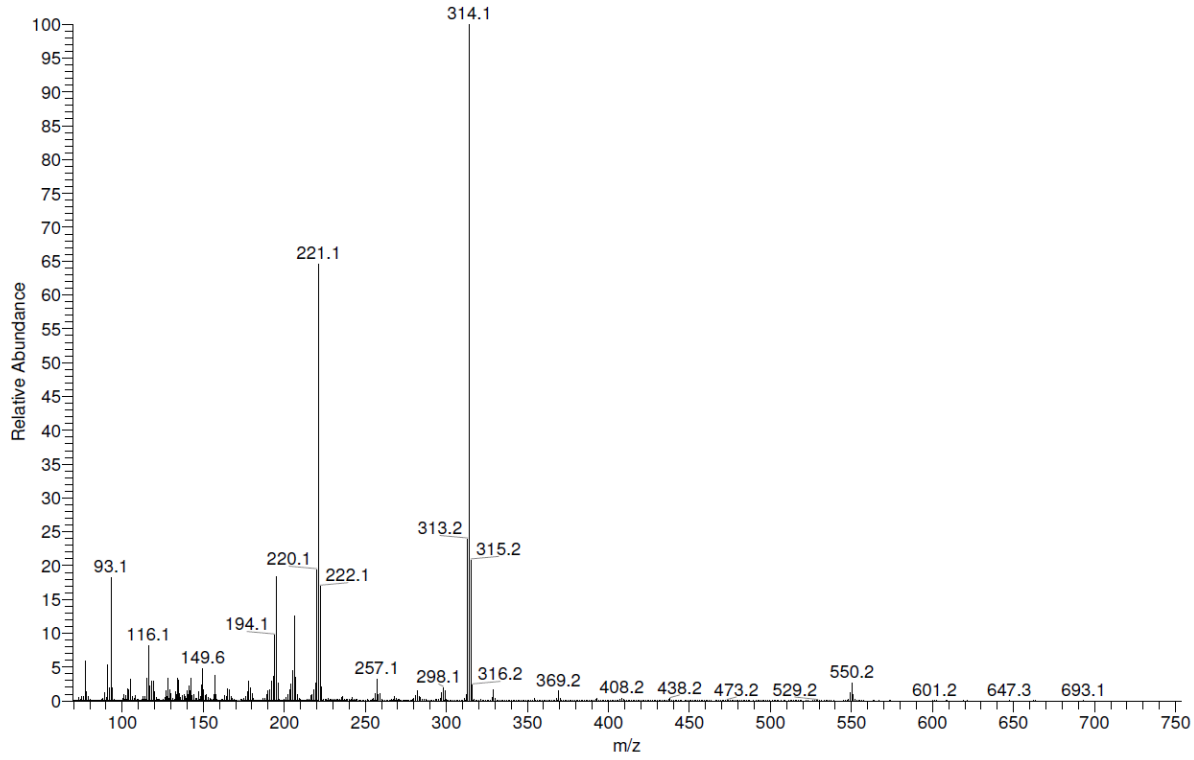

Figure 7.1.35. EI-MS spectrum of **8**.

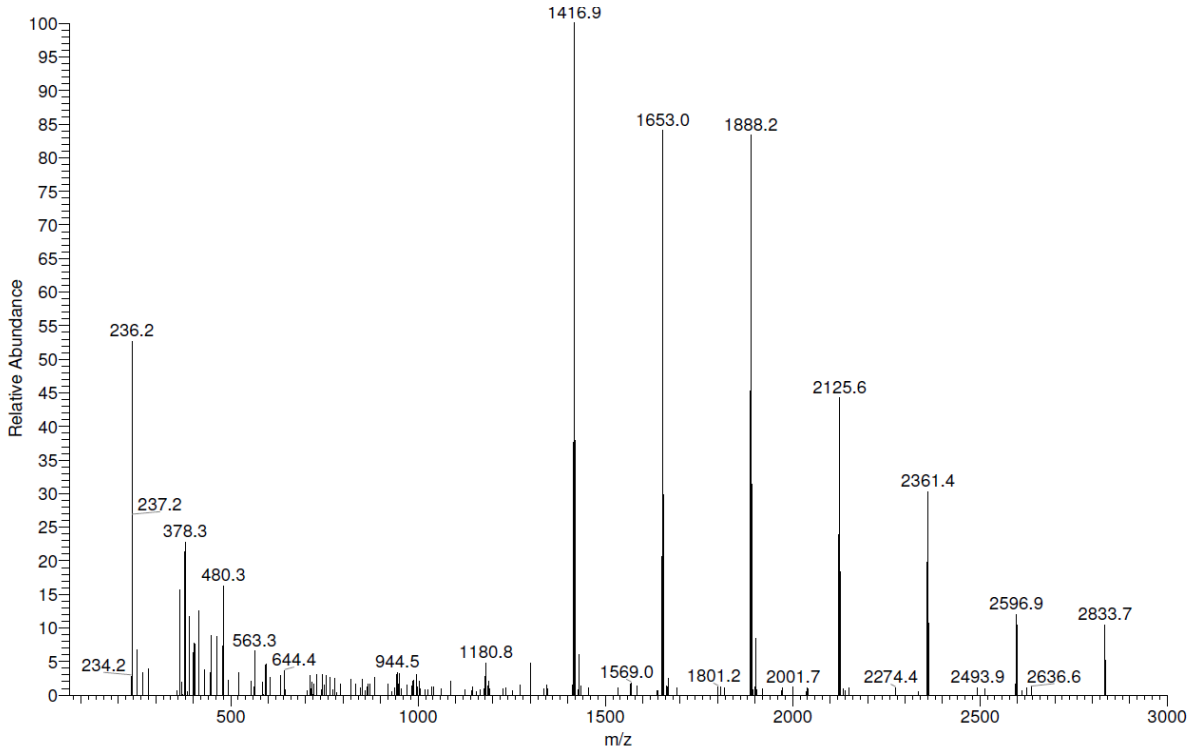

Figure 7.1.36. Secondary ion mass spectrometry (SIMS) spectrum of **13'**.

IR Spectra

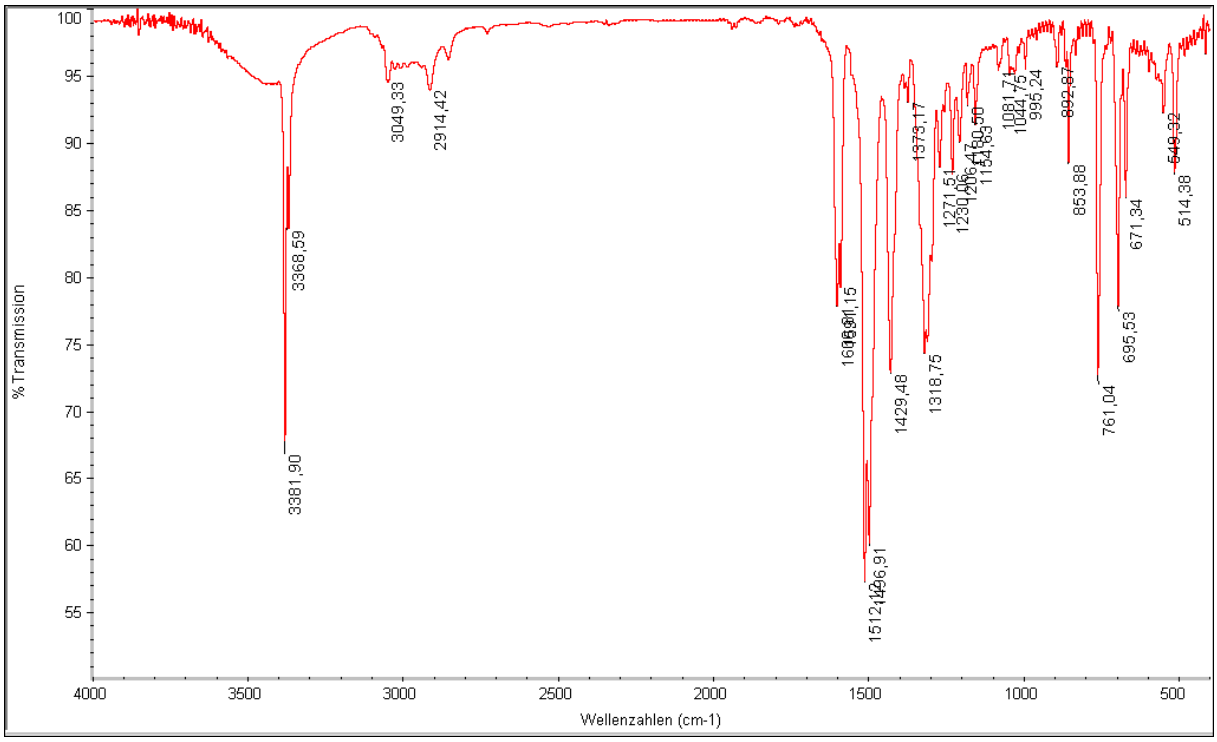

Figure 7.1.37. IR spectrum of **7**.

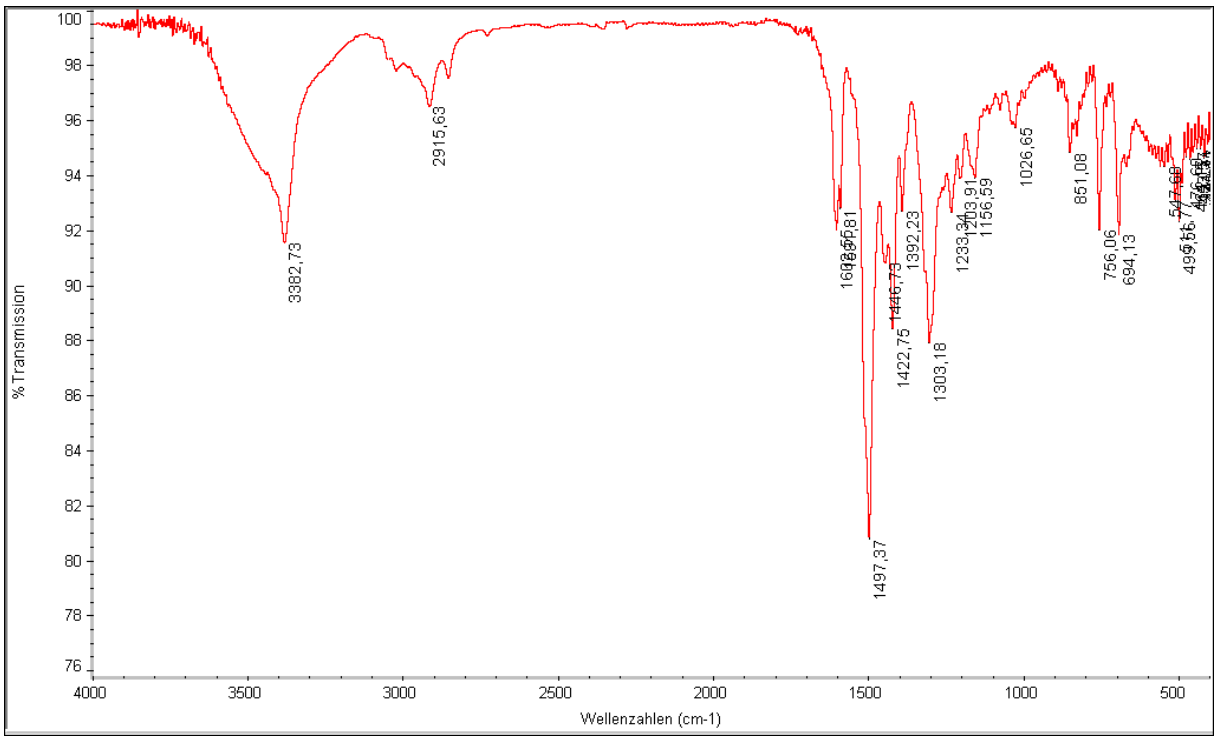

Figure 7.1.38. IR spectrum of **8**.

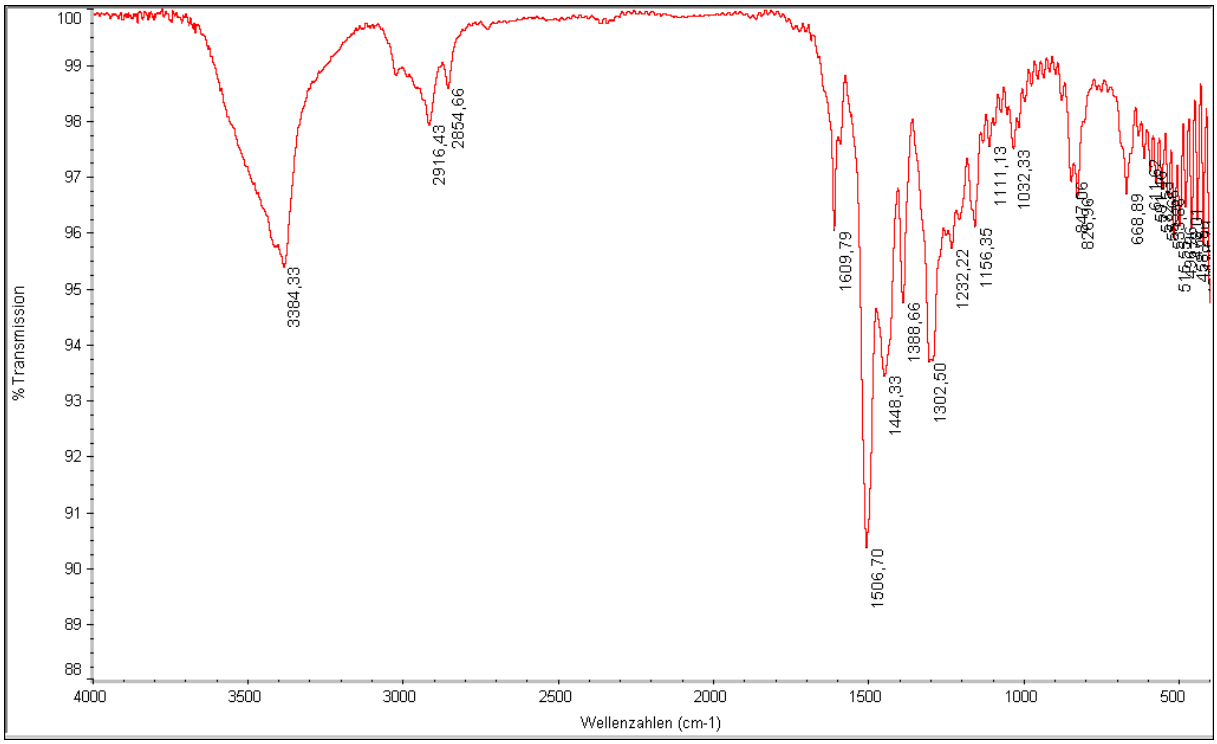

Figure 7.1.39. IR spectrum of **13'**.

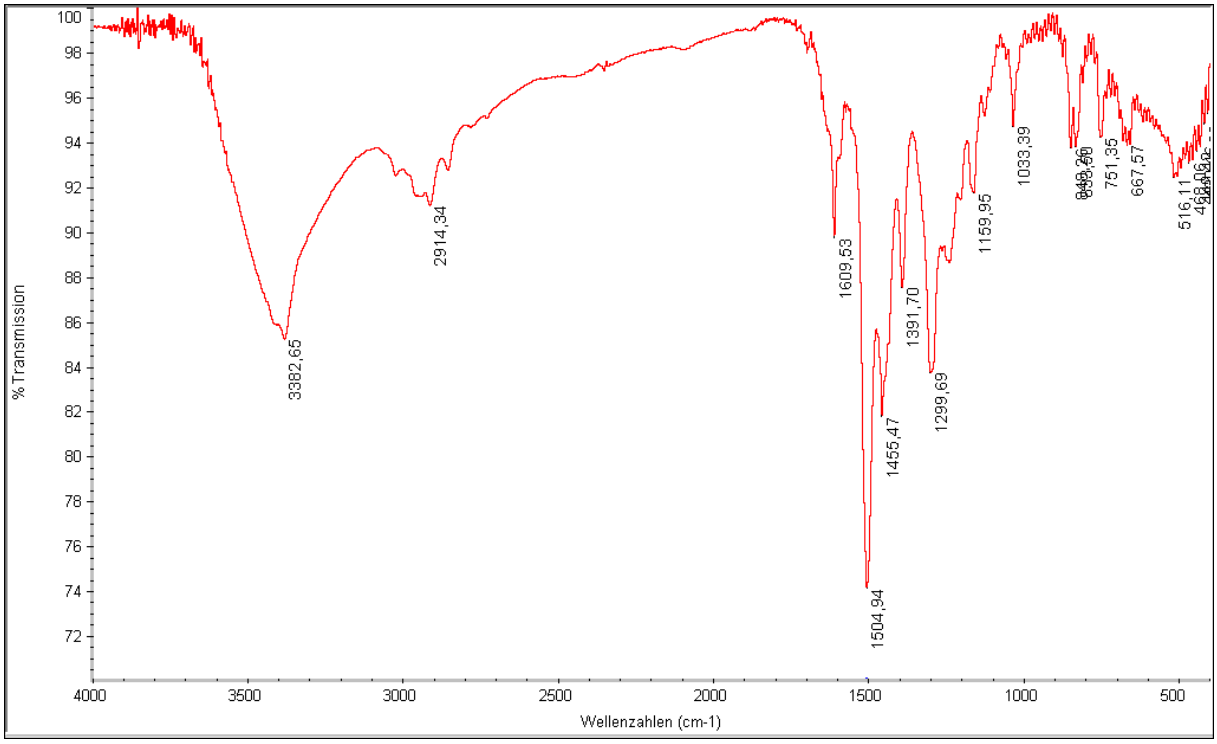

Figure 7.1.40. IR spectrum of the dried insoluble solid of the cross-linking reaction of **13'** with $Zr(NMe_2)_4$.

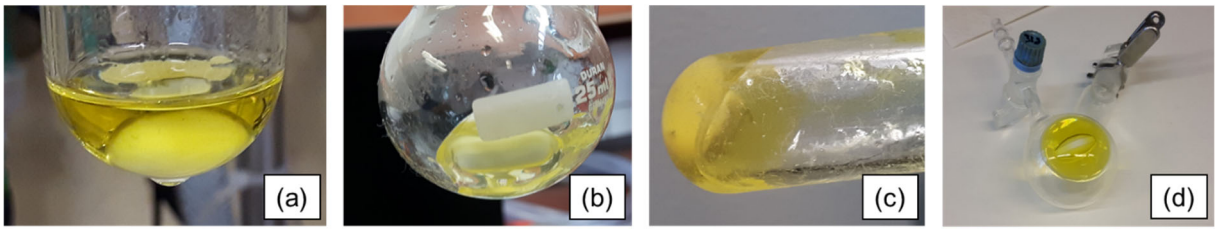

Figure 7.1.41. (a) Solution of the reaction of **7** with $Zr(NMe_2)_4$ and THF heated at 120 °C in 1,2-dichlorobenzene (*o*-DCB) for 45 min, (b) polymer **13'** cross-linked with 4 mol% of $Zr(NMe_2)_4$ swollen by *o*-DCB, (c) polymer **13'** cross-linked with 40 mol% of $Zr(NMe_2)_4$ swollen by *o*-DCB, (d) polymer **13'** cross-linked with 100 mol% of $Zr(NMe_2)_4$ swollen by *o*-DCB.

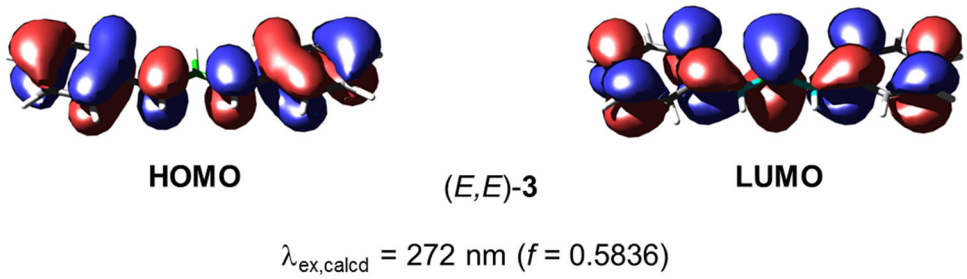

Figure 7.1.42. Calculated frontier orbitals (isovalue 0.022 a.u.) of (*E*,*E*)-**3** relevant for lowest-energy vertical excitation and corresponding calculated wavelength (*f*: oscillator strength).

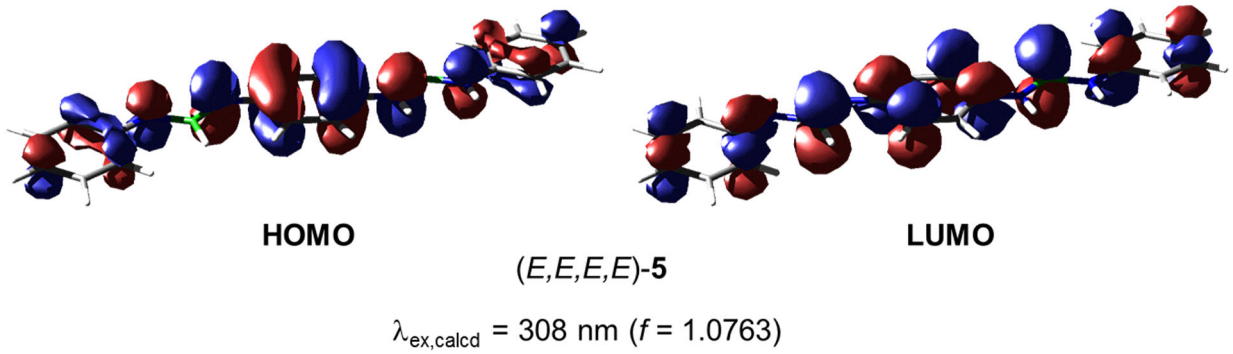

Figure 7.1.43. Calculated frontier orbitals (isovalue 0.022 a.u.) of (*E*,*E*,*E*,*E*)-**5** relevant for lowest-energy vertical excitation and corresponding calculated wavelength (*f*: oscillator strength).

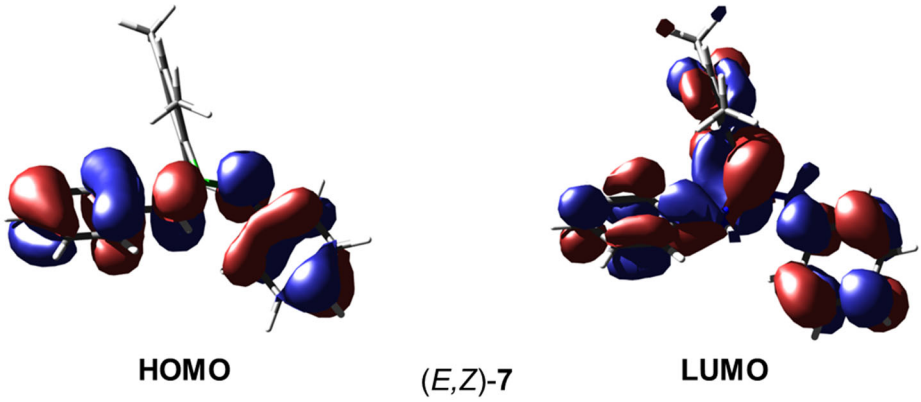

Figure 7.1.44. Calculated frontier orbitals (isovalue 0.022 a.u.) of (*E*,*Z*)-**7** relevant for lowest-energy vertical excitation and corresponding calculated wavelength (*f*: oscillator strength).

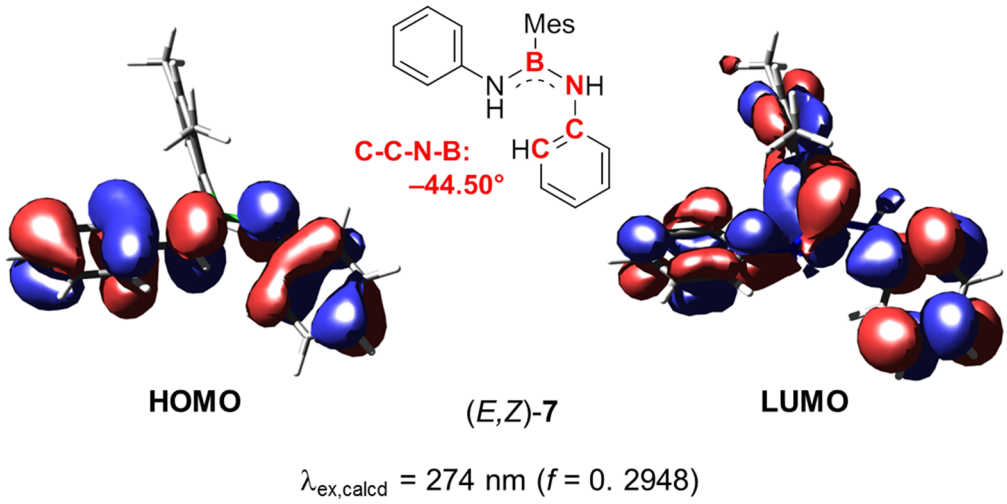

Figure 7.1.45. Calculated frontier orbitals (isovalue 0.022 a.u.) of (E,Z)-**7**, with the dihedral angle indicated in the drawing set to a fix value (–44.50°), relevant for lowest-energy vertical excitation and corresponding calculated wavelength (**f**: oscillator strength).

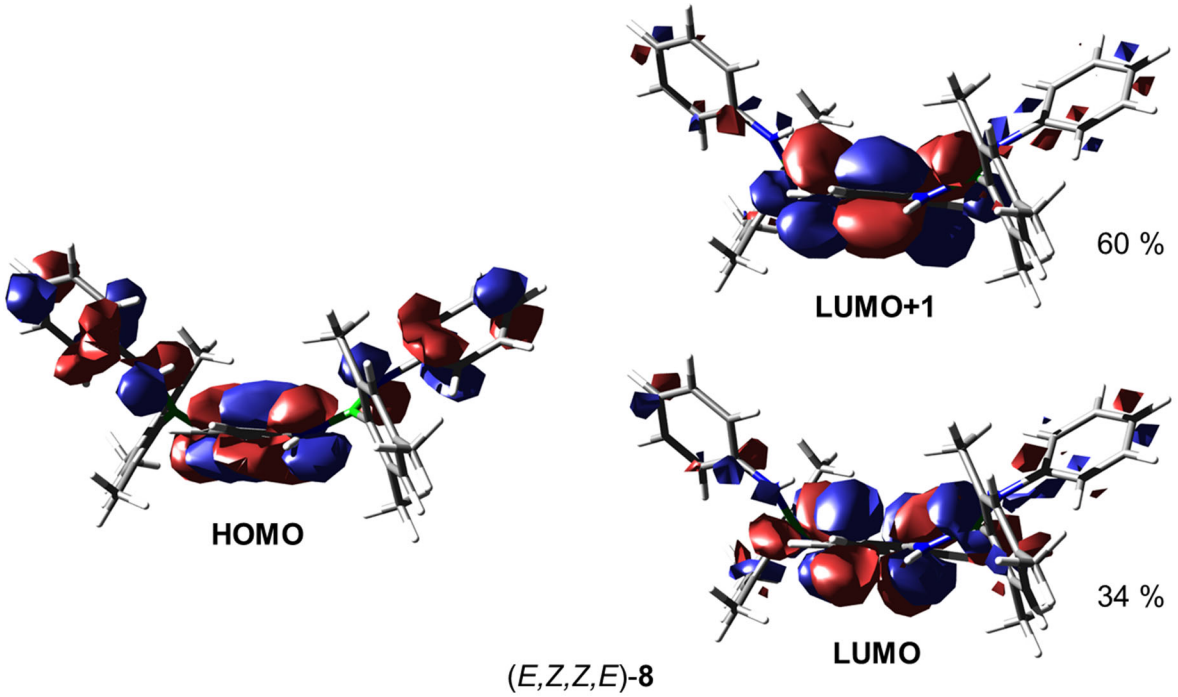

Figure 7.1.46. Calculated frontier orbitals (isovalue 0.022 a.u.) of (*E*,*Z*,*Z*,*E*)-**8** (with relative contributions in %) relevant for lowest-energy vertical excitation and corresponding calculated wavelength (*f*: oscillator strength).

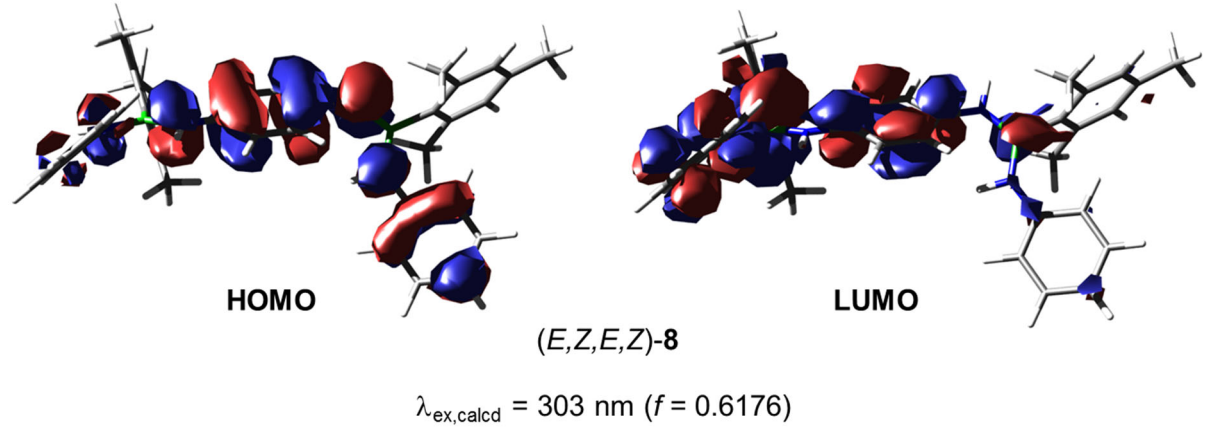

Figure 7.1.47. Calculated frontier orbitals (isovalue 0.022 a.u.) of (*E*,*Z*,*E*,*Z*)-**8** relevant for lowest-energy vertical excitation and corresponding calculated wavelength (*f*: oscillator strength).

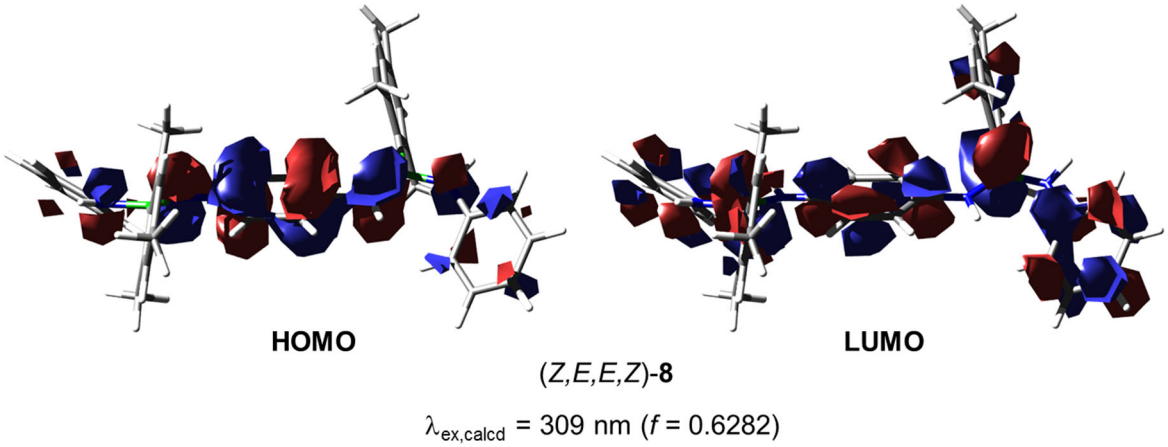

Figure 7.1.48. Calculated frontier orbitals (isovalue 0.022 a.u.) of (*Z*,*E*,*E*,*Z*)-**8** relevant for lowest-energy vertical excitation and corresponding calculated wavelength (*f*: oscillator strength).

Cartesian Coordinates [Å], Total Energies, Enthalpies, and Free Energies [a.u.] of Optimized Stationary Points

(*E*,*E*)-**3**
Total energy (B3LYP/6-31G(d,p): -599.569587288
Sum of electronic and thermal Enthalpies= -599.326117
Sum of electronic and thermal Free Energies= -599.381633

C	-4.213060	1.490385	-0.000906
C	-5.249987	0.555144	-0.000926
C	-4.932317	-0.803086	-0.000327
C	-3.602399	-1.216809	0.000239
C	-2.555886	-0.279875	0.000261
C	-2.879982	1.087008	-0.000277
N	-1.227946	-0.742998	0.000867
B	-0.000003	-0.022517	0.000193
N	1.227943	-0.742992	0.001764
C	2.555882	-0.279865	0.000714
C	3.602391	-1.216805	-0.000993
C	4.932312	-0.803093	-0.001877
C	5.249991	0.555135	-0.001125
C	4.213068	1.490381	0.000621
C	2.879988	1.087014	0.001611
H	5.721527	-1.549571	-0.003188
H	3.366671	-2.279148	-0.001689
H	-3.366686	-2.279153	0.000662
H	1.182893	-1.755259	0.002986
H	-1.182877	-1.755264	0.001939
H	-5.721538	-1.549559	-0.000313
H	6.285615	0.879846	-0.001819
H	-6.285609	0.879859	-0.001375
H	-0.000005	1.164795	-0.001706
H	4.441310	2.552608	0.001343

H	2.091364	1.829776	0.003179
H	-2.091348	1.829760	-0.000162
H	-4.441295	2.552615	-0.001323

(*E,Z*)-**3**

Total energy (B3LYP/6-31G(d,p): -599.569467239

Sum of electronic and thermal Enthalpies= -599.325836

Sum of electronic and thermal Free Energies= -599.379831

C	-2.207811	0.562688	0.750553
C	-2.371320	-0.652125	0.063175
C	-3.583281	-0.885876	-0.607854
C	-4.593335	0.072457	-0.605858
C	-4.415171	1.289253	0.055948
C	-3.218750	1.523618	0.733826
N	-1.367734	-1.640624	0.058165
B	0.056519	-1.539570	0.045305
N	0.742181	-0.297733	-0.040674
C	2.124694	-0.040718	-0.051334
C	2.583702	1.218147	-0.472814
C	3.945180	1.511414	-0.490637
C	4.880332	0.555413	-0.092894
C	4.428461	-0.695999	0.330607
C	3.068452	-0.995878	0.360755
H	0.664521	-2.564373	0.074527
H	-5.521827	-0.130842	-1.131804
H	-3.722662	-1.823361	-1.140687
H	1.863492	1.966846	-0.795535
H	-1.733571	-2.573506	-0.072750
H	0.189428	0.532059	-0.216574
H	4.273557	2.492718	-0.821470
H	-5.200855	2.038065	0.051102
H	5.941640	0.782418	-0.107506
H	-3.073126	2.454996	1.273787
H	-1.308469	0.732290	1.332875
H	2.735432	-1.965657	0.711665
H	5.141797	-1.449672	0.652568

(*Z,Z*)-**3**

Total energy (B3LYP/6-31G(d,p): -599.562037741

Sum of electronic and thermal Enthalpies= -599.318463

Sum of electronic and thermal Free Energies= -599.371755

C	-1.277669	-0.177498	-0.957699
C	-1.818097	0.702529	-0.007616
C	-2.968266	0.311809	0.697588
C	-3.558014	-0.928164	0.464070
C	-3.008514	-1.806481	-0.471622
C	-1.867666	-1.421113	-1.177039
N	-1.271589	1.981671	0.220140
B	0.000003	2.589293	-0.000007
N	1.271601	1.981699	-0.220164
C	1.818101	0.702549	0.007605

C	1.277752	-0.177401	0.957802
C	1.867741	-1.421016	1.177161
C	3.008505	-1.806456	0.471646
C	3.557929	-0.928214	-0.464159
C	2.968185	0.311759	-0.697696
H	4.447983	-1.209050	-1.020127
H	3.394777	0.987349	-1.435565
H	-3.394919	0.987459	1.435367
H	1.973591	2.637566	-0.536260
H	-1.973578	2.637549	0.536214
H	-4.448131	-1.208941	1.019965
H	3.465695	-2.774430	0.651702
H	-3.465712	-2.774454	-0.651664
H	1.433882	-2.088773	1.915926
H	0.408573	0.121694	1.531369
H	-0.408421	0.121529	-1.531196
H	-1.433746	-2.088927	-1.915716
H	-0.000026	3.787558	-0.000055

(*E,E,E,E*)-**5**

Total energy (B3LYP/6-31G(d,p): -966.879159460

Sum of electronic and thermal Enthalpies= -966.498220

Sum of electronic and thermal Free Energies= -966.577117

C	-6.772179	-1.080053	-0.000182
C	-6.477693	0.293788	0.000081
C	-7.545309	1.207030	0.000502
C	-8.865633	0.763844	0.000668
C	-9.153527	-0.601066	0.000426
C	-8.095958	-1.512899	0.000001
N	-5.160994	0.785637	-0.000106
B	-3.916184	0.091604	-0.000124
N	-2.704397	0.834485	-0.000205
C	-1.365738	0.394145	-0.000252
C	-0.329347	1.339863	0.000069
C	1.009031	0.961642	0.000026
C	1.365747	-0.394182	-0.000337
C	0.329355	-1.339900	-0.000667
C	-1.009022	-0.961679	-0.000639
N	2.704406	-0.834523	-0.000402
B	3.916191	-0.091641	-0.000065
N	5.161007	-0.785663	-0.000198
C	6.477696	-0.293785	0.000020
C	7.545334	-1.207001	0.000920
C	8.865647	-0.763785	0.001132
C	9.153506	0.601132	0.000469
C	8.095914	1.512939	-0.000435
C	6.772146	1.080062	-0.000693
H	9.671177	-1.492692	0.001826
H	7.333566	-2.274355	0.001480
H	0.575308	-2.399924	-0.000968
H	5.137622	-1.798611	-0.000288

H	2.766896	-1.845723	-0.000794
H	-1.776281	-1.726566	-0.000930
H	10.181715	0.948632	0.000633
H	3.891208	1.096024	0.000338
H	8.300385	2.580043	-0.000998
H	5.967231	1.805123	-0.001482
H	1.776288	1.726530	0.000275
H	-0.575300	2.399887	0.000366
H	-2.766888	1.845685	-0.000133
H	-3.891201	-1.096060	-0.000057
H	-5.137588	1.798585	-0.000107
H	-5.967284	-1.805135	-0.000536
H	-7.333514	2.274379	0.000706
H	-9.671145	1.492771	0.000995
H	-10.181744	-0.948542	0.000556
H	-8.300457	-2.579998	-0.000207

(*E,Z,Z,E*)-**5**

Total energy (B3LYP/6-31G(d,p): -966.879400322

Sum of electronic and thermal Enthalpies= -966.498094

Sum of electronic and thermal Free Energies= -966.573621

C	-6.319890	0.209756	-0.641876
C	-5.095415	0.549112	-0.043155
C	-5.077329	1.581900	0.908814
C	-6.245537	2.261039	1.246728
C	-7.457607	1.929205	0.640628
C	-7.481098	0.900913	-0.303627
N	-3.897120	-0.118320	-0.352898
B	-3.595694	-0.971664	-1.449547
N	-2.322301	-1.592308	-1.618669
C	-1.172252	-1.587929	-0.802561
C	-1.255667	-1.615804	0.599288
C	-0.105220	-1.596732	1.382366
C	1.172269	-1.587857	0.802737
C	1.255673	-1.616493	-0.599100
C	0.105233	-1.597475	-1.382188
N	2.322324	-1.592193	1.618858
B	3.595739	-0.971610	1.449638
N	3.897164	-0.118364	0.352908
C	5.095427	0.549090	0.043099
C	6.319867	0.210074	0.642086
C	7.481040	0.901243	0.303741
C	7.457552	1.929219	-0.640859
C	6.245517	2.260722	-1.247211
C	5.077344	1.581566	-0.909211
H	-6.203690	3.056077	1.985911
H	-4.135638	1.855874	1.379640
H	0.197731	-1.603979	-2.465480
H	-3.136051	0.142977	0.261524
H	-2.169500	-2.028788	-2.517090
H	2.227019	-1.683225	-1.077656

H	-8.368361	2.458540	0.902213
H	-8.417489	0.623006	-0.779499
H	-6.361563	-0.598472	-1.362572
H	-2.227035	-1.681952	1.077885
H	-0.197720	-1.602634	2.465660
H	2.169468	-2.028472	2.517366
H	3.136103	0.142805	-0.261574
H	6.361544	-0.597895	1.363071
H	4.135680	1.855277	-1.380243
H	6.203669	3.055512	-1.986659
H	8.368280	2.458566	-0.902509
H	8.417403	0.623601	0.779821
H	4.406879	-1.175616	2.298760
H	-4.406866	-1.175825	-2.298604

(*E,Z,E,Z*)-**5**

Total energy (B3LYP/6-31G(d,p): -966.879405433

Sum of electronic and thermal Enthalpies= -966.498081

Sum of electronic and thermal Free Energies= -966.573559

C	-6.551890	-1.020275	-1.051424
C	-5.576372	-0.234029	-0.415808
C	-5.284257	-0.488955	0.935063
C	-5.930433	-1.522630	1.613119
C	-6.890339	-2.306123	0.972425
C	-7.203192	-2.039835	-0.362283
N	-4.940845	0.801216	-1.128776
B	-3.612815	1.321098	-1.058152
N	-2.607653	0.767567	-0.220756
C	-1.275258	1.181172	-0.037773
C	-0.353178	0.309009	0.558564
C	0.970366	0.686676	0.771460
C	1.430430	1.947725	0.364477
C	0.503797	2.822968	-0.222639
C	-0.824864	2.458529	-0.408355
N	2.768131	2.356571	0.563207
B	3.990458	1.631197	0.465436
N	4.044849	0.270654	0.051620
C	5.154269	-0.581367	-0.077470
C	6.402888	-0.280176	0.492014
C	7.474506	-1.156431	0.337047
C	7.331340	-2.351553	-0.370732
C	6.090002	-2.660244	-0.927979
C	5.014542	-1.786651	-0.786083
H	5.954068	-3.585336	-1.481237
H	4.053802	-2.032558	-1.233339
H	0.832162	3.811168	-0.535513
H	3.189038	-0.146473	-0.292994
H	2.862763	3.353176	0.699667
H	-1.516991	3.169301	-0.844610
H	8.170561	-3.030934	-0.481666
H	8.431479	-0.902971	0.784988

H	6.528768	0.633456	1.061053
H	1.642256	0.009119	1.287760
H	-0.680440	-0.678644	0.875716
H	-5.499555	1.153394	-1.893684
H	-4.586160	0.151785	1.463094
H	-6.788693	-0.830896	-2.095579
H	-7.954162	-2.634291	-0.874820
H	-7.394279	-3.105405	1.506491
H	-5.692181	-1.700923	2.657955
H	4.991247	2.226905	0.720356
H	-2.817046	-0.101514	0.254285
H	-3.360381	2.241240	-1.773139

(*Z,E,E,Z*)-**5**

Total energy (B3LYP/6-31G(d,p): -966.878889196

Sum of electronic and thermal Enthalpies= -966.497538

Sum of electronic and thermal Free Energies= -966.572720

C	-5.648373	-0.255273	0.983776
C	-5.928931	0.630663	-0.070933
C	-7.195074	0.570222	-0.677673
C	-8.143496	-0.357101	-0.254474
C	-7.849967	-1.252372	0.776322
C	-6.599158	-1.191006	1.390931
N	-4.991286	1.586019	-0.505567
B	-3.563830	1.547953	-0.578849
N	-2.801711	0.394224	-0.261466
C	-1.403163	0.219365	-0.268068
C	-0.507226	1.297699	-0.254364
C	0.866200	1.076754	-0.265205
C	1.403192	-0.219292	-0.267975
C	0.507258	-1.297623	-0.254177
C	-0.866168	-1.076681	-0.265120
N	2.801743	-0.394175	-0.261265
B	3.563811	-1.547846	-0.578978
N	4.991262	-1.586004	-0.505679
C	5.928932	-0.630712	-0.070990
C	5.648273	0.255325	0.983606
C	6.599054	1.191033	1.390824
C	7.849955	1.252278	0.776388
C	8.143571	0.356920	-0.254310
C	7.195153	-0.570376	-0.677577
H	-9.115202	-0.384301	-0.739443
H	-7.426033	1.251930	-1.492685
H	-1.538641	-1.931824	-0.266053
H	-3.301716	-0.469062	-0.090695
H	0.883198	-2.313886	-0.230300
H	-8.588047	-1.979045	1.100721
H	-3.023446	2.540601	-0.959695
H	-6.362300	-1.864211	2.210085
H	-4.703868	-0.178540	1.511570
H	-0.883162	2.313966	-0.230638

H	1.538672	1.931898	-0.266223
H	3.301762	0.469088	-0.090409
H	3.023372	-2.540412	-0.959966
H	4.703669	0.178706	1.511241
H	7.426184	-1.252145	-1.492518
H	9.115344	0.384032	-0.739148
H	8.588032	1.978932	1.100832
H	6.362111	1.864324	2.209882
H	-5.421405	2.389215	-0.942633
H	5.421329	-2.389178	-0.942839

(*E,E*)-**7**

Total energy (B3LYP/6-31G(d,p): -948.591632325

Sum of electronic and thermal Enthalpies= -948.173543

Sum of electronic and thermal Free Energies= -948.252201

C	3.514076	-2.408527	0.366766
C	2.572560	-1.463188	-0.078559
C	3.043637	-0.250183	-0.608956
C	4.413086	0.003808	-0.666382
C	5.342109	-0.937003	-0.219923
C	4.880045	-2.149760	0.292982
N	1.205091	-1.787561	0.002959
B	-0.000620	-1.004433	-0.001077
N	-1.207715	-1.785396	-0.005247
C	-2.574670	-1.458940	0.076949
C	-3.043768	-0.245078	0.607169
C	-4.412841	0.010846	0.665211
C	-5.343423	-0.928813	0.219591
C	-4.883332	-2.142399	-0.293128
C	-3.517769	-2.403097	-0.367554
C	0.000929	0.575325	-0.000344
C	-0.348447	1.295857	-1.165186
C	-0.339865	2.694321	-1.146869
C	-0.002936	3.412947	0.003842
C	0.331629	2.691940	1.153550
C	0.346591	1.293315	1.167000
C	-0.746089	0.573721	-2.435411
C	0.738688	0.568497	2.437434
C	0.024181	4.923139	-0.003021
H	5.583757	-2.899671	0.643211
H	3.164894	-3.353248	0.778710
H	-3.170152	-3.348467	-0.779342
H	1.081188	-2.779148	0.172730
H	-1.085482	-2.777153	-0.175259
H	-5.588272	-2.891453	-0.642726
H	6.406451	-0.731323	-0.275589
H	-6.407444	-0.721605	0.275729
H	4.754245	0.949283	-1.078838
H	2.341743	0.485774	-0.978260
H	-2.340842	0.490188	0.975872
H	-4.752373	0.956999	1.077435

H	0.790351	1.257739	3.284833
H	1.721112	0.093376	2.335067
H	0.023720	-0.221376	2.692999
H	0.590131	3.231663	2.062385
H	-0.608437	3.236022	-2.051659
H	-0.033151	-0.216957	-2.694097
H	-1.729020	0.100122	-2.330943
H	-0.798865	1.264279	-3.281671
H	-0.183888	5.331991	0.990353
H	1.007578	5.301342	-0.310023
H	-0.712120	5.334108	-0.700473

(*E,Z*)-**7**

Total energy (B3LYP/6-31G(d,p): -948.594778702

Sum of electronic and thermal Enthalpies= -948.176629

Sum of electronic and thermal Free Energies= -948.256054

C	3.459404	-0.051687	-0.753131
C	2.856519	-1.054351	0.026644
C	3.685101	-1.914516	0.767892
C	5.069247	-1.767749	0.741600
C	5.660917	-0.752988	-0.014053
C	4.846325	0.098906	-0.759772
N	1.460047	-1.236094	0.054950
B	0.365321	-0.301481	0.013111
N	0.647280	1.099072	0.035153
C	-0.171514	2.241496	-0.031745
C	-1.476357	2.218672	-0.552417
C	-2.231150	3.389540	-0.602959
C	-1.709961	4.604393	-0.155497
C	-0.410106	4.634430	0.351389
C	0.348944	3.468954	0.415813
C	-1.086151	-0.935840	0.016591
C	-1.622631	-1.529346	-1.147312
C	-2.884651	-2.134843	-1.103891
C	-3.637757	-2.179943	0.070974
C	-3.097310	-1.593464	1.220522
C	-1.845149	-0.973869	1.210121
C	-0.863769	-1.492958	-2.458446
C	-1.321331	-0.335904	2.479529
C	-4.995186	-2.841794	0.108061
H	5.688089	-2.446070	1.322178
H	3.231416	-2.695733	1.372916
H	1.357905	3.502060	0.821308
H	1.190825	-2.188168	0.264593
H	1.612130	1.342796	0.225452
H	0.018385	5.568633	0.703468
H	6.739817	-0.635215	-0.027918
H	-2.304130	5.511497	-0.204582
H	5.290914	0.879073	-1.371311
H	2.843133	0.580137	-1.383576
H	-1.895327	1.289935	-0.917951

H	-3.238272	3.347874	-1.008522
H	-1.381289	-2.066547	-3.232244
H	0.147202	-1.899371	-2.353653
H	-0.754019	-0.465727	-2.827912
H	-3.286740	-2.583798	-2.009802
H	-3.666341	-1.619064	2.148015
H	-0.296782	-0.654227	2.701695
H	-1.305472	0.756834	2.395075
H	-1.945786	-0.594117	3.339308
H	-5.266917	-3.251916	-0.868485
H	-5.019767	-3.662778	0.834056
H	-5.777471	-2.132404	0.402133

(*Z,Z*)-**7**

Total energy (B3LYP/6-31G(d,p): -948.589218899

Sum of electronic and thermal Enthalpies= -948.171299

Sum of electronic and thermal Free Energies= -948.252084

C	1.906638	2.757459	-1.182621
C	1.474765	1.764861	-0.287443
C	2.314959	1.406908	0.778182
C	3.558753	2.017988	0.926712
C	3.984651	3.001863	0.033303
C	3.146491	3.371096	-1.020263
N	0.194781	1.197600	-0.454853
B	-0.447638	-0.000252	-0.000380
N	0.196517	-1.197157	0.454179
C	1.477071	-1.762994	0.286415
C	2.316777	-1.403931	-0.779215
C	3.561179	-2.013713	-0.928031
C	3.988196	-2.997359	-0.034907
C	3.150538	-3.367684	1.018678
C	1.910087	-2.755351	1.181321
C	-2.037856	-0.001133	-0.000092
C	-2.759765	-0.672287	-1.013379
C	-4.158727	-0.662931	-0.998498
C	-4.878131	-0.007314	0.004247
C	-4.158389	0.647676	1.007648
C	-2.759786	0.665242	1.016794
C	-2.036584	-1.401953	-2.127574
C	-2.036009	1.391079	2.133114
C	-6.388511	0.015661	-0.009575
H	-4.700303	-1.181344	-1.787357
H	-6.798049	-0.864879	-0.513699
H	-6.767799	0.898811	-0.539257
H	-6.798029	0.047410	1.004783
H	-4.699660	1.156213	1.803183
H	-2.740665	1.798323	2.863310
H	-1.349505	0.725461	2.669012
H	-1.431666	2.220887	1.750855
H	-1.431846	-2.230583	-1.743384
H	-1.350580	-0.737760	-2.665852

H	-2.741625	-1.811346	-2.856201
H	-0.436489	-1.833362	0.921663
H	4.197151	-1.720780	-1.758535
H	4.956790	-3.471252	-0.160098
H	3.463466	-4.134121	1.722147
H	1.266105	-3.040808	2.009975
H	1.987528	-0.659326	-1.494056
H	-0.439100	1.833009	-0.922224
H	1.986541	0.662114	1.493208
H	4.195129	1.725893	1.757201
H	4.952780	3.476767	0.158261
H	3.458567	4.137683	-1.723946
H	1.262272	3.042047	-2.011274

(*E,Z*)-**7** constraint geometry
Total energy (B3LYP/6-31G(d,p): -948.594681562

C	0.000567	-0.030913	0.011673
C	0.017021	-0.005201	1.424255
C	1.265113	0.014079	2.088620
C	2.450482	0.011894	1.346276
C	2.442352	-0.014174	-0.051551
C	1.204891	-0.039580	-0.700042
B	-1.338537	-0.075516	2.240210
N	-2.244741	1.013247	2.425282
C	-2.198688	2.371745	2.062336
C	-1.004213	3.041473	1.747229
C	-1.027565	4.392605	1.404944
C	-2.223854	5.110904	1.380632
C	-3.411194	4.453347	1.705181
C	-3.400678	3.101675	2.038760
C	1.335854	0.063836	3.601287
C	3.732761	0.009277	-0.836394
C	-1.309994	-0.037311	-0.746784
N	-1.681541	-1.365245	2.781665
C	-2.807555	-1.790766	3.516768
C	-3.323827	-1.025853	4.576846
C	-4.434964	-1.471809	5.293182
C	-5.034915	-2.693961	4.989229
C	-4.508294	-3.471679	3.955556
C	-3.411908	-3.024633	3.222663
H	-4.958572	-4.429590	3.711058
H	-3.018397	-3.626311	2.407178
H	-4.333603	2.596962	2.280428
H	-1.127416	-2.132488	2.424928
H	-3.144061	0.763401	2.820049
H	-4.354815	4.991714	1.695932
H	-5.894198	-3.040567	5.554642
H	-2.230354	6.164063	1.117781
H	-4.818587	-0.865413	6.108873
H	-2.830782	-0.100763	4.856657
H	-0.062995	2.507512	1.773344

H	-0.091723	4.889124	1.163662
H	2.369257	-0.000324	3.952775
H	0.769238	-0.752495	4.060550
H	0.912615	0.998764	3.989160
H	3.403324	0.026967	1.871864
H	1.175590	-0.067975	-1.787480
H	-1.994496	-0.805446	-0.370107
H	-1.826009	0.925133	-0.651804
H	-1.150275	-0.225084	-1.812185
H	4.534330	-0.514428	-0.306238
H	3.613043	-0.458629	-1.818129
H	4.075829	1.037718	-1.006377

(*E,Z,Z,E*)-**8**

Total energy (B3LYP/6-31G(d,p): -1664.93010459

Sum of electronic and thermal Enthalpies= -1664.199806

Sum of electronic and thermal Free Energies= -1664.326073

C	-3.862421	2.593574	2.384440
C	-4.450504	1.857532	1.339969
C	-5.836079	1.976134	1.137359
C	-6.597771	2.796381	1.968244
C	-6.008738	3.522665	3.004132
C	-4.631499	3.416315	3.202780
N	-3.619914	1.057395	0.534509
B	-3.876327	-0.007144	-0.384288
C	-5.297019	-0.646320	-0.670109
C	-6.006571	-0.339401	-1.851743
C	-7.234158	-0.961676	-2.110122
C	-7.784211	-1.895158	-1.229290
C	-7.072661	-2.196694	-0.062845
C	-5.849266	-1.588448	0.229053
C	-5.468792	0.679690	-2.835390
C	-5.135546	-1.932144	1.519432
N	-2.767548	-0.604407	-1.079940
C	-1.391268	-0.292641	-1.079416
C	-0.930091	1.034450	-1.108863
C	0.432777	1.317344	-1.088310
C	1.391165	0.292476	-1.079379
C	0.929987	-1.034614	-1.108922
C	-0.432883	-1.317510	-1.088394
N	2.767437	0.604270	-1.079879
B	3.876243	0.007057	-0.384224
N	3.619952	-1.057587	0.534486
C	4.450696	-1.857595	1.339923
C	5.836213	-1.976289	1.136981
C	6.598089	-2.796385	1.967844
C	6.009290	-3.522439	3.004027
C	4.632104	-3.416004	3.203002
C	3.862846	-2.593398	2.384692
C	5.296905	0.646267	-0.670112
C	6.006289	0.339565	-1.851896

C	7.233830	0.961906	-2.110351
C	7.783993	1.895242	-1.229438
C	7.072602	2.196570	-0.062839
C	5.849257	1.588264	0.229128
C	5.468343	-0.679320	-2.835667
C	5.135619	1.931826	1.519589
H	-1.644847	1.848458	-1.169496
H	0.762928	2.353181	-1.092485
H	2.791293	-2.511780	2.554447
H	2.979661	1.474294	-1.549647
H	2.640211	-1.234623	0.722770
H	4.149982	-3.972981	4.001542
H	6.611399	-4.161668	3.642069
H	-0.763036	-2.353345	-1.092646
H	1.644737	-1.848620	-1.169641
H	6.312814	-1.431378	0.332466
H	7.667769	-2.871611	1.792651
H	6.105411	-0.751006	-3.721466
H	4.455428	-0.426822	-3.165997
H	5.414441	-1.678323	-2.385692
H	7.770639	0.712582	-3.023275
C	9.106086	2.565260	-1.521505
H	7.482142	2.922466	0.637206
H	4.080697	2.172951	1.348425
H	5.161186	1.089640	2.220910
H	5.599315	2.790067	2.013913
H	-2.979802	-1.474403	-1.549747
H	-7.771094	-0.712191	-3.022928
C	-9.106349	-2.565115	-1.521293
H	-7.482105	-2.922715	0.637128
H	-4.080330	-2.172015	1.348370
H	-5.162199	-1.090450	2.221312
H	-5.598456	-2.791202	2.013078
H	-5.415191	1.678671	-2.385327
H	-6.105805	0.751287	-3.721237
H	-4.455786	0.427474	-3.165644
H	-2.640142	1.234374	0.722687
H	-6.312867	1.431047	0.333074
H	-7.667497	2.871534	1.793305
H	-6.610708	4.162004	3.642194
H	-4.149193	3.973471	4.001084
H	-2.790820	2.512037	2.553938
H	9.532973	2.213699	-2.464868
H	8.996037	3.653846	-1.589768
H	9.837499	2.367632	-0.729341
H	-9.533377	-2.213367	-2.464522
H	-8.996312	-3.653688	-1.589788
H	-9.837643	-2.367643	-0.728981

(*E,Z,E,Z*)-**8**
Total energy (B3LYP/6-31G(d,p): -1664.93027956

Sum of electronic and thermal Enthalpies= -1664.199856
Sum of electronic and thermal Free Energies= -1664.324650

C	5.523480	1.483887	0.062272
C	4.850306	0.541067	-0.747288
C	5.410741	0.199588	-1.999412
C	6.610605	0.789522	-2.411746
C	7.278237	1.727397	-1.619477
C	6.717190	2.060390	-0.383437
B	3.461966	-0.067194	-0.285468
N	3.299218	-1.082014	0.710116
C	4.210344	-1.852043	1.453774
C	5.551820	-2.031275	1.074258
C	6.401444	-2.816819	1.851466
C	5.943138	-3.451107	3.007077
C	4.608815	-3.286573	3.381550
C	3.753968	-2.496034	2.618291
C	4.744481	-0.827794	-2.892030
C	8.553235	2.382542	-2.096037
C	4.978979	1.864605	1.422883
N	2.291216	0.500436	-0.893442
C	0.919872	0.187198	-0.760539
C	-0.041419	1.209617	-0.765050
C	-1.401972	0.936066	-0.672440
C	-1.858072	-0.386055	-0.537811
C	-0.897856	-1.410295	-0.538887
C	0.461467	-1.135823	-0.663301
N	-3.220201	-0.729105	-0.440301
B	-4.386660	0.015084	-0.087444
C	-4.386067	1.518267	0.411570
C	-4.825532	2.562604	-0.434269
C	-4.862539	3.877503	0.042365
C	-4.484174	4.196353	1.349459
C	-4.052588	3.157990	2.179591
C	-3.996370	1.833845	1.732953
C	-5.229959	2.281349	-1.867378
C	-4.566593	5.616037	1.858924
C	-3.497330	0.755338	2.671518
N	-5.671228	-0.635405	-0.122108
C	-6.066194	-1.922959	-0.534283
C	-7.103792	-2.583194	0.146467
C	-7.525712	-3.848422	-0.252527
C	-6.916064	-4.492185	-1.331754
C	-5.892285	-3.840057	-2.018638
C	-5.474767	-2.564820	-1.636640
H	-2.111473	1.753180	-0.697501
H	0.285183	2.243245	-0.849771
H	2.718273	-2.366730	2.925160
H	2.455254	1.341333	-1.430480
H	2.345618	-1.229930	1.019263
H	4.227879	-3.772169	4.275723
H	6.611766	-4.065151	3.602240

H	-1.223178	-2.445276	-0.458711
H	1.168720	-1.956826	-0.715723
H	5.924767	-1.560481	0.173800
H	7.434822	-2.939537	1.538915
H	5.269616	-0.925023	-3.846185
H	3.702653	-0.565850	-3.102688
H	4.731232	-1.818107	-2.420110
H	7.034089	0.510227	-3.374539
H	7.223080	2.785661	0.251020
H	3.915258	2.122648	1.377716
H	5.077279	1.035586	2.133274
H	5.514900	2.723020	1.837466
H	-3.363881	-1.723444	-0.569907
H	-6.409857	-0.128555	0.347319
H	-3.750103	3.384657	3.200111
H	-5.195548	4.672015	-0.622501
H	-4.386583	1.894948	-2.452875
H	-6.022521	1.528237	-1.924185
H	-5.587711	3.187549	-2.363665
H	-3.399176	1.133713	3.692807
H	-2.515314	0.381925	2.358779
H	-4.173458	-0.106311	2.697059
H	-4.719272	-2.046881	-2.217721
H	-7.571810	-2.096526	0.998719
H	-5.422703	-4.316142	-2.874880
H	-7.240943	-5.481770	-1.637051
H	-8.330594	-4.336986	0.289336
H	9.094376	1.741660	-2.798585
H	8.345785	3.328451	-2.612459
H	9.222656	2.611200	-1.260953
H	-3.791044	5.820449	2.603419
H	-4.456121	6.340165	1.046174
H	-5.534503	5.810748	2.338059

(*Z,E,E,Z*)-**8**

Total energy (B3LYP/6-31G(d,p): -1664.92991316

Sum of electronic and thermal Enthalpies= -1664.199446

Sum of electronic and thermal Free Energies= -1664.324173

C	6.538379	4.140875	-1.867855
C	7.181929	3.568368	-0.768415
C	6.740601	2.357589	-0.242181
C	5.647759	1.680519	-0.811436
C	5.020560	2.249104	-1.934273
C	5.459344	3.471132	-2.444650
N	5.235477	0.448001	-0.271347
B	3.936217	-0.160010	-0.127226
C	3.924238	-1.612367	0.506845
C	4.297749	-2.742111	-0.257063
C	4.331070	-4.007528	0.338138
C	4.013660	-4.193382	1.686901
C	3.646399	-3.071879	2.435079

C	3.594749	-1.793662	1.868894
C	4.631670	-2.605198	-1.728704
C	3.163822	-0.620656	2.724068
N	2.773054	0.577281	-0.497063
C	1.398865	0.259392	-0.487504
C	0.458209	1.301562	-0.492266
C	-0.911233	1.056027	-0.504608
C	-1.398859	-0.259377	-0.487373
C	-0.458199	-1.301547	-0.492546
C	0.911239	-1.056008	-0.505020
N	-2.773034	-0.577288	-0.496802
B	-3.936253	0.160022	-0.127167
N	-5.235471	-0.448045	-0.271416
C	-5.647599	-1.680619	-0.811522
C	-6.740317	-2.357864	-0.242246
C	-7.181487	-3.568691	-0.768503
C	-6.537890	-4.141067	-1.867983
C	-5.458968	-3.471153	-2.444794
C	-5.020351	-2.249075	-1.934396
C	-3.924363	1.612411	0.506818
C	-4.297759	2.742104	-0.257241
C	-4.331162	4.007559	0.337857
C	-4.013971	4.193513	1.686668
C	-3.646817	3.072074	2.434980
C	-3.595078	1.793810	1.868889
C	-4.631413	2.605082	-1.728930
C	-3.164188	0.620891	2.724203
H	-8.028835	-4.071366	-0.310715
H	-7.236675	-1.927888	0.624405
H	-0.806449	-2.332202	-0.491558
H	-5.978344	0.035551	0.215481
H	-2.927967	-1.553535	-0.717928
H	1.600231	-1.890726	-0.523516
H	-6.878179	-5.088796	-2.273095
H	-4.960671	-3.890455	-3.314437
H	-4.218496	-1.712338	-2.429876
H	-1.600220	1.890756	-0.522792
H	0.806459	2.332217	-0.491051
H	-4.968027	3.556404	-2.150036
H	-5.417026	1.861727	-1.898067
H	-3.758615	2.277943	-2.307585
H	-4.613018	4.868311	-0.265587
C	-4.094654	5.561454	2.322375
H	-3.392152	3.195578	3.485788
H	-3.857209	-0.223033	2.636556
H	-2.175906	0.254775	2.423087
H	-3.108539	0.899878	3.780167
H	2.927991	1.553533	-0.718169
H	5.978251	-0.035626	0.215670
H	3.391580	-3.195313	3.485859
C	4.094151	-5.561283	2.322720

H	4.613033	-4.868315	-0.265207
H	3.758990	-2.278074	-2.307544
H	5.417333	-1.861873	-1.897746
H	4.968343	-3.556553	-2.149685
H	3.107416	-0.899732	3.779968
H	2.175883	-0.254083	2.422390
H	3.857264	0.222981	2.636940
H	4.218624	1.712500	-2.429764
H	7.236930	1.927515	0.624437
H	4.961078	3.890530	-3.314265
H	6.878793	5.088568	-2.272947
H	8.029367	4.070902	-0.310639
H	3.414270	-5.647079	3.175712
H	3.843165	-6.351150	1.607983
H	5.106470	-5.769372	2.691996
H	-3.843160	6.351259	1.607754
H	-5.107183	5.769676	2.691021

7.2 Poly(*p*-phenylene iminoborane): A Boron–Nitrogen Analogue of Poly(*p*-phenylene vinylene)

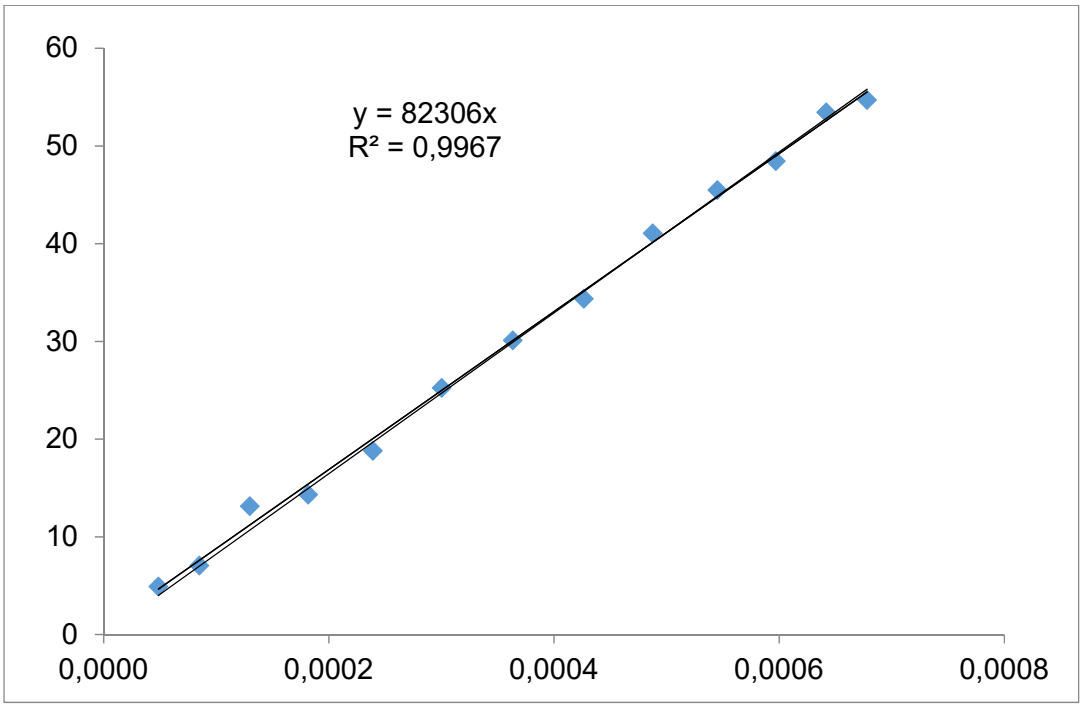

Figure 7.2.1. Plot of decay rates against the squared length of the scattering vector q^2 for the DLS measurement of **8'** in THF.

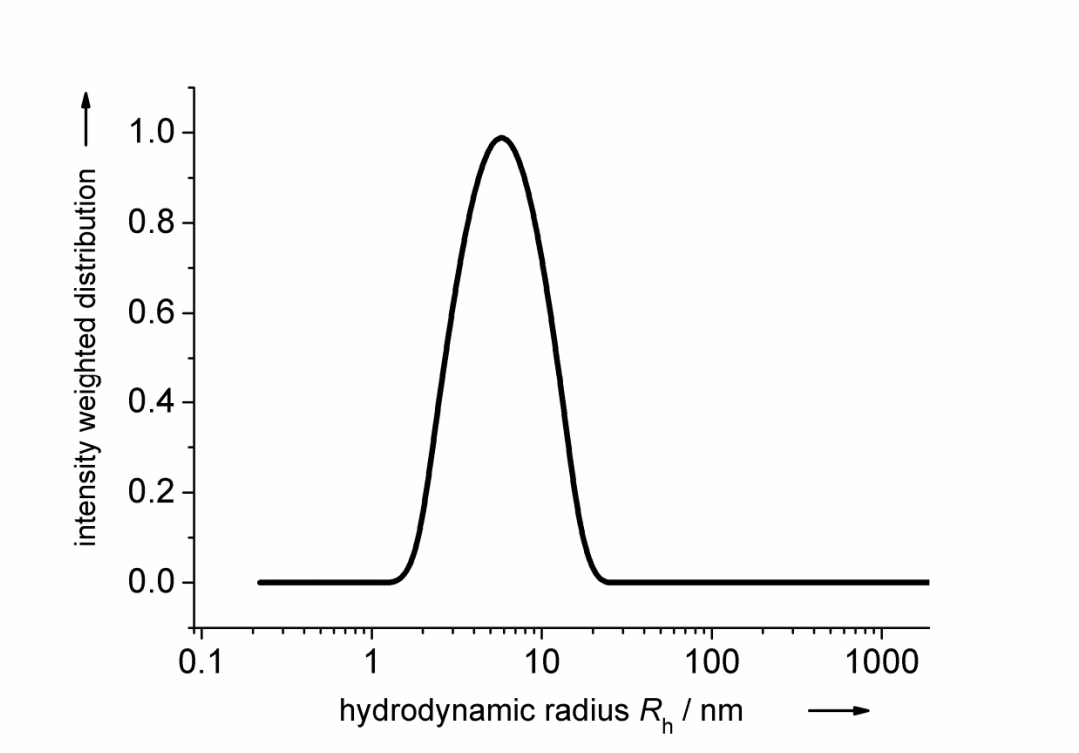

Figure 7.2.2. Intensity weighted size distribution of particles of **8'** in THF by DLS ($\theta = 90°$).

Small-angle X-ray scattering (SAXS) of 8'

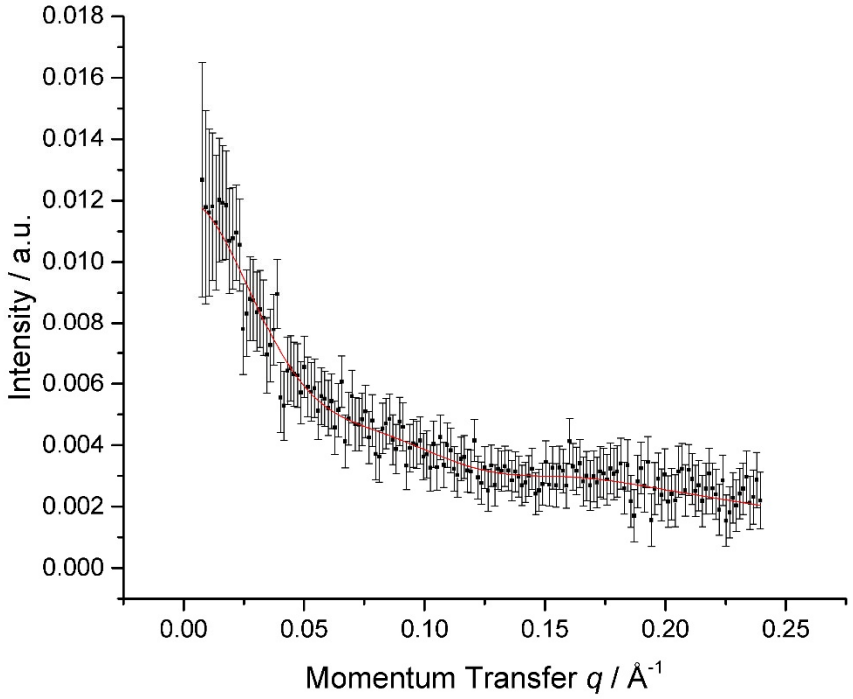

Figure 7.2.3. SAXS profile of **8'** in THF.

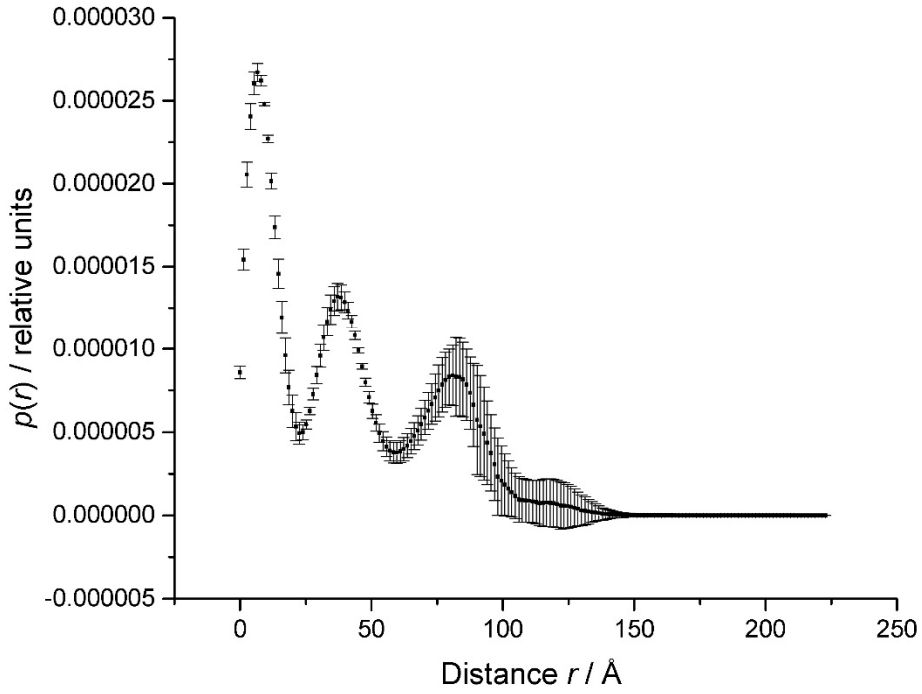

Figure 7.2.4. Bayesian weighted distance distribution function of **8'** in THF.

Gel permeation chromatography (GPC) of 8'

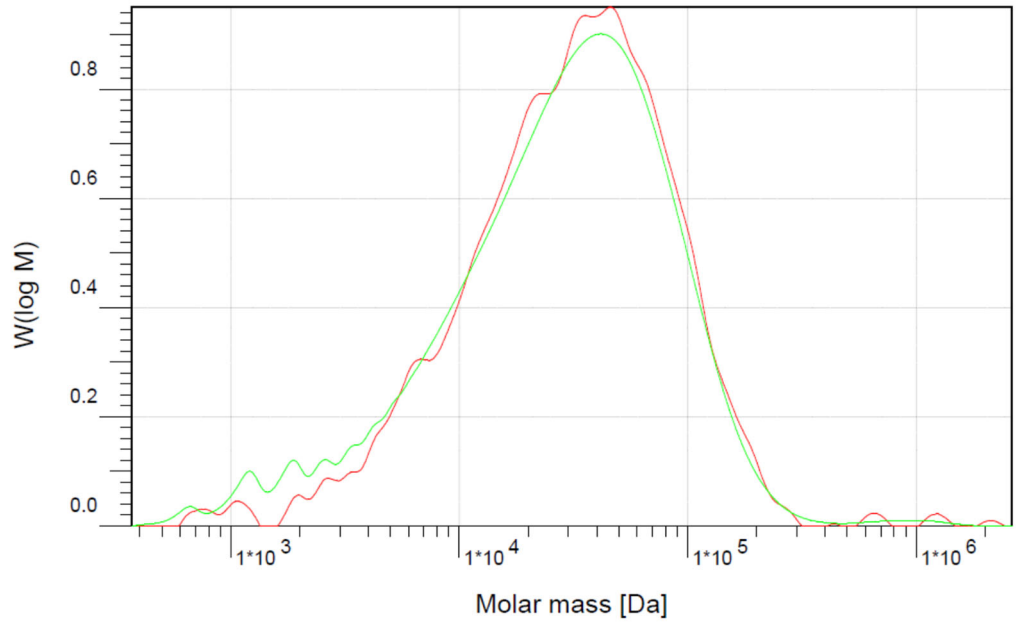

Figure 7.2.5. Gel permeation chromatography (GPC) trace of **8'** (in THF); red line: detection by RI signal; green line: detection by UV signal.

NMR spectra

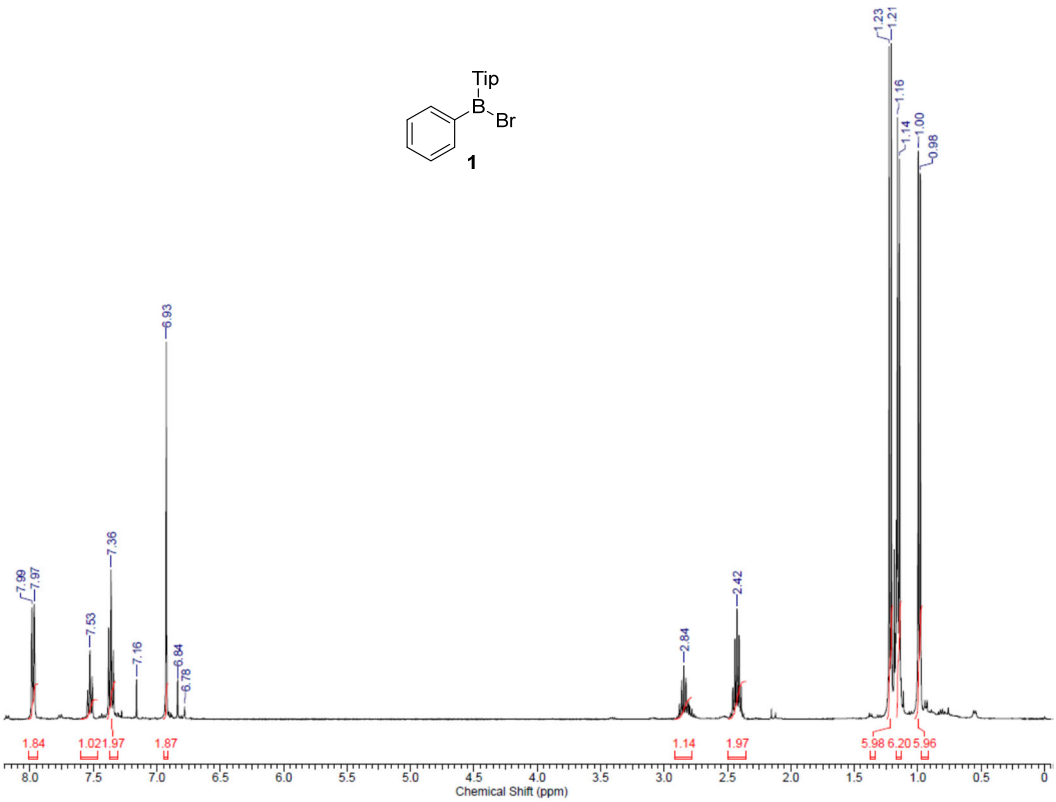

Figure 7.2.6. ^{1}H NMR spectrum of **1** (in $CDCl_3$).

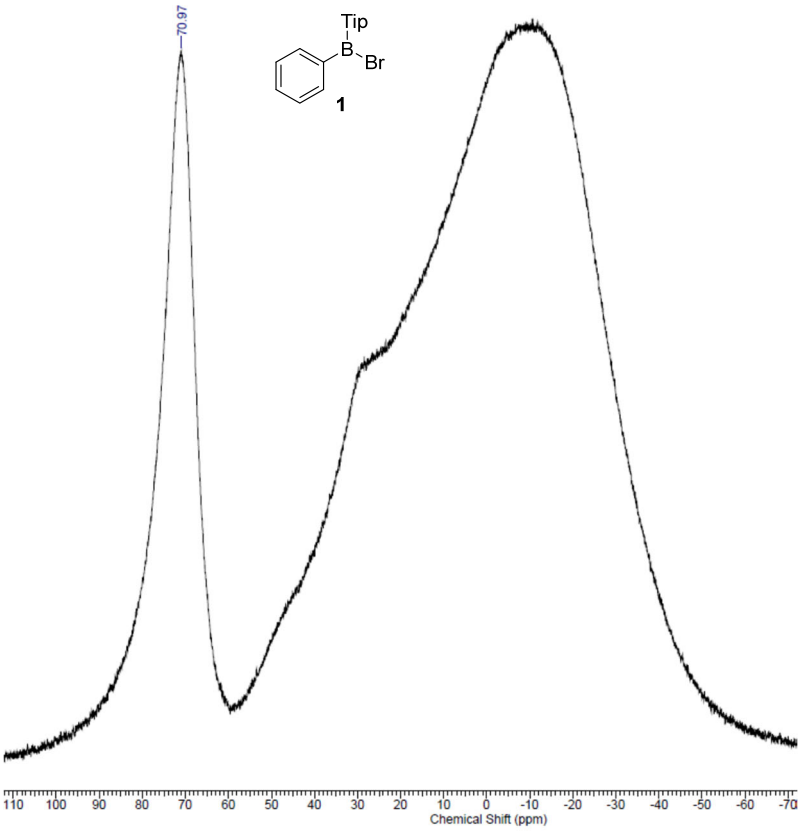

Figure 7.2.7. $^{11}B\{^{1}H\}$ NMR spectrum of **1** (in $CDCl_3$).

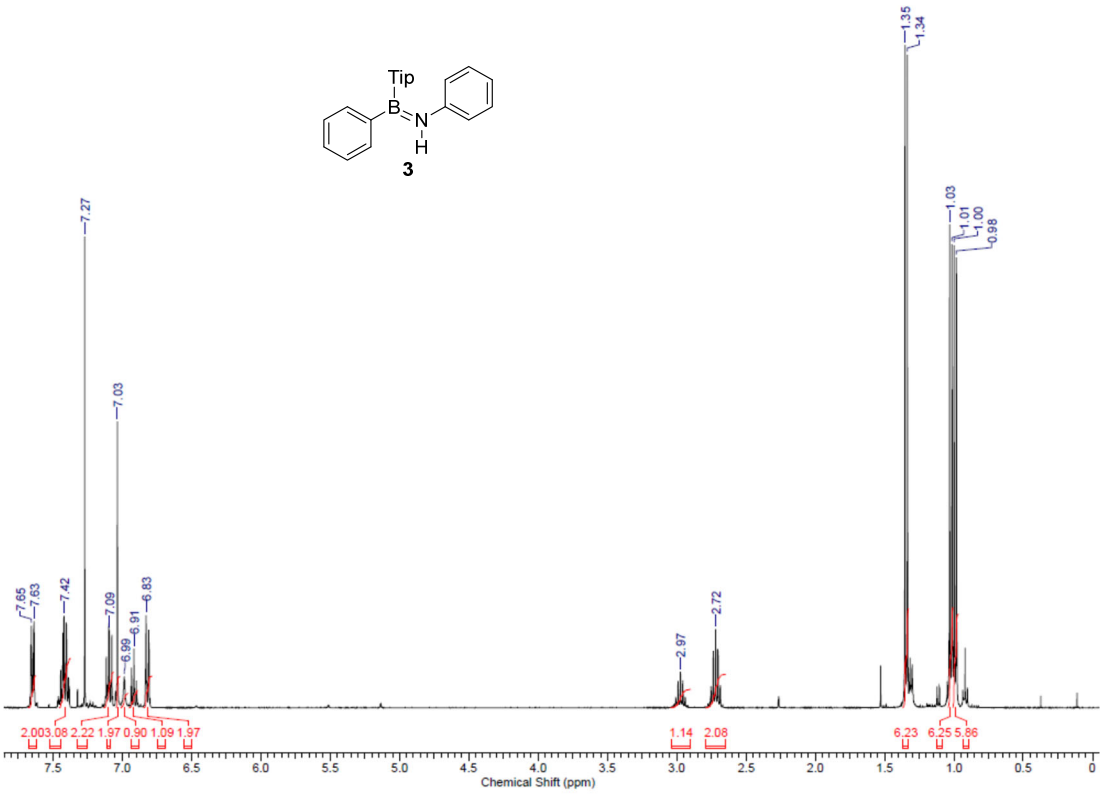

Figure 7.2.8. ^{1}H NMR spectrum of **3** (in $CDCl_3$).

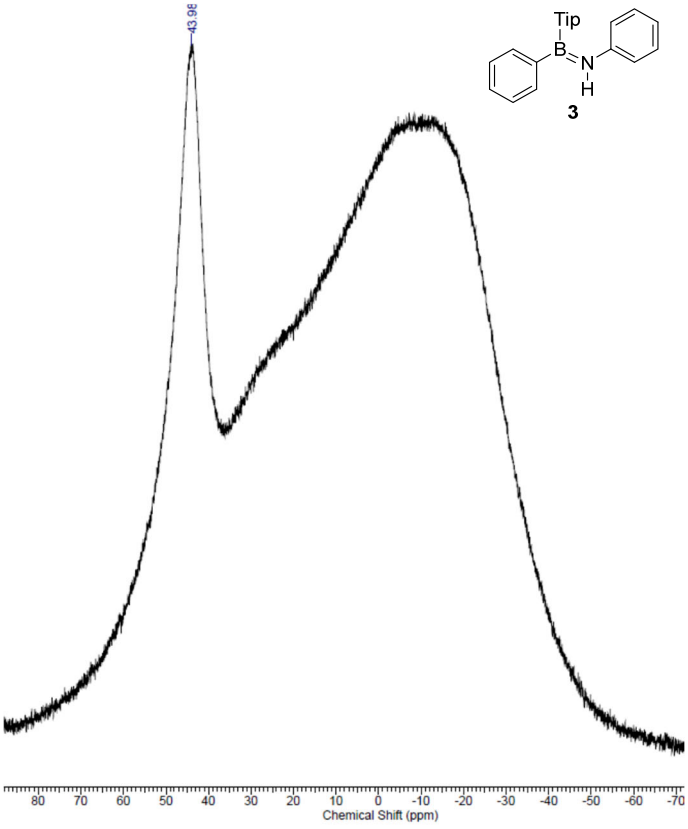

Figure 7.2.9. $^{11}B\{^{1}H\}$ NMR spectrum of **3** (in $CDCl_3$).

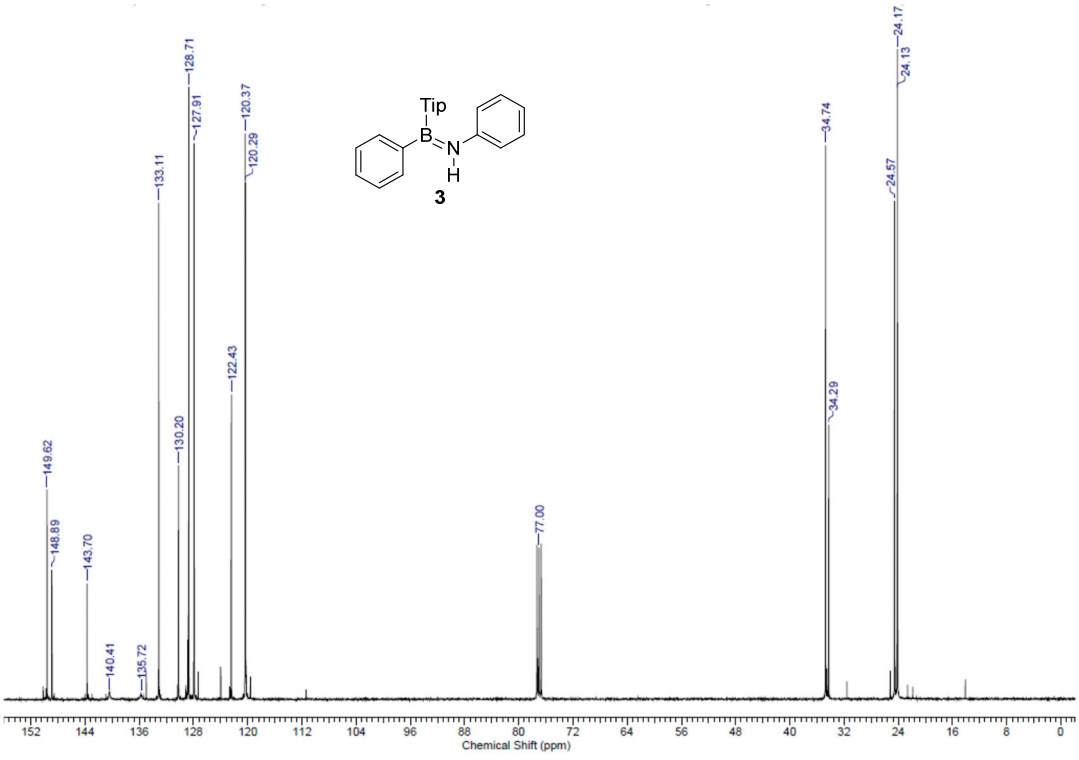

Figure 7.2.10. $^{13}C\{^{1}H\}$ NMR spectrum of **3** (in $CDCl_3$).

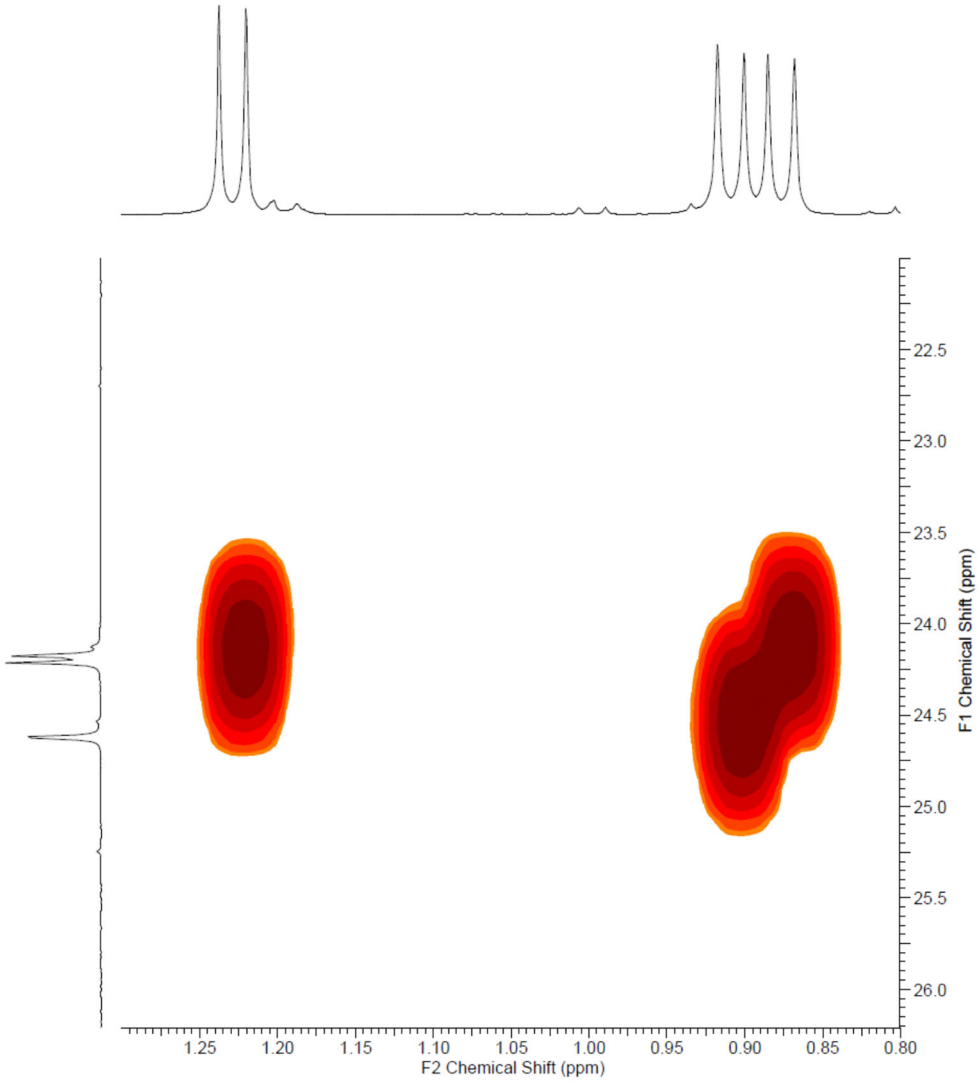

Figure 7.2.11. Detail of the $^{1}H,^{13}C$ HSQC spectrum of **3** (in $CDCl_3$).

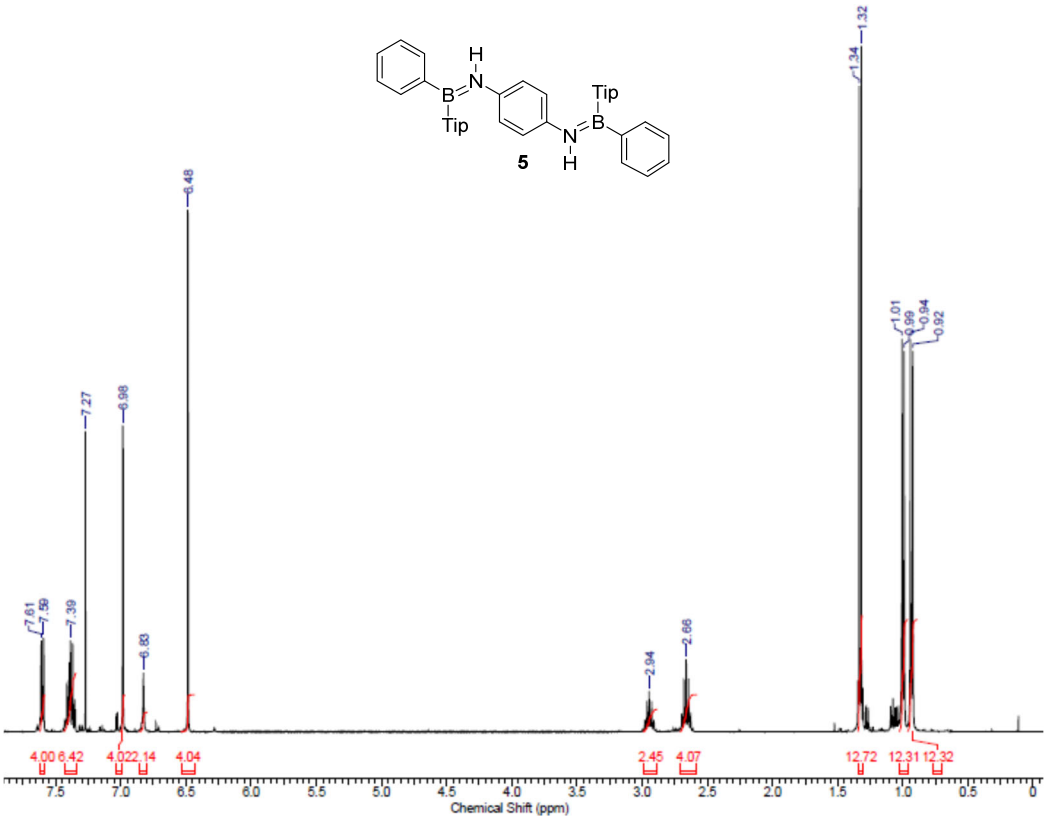

Figure 7.2.12. ^{1}H NMR spectrum of **5** (in $CDCl_3$).

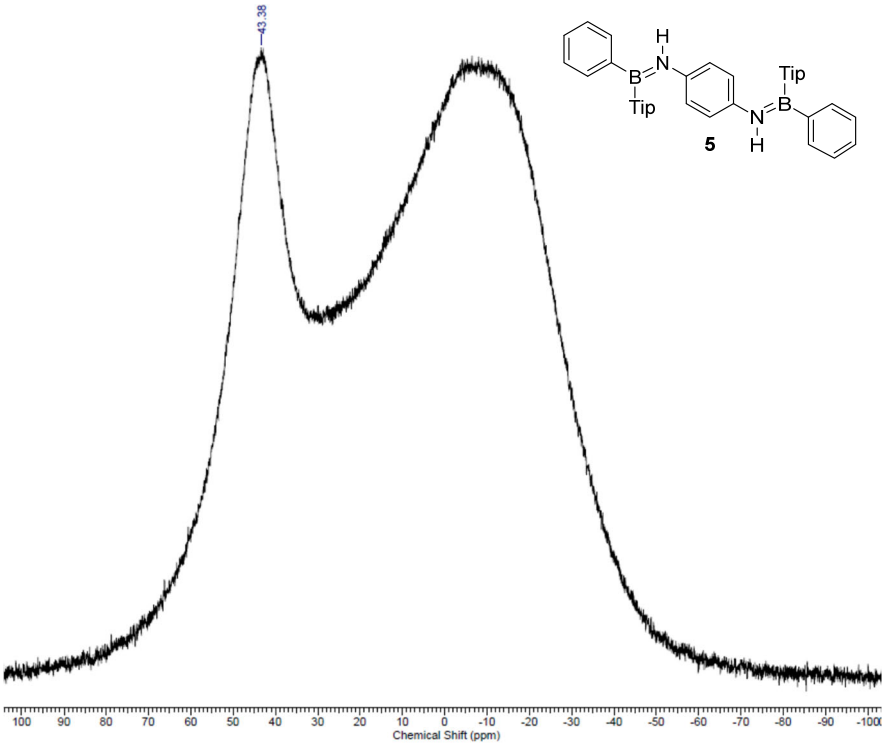

Figure 7.2.13. ^{11}B{^{1}H} NMR spectrum of **5** (in $CDCl_3$).

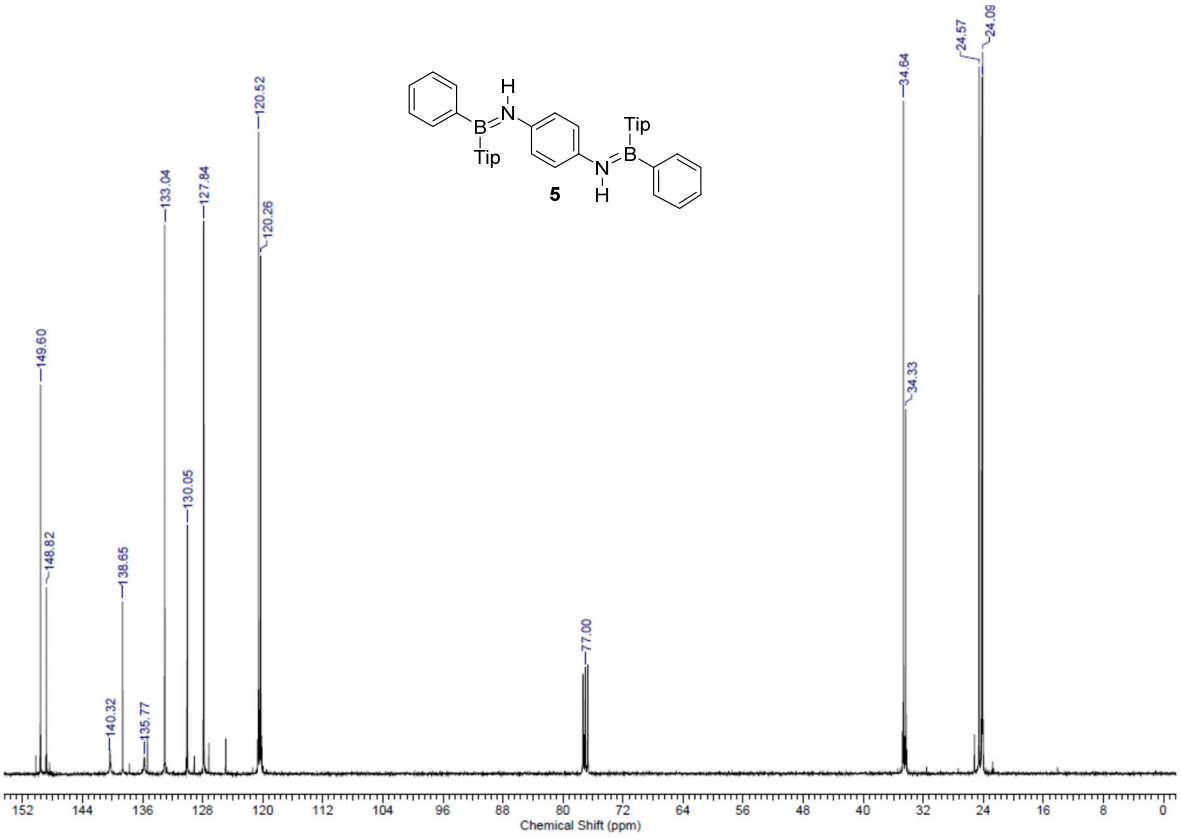

Figure 7.2.14. $^{13}C\{^{1}H\}$ NMR spectrum of **5** (in $CDCl_3$).

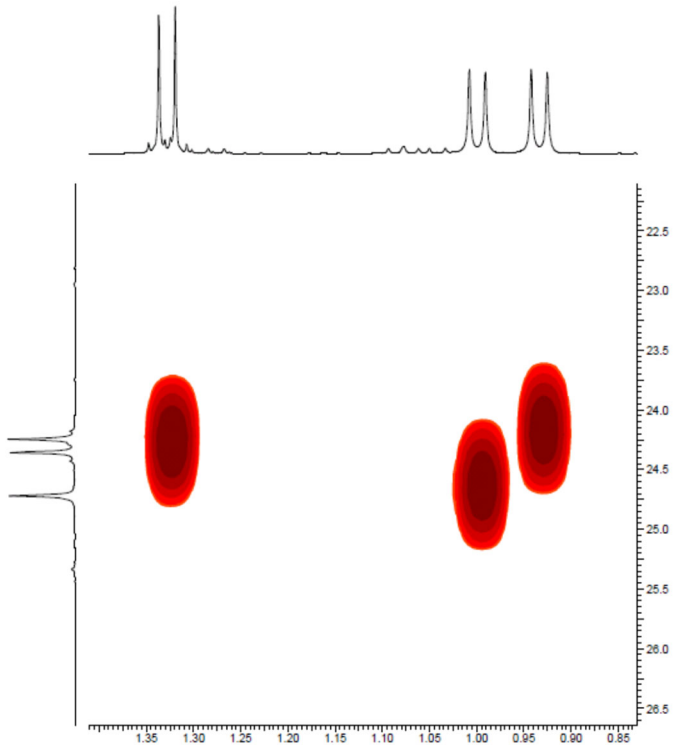

Figure 7.2.15. Detail of the $^{1}H,^{13}C$ HSQC spectrum of **5** (in $CDCl_3$).

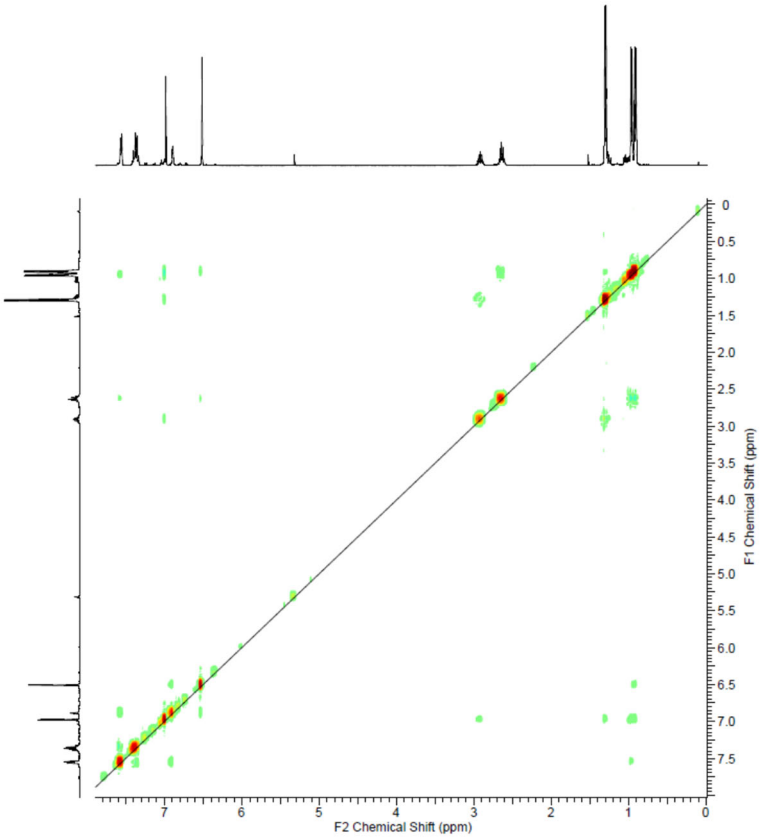

Figure 7.2.16. NOESY spectrum of **5** (in CD_2Cl_2).

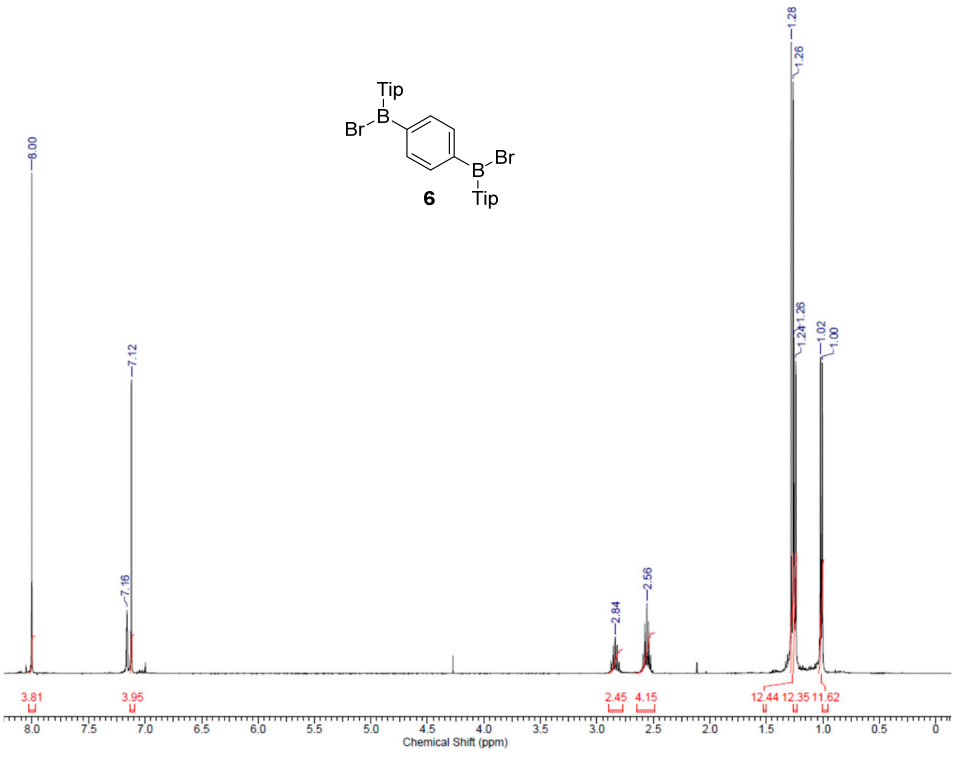

Figure 7.2.17. ^1H NMR spectrum of **6** (in C_6D_6).

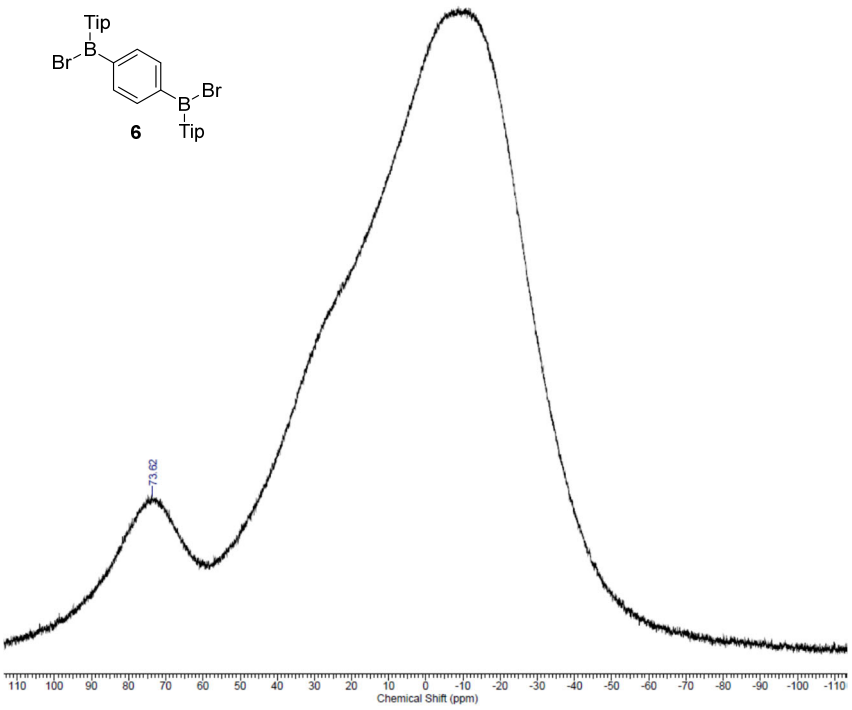

Figure 7.2.18. $^{11}B\{^{1}H\}$ NMR spectrum of **6** (in C_6D_6).

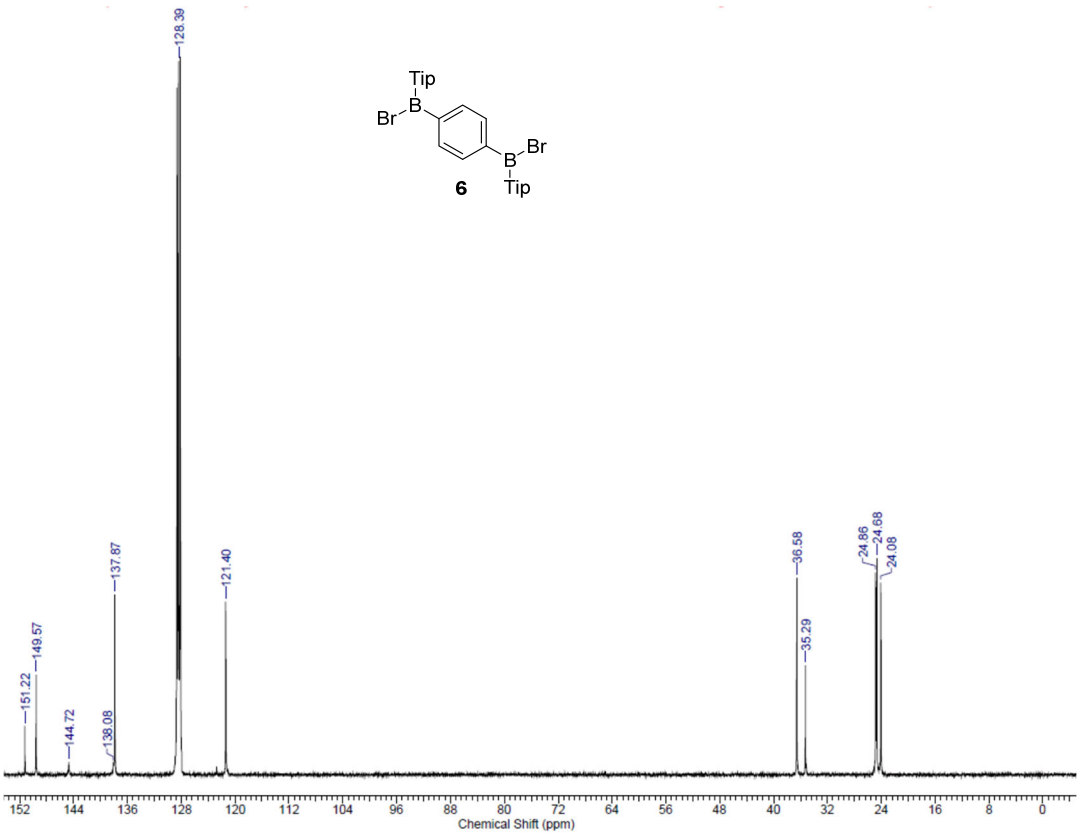

Figure 7.2.19. $^{13}C\{^{1}H\}$ NMR spectrum of **6** (in C_6D_6).

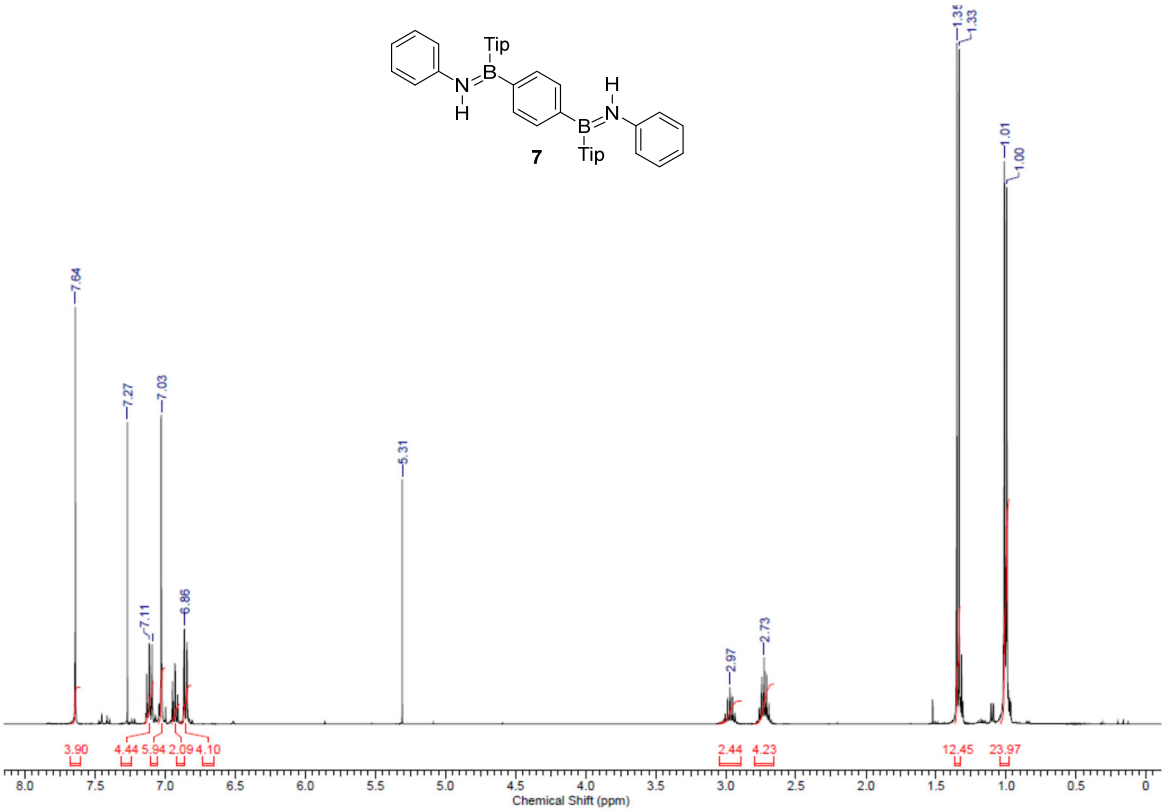

Figure 7.2.20. ^{1}H NMR spectrum of **7** (in $CDCl_3$).

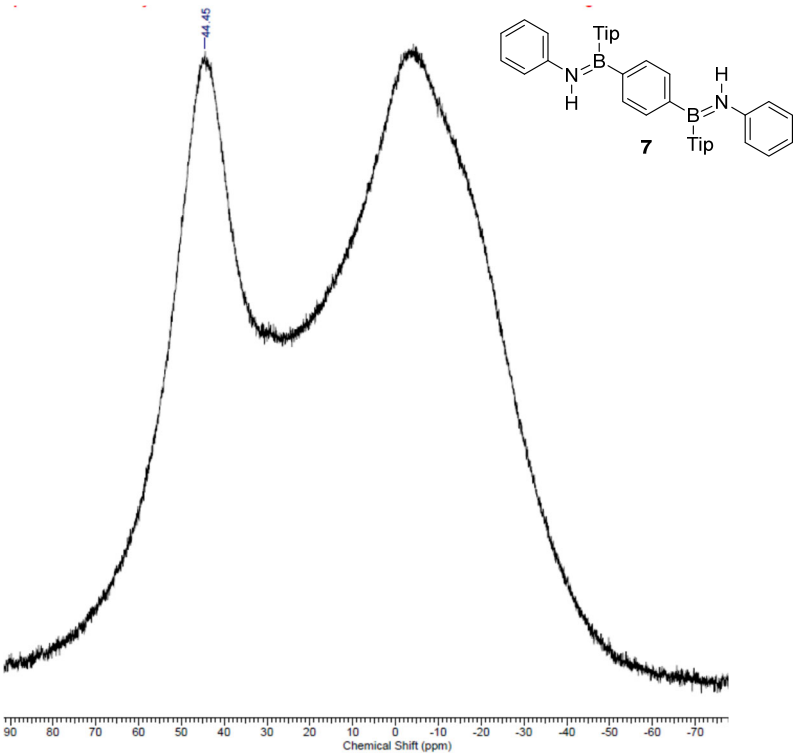

Figure 7.2.21. $^{11}B\{^{1}H\}$ NMR spectrum of **7** (in $CDCl_3$).

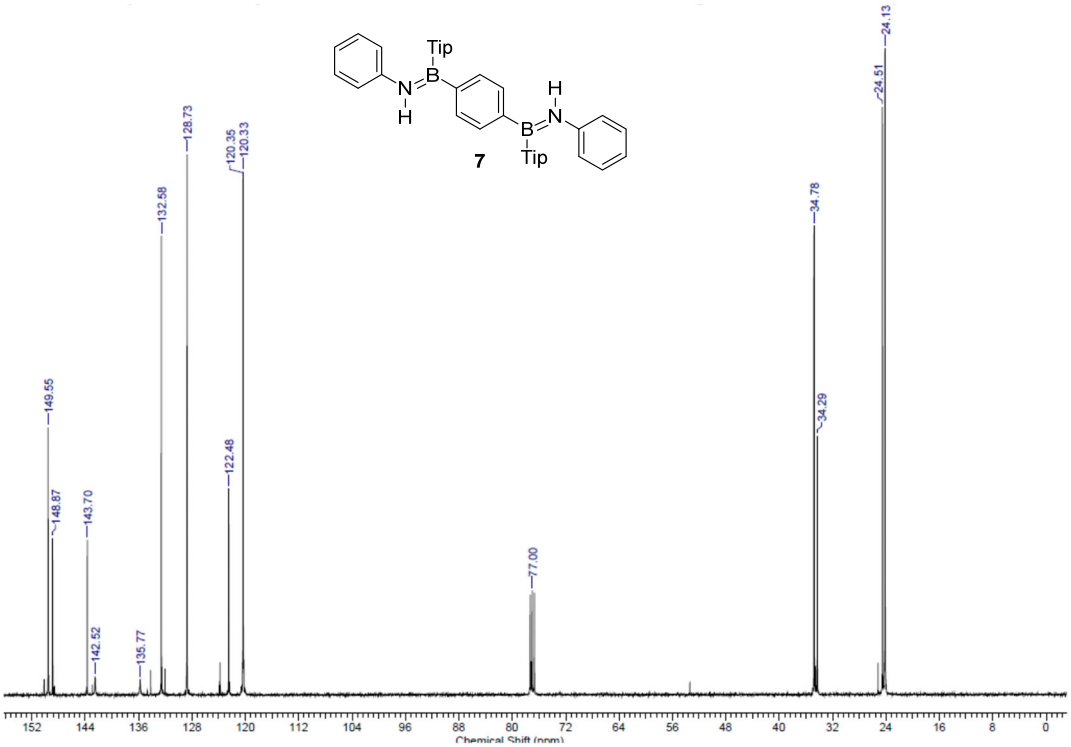

Figure 7.2.22. $^{13}C\{^{1}H\}$ NMR spectrum of **7** (in $CDCl_3$).

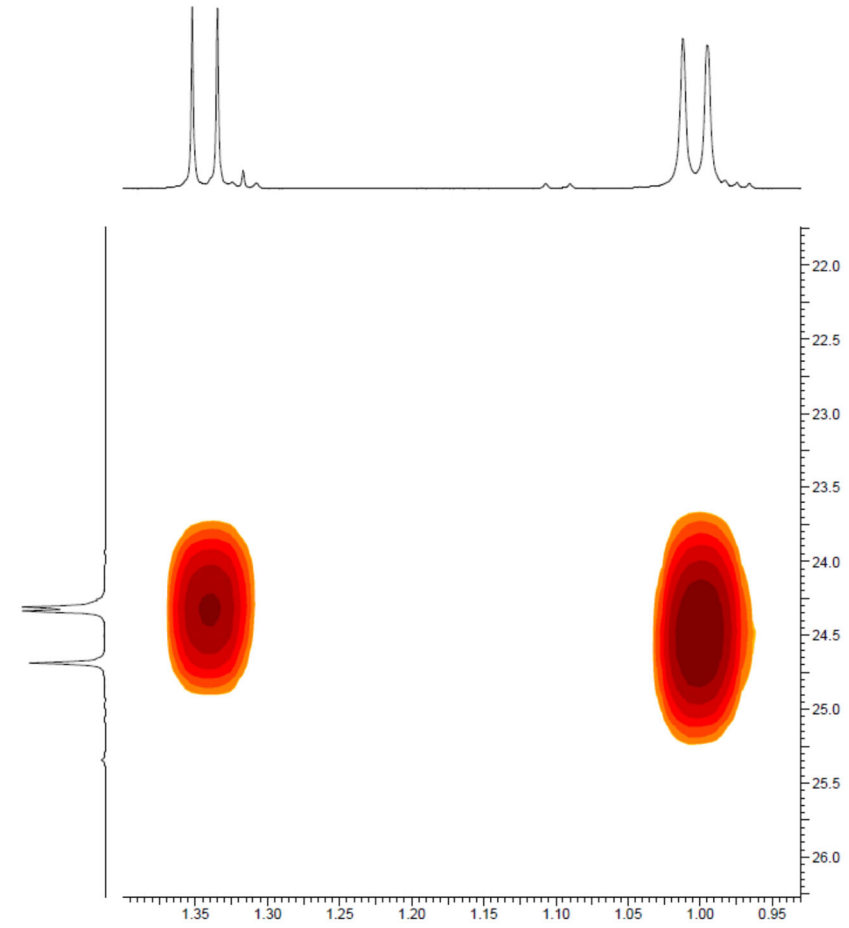

Figure 7.2.23. Detail of the $^{1}H,^{13}C$ HSQC spectrum of **7** (in $CDCl_3$).

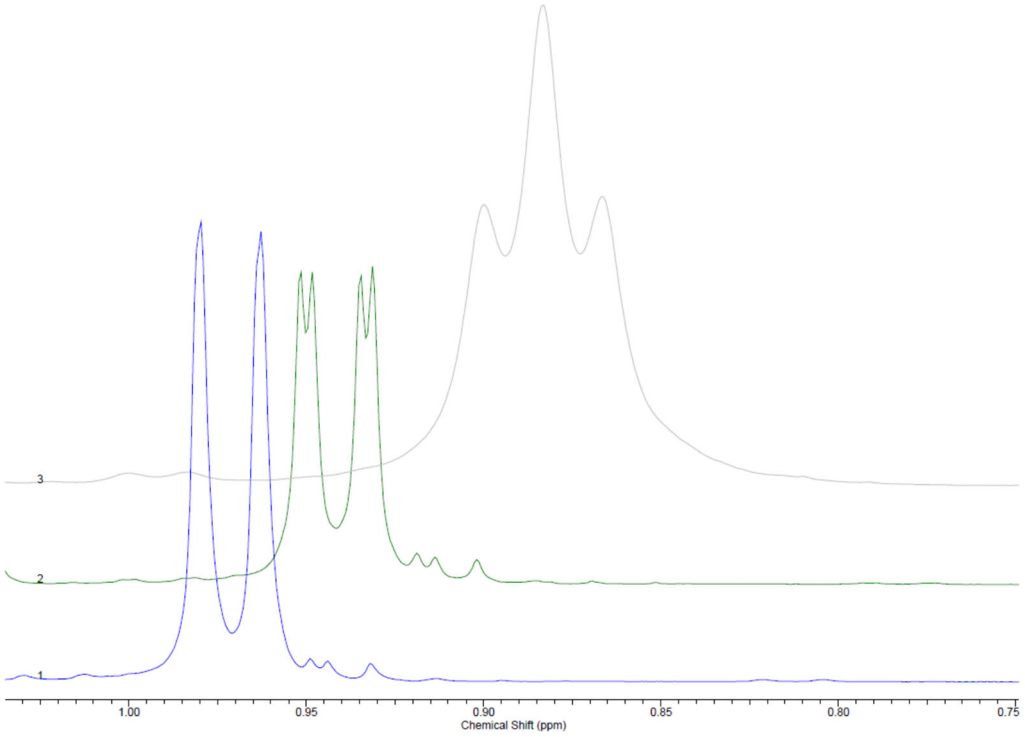

Figure 7.2.24. Detail of the ^{1}H NMR spectrum of **7** (in CD_2Cl_2; T = 23 °C (blue (1)), T = 0 °C (green (2)), T = –80 °C (grey (3)).

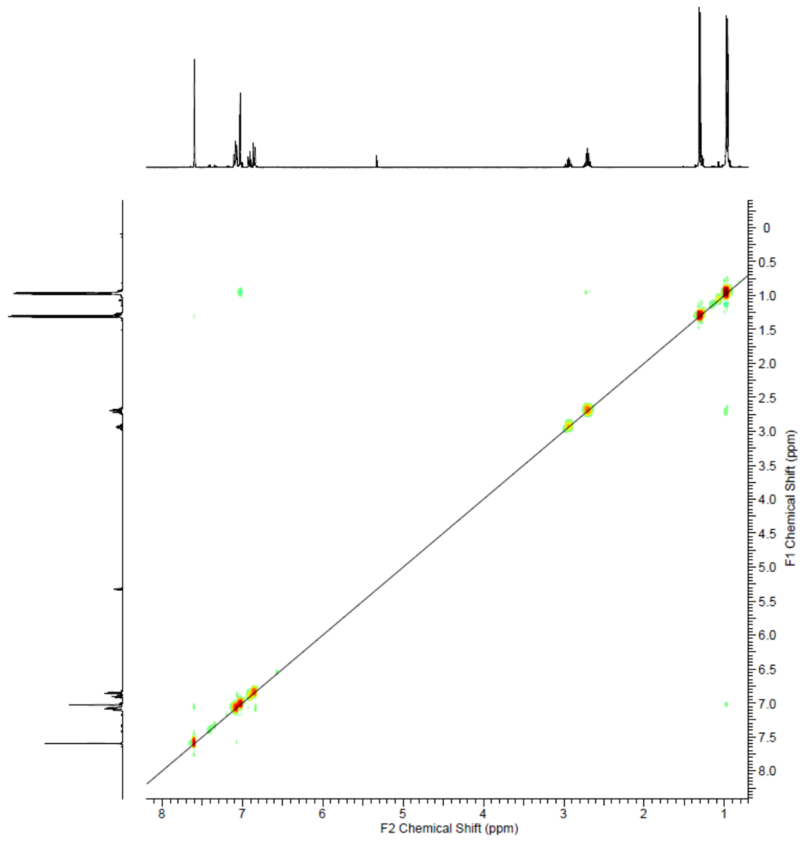

Figure 7.2.25. NOESY spectrum of **7** (in CD_2Cl_2; T = 23 °C).

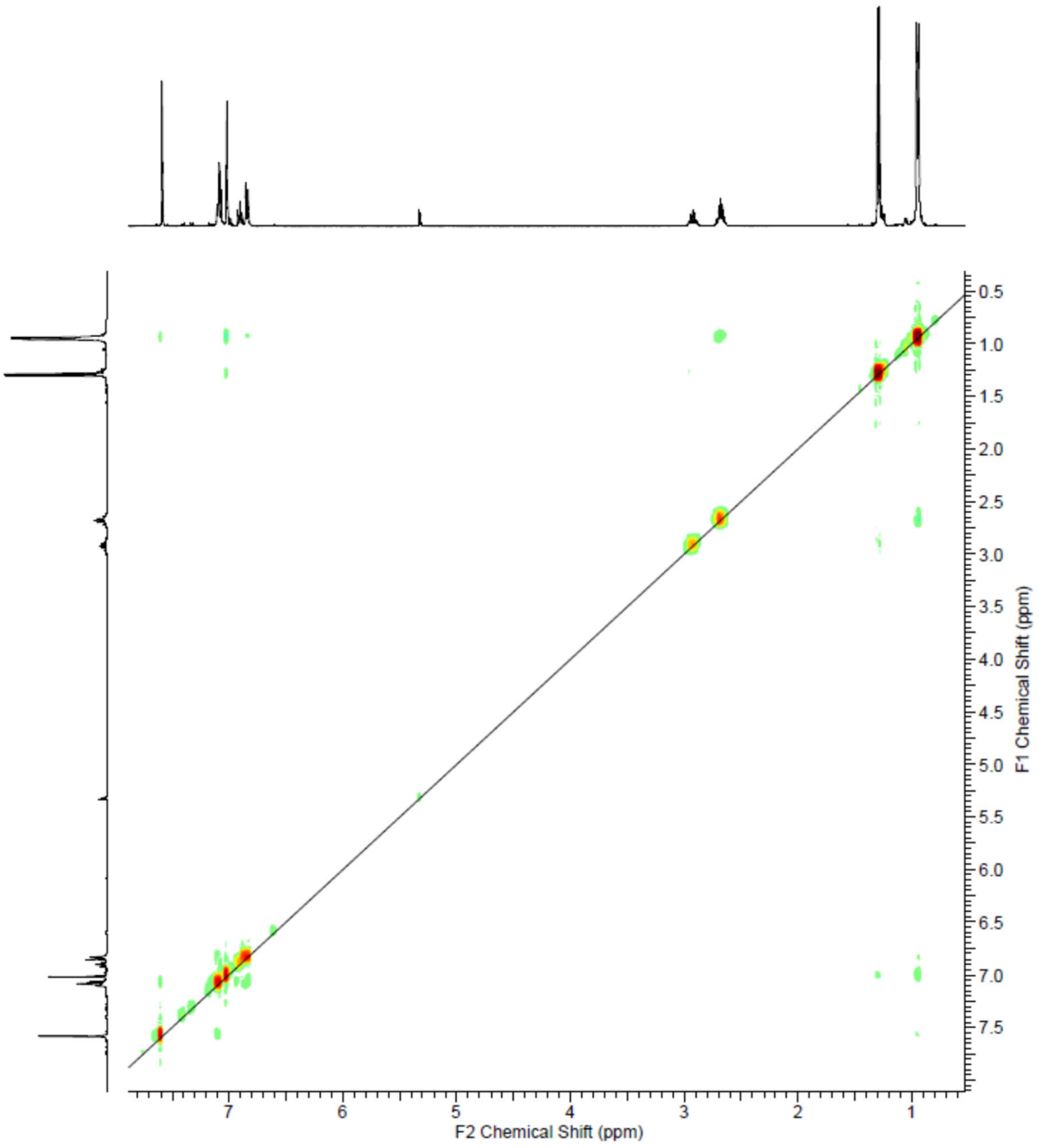

Figure 7.2.26. NOESY spectrum of **7** (in CD_2Cl_2; T = 0 °).

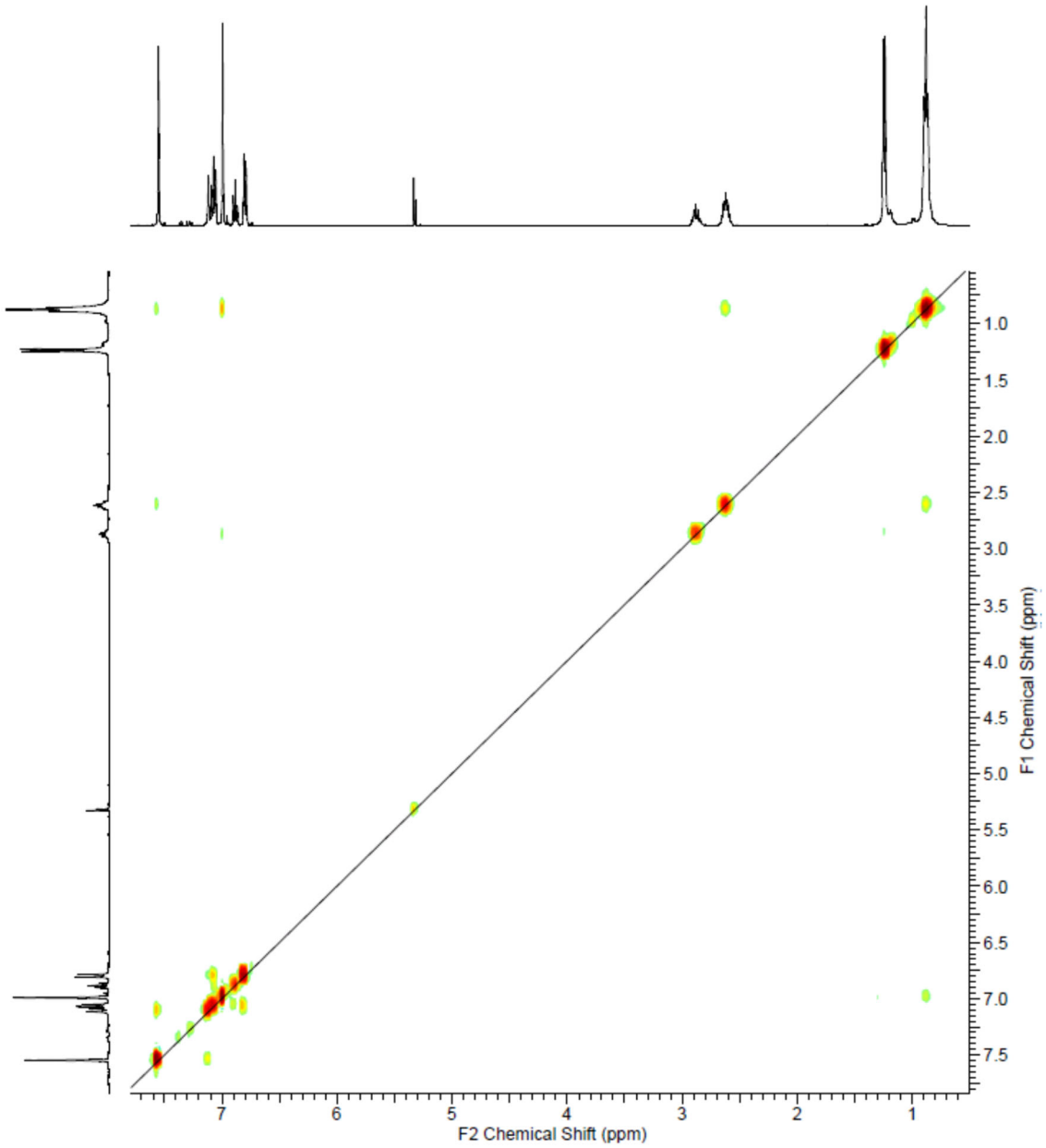

Figure 7.2.27. NOESY spectrum of **7** (in CD_2Cl_2; T = –80 °).

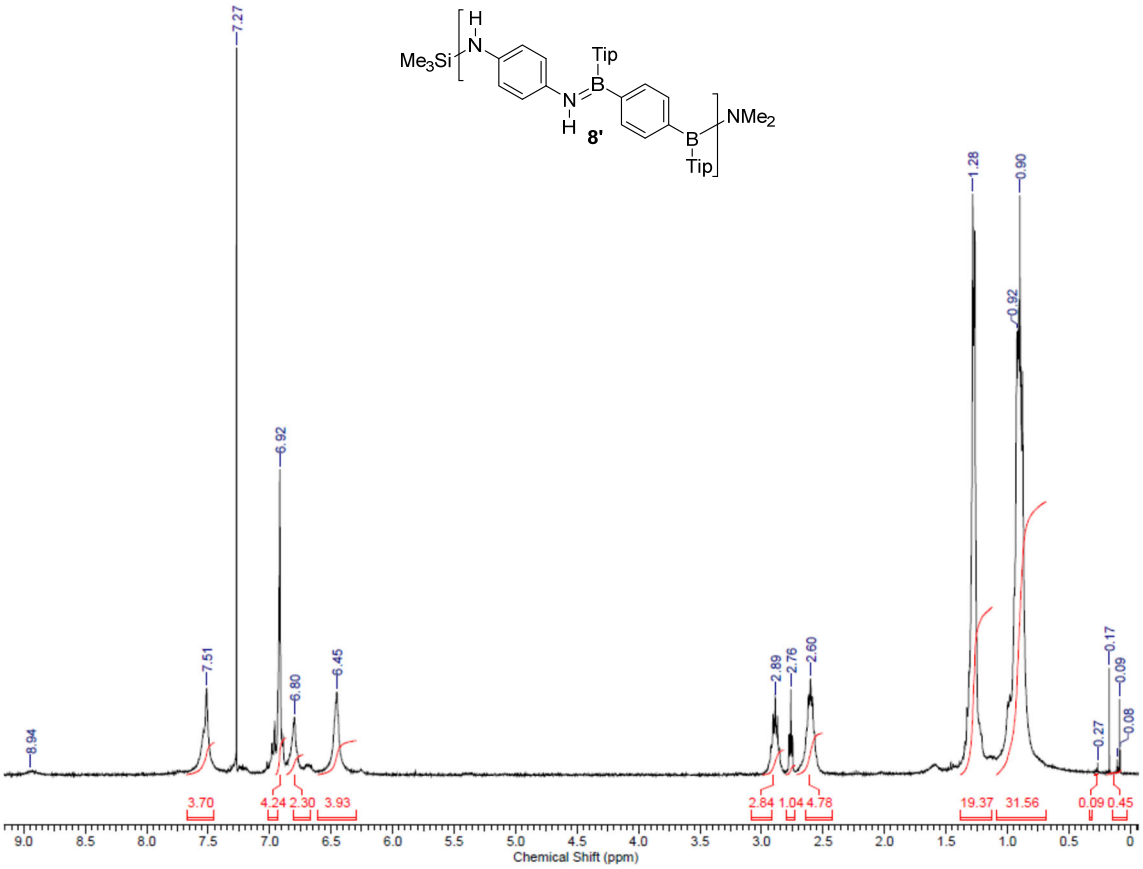

Figure 7.2.28. ^{1}H NMR spectrum of **8'** (in $CDCl_3$).

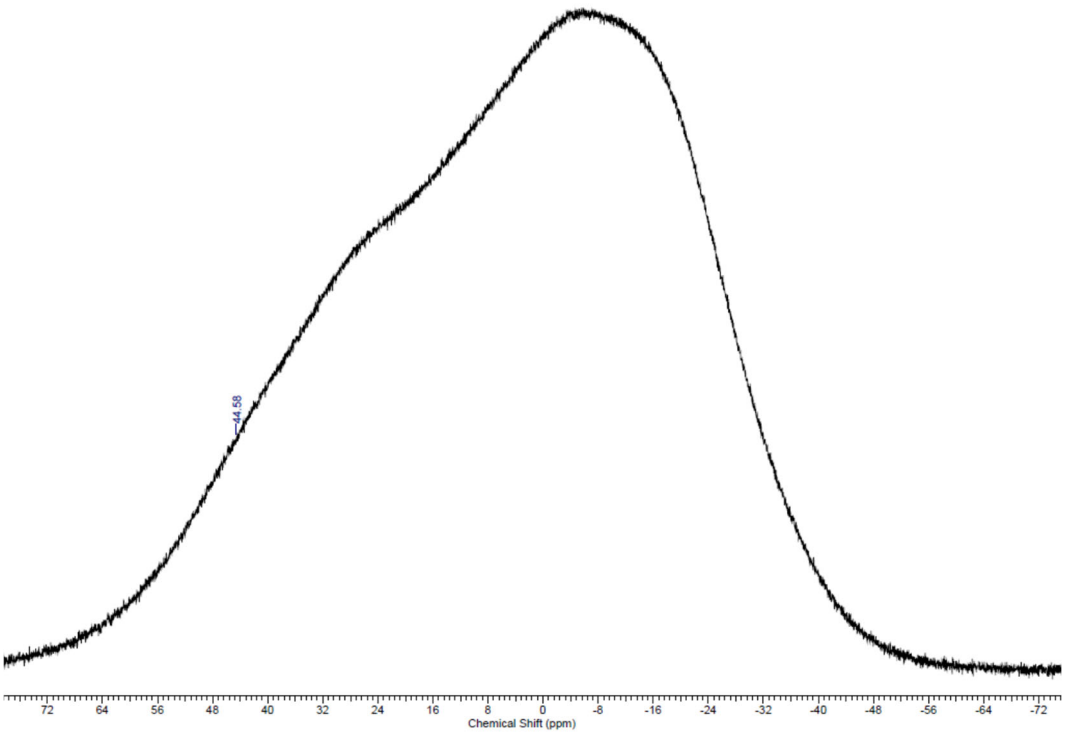

Figure 7.2.29. $^{11}B\{^{1}H\}$ NMR spectrum (in $CDCl_3$) of the reaction mixture of the polymerization of **4** with **6** (1:1 ratio) after 20 min.

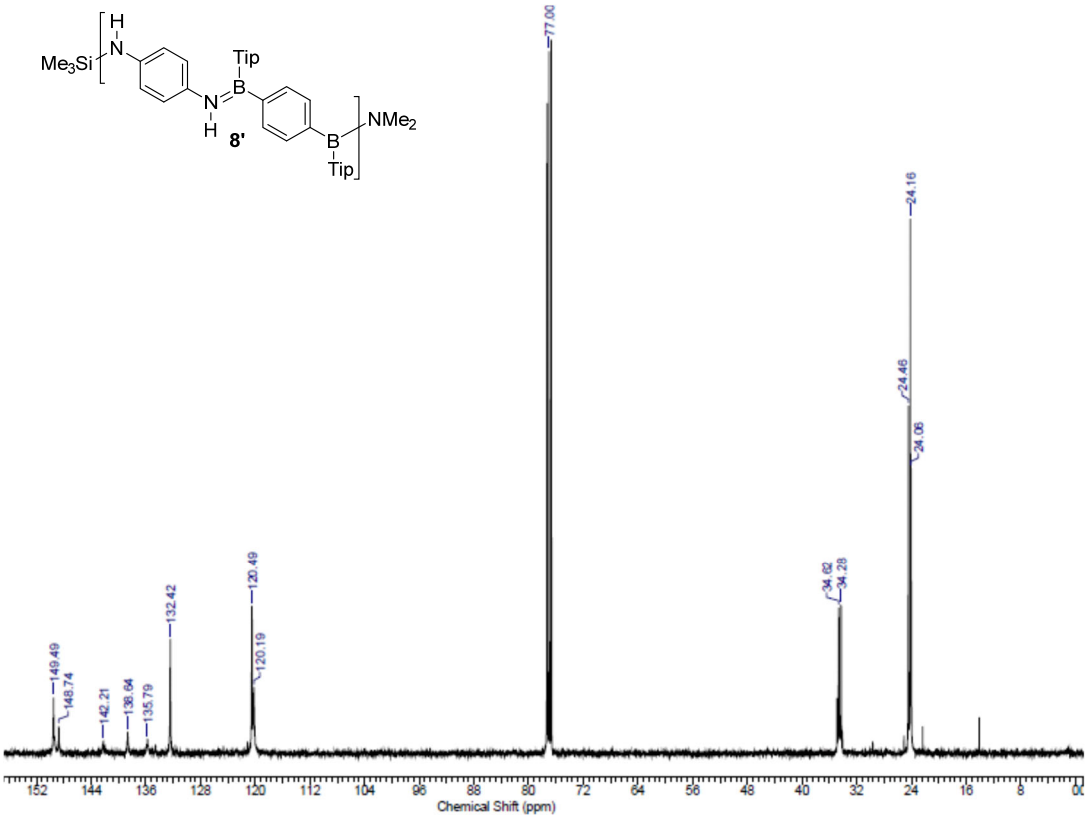

Figure 7.2.30. $^{13}C\{^{1}H\}$ NMR spectrum of **8'** (in $CDCl_3$).

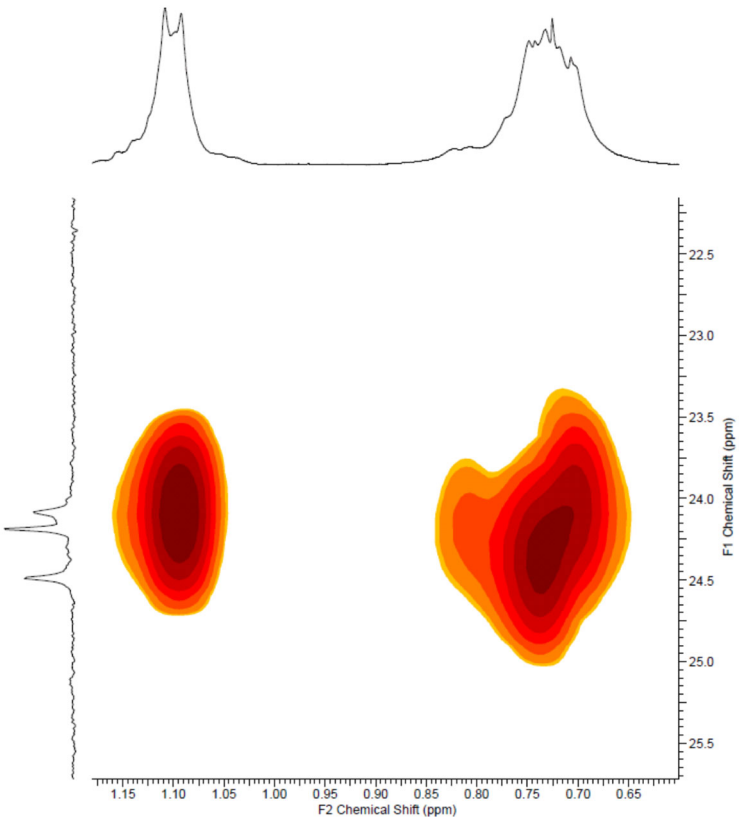

Figure 7.2.31. Detail of the $^{1}H,^{13}C$ HSQC of polymer **8'** (in $CDCl_3$).

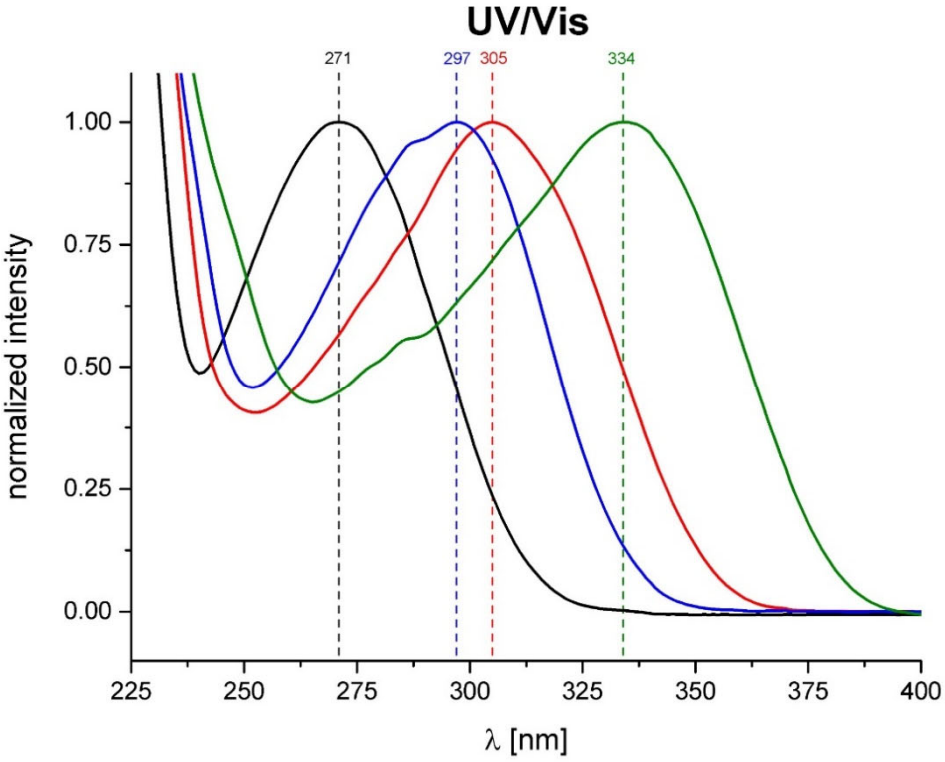

Figure 7.2.32. UV–vis spectrum of **3** (black), **5** (blue), **7** (red), **8'** (green) (in CH_2Cl_2).

MS spectra

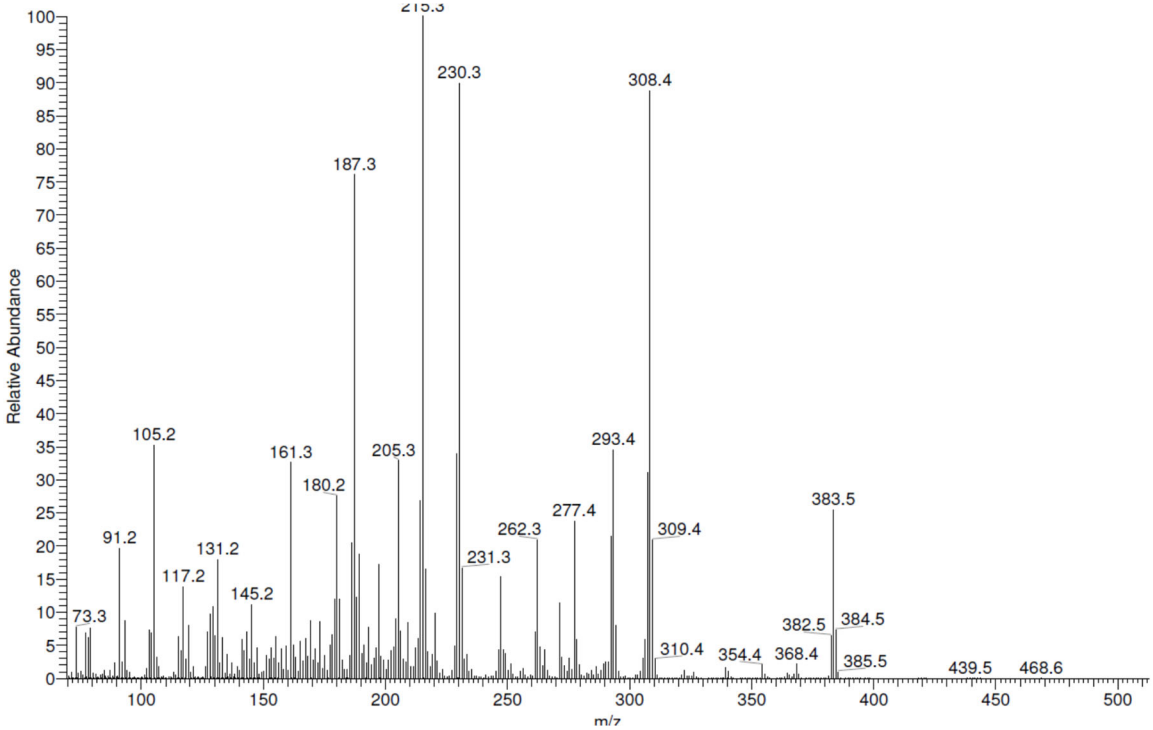

Figure 7.2.33. EI-MS spectrum of **3**.

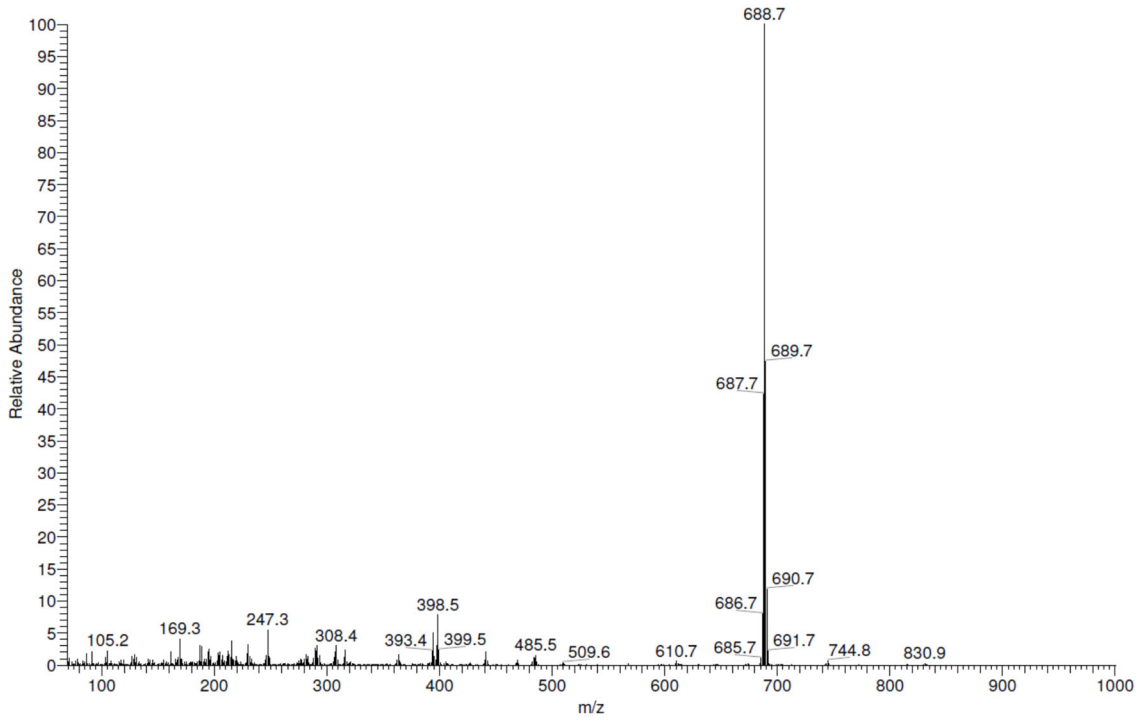

Figure 7.2.34. EI-MS spectrum of **5**.

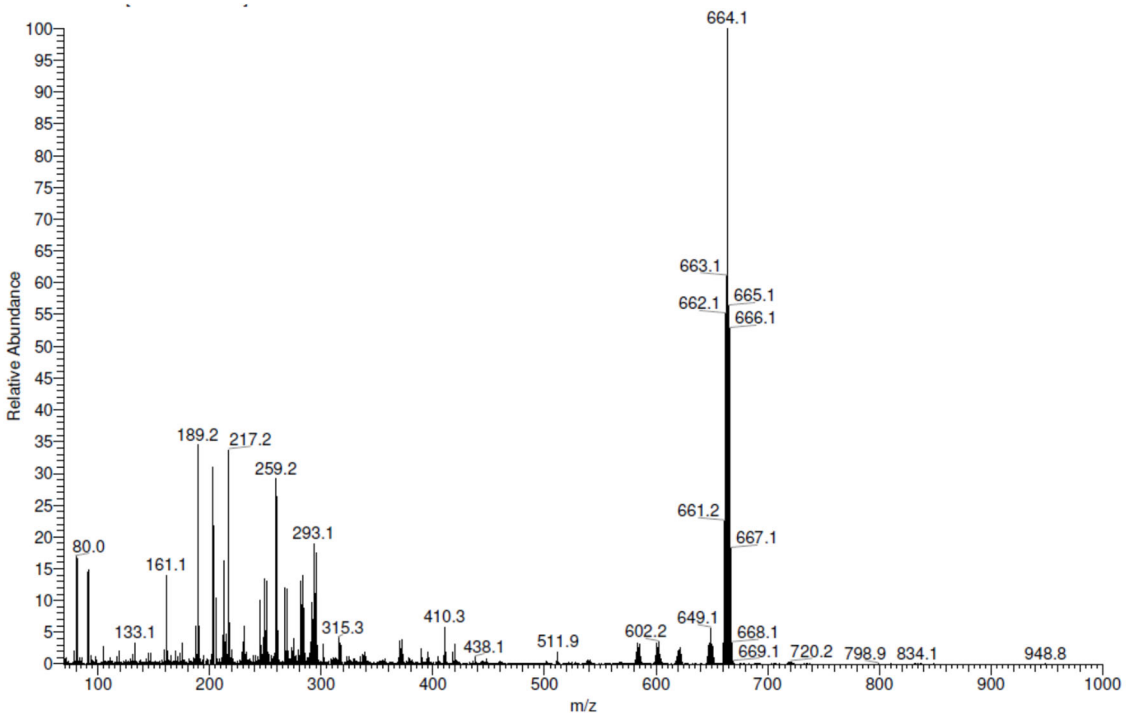

Figure 7.2.35. EI-MS spectrum of **6**.

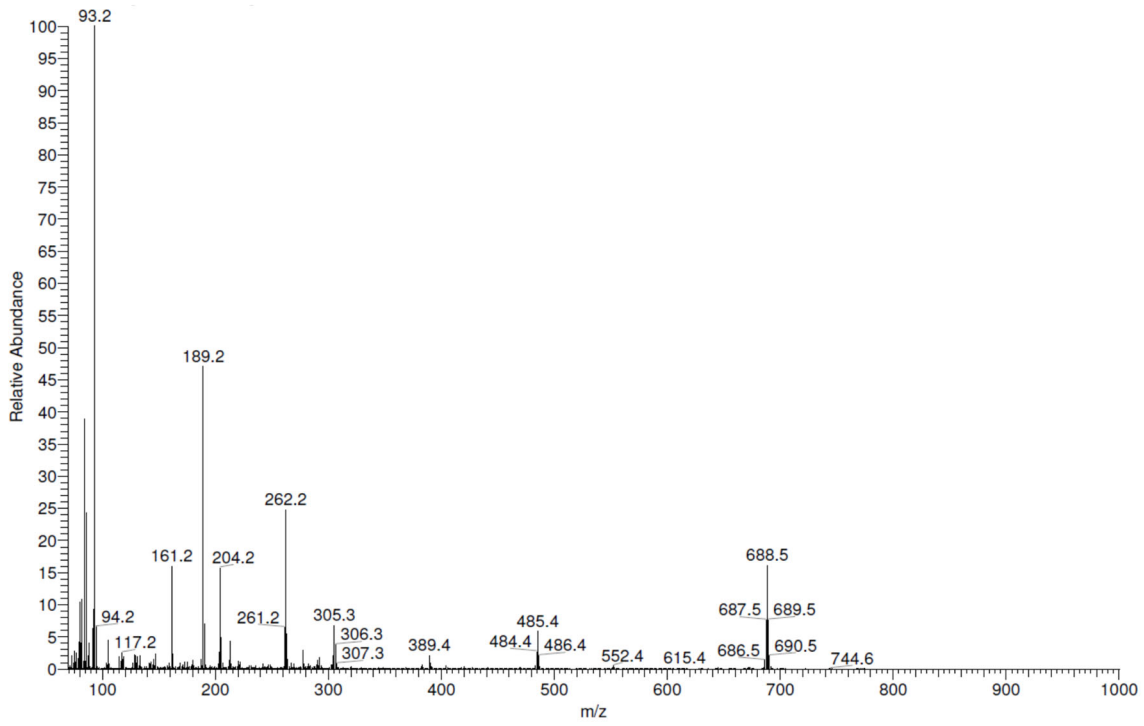

Figure 7.2.36. EI-MS spectrum of **7**.

Table 7.2-1. Results from TD-DFT calculations.

Compound	λ / nm	Oscillator strength *f*	Orbital contributions	$\|c\|^2$ / %
3	294.4	0.1207	HOMO → LUMO	79.7
			HOMO–2 → LUMO	10.2
			HOMO–1 → LUMO	9.0
5	333.1	0.8010	HOMO → LUMO	98.3
7	328.4	0.6671	HOMO → LUMO	93.7

Frontier orbitals

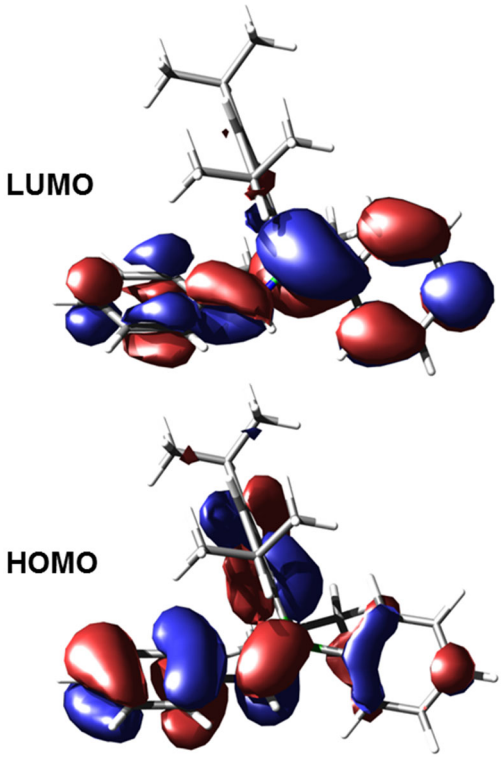

Figure 7.2.37. Calculated frontier orbitals (isovalue 0.025 a.u.) of **3**.

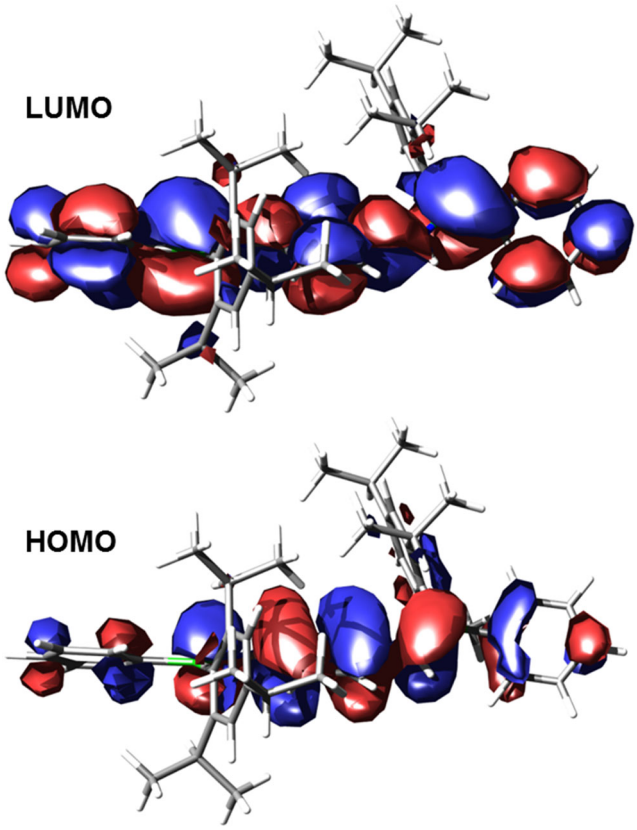

Figure 7.2.38. Calculated frontier orbitals (isovalue 0.015 a.u.) of **5**.

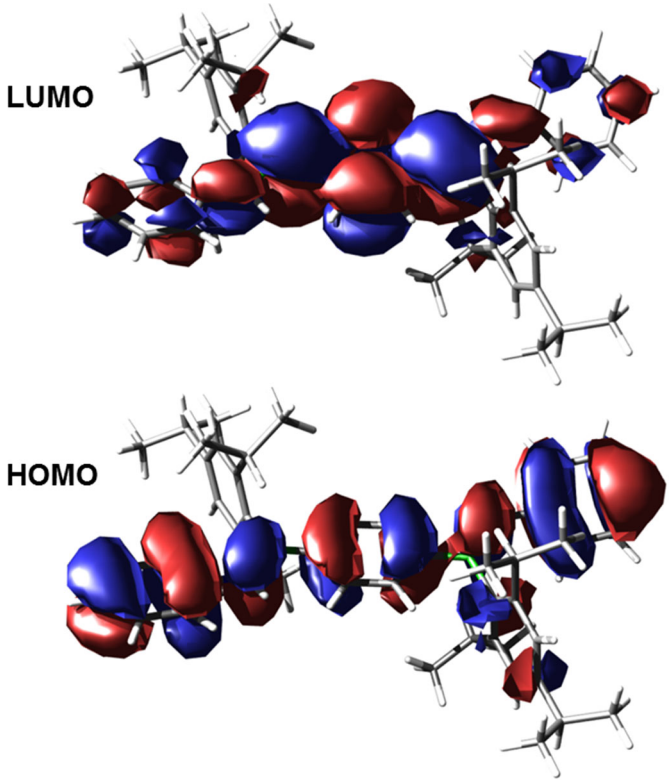

Figure 7.2.39. Calculated frontier orbitals (isovalue 0.015 a.u.) of **7**.

Cartesian coordinates (Å) and total energies (a.u.) of optimized stationary points

Compound **3**
Total energy (B3LYP-D3/def2-SV(P)): -1127.538223457

C	-3.426837	3.745126	1.266858
C	-2.233385	3.885638	2.004454
C	-1.930891	5.167869	2.505822
C	-2.787642	6.253303	2.303056
C	-3.967713	6.084384	1.571544
C	-4.284449	4.825447	1.048228
B	-1.246581	2.688917	2.275691
C	0.255253	2.980910	2.661111
C	0.696683	2.859542	3.998340
C	2.030128	3.145145	4.314633
C	2.949726	3.549347	3.338362
C	2.497349	3.671752	2.020222
C	1.168841	3.397190	1.669345
C	-0.262140	2.440004	5.108116
C	4.397774	3.845476	3.696620
C	0.726115	3.535052	0.216207
N	-1.769801	1.372799	2.205859
C	-1.169606	0.120373	2.446346
C	0.200610	-0.112897	2.235303
C	0.750224	-1.365040	2.515284
C	-0.046867	-2.409902	2.994860
C	-1.413903	-2.188405	3.187057

C	-1.968814	-0.936484	2.917071
H	-2.778794	1.297917	2.099624
H	-1.002174	5.311099	3.066864
H	-2.532068	7.236484	2.711035
H	-4.637574	6.933725	1.403013
H	-5.200294	4.689185	0.464090
H	-3.686928	2.773966	0.829167
H	2.363208	3.049052	5.352771
H	3.207687	3.988885	1.249262
C	0.752226	5.001188	-0.244416
C	1.538499	2.632228	-0.726697
H	-0.324009	3.197245	0.154648
C	-0.485183	3.580259	6.115890
H	-1.239084	2.226361	4.642710
C	0.191660	1.148775	5.809311
H	-3.037795	-0.765239	3.084750
H	-2.056385	-2.993863	3.556449
H	0.391670	-3.388693	3.209923
H	1.820079	-1.524826	2.348251
H	0.834603	0.686662	1.854929
H	4.908684	4.143245	2.762632
C	4.512616	5.022190	4.680041
C	5.115034	2.596814	4.236689
H	0.384763	5.093216	-1.283177
H	0.113149	5.626461	0.402844
H	1.778419	5.411171	-0.210019
H	1.149197	2.696415	-1.759394
H	2.603245	2.927019	-0.751981
H	1.488931	1.575802	-0.407766
H	-0.559068	0.827056	6.554410
H	0.327576	0.330120	5.082263
H	1.149123	1.295581	6.342085
H	-1.222349	3.285334	6.885469
H	0.454147	3.847543	6.633727
H	-0.861386	4.487367	5.610136
H	6.182100	2.810040	4.432865
H	4.660622	2.254096	5.184291
H	5.056062	1.762190	3.515813
H	5.572571	5.264927	4.880367
H	4.021287	5.925609	4.277480
H	4.034316	4.782572	5.647388

Compound **5**

Total energy (B3LYP-D3/def2-SV(P)): -2023.142590

C	0.189575	-0.021438	-0.068774
C	0.102137	0.113671	1.333064
C	1.280687	0.343213	2.078254
C	2.512821	0.420074	1.418202
C	2.615210	0.274821	0.028628
C	1.439324	0.057978	-0.697607
B	-1.303524	0.037194	2.046477

C	-2.281342	1.270064	1.980708
C	-1.774881	2.548301	1.669432
C	-2.605421	3.670921	1.613422
C	-3.977198	3.537365	1.851196
C	-4.509563	2.276912	2.146080
C	-3.668556	1.163905	2.210210
C	1.228305	0.524749	3.591718
C	3.960627	0.362770	-0.675039
C	-1.062674	-0.270443	-0.902834
N	-1.719262	-1.097272	2.786216
C	-1.091585	-2.330319	3.053939
C	-1.481865	-3.065679	4.186214
C	-0.899448	-4.289830	4.506626
C	0.119787	-4.824534	3.700191
C	0.502065	-4.093767	2.561525
C	-0.090964	-2.877052	2.233437
N	0.758764	-6.050902	3.968051
B	0.849425	-6.854598	5.131203
C	1.670408	-8.196038	5.036276
C	1.967394	-8.833167	3.813849
C	2.698281	-10.021925	3.764278
C	3.157701	-10.608193	4.949329
C	2.872414	-10.001851	6.176836
C	2.131629	-8.817371	6.214816
C	0.193573	-6.441520	6.505705
C	-1.018468	-7.035166	6.915920
C	-1.588130	-6.672161	8.143592
C	-0.982889	-5.732651	8.985466
C	0.227996	-5.161806	8.572263
C	0.822823	-5.501368	7.351414
C	-1.716979	-8.058206	6.026905
C	2.143562	-4.852701	6.951165
C	-1.615892	-5.358315	10.316615
H	-2.583496	-0.993056	3.312494
H	-0.704824	2.658716	1.467954
H	-2.183485	4.653059	1.377288
H	-4.632874	4.412606	1.800880
H	-5.584388	2.162912	2.320338
H	-4.113888	0.184620	2.422698
H	3.419998	0.599069	2.003625
H	1.507495	-0.053838	-1.785047
C	-1.363677	0.913248	-1.835736
C	-0.988318	-1.597026	-1.676647
H	-1.915489	-0.354959	-0.205766
C	1.634488	1.950692	4.000354
H	0.180766	0.384736	3.908518
C	2.063388	-0.533360	4.330463
H	-2.266377	-2.667667	4.839119
H	-1.237616	-4.826512	5.390997
H	1.286878	-4.491685	1.908784
H	0.231256	-2.349579	1.337223

H	1.312886	-6.361425	3.173570
H	2.906630	-10.497702	2.800533
H	1.602387	-8.407626	2.871399
H	3.731476	-11.539894	4.914925
H	3.224200	-10.457624	7.107897
H	1.901403	-8.356887	7.180465
H	2.426032	-5.254717	5.962787
C	2.006293	-3.329756	6.792117
C	3.275227	-5.219807	7.924929
H	0.721825	-4.431059	9.220382
H	-2.532325	-7.128408	8.459798
C	-1.730891	-9.451146	6.676162
C	-3.129718	-7.605925	5.622552
H	-1.130007	-8.143691	5.094730
H	-2.583088	-5.890210	10.376627
C	-0.755248	-5.832395	11.500306
C	-1.911182	-3.852567	10.411889
H	3.779388	0.164054	-1.747292
C	4.562591	1.773939	-0.563137
C	4.945546	-0.703603	-0.168468
H	-1.250370	-5.607047	12.462987
H	-0.576412	-6.920984	11.449734
H	0.229676	-5.330264	11.501179
H	-2.435058	-3.614902	11.355993
H	-0.979679	-3.258042	10.387628
H	-2.544781	-3.517658	9.571489
H	5.891085	-0.667492	-0.740311
H	5.192925	-0.547463	0.897438
H	4.519569	-1.717689	-0.268694
H	5.511872	1.843388	-1.125886
H	3.867764	2.534223	-0.961501
H	4.774997	2.032725	0.490450
H	-2.192325	-10.194988	6.000734
H	-0.704236	-9.785525	6.906332
H	-2.307580	-9.446015	7.619402
H	-3.588201	-8.332531	4.926797
H	-3.793634	-7.520042	6.501971
H	-3.103023	-6.621907	5.121514
H	2.950022	-2.886384	6.425577
H	1.209386	-3.078713	6.072025
H	1.760309	-2.846089	7.755590
H	4.235718	-4.786620	7.590046
H	3.070442	-4.838197	8.941920
H	3.398343	-6.315282	7.993498
H	-2.300701	0.742409	-2.397114
H	-1.474240	1.847770	-1.258596
H	-0.550378	1.059817	-2.570236
H	-1.932309	-1.785353	-2.220342
H	-0.170385	-1.586344	-2.419776
H	-0.812029	-2.446584	-0.992964
H	1.947038	-0.429145	5.424489

H	1.747896	-1.552342	4.049597
H	3.139642	-0.432794	4.097993
H	1.541290	2.086920	5.093655
H	2.682637	2.164444	3.721721
H	0.993620	2.701669	3.505061

Compound **7**

Total energy (B3LYP-D3/def2-SV(P)): -2023.141732504

C	-1.926897	-0.367733	4.707087
C	-1.229461	0.367358	3.731594
C	0.045789	-0.076525	3.338545
C	0.605518	-1.211461	3.927792
C	-0.088244	-1.933111	4.904983
C	-1.363590	-1.505615	5.286296
N	-1.837660	1.515960	3.187887
B	-1.298091	2.676264	2.578642
C	0.251106	2.894646	2.377877
C	1.074698	3.274081	3.461519
C	2.442079	3.485429	3.249475
C	3.024364	3.331552	1.984564
C	2.195133	2.964063	0.919332
C	0.822163	2.746925	1.096247
C	0.491381	3.471049	4.856997
C	4.513533	3.555083	1.771856
C	-0.040915	2.338366	-0.092950
C	-2.304817	3.802156	2.130539
C	-1.839637	5.117763	1.926794
C	-2.702041	6.143631	1.542848
C	-4.076109	5.917342	1.323388
C	-4.535812	4.596576	1.510490
C	-3.676051	3.571232	1.904466
B	-5.096158	7.038508	0.883616
N	-4.621004	8.369210	0.777200
C	-5.222699	9.595170	0.437246
C	-4.448396	10.765925	0.546670
C	-4.981143	12.015384	0.228818
C	-6.304570	12.127559	-0.207088
C	-7.078704	10.968374	-0.320905
C	-6.553140	9.713468	-0.007132
C	-6.594518	6.637001	0.596676
C	-7.557002	6.699600	1.624411
C	-8.880736	6.325814	1.355328
C	-9.277504	5.883379	0.088636
C	-8.305866	5.811783	-0.919280
C	-6.976164	6.178601	-0.682706
C	-7.168138	7.175096	3.019515
C	-5.950794	6.097155	-1.808254
C	-10.721420	5.489494	-0.181782
H	-2.835908	1.541426	3.382393
H	-0.776694	5.332561	2.073402
H	-2.274974	7.144321	1.403451

H	-5.592882	4.374962	1.337079
H	-4.087328	2.560686	2.015027
H	3.073022	3.778101	4.094556
H	2.639872	2.843311	-0.074230
C	-0.145770	3.468299	-1.129536
C	0.439119	1.025593	-0.733377
H	-1.062461	2.153550	0.285476
C	0.582014	4.940730	5.300978
H	-0.580687	3.214589	4.809465
C	1.131384	2.529091	5.890212
H	-2.921838	-0.032167	5.019805
H	-1.926607	-2.058016	6.045101
H	0.357742	-2.822331	5.359797
H	1.600653	-1.537788	3.609569
H	0.598328	0.466653	2.573641
H	-3.642394	8.502921	1.019570
H	-7.176815	8.827792	-0.107252
H	-8.116268	11.034738	-0.663329
H	-6.726808	13.105268	-0.456472
H	-4.353941	12.907260	0.324816
H	-3.410428	10.689719	0.889966
C	-5.744941	4.651685	-2.288136
H	-4.982839	6.441116	-1.400670
C	-6.304688	7.037960	-2.971955
H	-8.594886	5.463346	-1.915908
H	-9.631377	6.379554	2.151119
C	-7.336807	6.060693	4.064789
H	-6.094135	7.432534	2.994319
C	-7.923936	8.452065	3.421994
H	-11.279912	5.639160	0.760336
C	-11.366695	6.390410	-1.248074
C	-10.844912	4.004002	-0.559960
H	4.718568	3.375166	0.700657
C	4.922568	5.004665	2.082220
C	5.358322	2.553878	2.577488
H	0.636570	2.635958	6.873070
H	1.043205	1.475987	5.572568
H	2.204436	2.755228	6.030391
H	0.109347	5.081511	6.290581
H	1.633764	5.271889	5.379161
H	0.071925	5.603696	4.579599
H	6.435101	2.686936	2.364511
H	5.210935	2.690921	3.664440
H	5.083031	1.513227	2.330654
H	5.993710	5.166720	1.861098
H	4.333625	5.720645	1.482088
H	4.759347	5.246048	3.148494
H	-0.810638	3.175947	-1.963150
H	-0.554060	4.385063	-0.669753
H	0.845101	3.711549	-1.555253
H	-0.244692	0.714418	-1.544339

H	1.448488	1.133985	-1.170311
H	0.479594	0.211160	0.011661
H	-4.961784	4.605184	-3.067080
H	-5.436554	4.000060	-1.451634
H	-6.674105	4.235593	-2.718819
H	-5.517560	7.014301	-3.747902
H	-7.256871	6.743560	-3.450327
H	-6.410206	8.079307	-2.620090
H	-11.905029	3.718554	-0.691012
H	-10.319123	3.788345	-1.508133
H	-10.406927	3.357591	0.221055
H	-12.433545	6.134685	-1.385393
H	-11.300716	7.454957	-0.961422
H	-10.864875	6.274289	-2.226174
H	-7.573348	8.820876	4.403523
H	-7.769519	9.252685	2.677611
H	-9.010854	8.266786	3.502182
H	-7.000979	6.402980	5.061018
H	-8.394160	5.750679	4.153163
H	-6.743953	5.170578	3.789113

7.3 BN- and BO-Doped Inorganic–Organic Hybrid Polymers with Sulfoximine Core Units

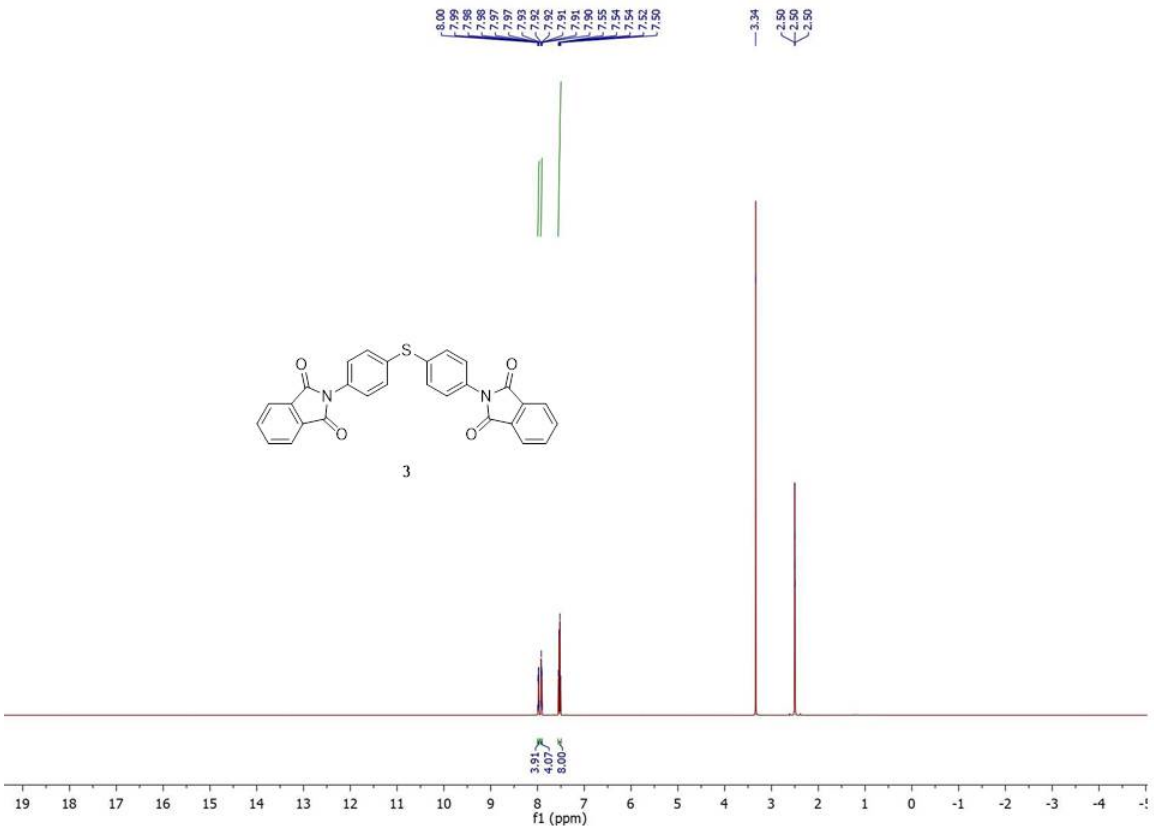

Figure 7.3.1. ^{1}H NMR spectrum of **3** (in DMSO-d_6).

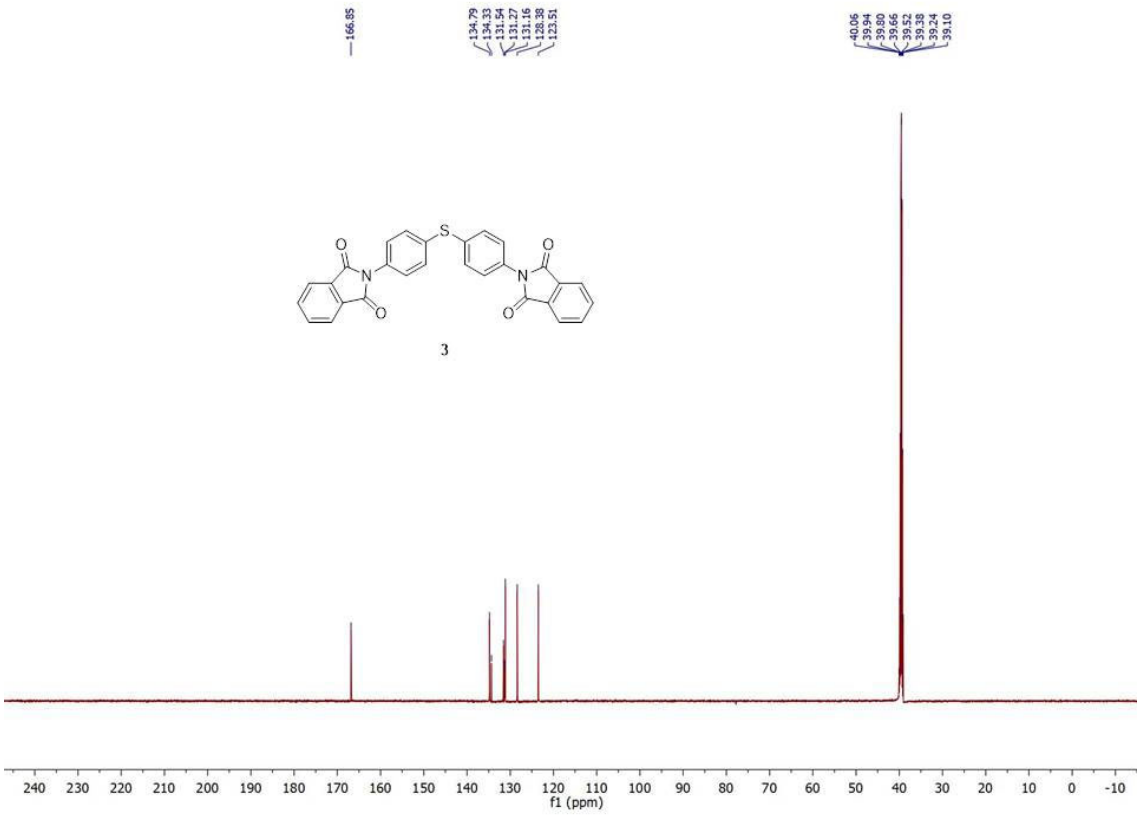

Figure 7.3.2. $^{13}C\{^{1}H\}$ NMR spectrum of **3** (in DMSO-d_6).

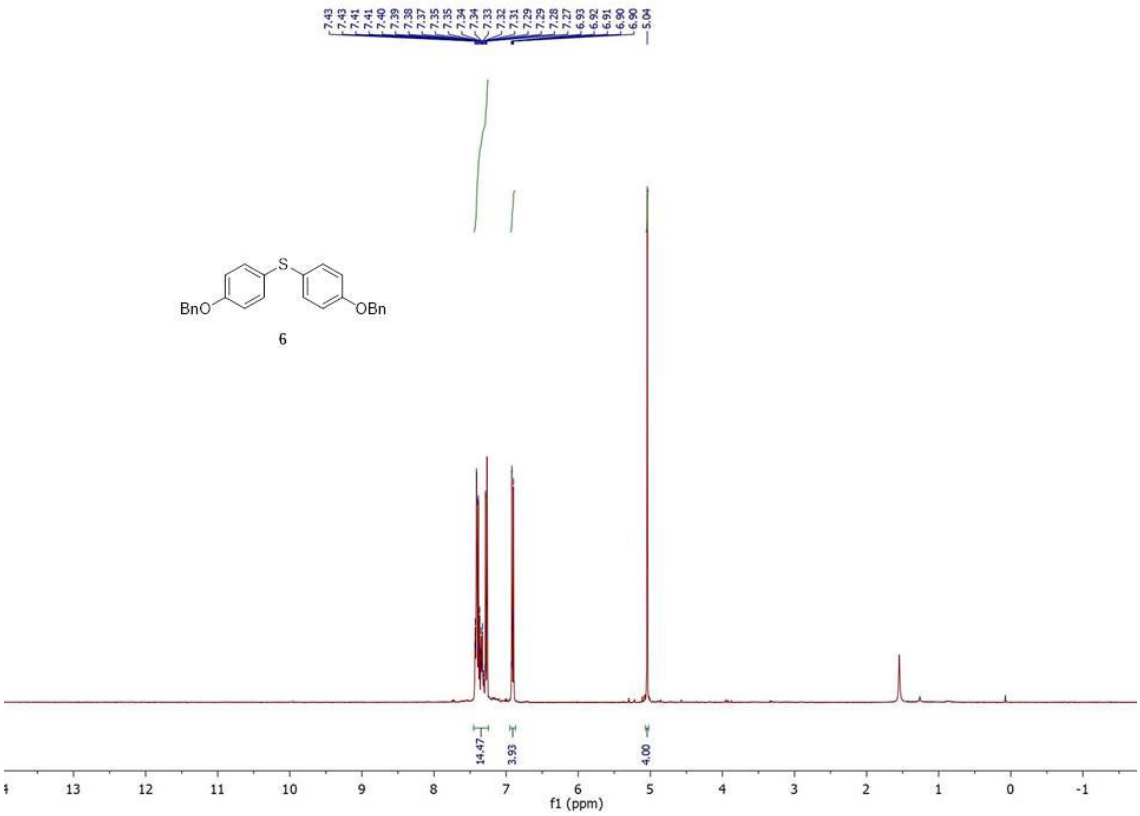

Figure 7.3.3. ^{1}H NMR spectrum of **6** (in $CDCl_3$).

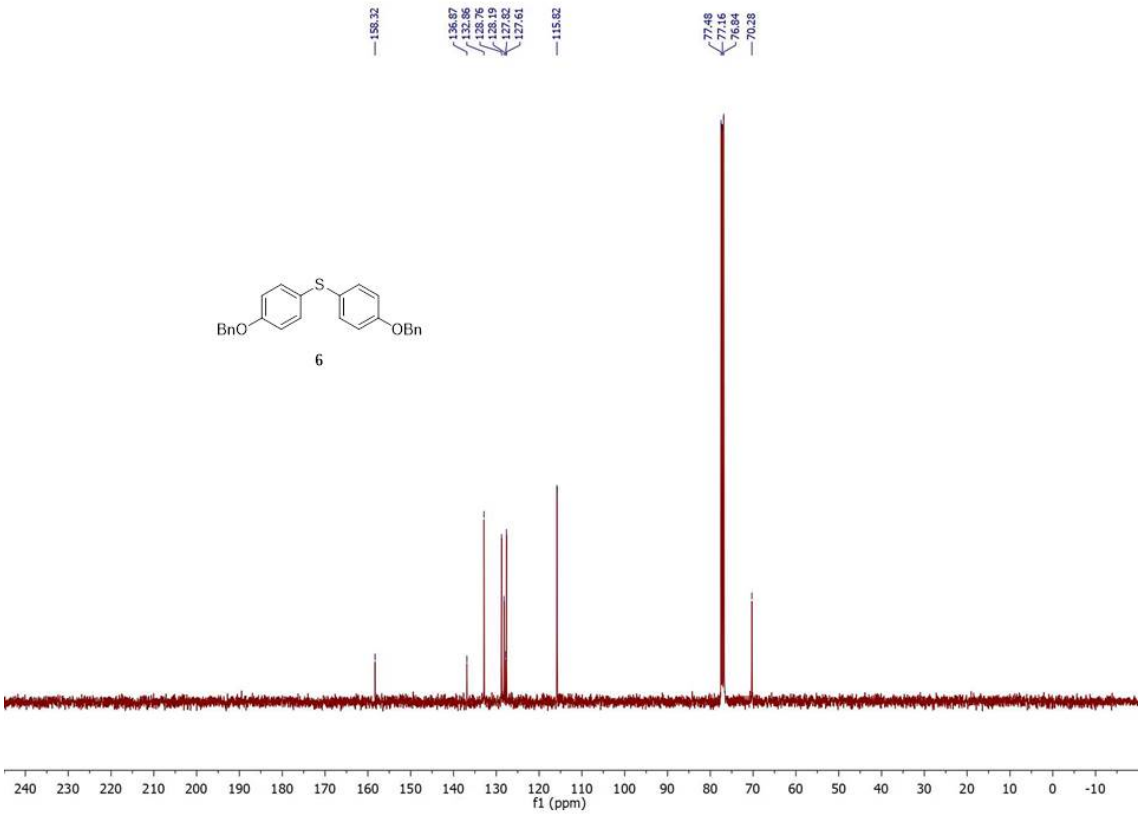

Figure 7.3.4. $^{13}C\{^{1}H\}$ NMR spectrum of **6** (in $CDCl_3$).

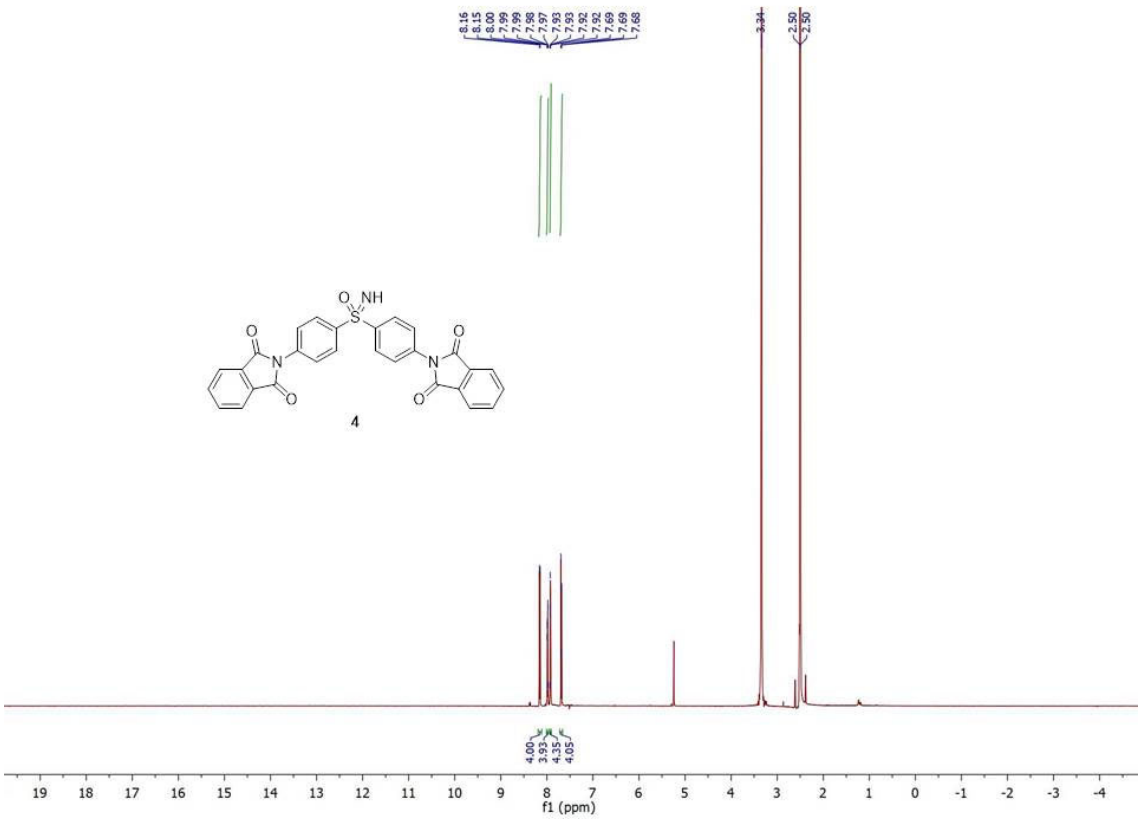

Figure 7.3.5. ^{1}H NMR spectrum of **4** (in DMSO-d_6).

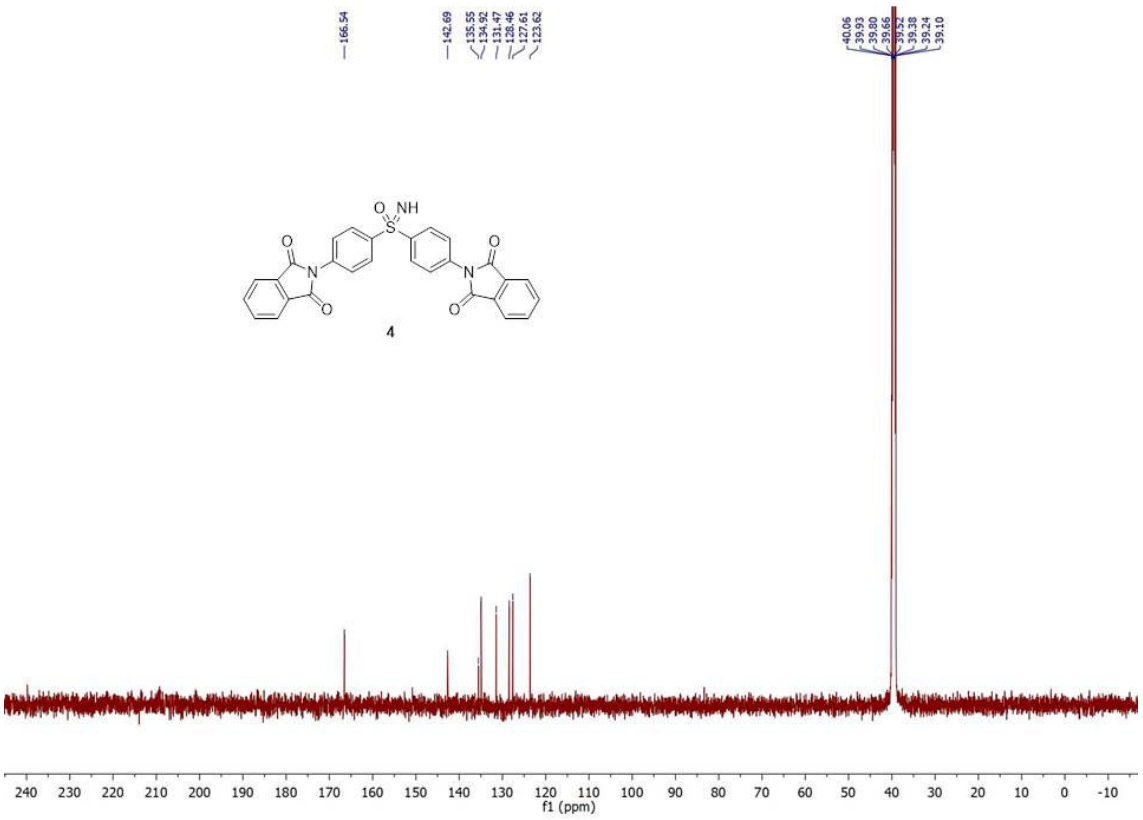

Figure 7.3.6. $^{13}C\{^{1}H\}$ NMR spectrum of **4** (in DMSO-d_6).

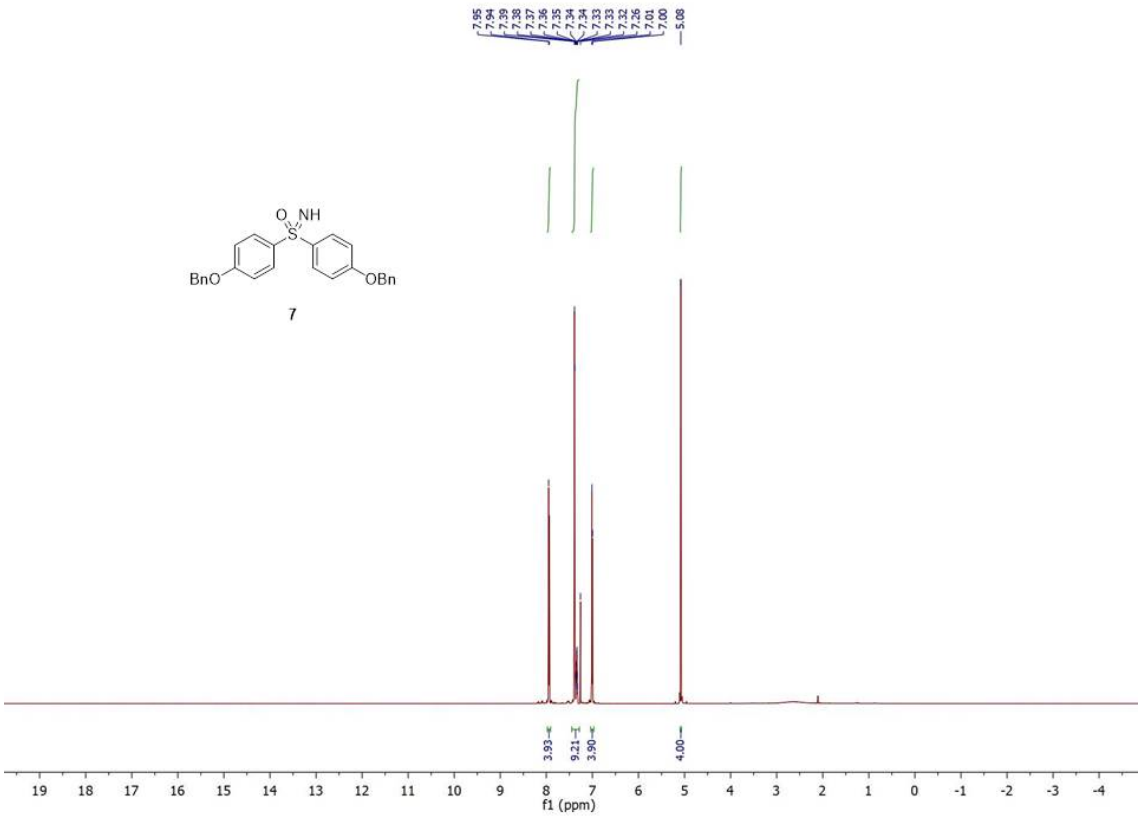

Figure 7.3.7. ^{1}H NMR spectrum of **7** (in $CDCl_3$).

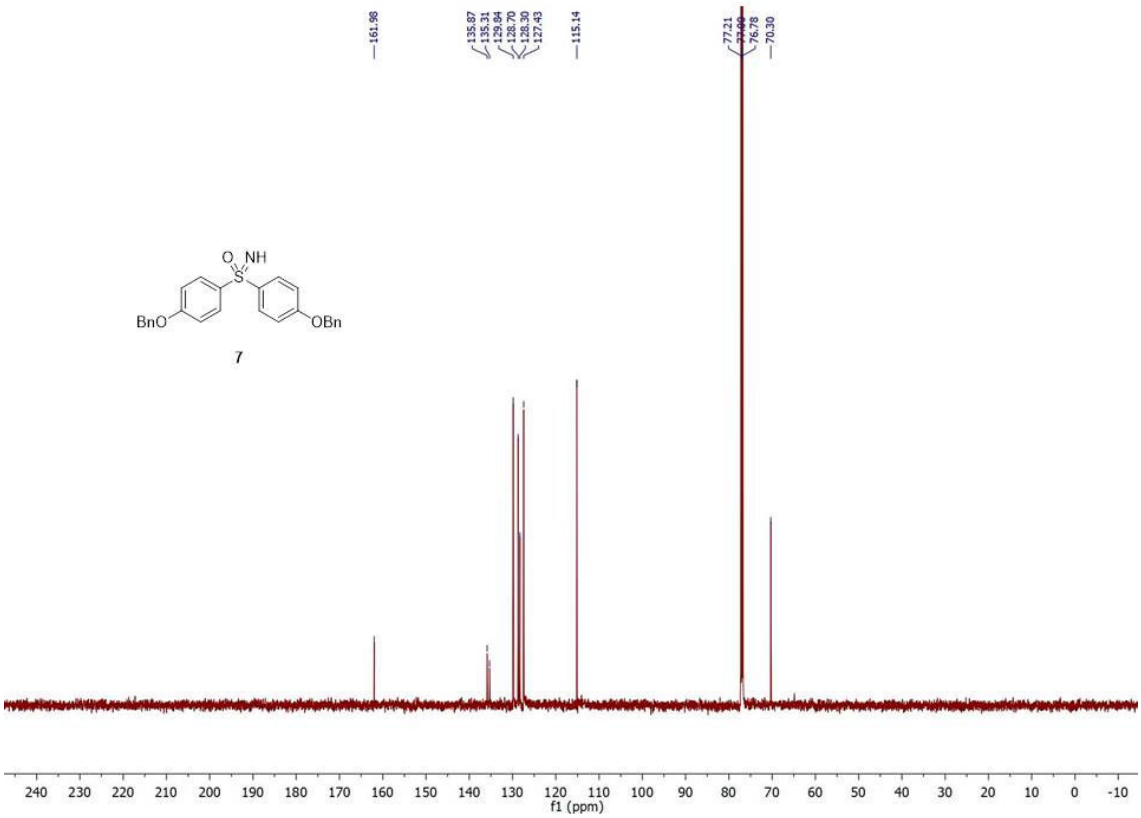

Figure 7.3.8. $^{13}C\{^{1}H\}$ NMR spectrum of **7** (in $CDCl_3$).

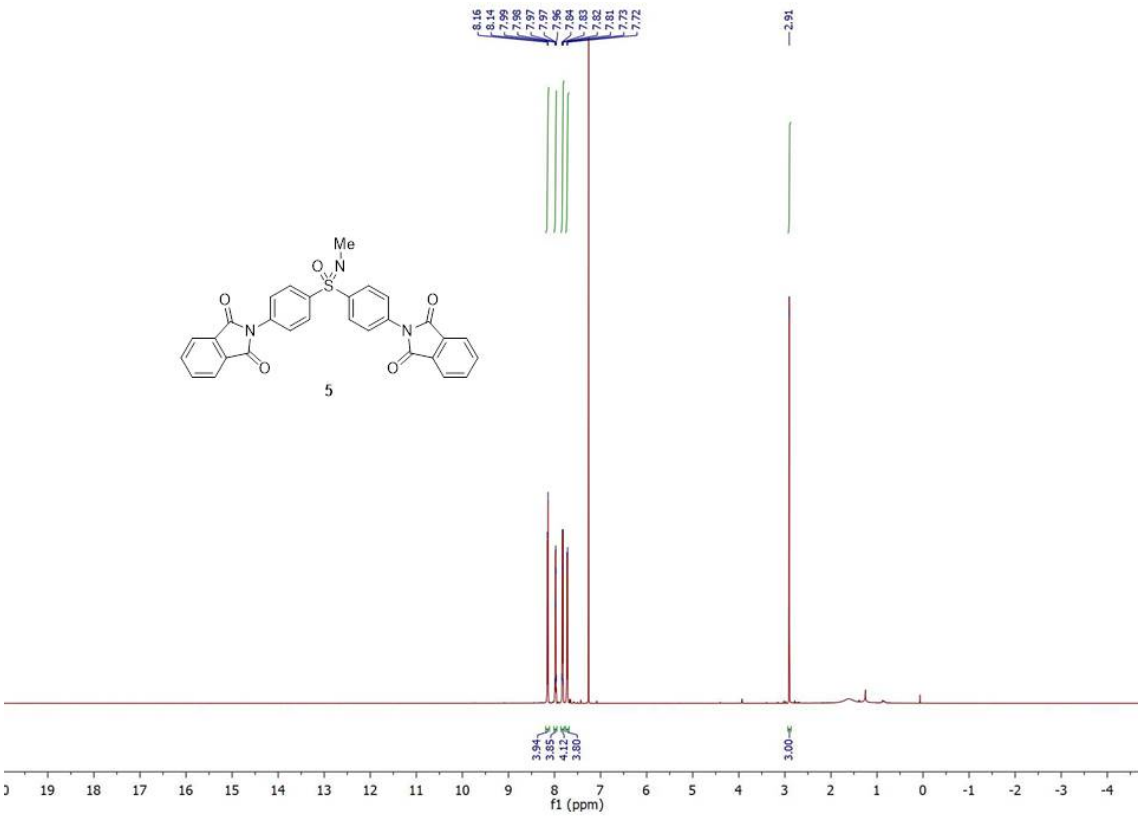

Figure 7.3.9. ^{1}H NMR spectrum of **5** (in $CDCl_3$).

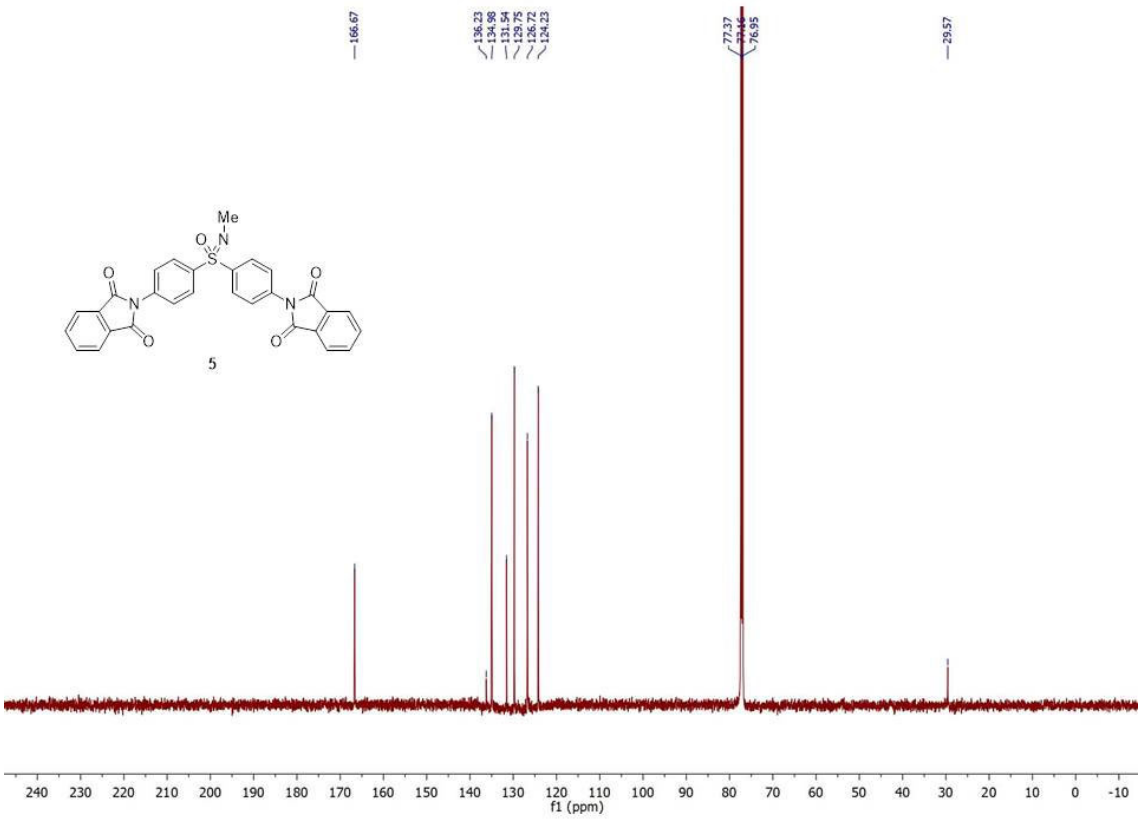

Figure 7.3.10. $^{13}C\{^{1}H\}$ NMR spectrum of **5** (in $CDCl_3$).

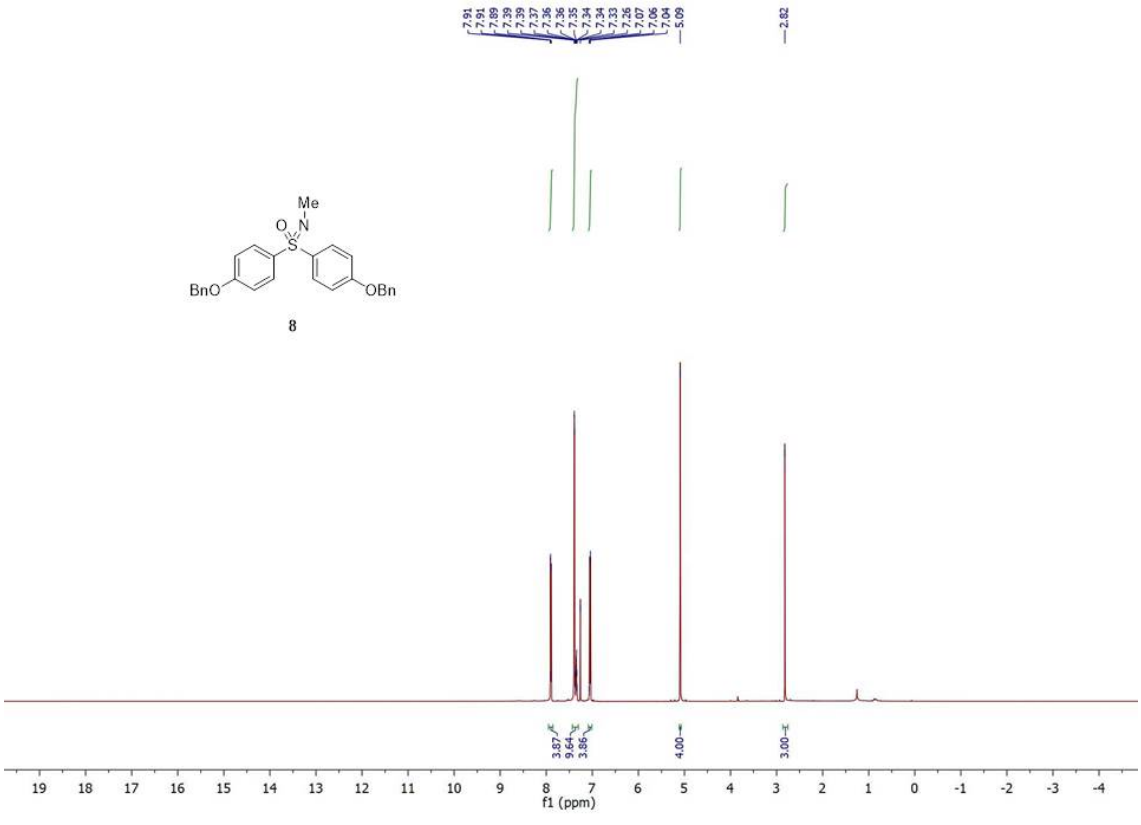

Figure 7.3.11. ^{1}H NMR spectrum of **8** (in $CDCl_3$).

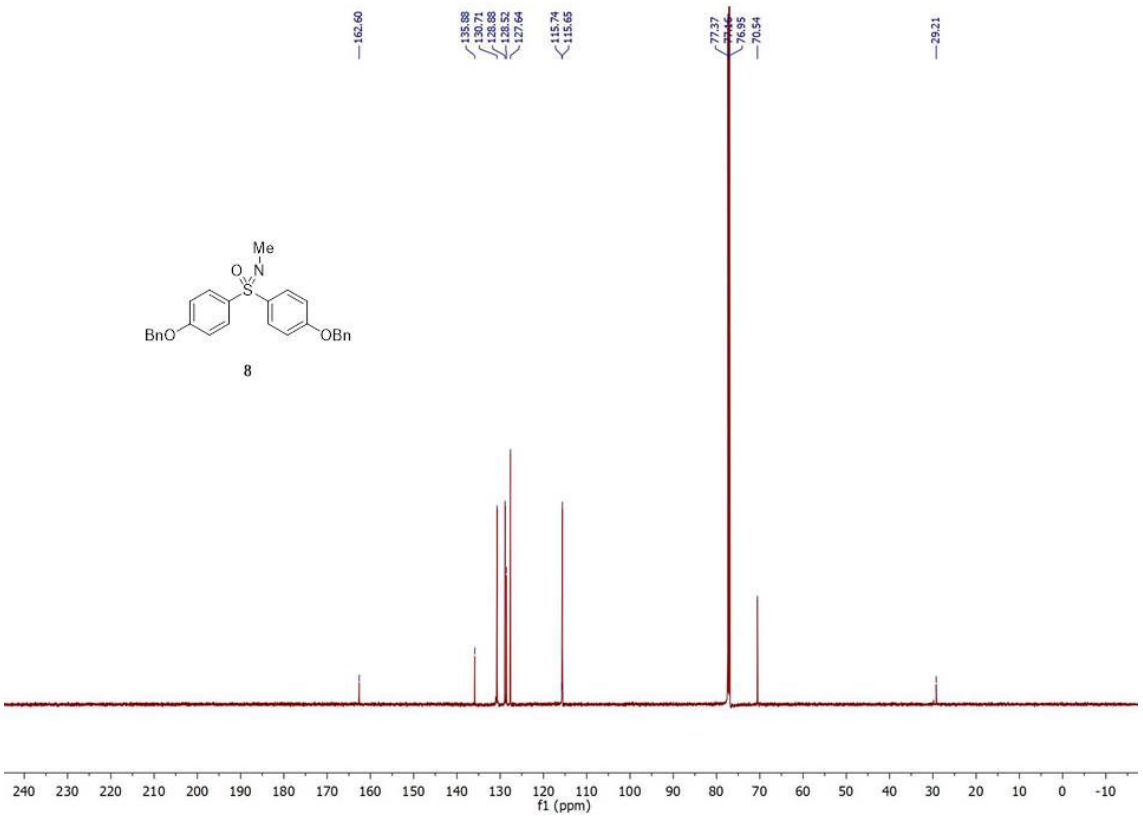

Figure 7.3.12. $^{13}C\{^{1}H\}$ NMR spectrum of **8** (in $CDCl_3$).

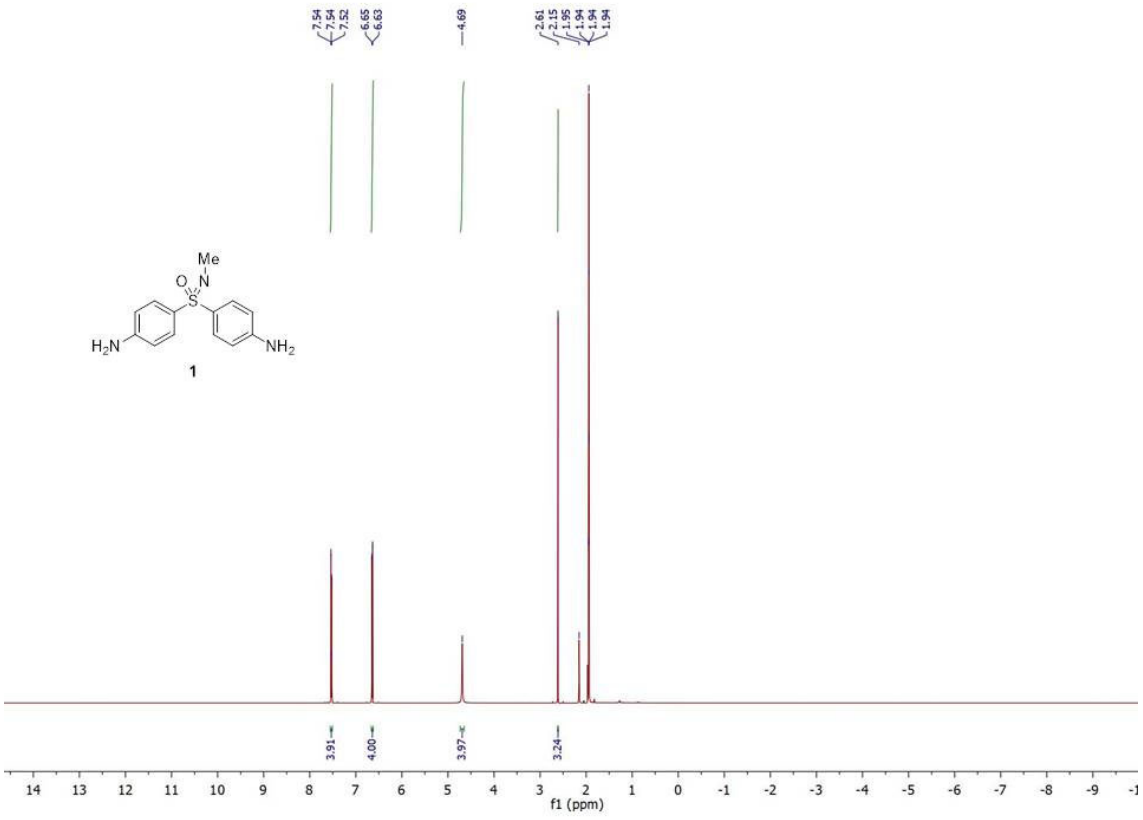

Figure 7.3.13. ^{1}H NMR spectrum of **1** (in MeCN-d_3).

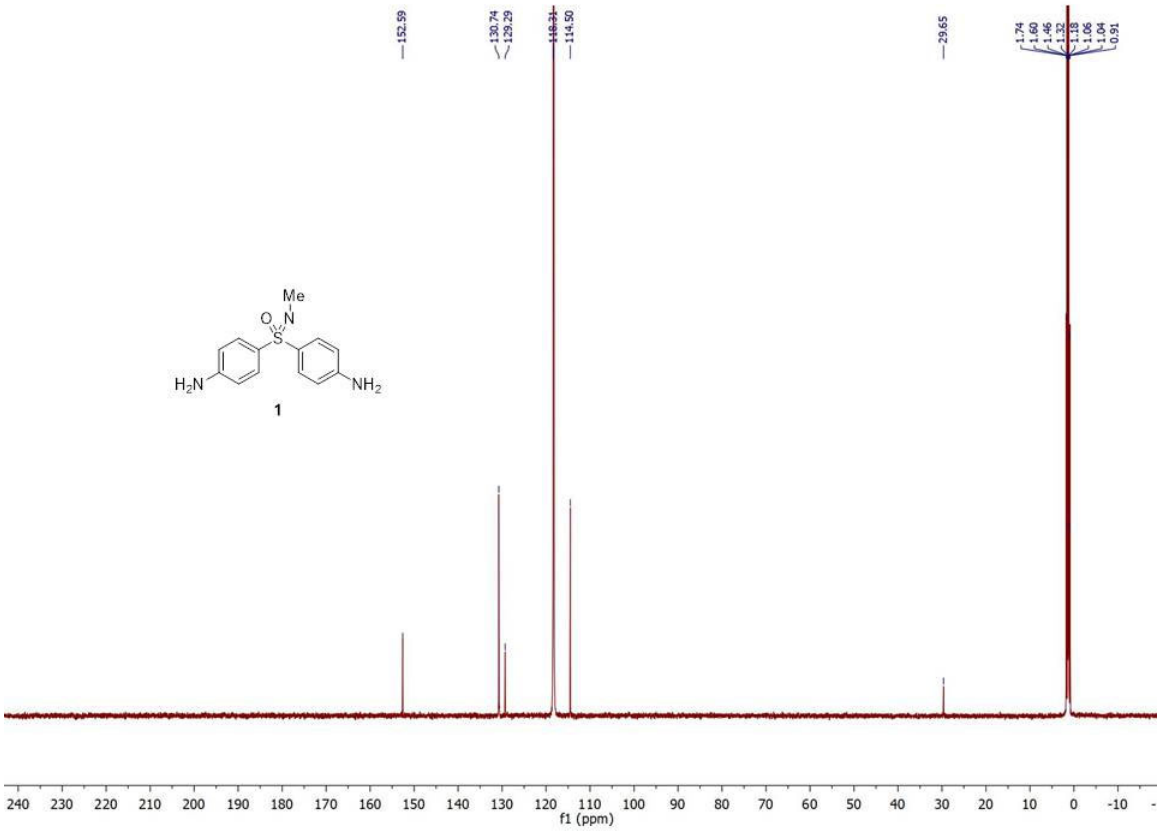

Figure 7.3.14. $^{13}C\{^{1}H\}$ NMR spectrum of **1** (in MeCN-*d*$_3$).

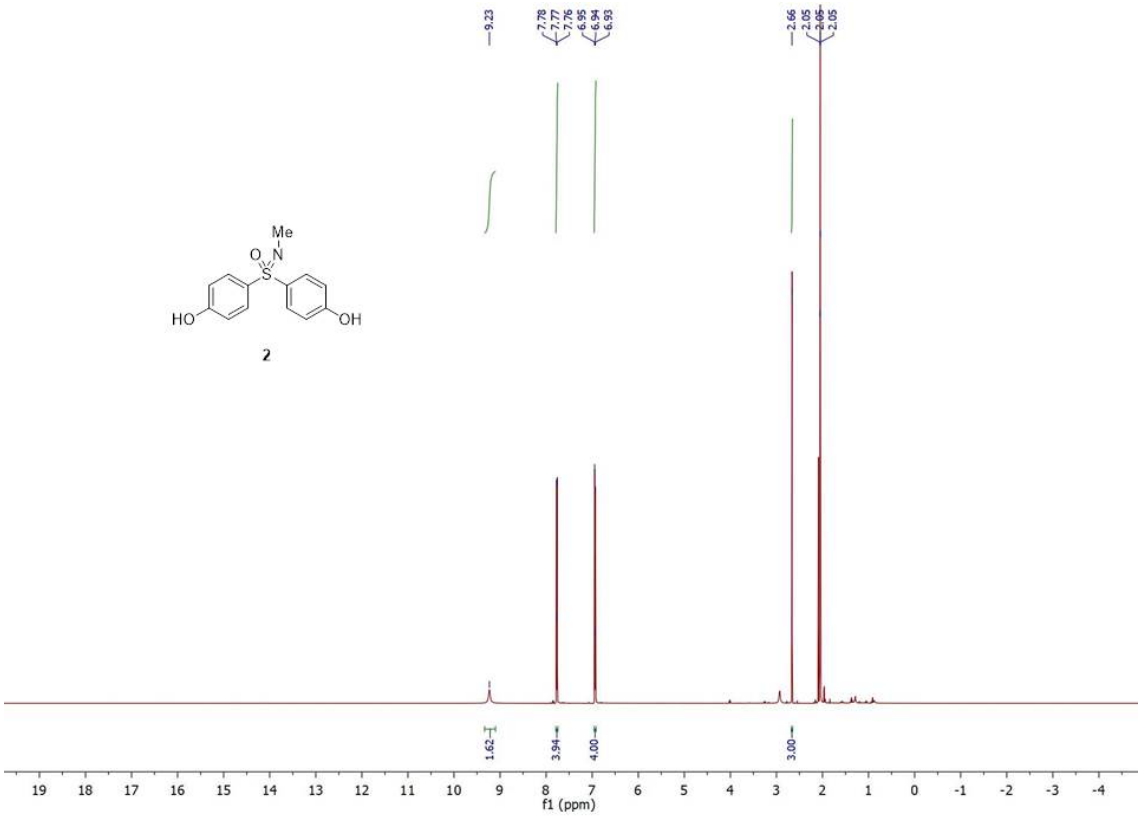

Figure 7.3.15. ^{1}H NMR spectrum of **2** (in Acetone-d_6).

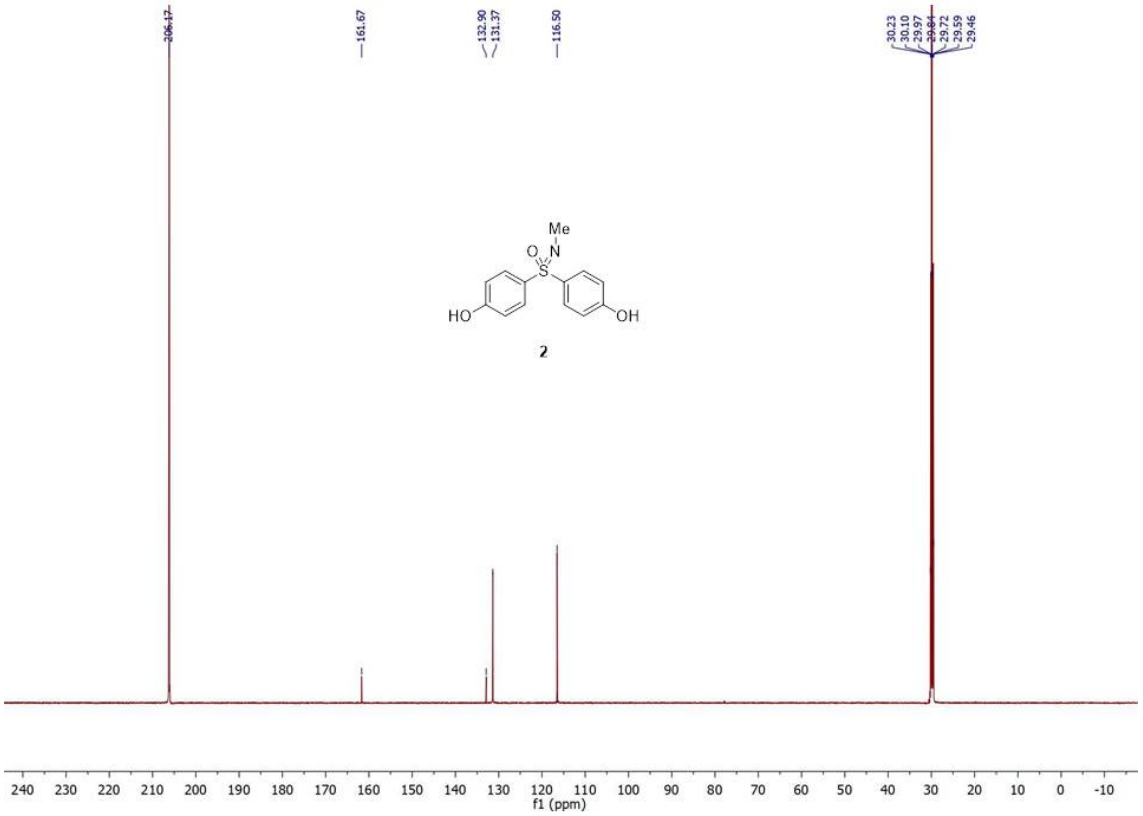

Figure 7.3.16. $^{13}C\{^{1}H\}$ NMR spectrum of **2** (in Acetone-d_6).

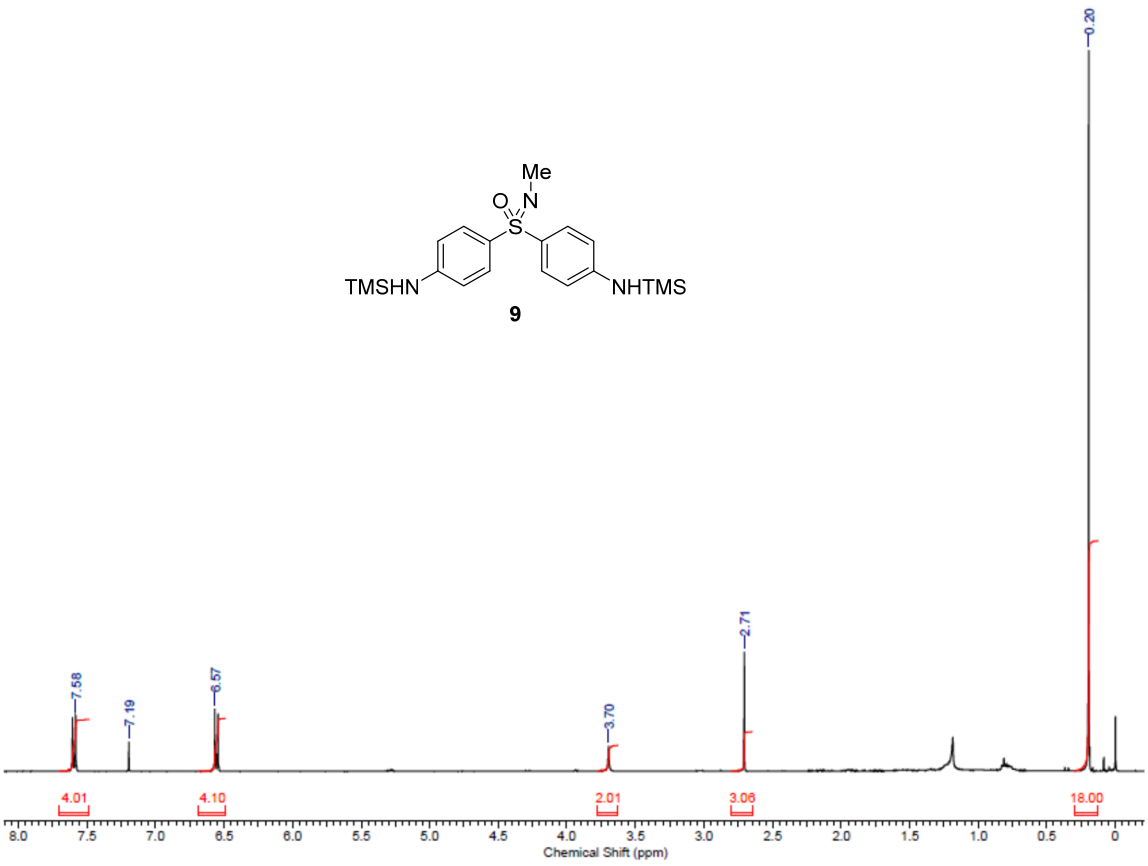

Figure 7.3.17. ^{1}H NMR spectrum of **9** (in $CDCl_3$).

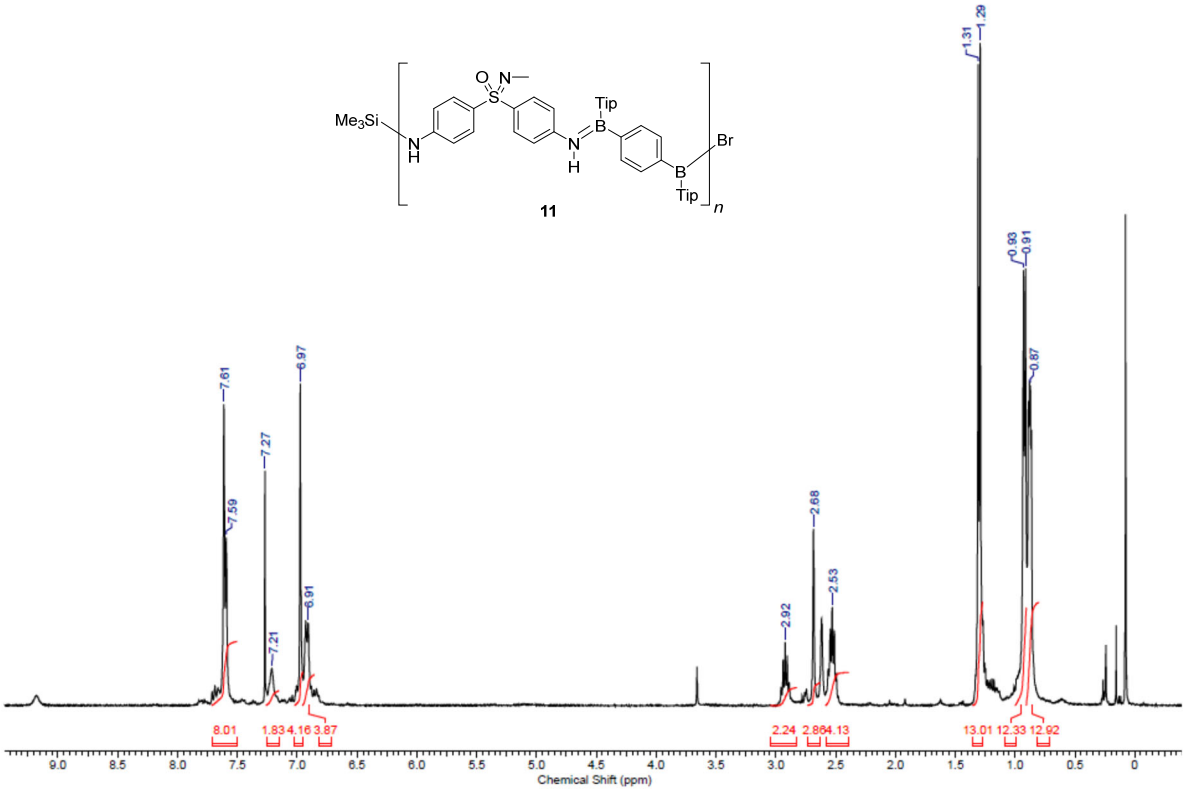

Figure 7.3.18. ^{1}H NMR spectrum of **11** (in $CDCl_3$).

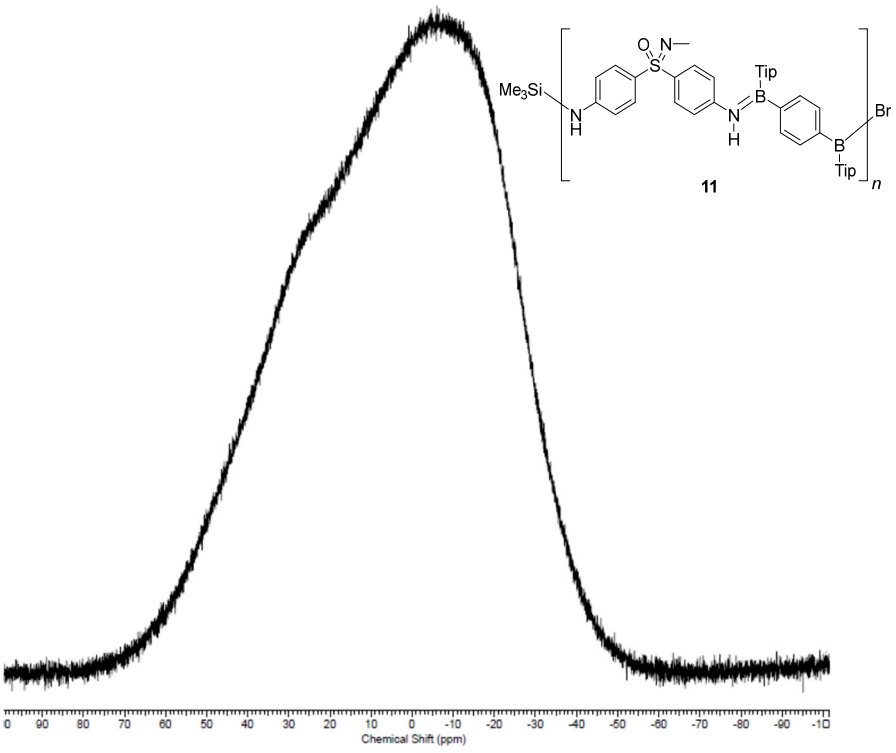

Figure 7.3.19. $^{11}B\{^{1}H\}$ NMR spectrum of **11** (in $CDCl_3$).

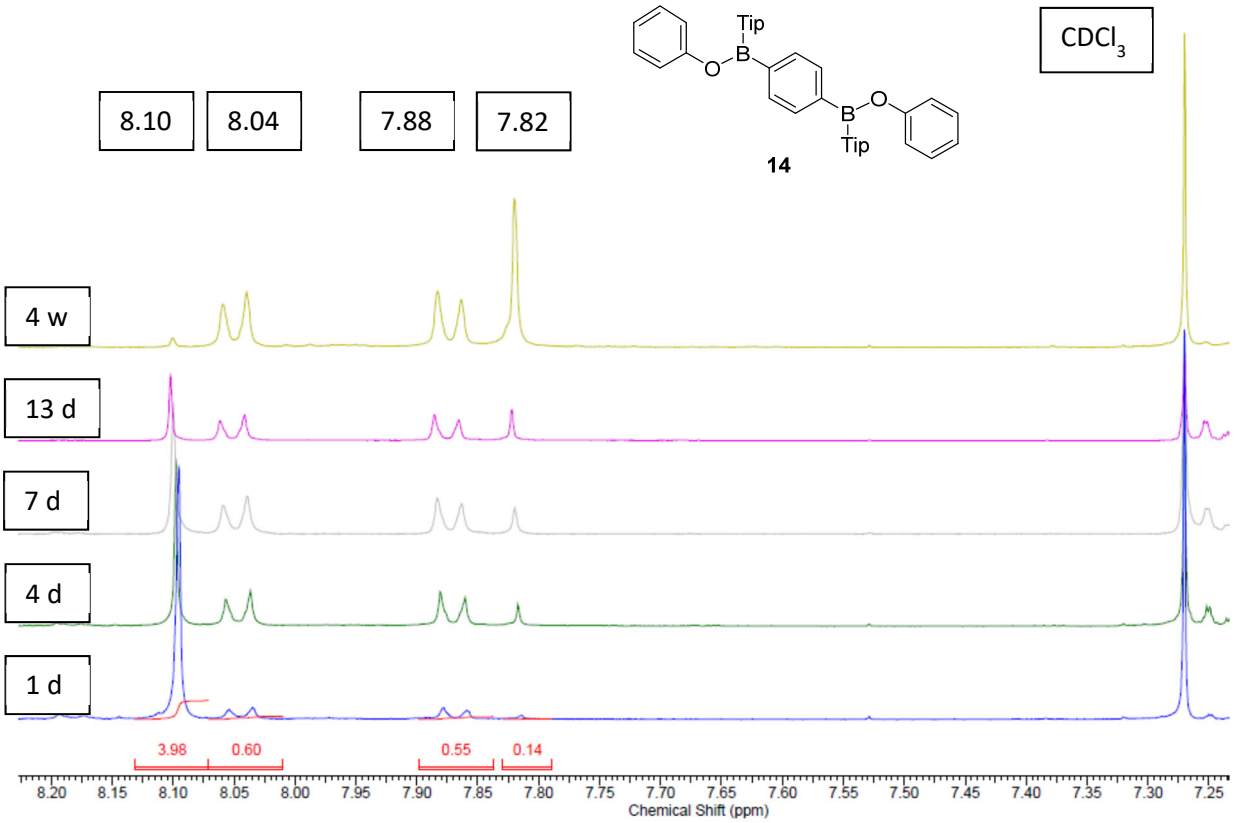

Figure 7.3.20. ^{1}H-NMR spectra: Attempted synthesis of **14** in DCM at room temperature.

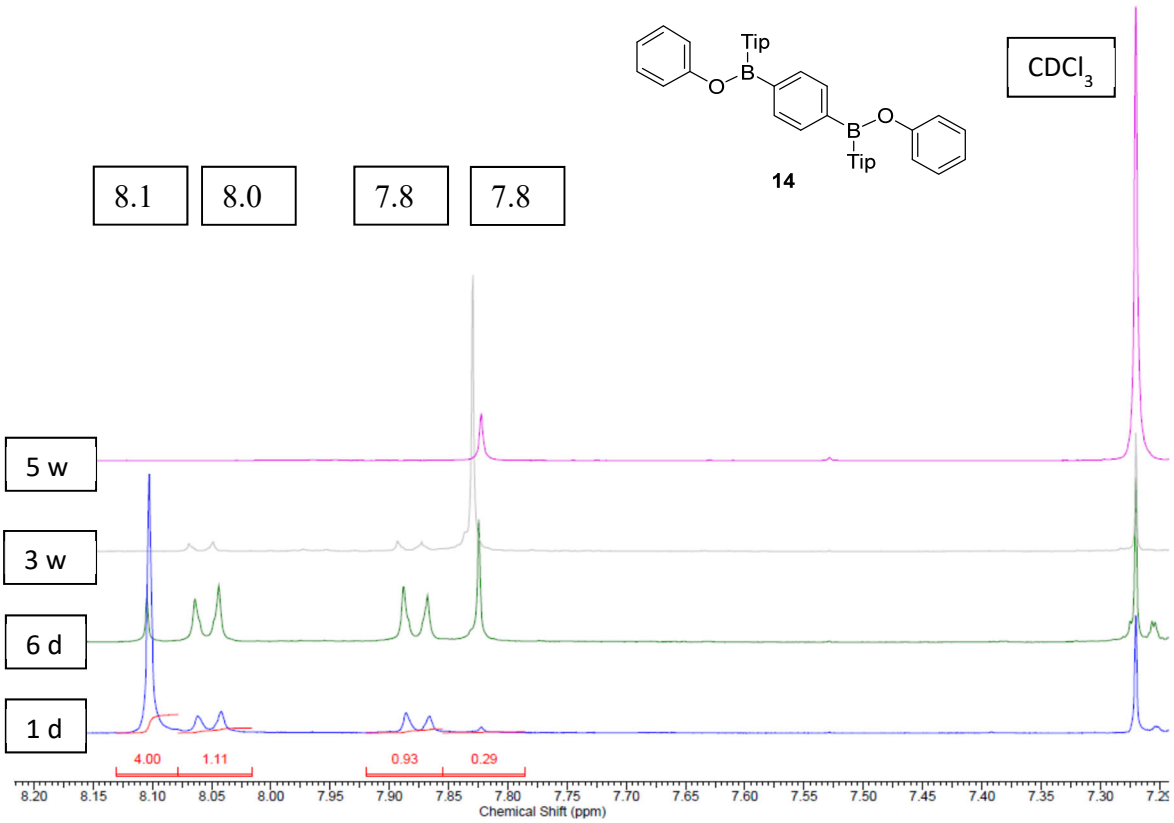

Figure 7.3.21. ^{1}H-NMR spectra: Attempted synthesis of **14** in *o*-DFB at 80 °C.

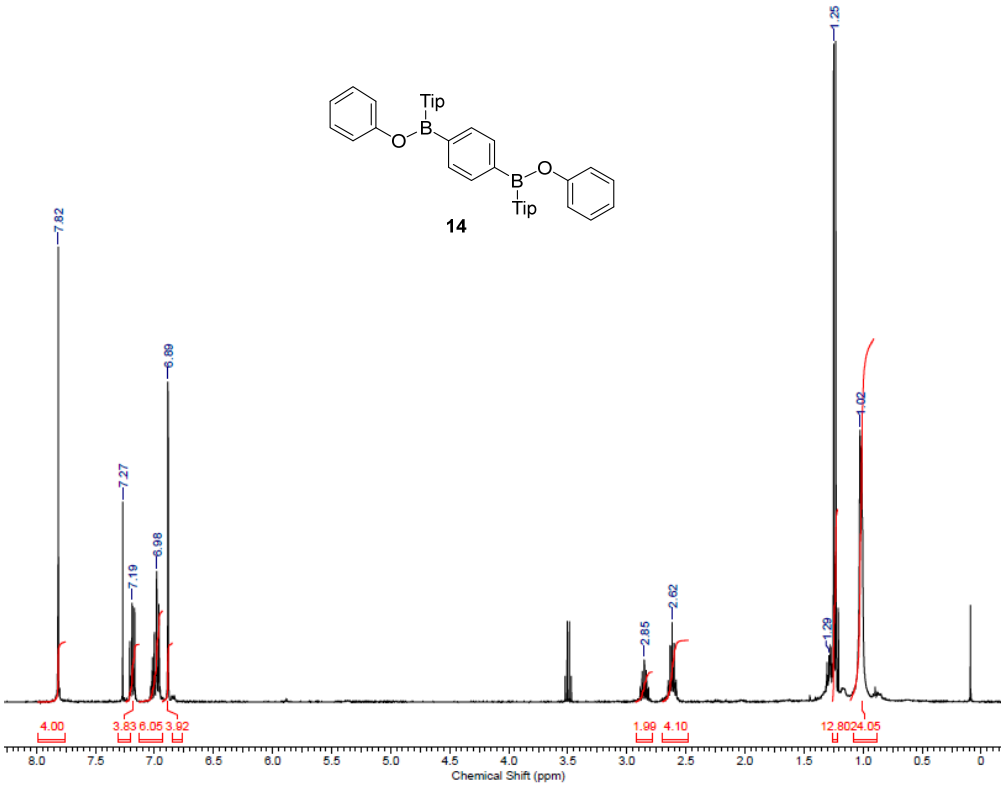

Figure 7.3.22. ^{1}H NMR spectrum of **14** (in $CDCl_3$).

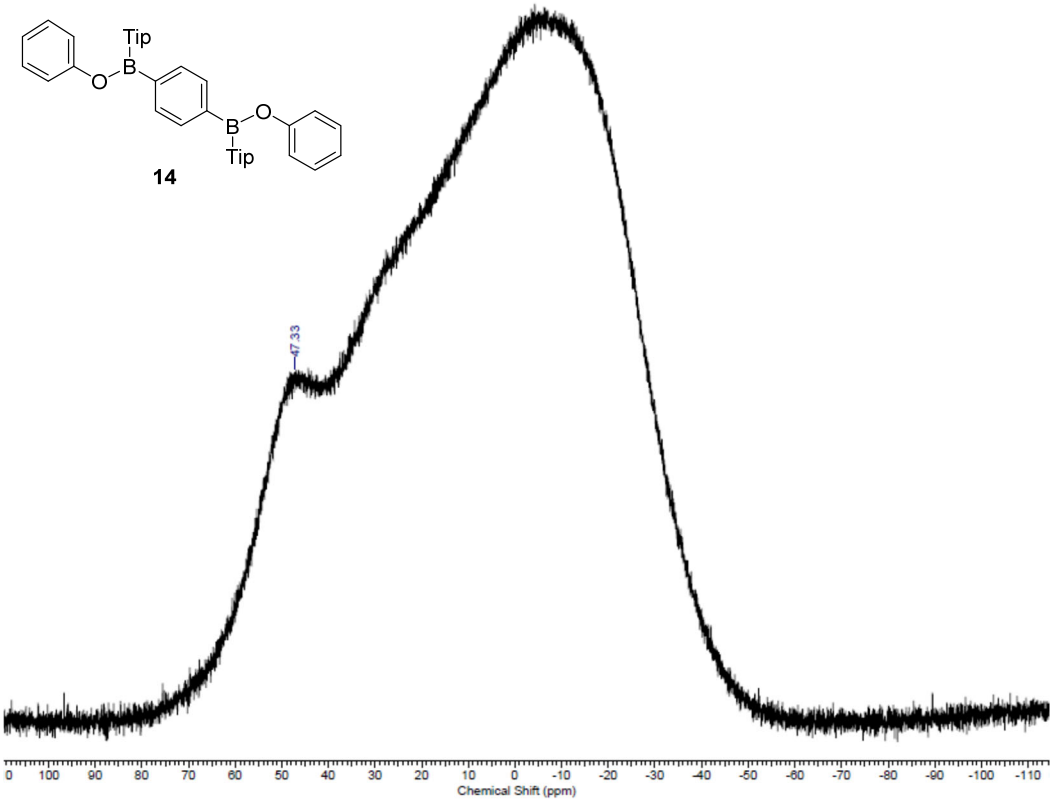

Figure 7.3.23. ^{1}H NMR spectrum of **14** (in $CDCl_3$).

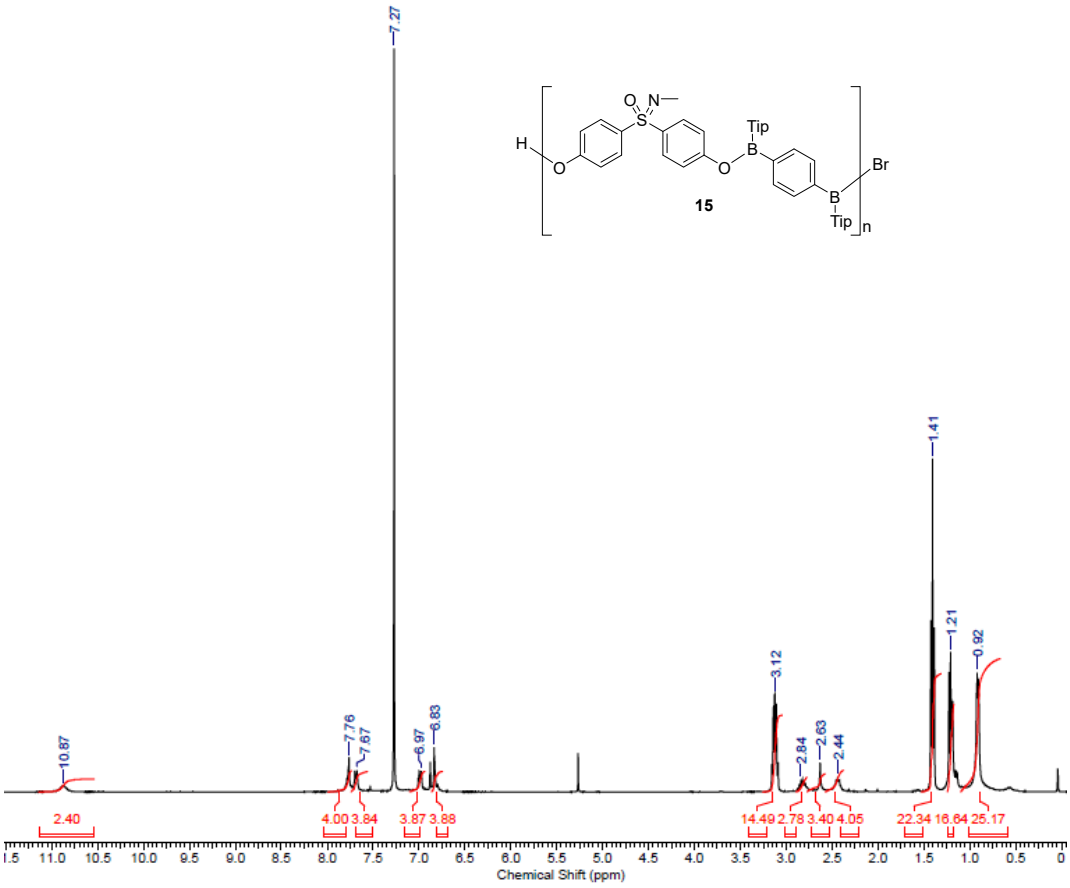

Figure 7.3.24. ^{1}H NMR spectrum of **15** (in $CDCl_3$).

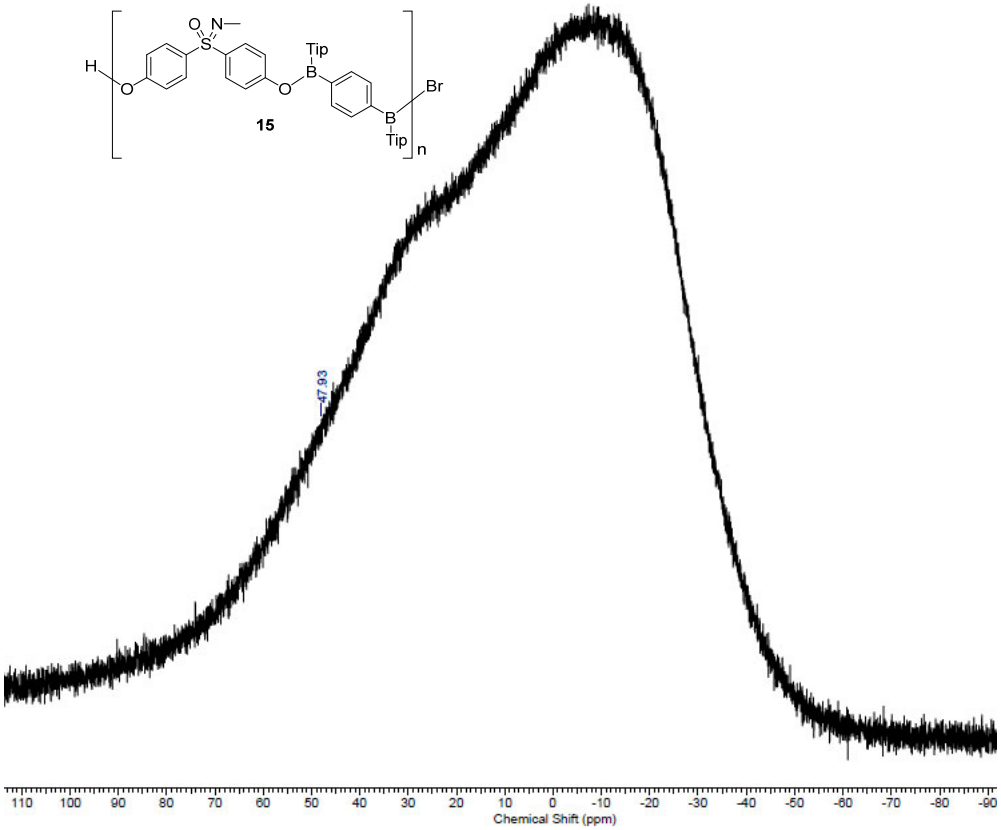

Figure 7.3.25. $^{11}B\{^{1}H\}$ NMR spectrum of **15** (in $CDCl_3$).

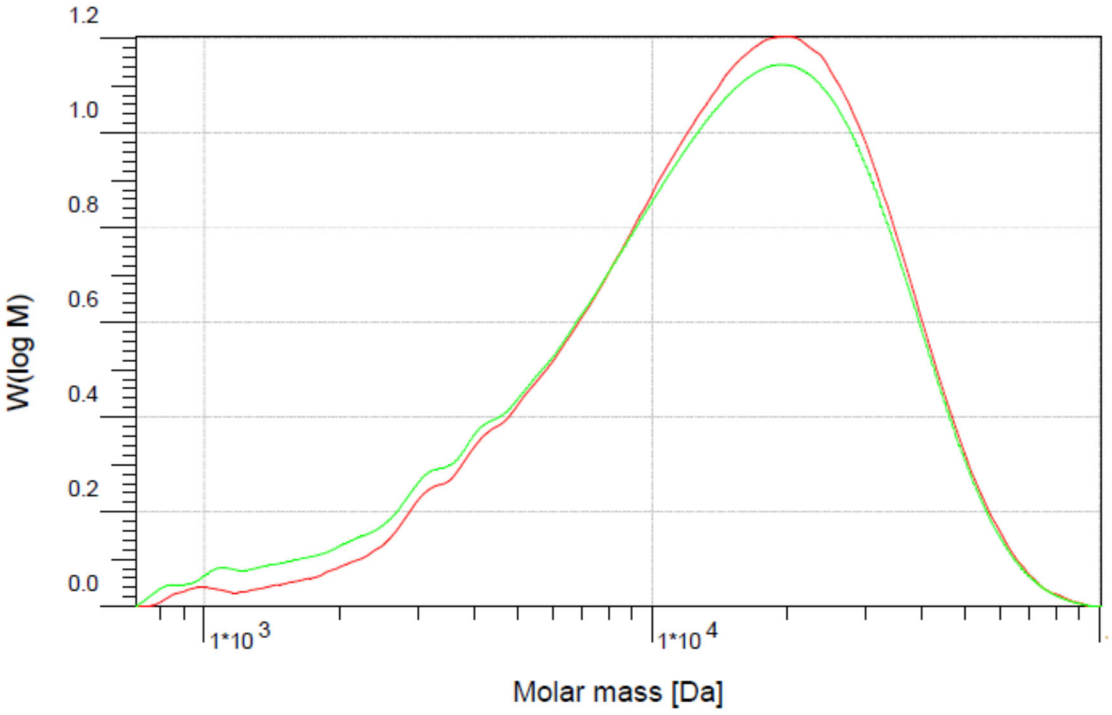

Figure 7.3.26. Gel permeation chromatography (GPC) trace of **11** (trial 1) (in THF); red line: detection by RI signal; green line: detection by UV signal.

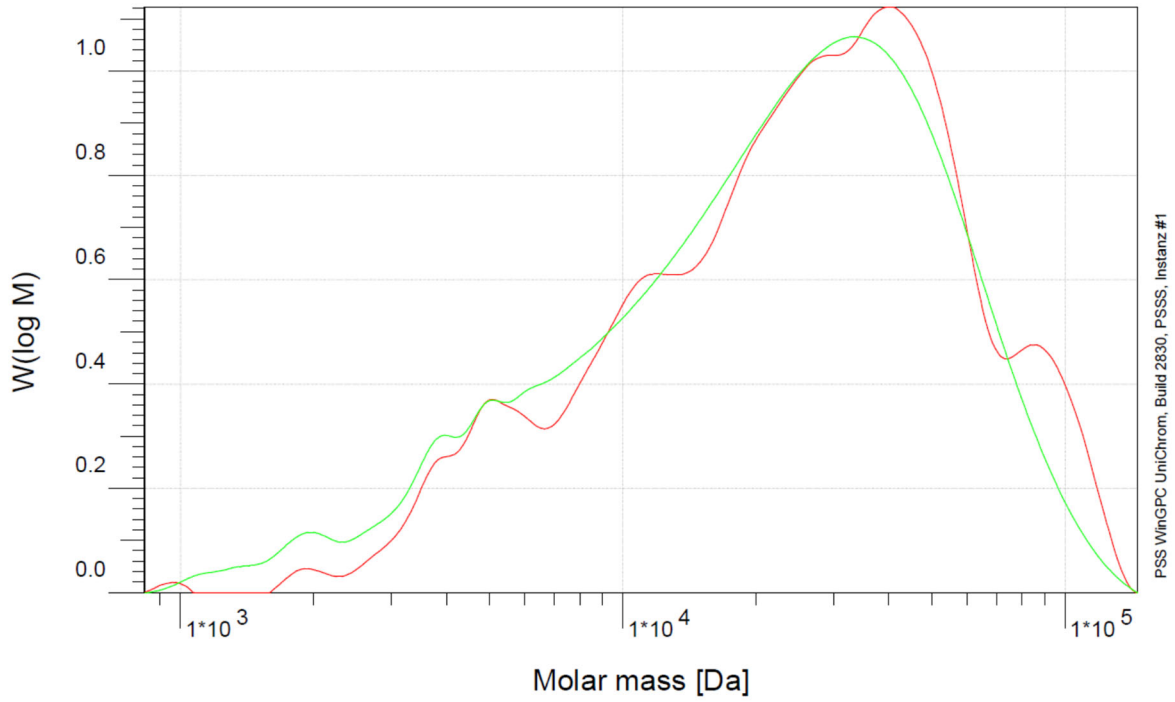

Figure 7.3.27. Gel permeation chromatography (GPC) trace of **11** (trial 2) (in THF); red line: detection by RI signal; green line: detection by UV signal.

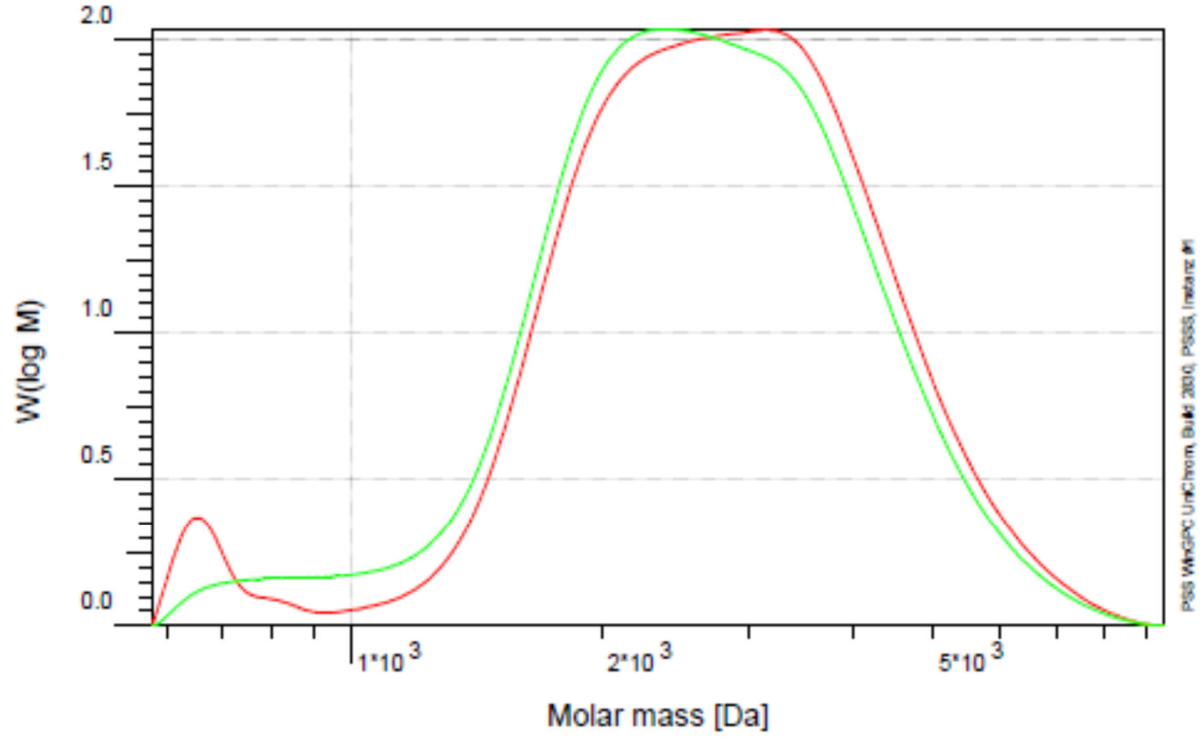

Figure 7.3.28. Gel permeation chromatography (GPC) trace of **15** (trial 1) (in THF); red line: detection by RI signal; green line: detection by UV signal.

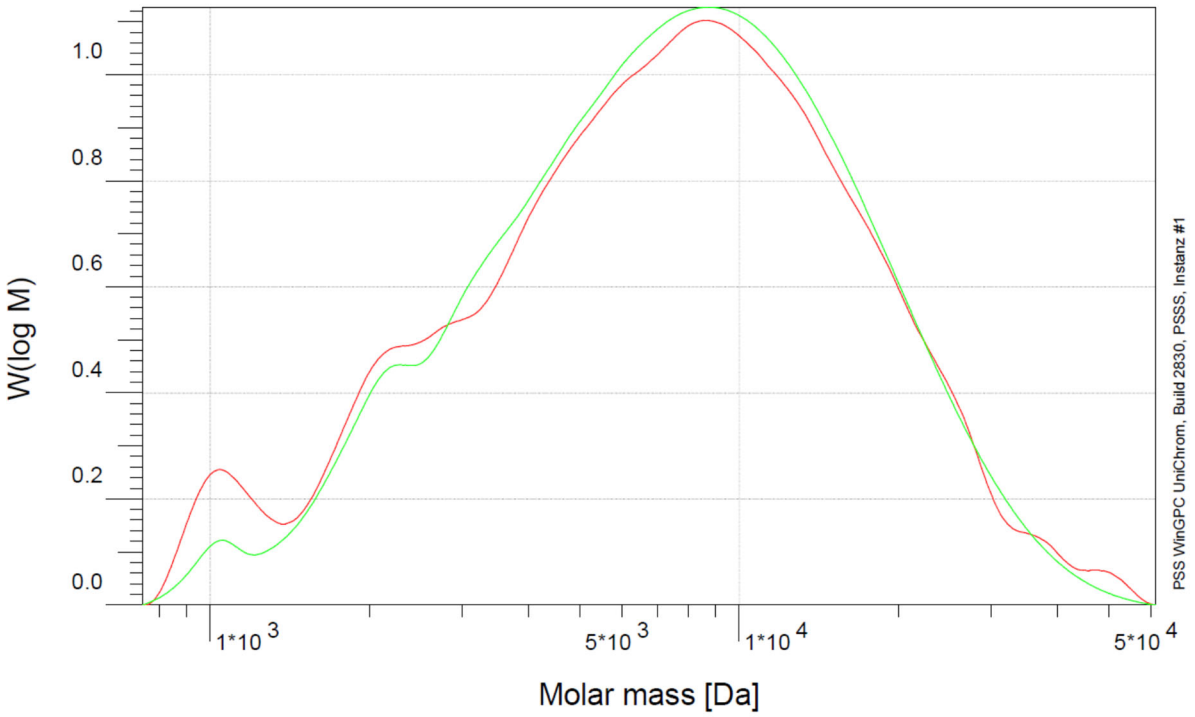

Figure 7.3.29. Gel permeation chromatography (GPC) trace of **15** (trial 2) (in THF); red line: detection by RI signal; green line: detection by UV signal.

7.4 Conjugated Oligomers with BP-Linkages

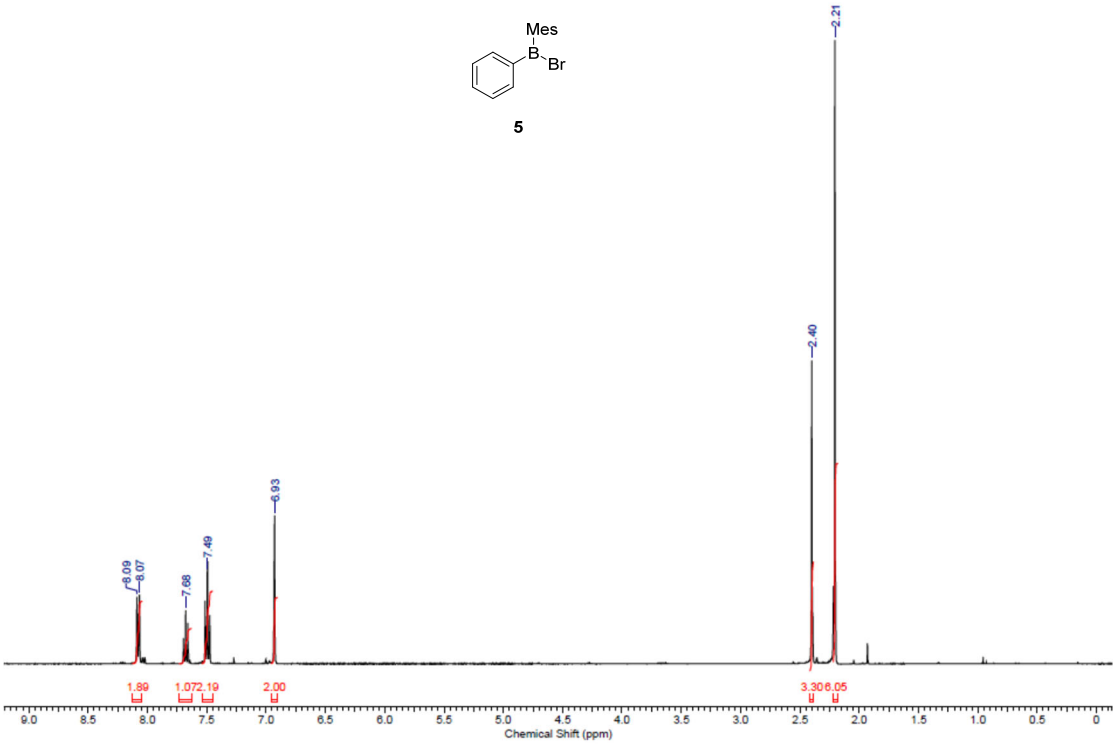

Figure 7.4.1. ^{1}H NMR spectrum of **5** (in $CDCl_3$).

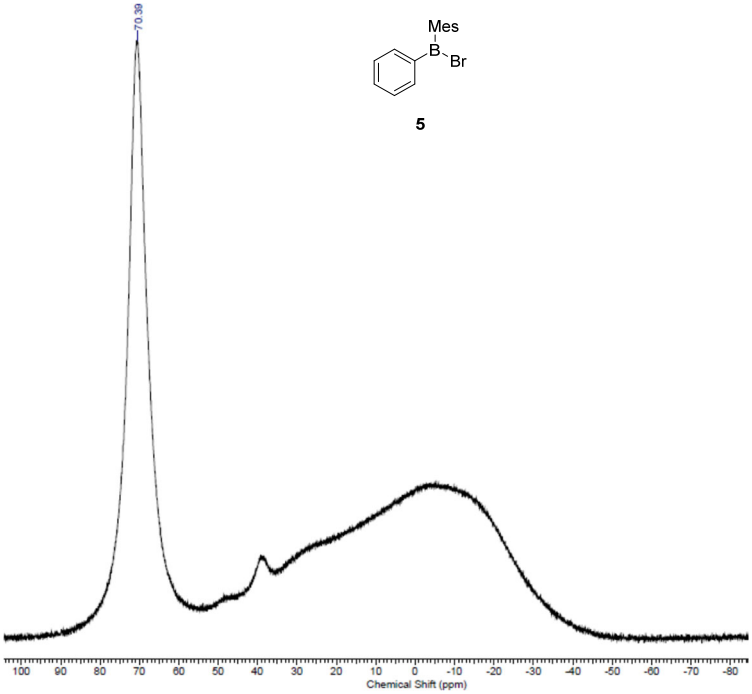

Figure 7.4.2. $^{11}B\{^{1}H\}$ NMR spectrum of **5** (in $CDCl_3$).

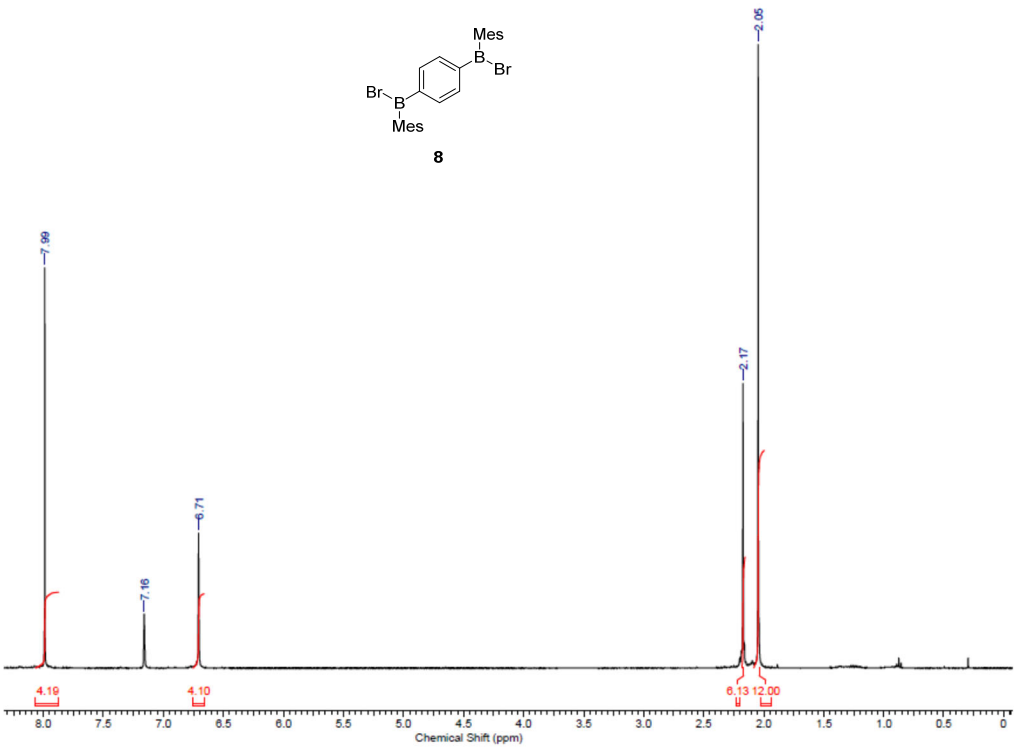

Figure 7.4.3. ^{1}H NMR spectrum of **8** (in C_6D_6).

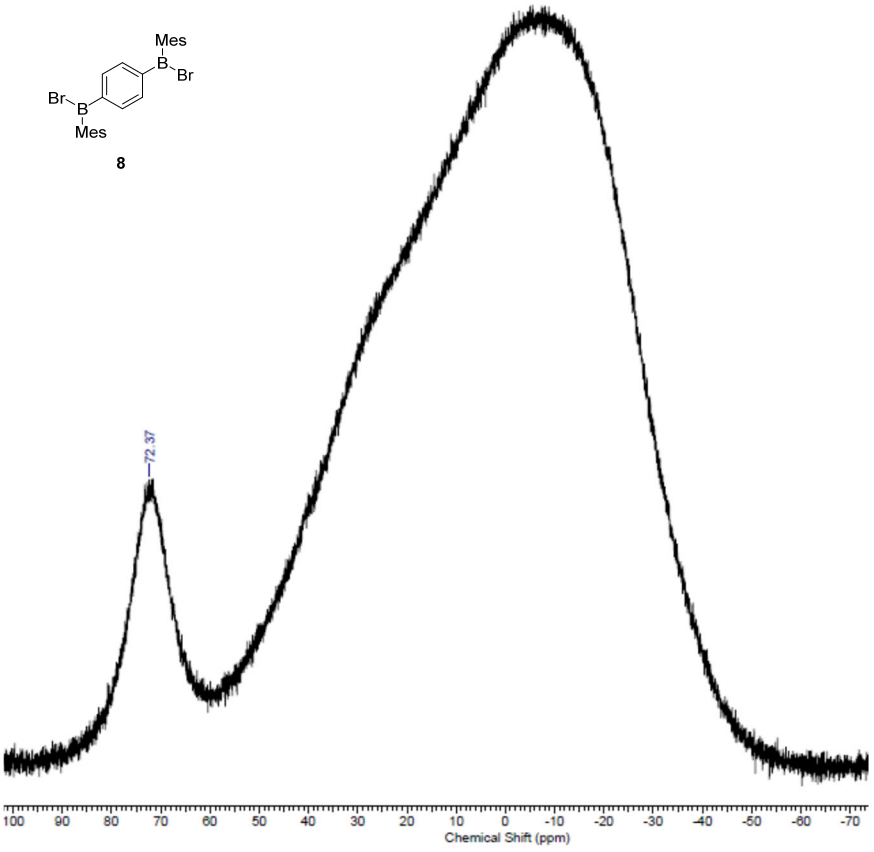

Figure 7.4.4. ^{11}B{^{1}H} NMR spectrum of **8** (in C_6D_6).

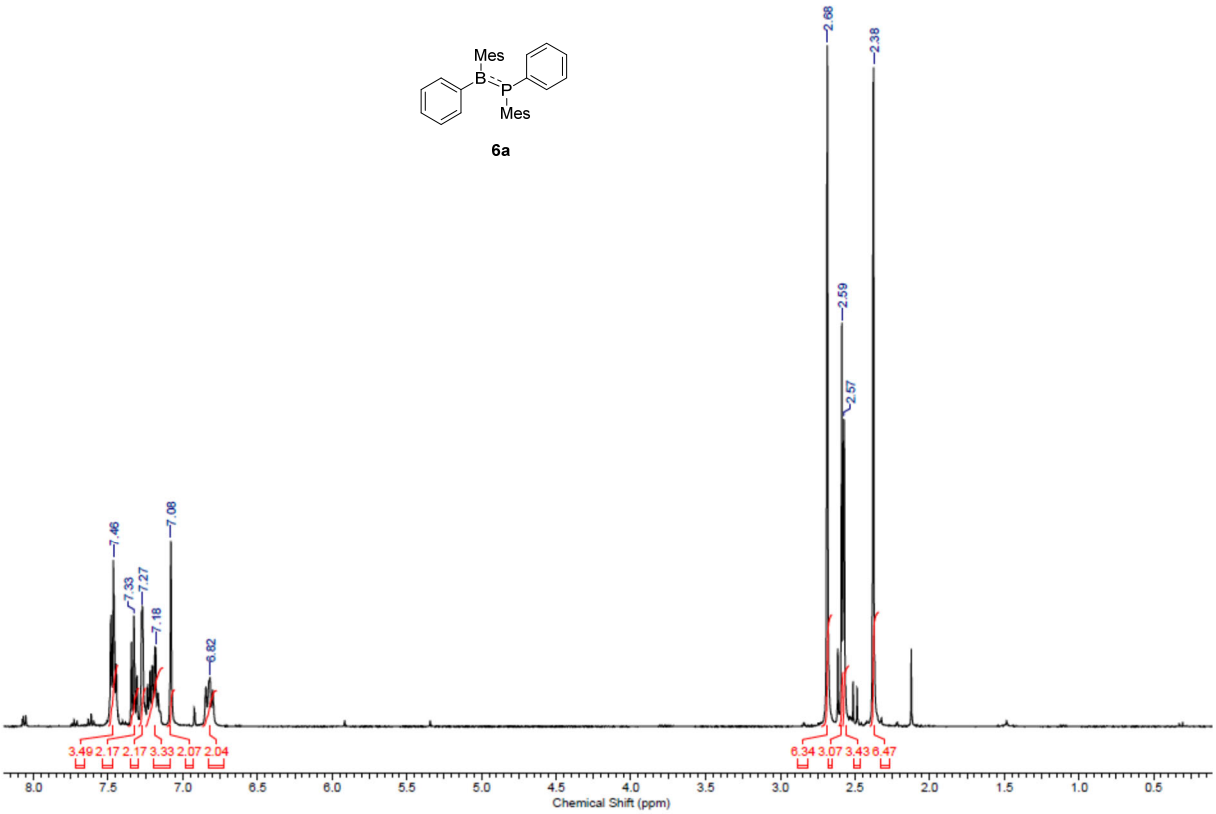

Figure 7.4.5. ^{1}H NMR spectrum of **6a** (in $CDCl_3$).

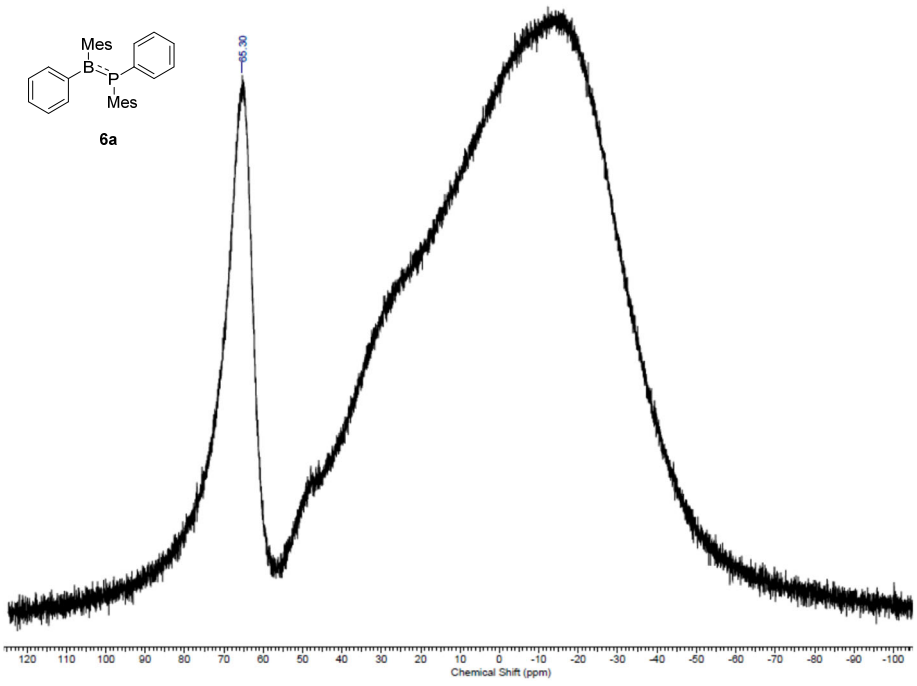

Figure 7.4.6. $^{11}B\{^{1}H\}$ NMR spectrum of **6a** (in $CDCl_3$).

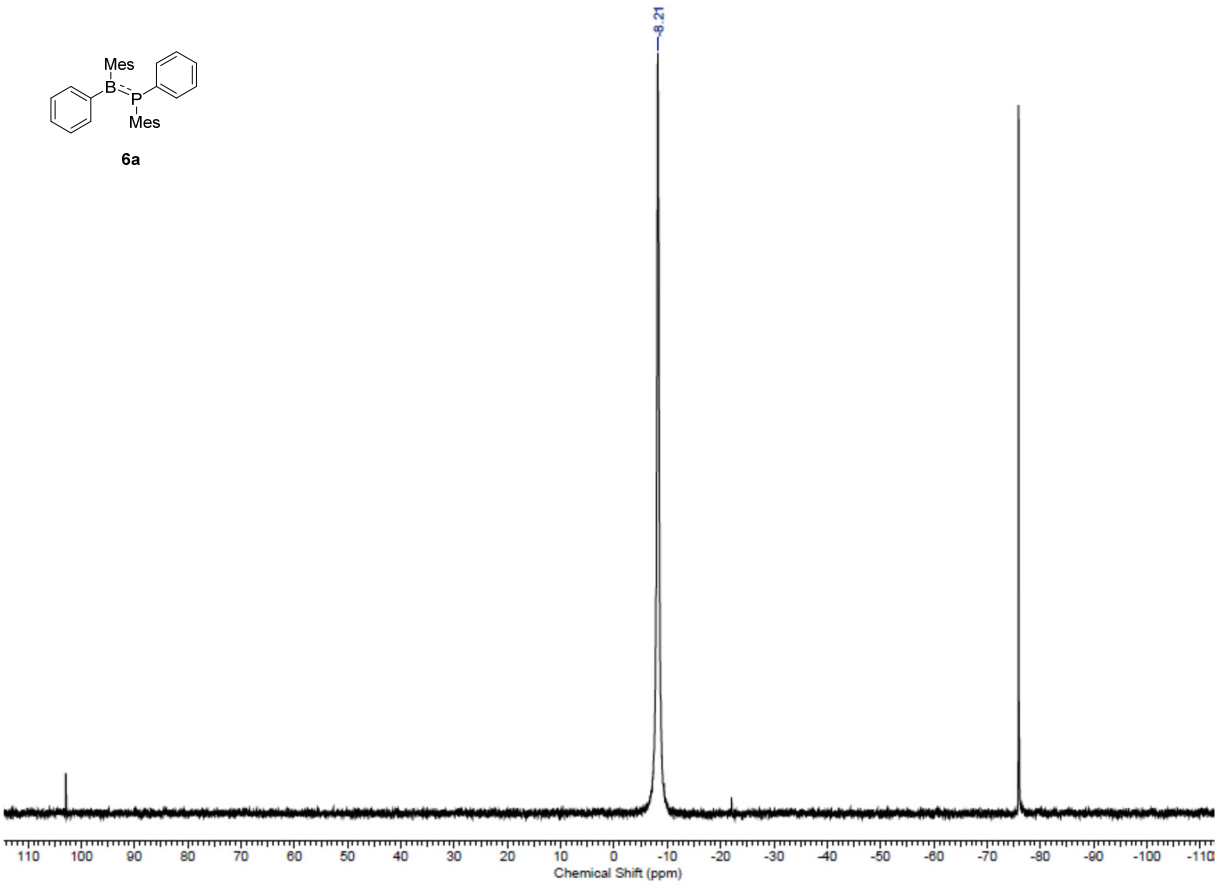

Figure 7.4.7. $^{31}P\{^{1}H\}$ NMR spectrum of **6a** (in $CDCl_3$).

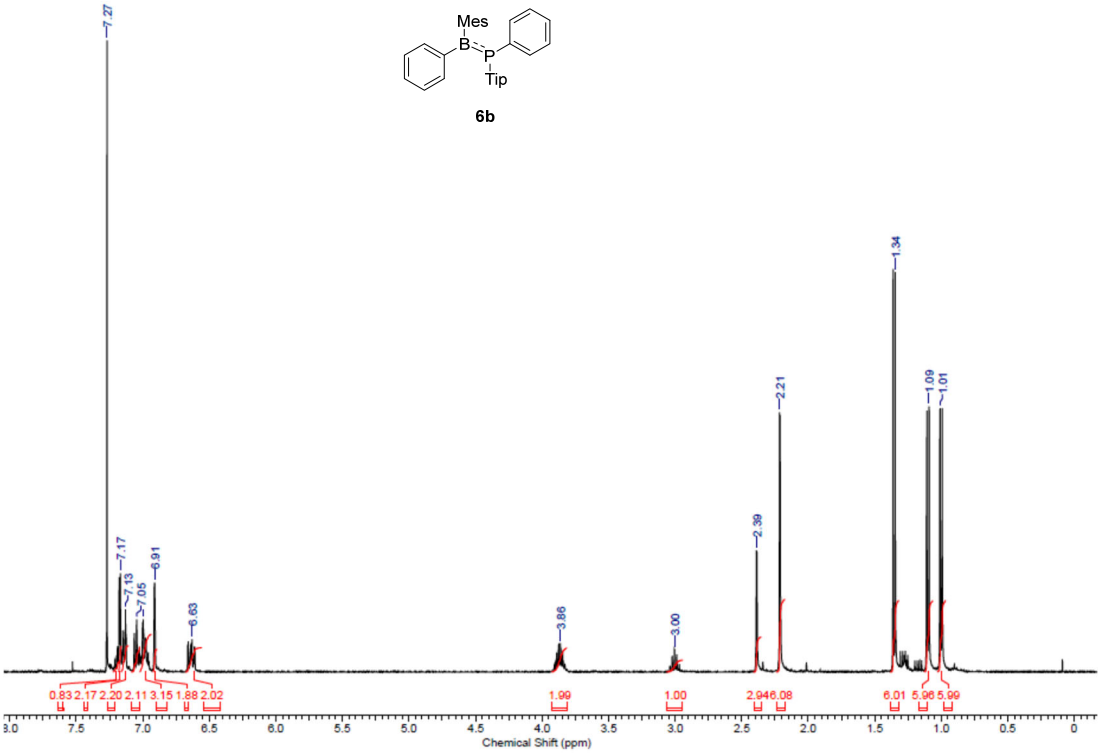

Figure 7.4.8. ^{1}H NMR spectrum of **6b** (in $CDCl_3$).

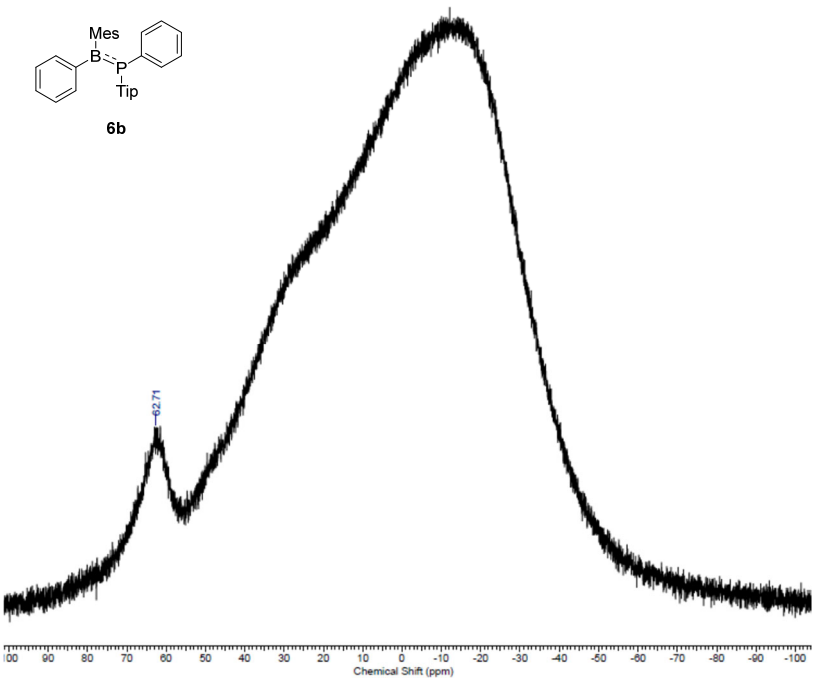

Figure 7.4.9. $^{11}B\{^{1}H\}$ NMR spectrum of **6b** (in $CDCl_3$).

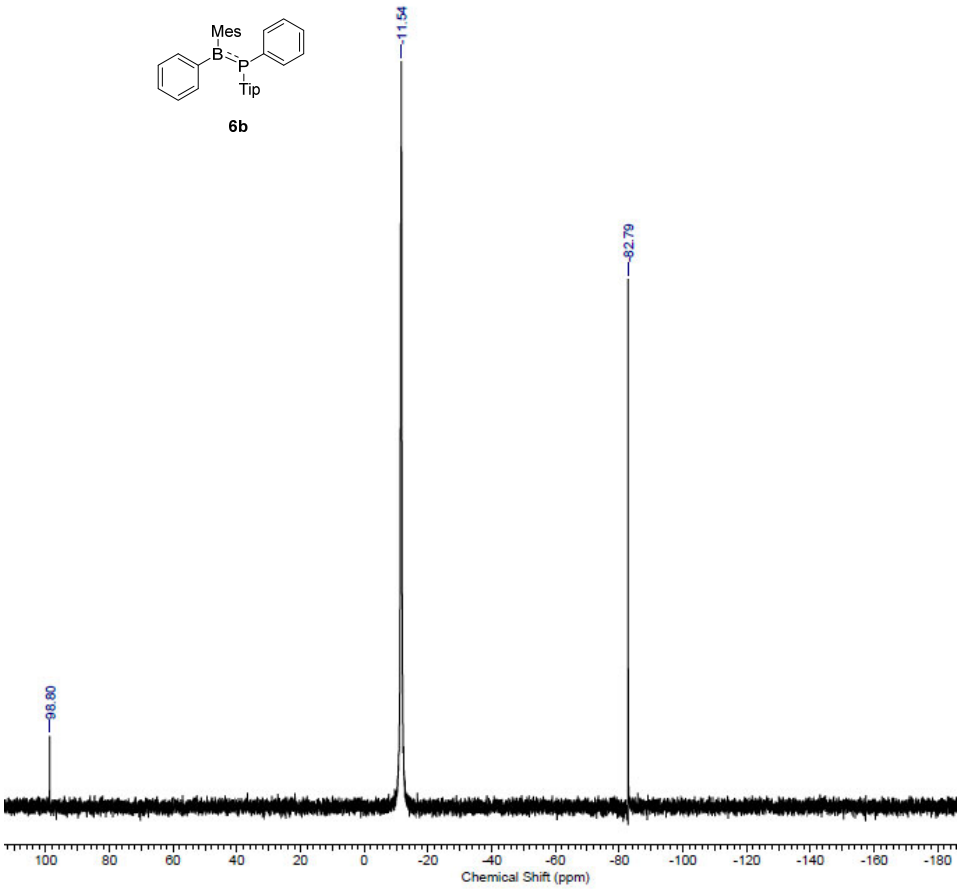

Figure 7.4.10. $^{31}P\{^{1}H\}$ NMR spectrum of **6b** (in $CDCl_3$).

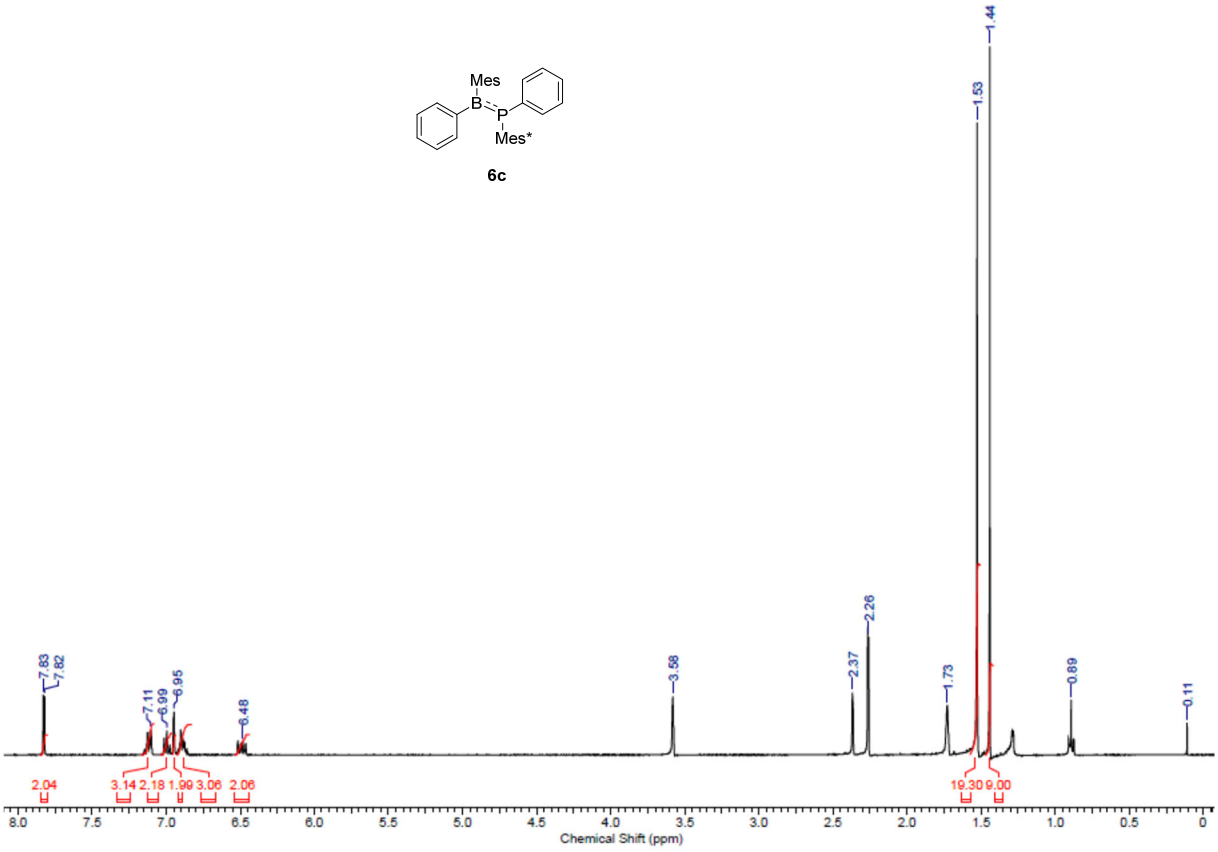

Figure 7.4.11. ^{1}H NMR spectrum of **6c** (in THF-d_8).

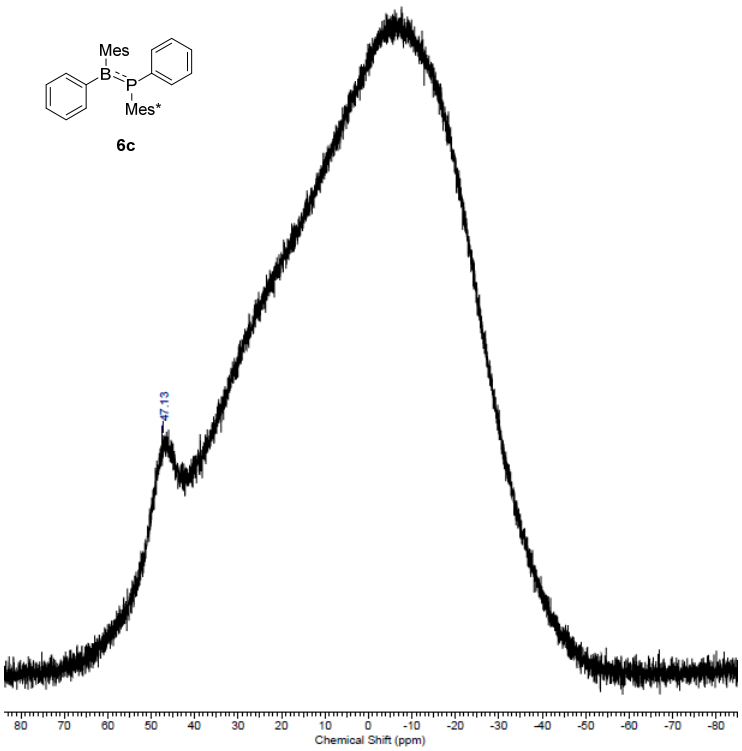

Figure 7.4.12. ^{11}B{^{1}H} NMR spectrum of **6c** (in THF-d_8).

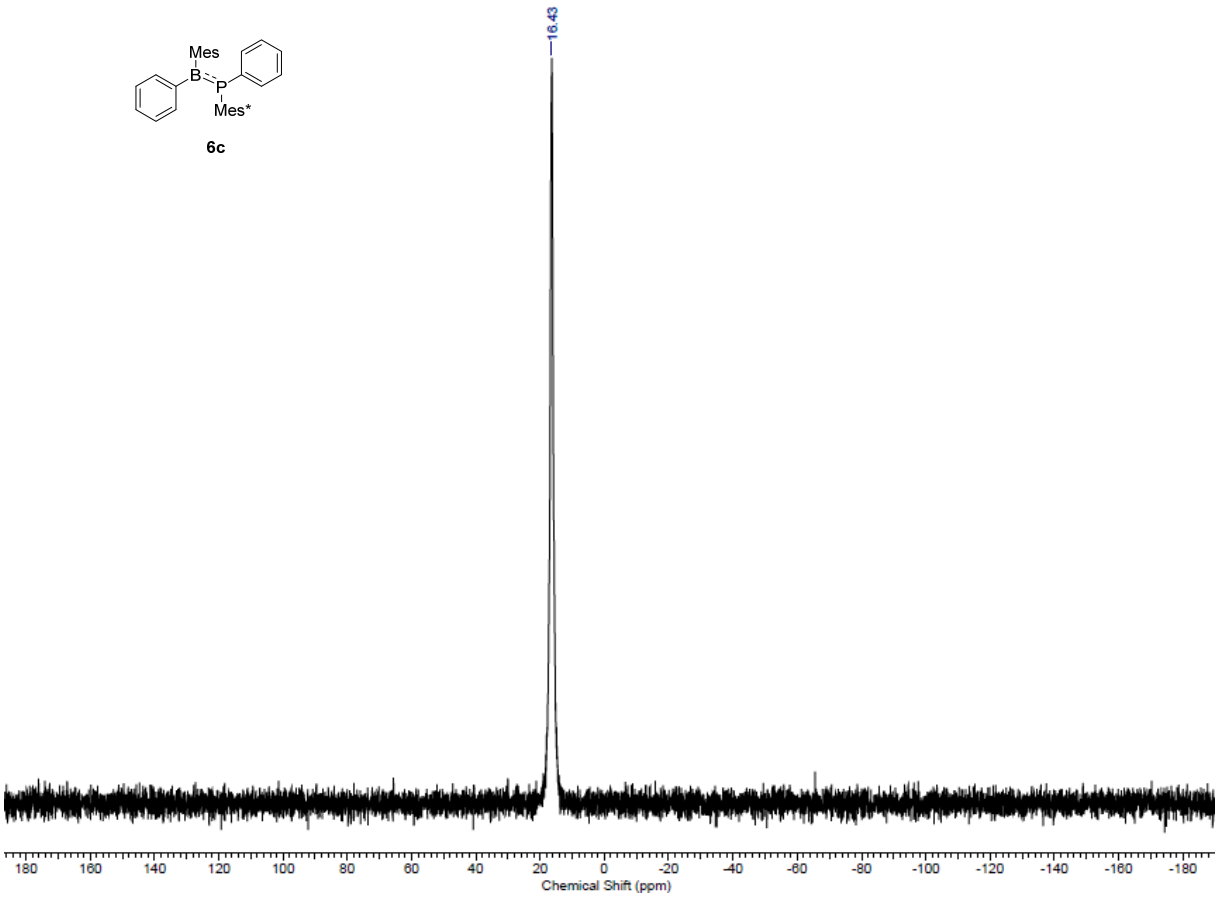

Figure 7.4.13. $^{31}P\{^{1}H\}$ NMR spectrum of **6c** (in THF-d_8).

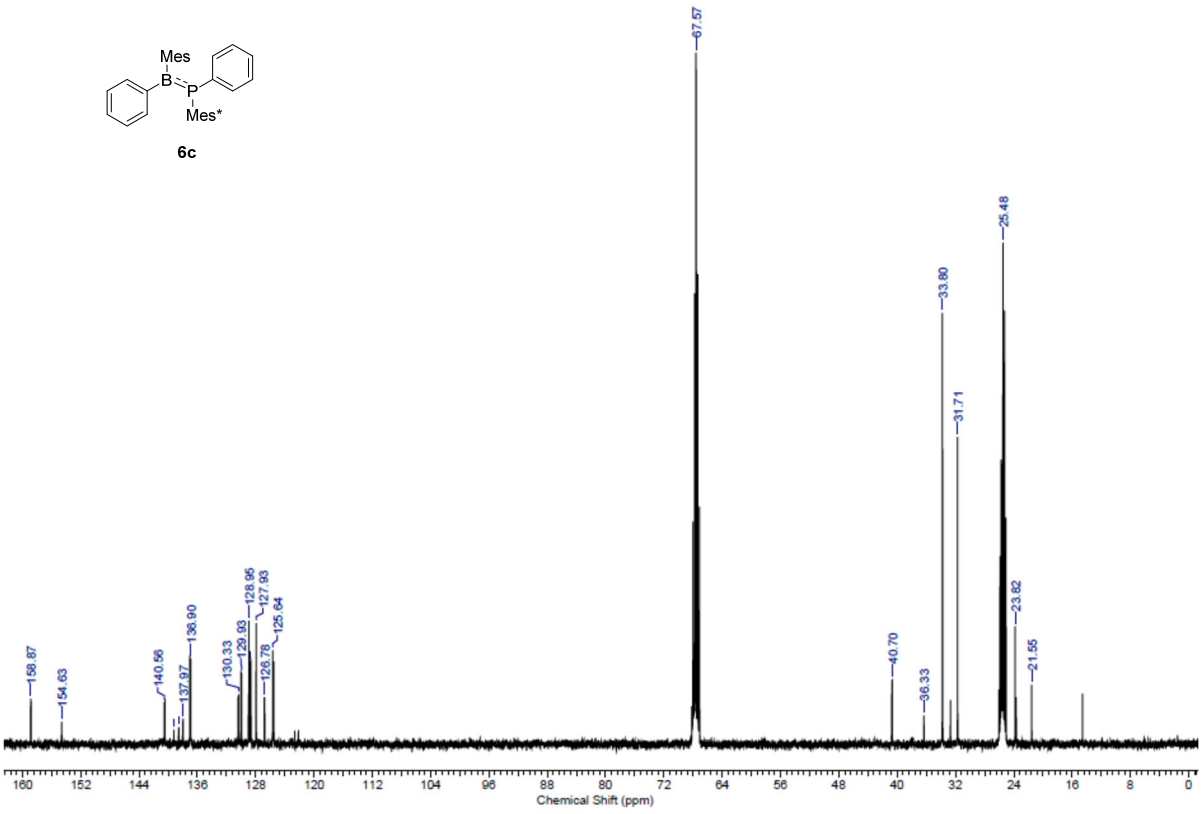

Figure 7.4.14. $^{13}C\{^{1}H\}$ NMR spectrum of **6c** (in THF-d_8).

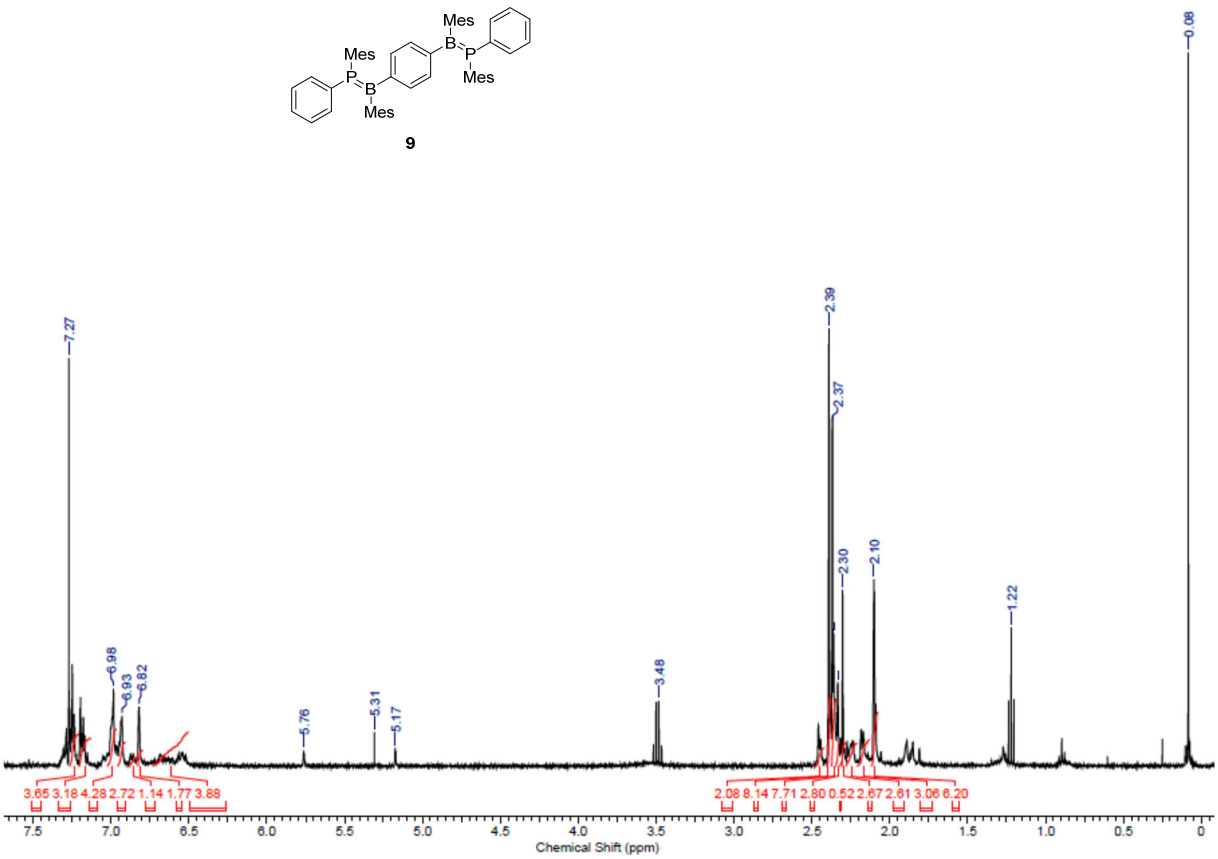

Figure 7.4.15. ^{1}H NMR spectrum of **9** (in $CDCl_3$).

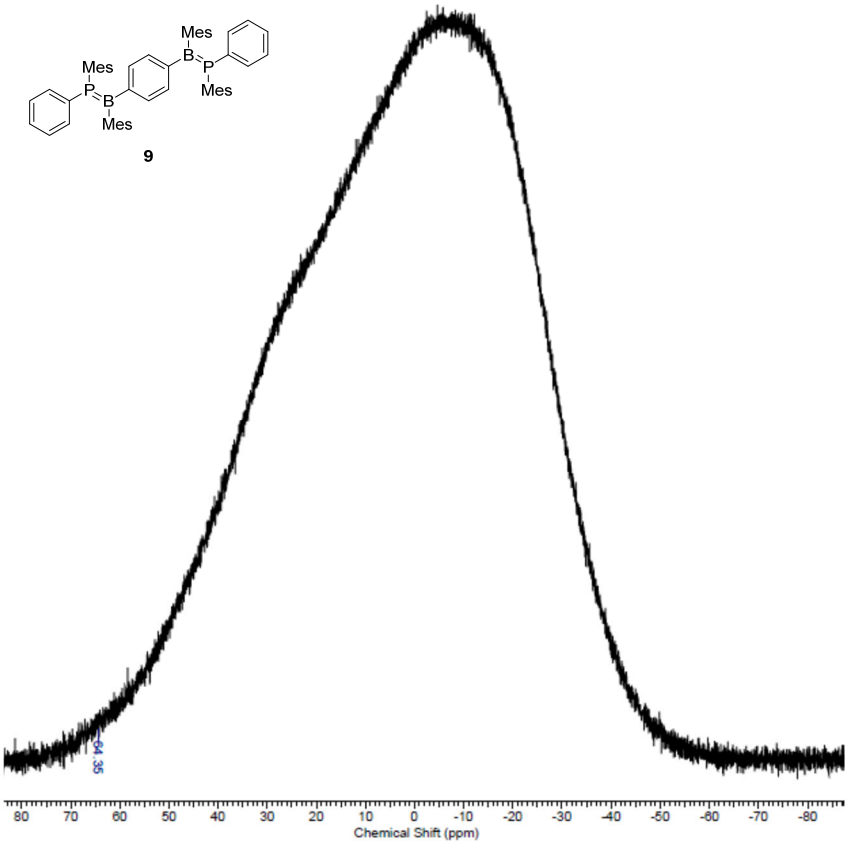

Figure 7.4.16. $^{11}B\{^{1}H\}$ NMR spectrum of **9** (in $CDCl_3$).

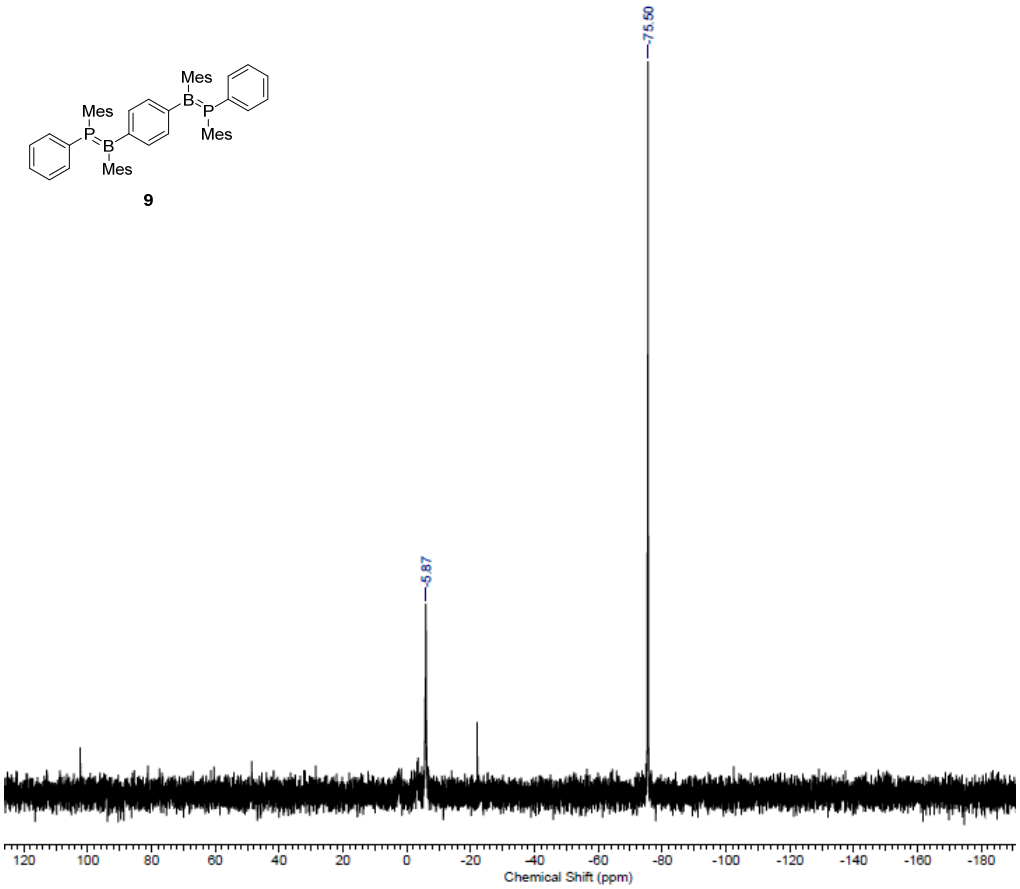

Figure 7.4.17. $^{31}P\{^{1}H\}$ NMR spectrum of **9** (in $CDCl_3$).

Erklärung zur Autorenschaft

“Poly(*p*-phenylene iminoborane): A Boron–Nitrogen Analogue of Poly(p-phenylene vinylene)”,

Thomas Lorenz, Merian Crumbach, Thomas Eckert, Artur Lik, and Holger Helten,* *Angew. Chem. Int. Ed*, **2017**, *56*, 2780-2784.

Detaillierte Darstellung der Anteile an der Veröffentlichung (in %)

Angabe Autoren/innen (ggf. Haupt- / Ko- / korrespondierende/r Autor/in) mit Vorname Nachname (Initialen)

Autor/in 1 (TL), Autor/in 2 (MC), Autor/in 3 (TE), Autor/in 4 (AL), Autor/in 5 (HH)

Autor	**A1**	**A2**	**A3**	**A4**	**A5**					**∑ in Prozent**
Idee/Ideenentwicklung/Konzept					14.28%					14.28%
Synthese	17.17%	4.29%								21.46%
Analyse	12.15%	0.71%	0.71%	0.71%						14.28%
Rechnung					14.28%					14.28%
Verfassen der Veröffentlichung	11.42%				2.86%					14.28%
Korrektur der Veröffentlichung	3.57%				3.57%					7.14%
Koordination der Veröffentlichung					14.28%					14.28%
Summe	44.31%	5.00%	0.71%	0.71%	49.27%					100%

Erklärung zur Autorenschaft

“Dehydrocoupling and Silazane Cleavage Routes to Organic–Inorganic Hybrid Polymers with NBN Units in the Main Chain”, Thomas Lorenz, Artur Lik, Felix A. Plamper, and Holger Helten*, *Angew. Chem. Int. Ed.*, **2016**, *55*, 7236-7241.

Detaillierte Darstellung der Anteile an der Veröffentlichung (in %)

Angabe Autoren/innen (ggf. Haupt- / Ko- / korrespondierende/r Autor/in) mit Vorname Nachname (Initialen)

Autor/in 1 (TL), Autor/in 2 (AL), Autor/in 3 (FP), Autor/in 4 (HH)										
Autor	**A1**	**A2**	**A3**	**A4**						**∑ in Prozent**
Idee/Ideenentwicklung/Konzept				14.28%						14.28%
Synthese	21.46%									21.46%
Analytik	12.86%	0.71%	0.71%							14.28%
Rechnung				14.28%						14.28%
Verfassen der Veröffentlichung	11.42%			2.86%						14.28%
Korrektur der Veröffentlichung	3.57%			3.57%						7.14%
Koordination der Veröffentlichung				14.28%						14.28%
Summe	49.31%	0.71%	0.71%	49.27%						100 %

Erklärung zur Autorenschaft

“BN- and BO-Doped Inorganic–Organic Hybrid Polymers with Sulfoximine Core Units”,

Felix Brosge, Thomas Lorenz, Holger Helten,* Carsten Bolm,* *Chem. Eur. J.*, **2019**, *25*, 12708-12711.

Detaillierte Darstellung der Anteile an der Veröffentlichung (in %)

Angabe Autoren/innen (ggf. Haupt- / Ko- / korrespondierende/r Autor/in) mit Vorname Nachname (Initialen)

Autor/in 1 (FB), Autor/in 2 (TL), Autor/in 3 (HH), Autor/in 4 (CB)

Autor	**A1**	**A2**	**A3**	**A4**						**∑ in Prozent**
Idee/Ideenentwicklung/Konzeption			8.33%	8.33%						16.66%
Synthese	8.35%	8.35%								16.70%
Analyse	8.34%	8.34%								16.68%
Verfassen der Veröffentlichung	8.33%	8.33%								16.66%
Korrektur der Veröffentlichung	4.16%	4.16%	4.16 %	4.16%						16.64%
Koordination der Veröffentlichung			12.5 %	4.16%						16.66%
Summe	29.18%	29.18%	24.99%	16.65%						100%